Chapter-2

Synthesis & Study of Small Non-planar molecules

Section A:
1,8-Disubstituted Naphthalenes

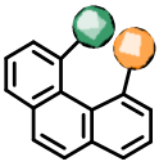

Section B:
4,5-Disubstituted Phenanthrenes

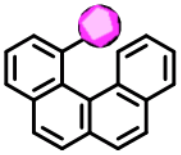

Section C:
1-Substituted Benzo[c]phenanthrenes

Table of Contents

2.1 Introduction to Small non-planar molecules: 32
2.2 Section A: 1,8-Disubstituted Naphthalenes: 33
2.2.1 Introduction: 33
2.2.2 Results and Discussion: 40
2.2.2.1 Synthesis of 1,8-Disubstituted naphthalenes: 40
2.2.2.2 Single Crustal XRD analysis: 43
2.2.2.3 Conclusion: 47
2.2.2.4 Experimental Section: 48
2.2.2.5 Spectral Data: 51
2.2.2.6 Crystallographic Data: 57
2.3 Section B: 4,5-Disubstituted Phenanthrenes: 59
2.3.1 Introduction: 59
2.3.2 Results and Discussion: 65
2.3.2.1 Synthesis of 4 and 5-Disubstituted Phenanthrenes: 65
2.3.2.2 NMR spectroscopy as a tool for detection of chirality: 69
2.3.2.3 Single Crystal XRD to determine degree of non-planarity: 73
2.3.2.4 Conclusion: 78
2.3.2.5 Experimental Section: 79
2.3.2.6 Spectral Data: 87
2.3.2.7 Crystallographic Data: 107
2.4 Section C: 1-Substituted Benzo[*c*]phenanthrenes: 109
2.4.1 Introduction: 109
2.4.2 Results and Discussion: 118
2.4.2.1 Synthesis of 1-Substituted Benzo[*c*]phenanthrenes: 118
2.4.2.2 Single Crystal XRD to determine degree of non-planarity: 125
2.4.2.3 Chiral HPLC Analysis: 135
2.4.2.4 Chiral Crystals: Absolute Asymmetric Synthesis: 139
2.4.2.4.1 SCXRD as a tool for detecting spontaneous resolution: 140
2.4.2.4.2 Solid State Circular Dichroism: 144
2.4.2.5 Conclusion: 146
2.4.2.6 Experimental Section: 147
2.4.2.7 Spectral Data: 156
2.4.2.8 Crystallographic Data: 178
2.5 References: 185

2.1 Introduction to Small non-planar molecules:

For many years, benzene and other six membered aromatic rings were considered to be conformationally rigid in their nature. But with the synthesis of hexa-substituted benzene **(1)** [1–3] and paracyclophanes **(2)**,[4,5] deformation of the molecule due to high steric strain has been reported. Later, the non-planarity of various polycyclic compounds like corannulenes **(3)**,[6–8] tetramethylfluoranthrene **(4)**[9] and coronenes **(5)**[10] was established and later confirmed by various theoretical investigations of such systems (Figure 1). Literature reports on corannulenes **(3)** and its derivatives revealed that the inversion barrier between the two bowl shaped conformations is low (10-12 kcal/mol) which was greatly affected by the nature of substituents present on it.[11,12] Hence, the non-planarity of these systems was attributed to intramolecular steric strain which develops in the molecule either due to the presence of bulky substituents or due to their topology. Such deformations in the molecular skeleton was also reported in biological systems. The deformation of pyrimidine ring in DNA lead to the conclusion that these aromatic systems are conformationally non-rigid.[13]

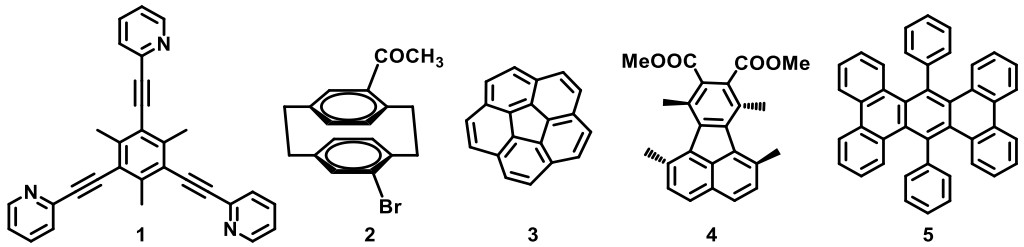

Figure 1 Non-planarity in various substituted polycyclic compounds

Interest in the study of overcrowded molecules remains attractive for a variety of reasons: such molecules pose synthetic challenges, they serve to test the limits of theoretical predictions and they provide exceptional insights into the effect of intramolecular strain on ground-state structures as well as internal mobility of electrons.[14] There are two principal ways in which the geometries of organic structures can be altered from their usual arrangements, the most widely studied of these is the construction of ring systems with forced bond angle deformations. The second method, which has not received the same degree of attention, is the use of bulky groups leading to non-bonded repulsions and eclipsing strains due to the close proximity of various substituents leading to deformation of molecular structure. In this case, the non-bonded repulsions involving large groups in turn induces bond-angle strain and other deformations in the molecule.[15]

Steric strain due to bulky substitution at interfering positions can be relieved by (a) stretching of bonds, (b) in-plane deflection of the substituent, (c) out-of-plane deflection of the substituent, and (d) distortion or buckling of the nucleus itself. Of these possibilities, (a) is practically excluded because of the large amounts of energy associated with even a small change in bond length. All of the other modes for relief of steric strain may come into play in overcrowded organic molecules. While in many cases considerable in-plane and out-of-plane deviations of the exocyclic bonds occur, reported cases of nuclear distortions are relatively limited. Such phenomena is pronounced not only in heavily substituted benzenes, but also its analogues of naphthalene, phenanthrene and benzo[*c*]phenanthrene which have been individually discussed in following sections.

2.2 Section A: 1,8-Disubstituted Naphthalenes:

2.2.1 Introduction:

In naphthalene molecule, the 1- and 8-positions are said to be *peri* to each other (Figure 2). The substituents located at these positions are in much closer proximity than similar substituents located *ortho* to each other (1- and 2- position). This close proximity has been responsible for several unique properties of *peri*-substituted naphthalenes. Such "proximity effects" have been reported by several groups over many years and this aspect of naphthalene chemistry has attracted increasing attention over the years.

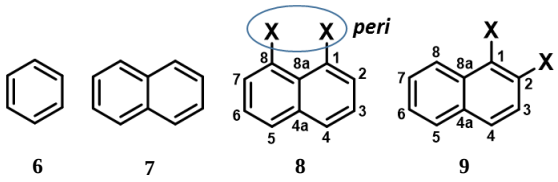

6 **7** **8** **9**

Figure 2 *Peri*-substitutions at 1 and 8-position of naphthalene

The unsubstituted naphthalene molecule is known to have a rigidly planar structure. The distance between the C1 and C8 carbon atoms is about 2.4-2.5 Å. Hence, with substituents other than hydrogen at the *peri* positions leads to development of considerable steric strain in naphthalene. In 1-substituted naphthalenes, the substituent undergoes in-plane and/or out-of-plane deformations because of *peri*-interaction with hydrogen atom present on 8-position.[16]

Many octasubstituted naphthalenes have been prepared and structurally characterized, including a variety of octaaryl **(10)**,[17–21] octahalo **(11)**,[22,23] octamethyl naphthalenes **(12)**,[24] octakis(aryloxy) naphthalenes **(13)**,[25] octakis(arylthio) **(14)**[26–28] as well as

octapyrrolyl naphthalene **(15)**,[29] and a few others with mixed substituents (Figure 3). The naphthalene core of these molecules are significantly distorted from a normal planar geometry, usually in the form of a twist of 20-30° between the planes containing the aromatic rings.

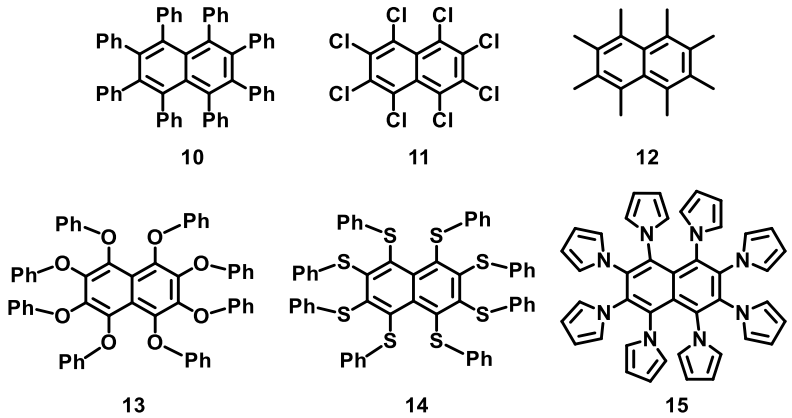

Figure 3 Some octa-substituted naphthalenes (10-15)

However, *tert*-butyl group has much greater steric demand than any of the substituents listed above and helps in clearly understanding the interactions in play. Leser *et al.* were the first to synthesize 1,8-di-*tert*-butylnaphtalene,[30] in which non-bonded repulsions result in a warped naphthalene ring. Later Madella and co-workers prepared its derivative namely 5-benzyl-1,3,8-tri-*tert*-butylnaphthalene **(20)** by using a similar procedure (Scheme 1).[31]

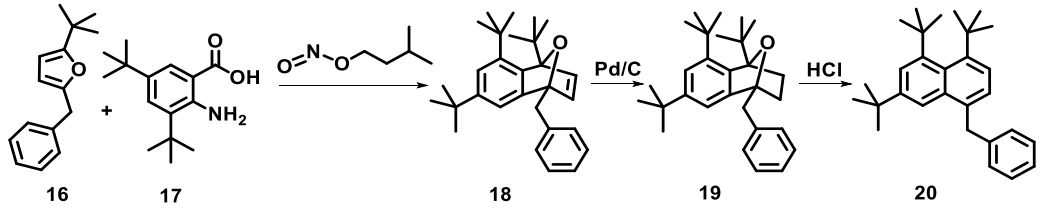

Scheme 1 Synthesis of 5-benzyl-1,3,8-tri-*tert*-butylnaphthalene (20)

The ^{1}H NMR **20** showed that the methylene protons appeared as an AB quartet at ambient temperatures proving for the first time that these protons were diastereotopic in nature. This showed that the *tert*-butyl groups at the *peri* positions caused sufficient bulk for the slow interconversion of the two enantiomers on NMR time scale. Further, from coalescence studies, it was determined that the free energy of barrier to racemization for this molecule was >20 kcal/mol. The crystal structure of one of the 1,8-di-*tert*-butyl naphthalene derivative was studied by Allinger *et al.* They were the first to report the crystal structure of 1,3,6,8-tetra-*tert*-butylnaphthalene **(21)** showing that each benzene ring of the naphthalene core was distorted into a flattened half chair shape. The *peri* carbons 1 and 8 are 0.29Å (21°)

and the *tert*-butyl group at C1 and C8 *peri* positions were deflected further by an angle of 10^{o} from the mean plane of the naphthalene moiety (Figure 4).[32]

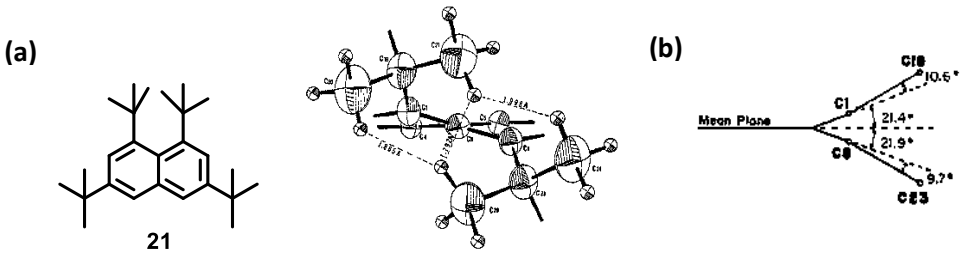

Figure 4 (a) Observed close contacts among hydrogens on *peri tert*-butyl groups (b) Projection of distortion of various atoms from the mean plane

Later, Anderson and co-workers carried out functionalization of 1,6,8-tri-*tert*-butylnaphthalene **(26)** (Scheme 2). The enantiotopic nature of parent 1,6,8-tri-*tert*-butylnaphthalene **(22)** was also confirmed by ^{1}H NMR for its derivative 2-(4,5,7-tri-*tert*-butylnaphthalen-1-yl)propan-2-ol **(26)** which showed a doublet (J=10.6 Hz at ambient temperature) for the two methyl groups of the -C(CH_3)$_2$OH substituent. This shift was temperature dependent (J=7.5 Hz at 100^{o}C) and the peaks of the doublet coalesce at 144°C into a singlet indicating that the barrier to flipping is 22.5 kcal mol^{-1}.[33]

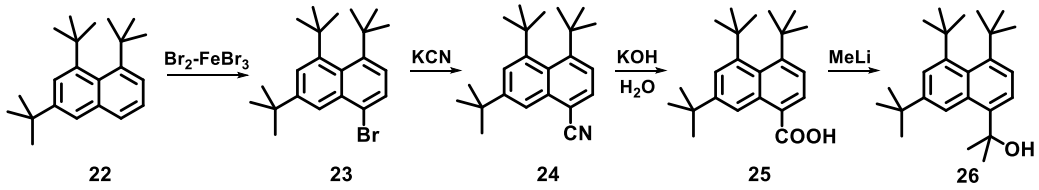

Scheme 2 Synthesis of 2-(4,5,7-tri-*tert*-butylnaphthalen-1-yl)propan-2-ol (26)

A relatively less bulky 1,8-diisopropyl naphthalene **(35)** was synthesized from 1,8-naphthalene dicarboxylic anhydride **(27)** by Wepster *et al* (Scheme 3).[34]

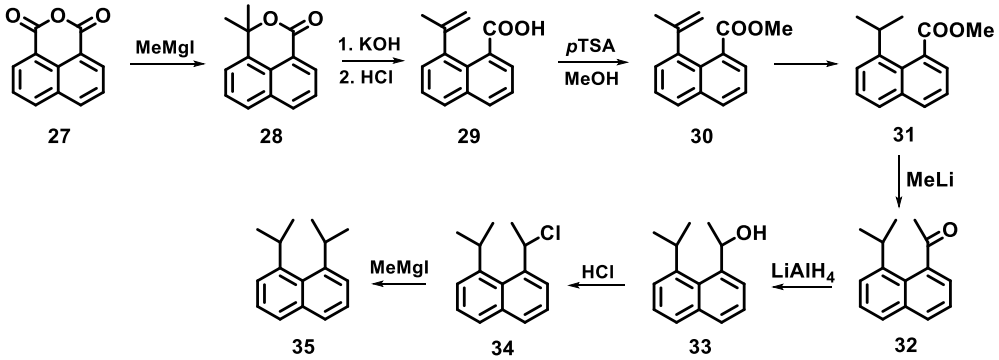

Scheme 3 Synthesis of 1,8-diisopropyl naphthalene (35)

A comparison of ^{1}H NMR of 1,8-diisopropyl naphthalene **(35)** with 2-isopropylnaphthalene revealed that the downfield shift of the methine proton by 0.93 ppm was a consequence of the high steric strain in this molecule.

Acetyl and benzoyl groups can provide sufficient bulk to the skeleton as well as act as a precursor to access various other functional groups like chloro, secondary alcohols *etc.* which are known to act as a handle for resolution. Rank and co-workers were the first to synthesize 1,8-diacetyl naphthalene **(38)** by carrying out oxidation of 1,2-dimethylacenaphthalene-l,2-diol **(37)** using chromic acid (Scheme 4).[35,36]

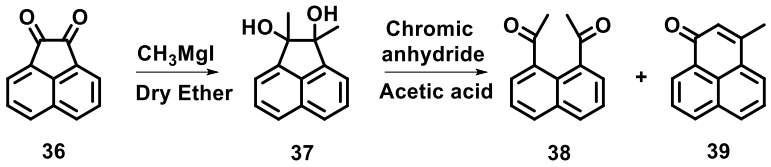

Scheme 4 Synthesis of 1,8-diacetyl naphthalene (38)

The yield of this reaction was very low as 3-methylphenalenone **(39)** was obtained as a side product due to facile cyclization of 1,8-diacetyl naphthalene **(38)** both in acidic as well as basic medium.

Recently, Okamoto and group have revealed that diaroylation at 1,8-positions of 2,7-dimethoxy naphthalene proceeds smoothly by carrying out condensation of 2,7-dimethoxy naphthalene **(40)** and benzoic acid using phosphorus pentoxide-methanesulfonic acid (P_2O_5–MsOH) giving a mixture of compounds which were carefully separated (Scheme 5). X-ray crystal structural study of the obtained 1,8-diaroylnaphthalene **(41)** has unique non-coplanar alignment of aromatic rings.[37]

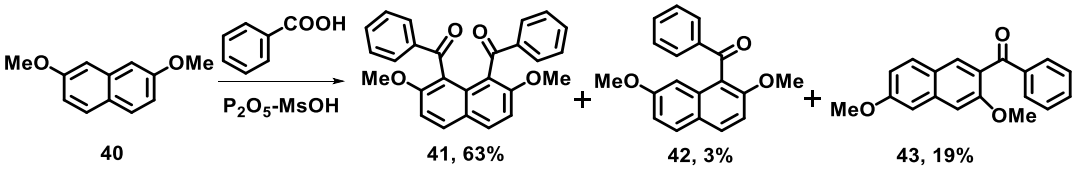

Scheme 5 Aroylation of 2,7-dimethoxy naphthalene (35)

VT-NMR showed that the signals at 7.34 and 7.70 ppm are broadened as the temperature was reduced from 293 to 213K and each of them splits into two broad signals at 193K. Both of the pairs of broad signals are sharpened again at 173K. This suggests that the C–C bond rotation between benzene ring and carbonyl of ketone group is gradually slowed down with

decreasing temperature leading to the development of magnetically non-equivalent environment on the aromatic ring.

A similar observation of restricted rotation around the C-O bond of the ester group present at the 1-position of 8-substituted naphthalene was reported by Cookset *et al.* They showed that in methyl 8-isopropyl-l-naphthalenecarboxylate **(44)**, the isopropyl methyl groups appeared as a doublet (J= 6.5 Hz) at **δ** 1.28 at ambient temperature, but at -100°C this signal appears as two equal doublets with a coupling constant of 17 Hz indicating that the barrier to rotation of the ester group is 8.9 kcal/mol. Likewise, 8-benzylnaphthalen-1-benzoyl naphthalene **(45)**, -CH_2 signal appeared as a singlet at **δ** 4.03 which splits at -30°C (J_{AB}=16.0 Hz) indicating that the barrier to rotation of the benzoyl group is 11.9 kcal/mol (Figure 5).[38]

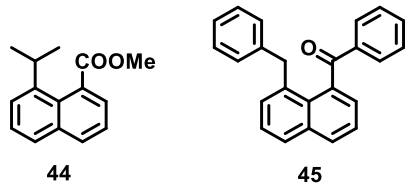

Figure 5 Structures of methyl 8-isopropyl-l-naphthalenecarboxylate (44) and 8-benzylnaphthalen-1-benzoyl naphthalene (45)

The first report of isomerism based on a 1,8-disubstituted naphthalene system was made by Clayden *et al.* who synthesized 8-substituted-1-naphthamides **(46)** and proved that such compounds can provide a barrier to Ar–CO bond rotation sufficiently large that they can be configurationally stable as the rotation is governed more by electronic factors than steric factors. Such compounds undergo highly stereoselective reactions (Scheme 6) on prochiral 2-substituents **(47)** as reagent approach is governed by differentiation of the two faces of the naphthalene ring by the steric and electronic properties of the amide group.[39–41]

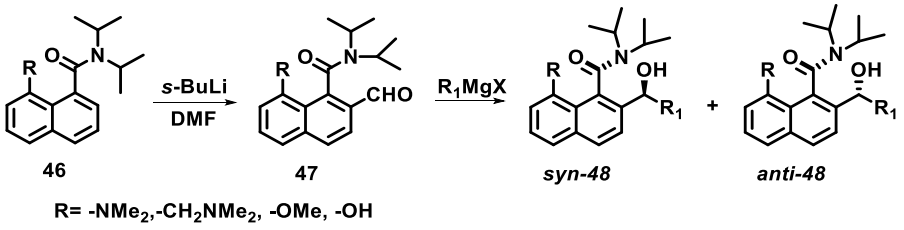

Scheme 6 8-Substituted 1-naphthamides (47) undergo stereoselective reaction on prochiral center

Both kinetic stereoselectivity and thermodynamically controlled equilibration favour the formation of *syn* atropisomeric alcohols (Scheme 7) from nucleophilic additions to 8-acyl substituted naphthamide (64-98% *de*).[42]

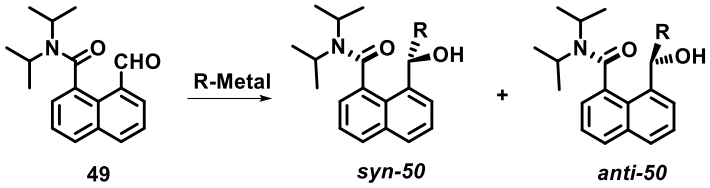

Scheme 7 **Stereoselective reaction on 8-acyl-1-naphthamides (49)**

The first report on the synthesis of optically pure 1,8-disubstituted naphthalene was made in 2013 by Yamaguchi *et al.* They synthesized **56** by the [4+2] cycloaddition reaction of 6-adamantyl benzyne and 2-adamantyl furan (Scheme 8). The enantiomers were resolved by forming diastereomeric ketopinic esters **(55)**.[43,44]

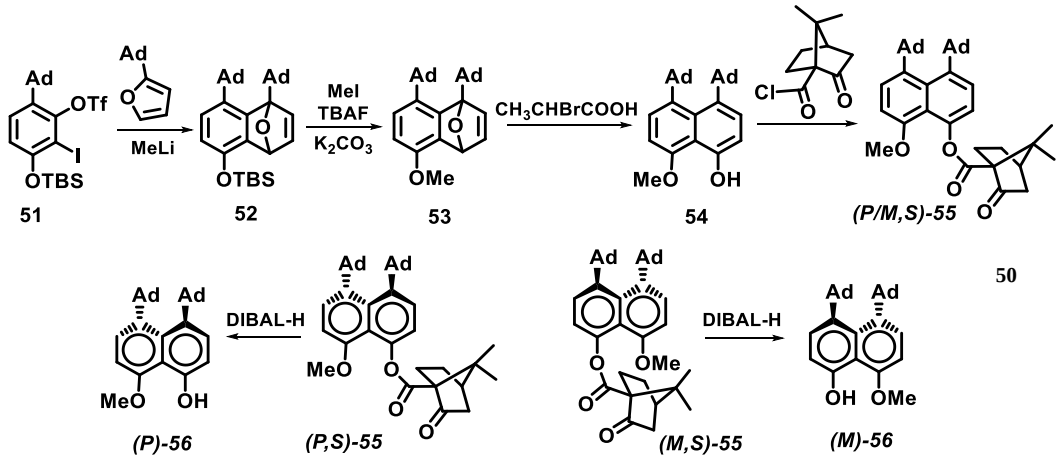

Scheme 8 **Synthesis of optically pure 1,8-diadamantyl derivative of naphthalene (56)**

It was known that the secondary structure of proteins is due to N-H···O=C hydrogen bonding between the amino acid residues along with XH···π binding (X = N, O, S). To understand such interactions, Steglenko *et al.* synthesized two types of protonated 9-dimethylamino-1-methylbenzo[*g*]indoles **(57)** and 1-dimethylamino-8(pyrrolyl) naphthalene **(58)** having a pyrrole nitrogen atom (Figure 6). The formation of intramolecular NH···N hydrogen bond was the first example of such kind of hydrogen bonding in pyrroles which was possible due to the close proximity of *peri* substituents.[45]

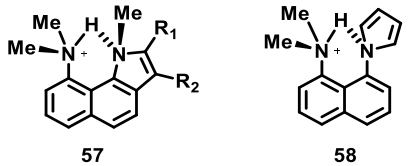

Figure 6 **Intramolecular interactions in 9-dimethylamino-1-methylbenzo[*g*]indoles (57) and 1-dimethylamino-8(pyrrolyl) naphthalene (58)**

Compounds **59-61** were synthesized by Starikova *et al.* and studied them as "push–pull" proton sponges (Figure 7). This phenomenon is ascribed to smaller steric demands of -CHO, their lower electrostatic repulsion, and specific packing forces. The naphthalene cores of all but one of the molecules are markedly twisted (21–26°).[46]

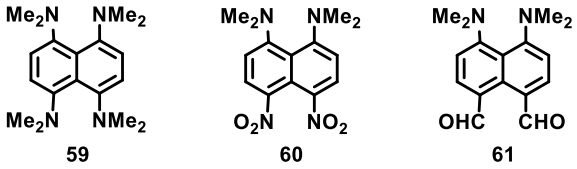

Figure 7 Showing some 1,8-Bis(dialkylamino)-4,5-disubstitutednaphthalenes (59-61)

Carboxylic acid recognition is biologically important because of their significant roles in metabolic processes. Many 'turn-off type' fluorescent probes for the recognition of the acids are known in the literature. Kusukawa *et al.* have synthesized a 1,8-diphenylnaphthalene-based diamidine **(66)** (Scheme 9) 'turn-on' fluorescent probe for the detection of dicarboxylic acids.[47]

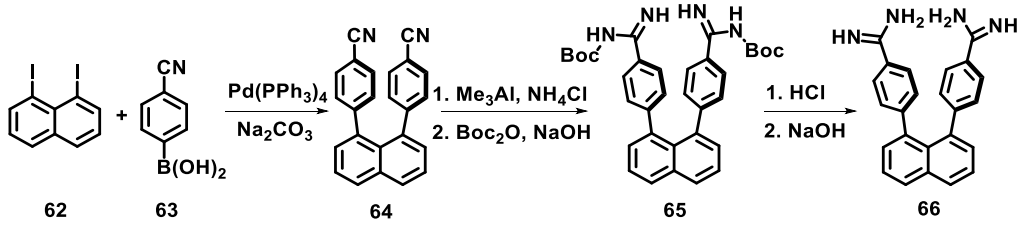

Scheme 9 Synthesis of 1,8-diphenylnaphthalene based diamidine (66)

2.2.2 Results and Discussion:

2.2.2.1 Synthesis of 1,8-Disubstituted naphthalenes:

Aromatic hydroxyketones are a class of important intermediates in the synthesis of biologically active compounds such as chalcones, flavanones, naphthoquinones and some are important drug intermediates.[48,49] The most common pathway to obtain such molecules is by the Friedel Crafts acylation of phenol derivatives, boron trifluoride in liquid HF[50] *etc*. These synthetic procedures suffer from numerous drawbacks in their practical applicability, such as their unpredictable regioselectivity, extremely corrosive nature of the reagents, requirement of extremely hazardous solvent systems, and the use of large amount of Lewis acid. Another limitation towards the application of these processes is the limited availability of the required, pure 2-substituted naphthalene derivatives on a large scale. Numerous literature on the acylation of benzene has been reported, but relatively less study on the acylation of naphthalene and other polyaromatic systems has been done. Although the *peri* interactions in naphthalenes have been greatly reviewed, but only a few reports on 1,8-diacyl naphthalene have been known in literature.[51,52] The thought that introduction of acyl substituents at these crowded positions may not only lead to a skeletal deformation of naphthalene core due to non-bonded interactions, but also restrict the C-C(O)CH_3 bond rotation leading to a fixed conformation was quite fascinating.

With this idea in mind, we attempted the synthesis of 1,1'-(2,7-dihydroxynaphthalene-1,8-diyl)bis(ethan-1-one) **(70)** utilizing the classical Fries rearrangement which is an effective method for C-C bond formation. Fries rearrangement is an acid-catalyzed reaction of the phenol esters resulting in the formation of phenolic ketones. Hence, 2,7-dihydroxy naphthalene **(67)** was almost quantitatively *O*-acetylated using acetic anhydride in acetic acid to give naphthalene-2,7-diyl diacetate **(68)**. The synthesized **(68)** was then subjected to Fries rearrangement using stoichiometric amount of $AlCl_3$ and heating the reaction mixture neat at 150^oC. High temperatures help in the formation of *o*-hydroxy ketone product by promoting the generation of acylium ions *in situ* leading to α-acylation of the phenol. However, it was observed that only 1-(2,7-dihydroxynaphthalen-1-yl)ethan-1-one **(69)** along with 2,7-dihydroxy naphthalene **(67)** was formed, with no traces of the target molecule **(70)** (Scheme 10). This could possibly happen due to the fact that after the first acylation, acyl group being strongly electron withdrawing in nature deactivates the

naphthalene ring preventing the second acylation to occur. Also the development of steric bulk in the *peri* region after the introduction of acetyl group at 1-position may also be a factor contributing to the inhibition of second acetyl migration at 8-position.

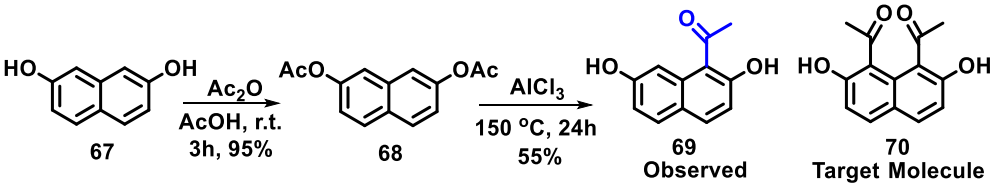

Scheme 10 Attempted synthesis of 1,1'-(2,7-dihydroxynaphthalene-1,8-diyl) bis(ethan-1-one) (70)

The formation of 1-(2,7-dihydroxynaphthalen-1-yl)ethan-1-one **(69)** was confirmed by ^{1}H NMR spectra, clearly showing a doublet of one proton at **δ** 7.47 with *J*=2.0 Hz corresponding to the proton at 8th position which is meta-coupled with the proton that appears at **δ** 6.98. Also a single peak for the –COC*H*$_3$ protons appears at **δ** 2.86 as a sharp singlet, confirming that the acyl migration has occurred only at 1-position. A characteristic broad singlet can be observed at **δ** 13.67 in the downfield region suggesting the possibility of intramolecular hydrogen bonding between the –O*H* and oxygen atom of -C*O*- group, restricting the rotation along the C-C bond. Modification of reaction conditions as well as the use of anhydrous $ZnCl_2$ or photofries conditions did not give us the desired target molecule.

Modifying our strategy, we planned to introduce another bulky substituent at 8-position of 1-(2,7-dihydroxynaphthalen-1-yl)ethan-1-one **(69)** and bromine atom was the ideal choice due to its large size, presence of non-bonded electrons and its ability to act as a precursor for introduction of a wide variety of functional groups.[53] 1-(2,7-Dihydroxy naphthalen-1-yl)ethan-1-one **(69)** was subjected to bromination using potassium bromate, potassium bromide and conc. HCl[54] giving 1-(8-bromo-2,7-dihydroxynaphthalen-1-yl) ethan-1-one **(71)** as a single product with good yield (Scheme 11).

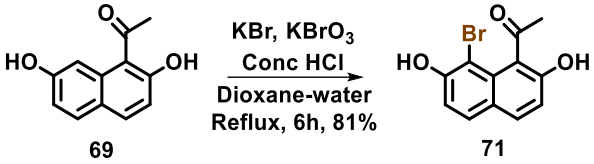

Scheme 11 Synthesis of 1-(8-bromo-2,7-dihydroxynaphthalen-1-yl)ethan-1-one (71)

The disappearance of the signal for the proton at 8th position in the ^{1}H NMR and its simplification clearly indicates the successful bromination at 1st position. An upfield shift in the signal for the –COC*H*$_3$ protons from **δ** 2.86 in **69** to **δ** 2.54 in **71** shows the shielding effect due to the non-bonding electrons of the neighbouring -Br atom. The broad singlet that appeared at **δ** 13.67 in 1-(2,7-dihydroxynaphthalen-1-yl)ethan-1-one **(69)** disappeared and a sharp singlet at **δ** 10.48 appeared. This was attributed to loss in the intramolecular hydrogen bonding and involvement of phenolic –O*H* in intermolecular hydrogen bonding. Hence the introduction of –Br atom at 8th position lead to electronic changes in the molecule leading to the loss in the rigidity along the ArC-C(O) bond.

In order to increase the rigidity of the molecule, we shifted our focus towards synthesis of naphthofurans. Naphthofuran derivatives have proved to be biologically active and have been well utilized for various pharmacological applications ranging from antimicrobial, analgesic, antibacterial, antitumor, anthelmintic to growth inhibitory activity which is well documented in the literature.[55,56] The most straight forward methodology for the formation of furan ring involves the intramolecular cyclization reaction of α-alkoxy phenols. Utilizing this strategy, we subjected **71** to diether formation by its reaction with bromo ethyl acetate using potassium carbonate as base in acetone. The diether **72** was then subjected to intramolecular cyclization by hydrolysis of the ester followed by anion generation at the active methylene group which attacks on the electrophilic ketone carbon to form a five-membered oxygen containing cyclic system. Its facile dehydration leads to the formation of furan ring with two free carboxylic groups. The subsequent esterification of -COOH leads to the formation of ethyl 9-bromo-8-(2-ethoxy-2-oxoethoxy)-1-methylnaphtho[2,1-b]furan-2-carboxylate **(73)** in moderate overall yield (Scheme 12).

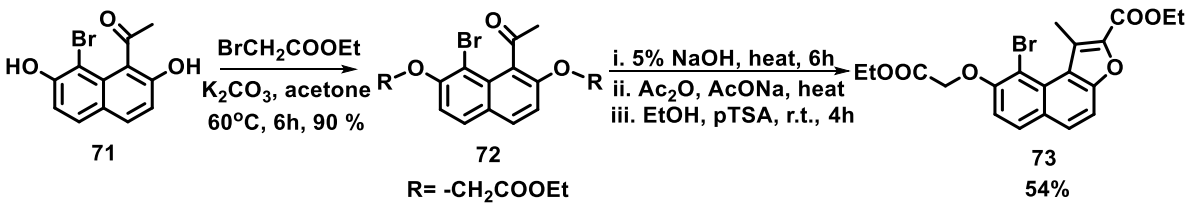

Scheme 12 Synthesis of naphthofuran derivative (73)

The ^{1}H NMR spectra for **73** was well in agreement with the structure, showing only one sharp singlet for two protons at **δ** 4.88 corresponding to the two protons of the ether linkage. A sharp singlet at **δ** 3.05 for three protons corresponds to the aromatic methyl group clearly

indicates the successful cyclization. This notable downfield shift of the –CH_3 signal suggests it is being deshielded due to the π-cloud of naphthalene core.

2.2.2.2 Single Crustal XRD analysis:

SCXRD is an important tool to determine the degree of deformation within the molecule as well as to study the variations in crystal packing that arise due to slight modifications in the molecular skeleton. Hence, crystals suitable for carrying out single crystal XRD were obtained from slow evaporation of 1-(8-bromo-2,7-dihydroxynaphthalen-1-yl)ethan-1-one **(71)** from ethyl acetate-petroleum ether mixture. It was found that **71** crystallizes out in P_{bca} space group showing only a slight deviation form planarity by 4.58° (Figure 8a). This means that the puckering of naphthalene skeleton only partly relieves the steric strain developed in the molecule. The major mode of steric relaxation is by out of the plane deflection of both the substituents from the naphthalene plane. The substituents at 1 and 8 position are bent out of the plane from the naphthalene skeleton which was measured in terms of interplanar angle formed between the plane containing C1-C9 or C8-Br bond and that of naphthalene ring which forming an angle of 9.56° and 4.69° respectively (Figure 8b & 8c).

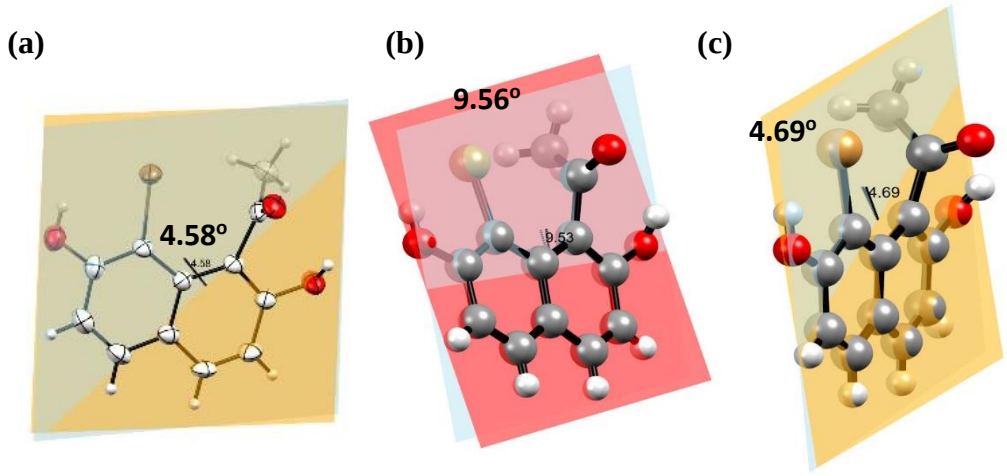

Figure 8 Showing (a) Interplanar angle between two aromatic rings of naphthalene (b) out-of-plane deviation of –OAc group (c) out-of-plane deviation of –Br group

Along with out of the plane deviation of the substituents at 1 and 8 position, the *peri* substituents are splayed apart by a distance of 3.03Å between the –Br and –C(O) of acetyl group. This causes a significant broadening of the angle formed between C1-C10-C9 to 126.58° whereas that formed between C4-C5-C6 is reduced to 119.82° from the mean value of 121.5° in unsubstituted naphthalene (Figure 9a). This is a characteristic feature for many 1,8-disubstitued naphthalenes. The introduction of -Br atom at 8-position not only leads to

molecular distortions, but the electronic factors also affect the bonding and packing of the molecules in a crystal lattice. An unusual Br-O(C) intramolecular bonding of 3.21Å (Figure 9b) which breaks the intramolecular hydrogen bonding between phenolic –O*H* and –*O*(C)Me which was seen in 2,7-dihydroxynaphthalen-1-ylethan-1-one **(69)**. However in **71**, the phenolic –O*H* undergoes intermolecular H-bonding (Figure 9c) which is also evident in ^{1}H NMR spectra which shows a broad singlet at **δ** 10.1.

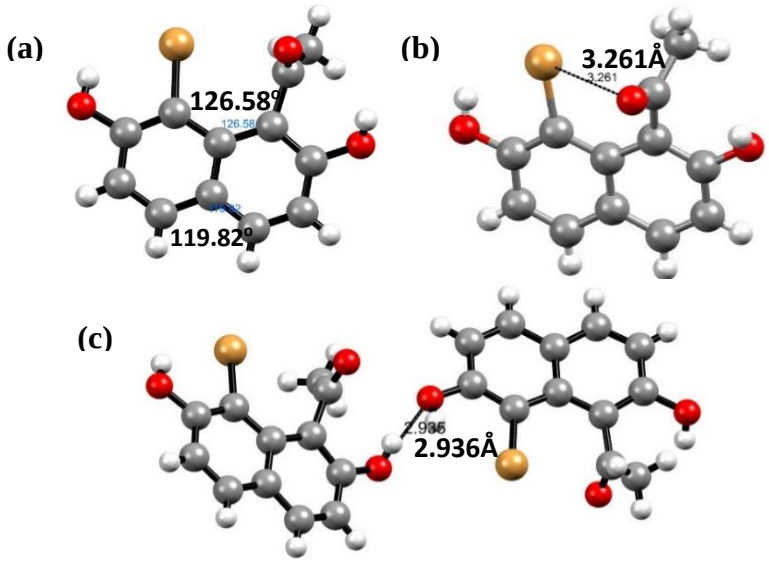

Figure 9 Showing (a) in-plane deviation of bond angles (b) intramolecular Br-O(C) short contact (c) intermolecular hydrogen bonding

A very interesting packing of these molecules in 3X3 box viewed along the c-axis was observed. The molecules arrange themselves in horizontally placed parallel columns of zig-zag chains (Figure 10).

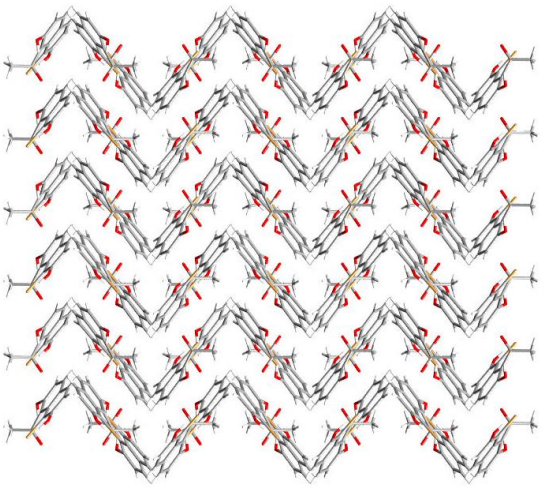

Figure 10 Packing in 3X3 box viewed along the c-axis showing a zigzag chain arrangement of molecules

Each chain comprises of molecules stacked in opposite directions while the molecules in the neighbouring chains are stacked parallel to each other where the distance between two chains is 8.7Å. These chains are held together by a number of H-bonds and short contacts. To study the difference in the crystal packing and non-covalent interactions due to the intramolecular cyclization of 1-(8-bromo-2,7-dihydroxynaphthalen-1-yl)ethan-1-one **(71)** into its naphthofuran derivative, we carried out SCXRD for ethyl 9-bromo-8-(2-ethoxy-2-oxoethoxy)-1-methylnaphtho[2,1-b]furan-2-carboxylate **(73)**. It crystallizes out in $C_{2/c}$ space group with an angle of 1.92° between the terminal aromatic rings (Figure 11a). Contrary to our expectation, the deformation of the naphthalene core further reduces due to the introduction of a furan ring. This may be attributed to the fact that furan ring contributes to a lesser extent towards the deformation of the naphthalene moiety due to its small in-

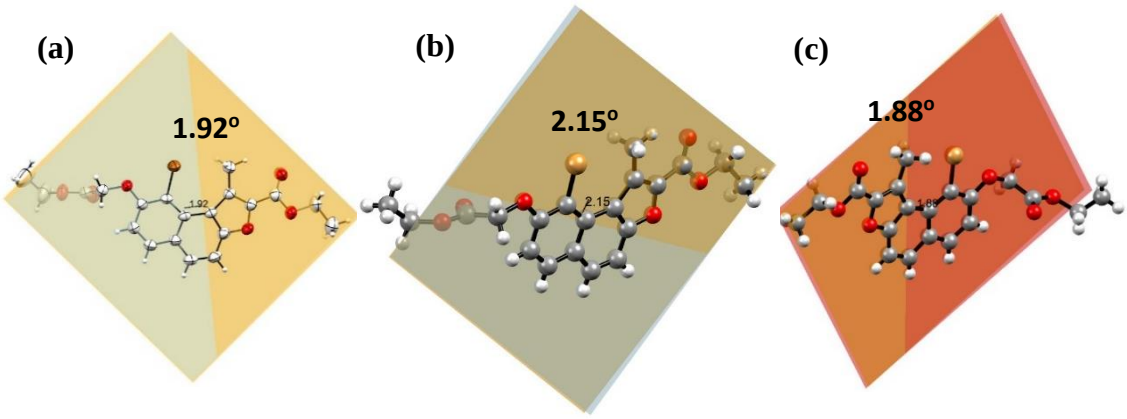

plane angle of 32°. The out of plane deflection of $–CH_3$ and -Br group seem to be the major factors contributing towards relieve in steric strain of the molecule (Figure 11b & 11c).

Figure 11 ORTEP diagram of 20 showing (a) interplanar angle between the two aromatic rings is 1.92°; out-of-plane deviation of (b) –Br atom (c) $–CH_3$ group

Crystal packing shows an increased hydrogen bonding in the system due to the presence of two ester linkages. Two molecules are held together by O-C(Ar) short contact of 3.15Å between the ester linkages of furan rings (Figure 12a). A short contact between ArO-H(Ar) of 2.554Å is also observed that holds two molecules together. These two molecules form stacks of molecules separated by a distance of 4.42Å in the form of columns which are almost perpendicular making an angle of 74.18° (Figure 12b). The more regular network of zigzag chains having a parallel arrangement which was observed for 1-(8-bromo-2,7-dihydroxynaphthalen-1-yl)ethan-1-one **(71)** has been disrupted completely and the molecules are now held in a crisscross fashion (Figure 12c) .

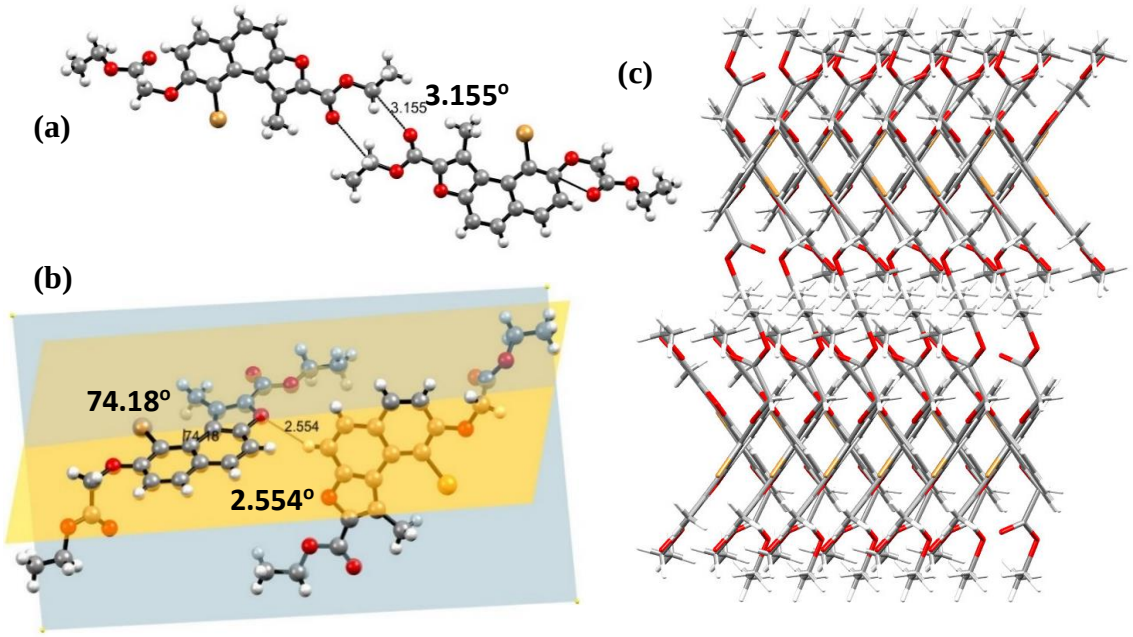

Figure 12 Showing (a) CO-C short contact (b) (Ar)O-H(Ar) short contact between two molecules forming an angle of 74.18° (c) Packing in 3X3 box viewed along the a-axis

Although the study and comparison of such crystal packing with variation in the ring structure is interesting, we however did not succeed in twisting the planar naphthalene skeleton to a notable extent so as to observe enantiomerism. This inspired us to focus on the synthesis of larger system *i.e.* phenanthrenes, where the furan ring is replaced by a benzene ring which has a larger in-plane angle and hence substitution at sterically hindered position may lead to the achievement of our objective.

2.2.2.3 Conclusion:

We attempted to synthesize non-planar 1,8-substituted naphthalenes. The introduction of acetyl group at 1st position and –Br group at 8th position of the naphthalene skeleton renders the molecule non-planar only by a small degree. Hence, the steric bulk at the *peri* positions is not sufficient enough to cause sufficient twist in the naphthalene moiety. We carried out the cyclization of the acetyl group into furan scaffold and observed that the introduction of this ring fused to the naphthalene core not only leads to an increase in the rigidity of the molecule, but also an increase in the planarity of the molecule. This can be attributed to the less in-plane angle of the furan ring as compared to that of the benzene ring. Hence for 1,8-substituted naphthalene, the major mode of steric strain relief is not the puckering of the aromatic rings, but the out of the plane deflection of the substituents present at the *peri* positions. This encouraged us to explore the next member of PAH series *i.e.* phenanthrenes.

2.2.2.4 Experimental Section:

Synthesis of 1-(2,7-dihydroxynaphthalen-1-yl)ethan-1-one (69):

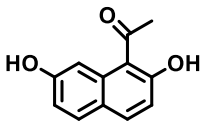

2,7-diacetyl naphthalene (0.5g; 2.02mmol) was taken in a clean and dry round bottom flask to which carefully weighed anhydrous $AlCl_3$ (0.54g; 4.08mmol) was added. The reaction mixture was heated in solvent free conditions to 150^oC for 24h. The completion of reaction is marked by the disappearance of starting material (TLC). The reaction mixture is allowed to cool down to room temperature and diluted with water (100mL). The water layer is extracted using ethyl acetate (3X50mL), collected and dried over anhy. Na_2SO_4. The vacuum distillation of organic layer gave residue which was purified using column chromatography. 1-Acetyl-2,7-dihydroxy naphthalene **(69)** is obtained as pale yellow solid (0.23g; Yield:55%)

^{1}H NMR (400MHz, $CDCl_3$): δ 13.67 (bs, 1H); 7.83-7.81 (d, *J*=8.8Hz, 1H); 7.70-7.68 (d, *J*=8.8Hz, 1H); 7.48-7.47 (d, *J*=2.0Hz, 1H); 6.99-6.97 (dd, *J*=8.8Hz, 2.0Hz, 1H); 2.86 (s, 3H)

^{13}C NMR (100MHz, $CDCl_3$): δ 204.5; 165.1; 155.9; 137.5; 133.9; 131.5; 123.7; 117.1; 114.6; 114.1; 108.6; 32.5

IR (KBr): ν 3432; 3232; 1735; 1618; 1580; 1473; 1372; 1331; 1237; 1142; 1018; 962; 844; 808; 691; 481 cm^{-1}

Synthesis of 1-(8-bromo-2,7-dihydroxynaphthalen-1-yl)ethan-1-one (71):

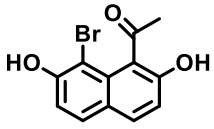

1-Acetyl-2,7-dihydroxy naphthalene **(69)** (0.1g; 0.5mmol); potassium bromide (0.025g; 0.02mmol) and potassium bromate (0.07g; 0.4mmol) were taken in a clean dry round bottom flask and dissolved in dioxane-water mixture (4:1; 5mL). To this solution, conc. HCl (0.06mL; 0.62mmol) was added carefully dropwise. The reaction mixture was then allowed to reflux for 6h after which no starting material could be seen on TLC. The reaction mixture was cooled and concentrated to remove dioxane. The residue was poured onto cold water and extracted using ethyl acetate (3X25mL). The combined organic layer was dried and concentrated to obtain brown residue which was subjected to column chromatography. 1-(8-Bromo-2,7-dihydroxynaphthalen-1-yl)ethan-1-one **(71)** was obtained as a yellow solid which turns brown gradually (0.11g; Yield: 81%)

^{1}H NMR (400MHz, $CDCl_3$): δ 10.48 (s, 1H); 7.75-7.73 (d, *J*=8.8Hz, 1H); 7.71-7.69 (d, *J*=8.8Hz, 1H); 7.20-7.18 (d, *J*=8.8Hz, 1H); 7.03-7.00 (d, *J*=8.8Hz, 1H); 6.23 (bs, 1H); 2.54 (s, 3H)

IR (KBr): ν 3486; 3262; 1666; 1617; 1569; 1513; 1444; 1356; 1318; 1204; 1162; 1060; 838; 823; 519; 440 cm^{-1}

Synthesis of diethyl 2,2'-((1-acetyl-8-bromonaphthalene-2,7-diyl)bis(oxy))diacetate (72):

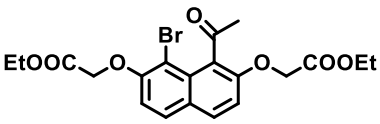

A clean and dry round bottom flask was charged with 1-(8-bromo-2,7-dihydroxynaphthalen-1-yl)ethan-1-one **(71)** (0.25g; 1.24mmol) and anhydrous potassium carbonate (0.83g; 6.2mmol) in 15mL of AR grade acetone. To this mixture, bromo ethyl acetate (0.4mL; 3.7mmol) was added carefully dropwise. The reaction mixture was then heated to 60°C for 6h when no starting material can be seen on TLC. The reaction mixture was concentrated to remove the solvent and then poured on cold water. The aqueous layer was extracted using ethyl acetate (3X30mL) and the combined organic layer was dried over anhy. Na_2SO_4, concentrated under vacuum to obtain residue. This reside was subjected to column chromatography to obtain diethyl 2,2'-((1-acetyl-8-bromonaphthalene-2,7-diyl)bis (oxy))diacetate **(72)** as pale yellow solid (0.36g; Yield 90%)

^{1}H NMR (400MHz, $CDCl_3$): δ 7.79-7.77 (d, *J*=8.8Hz, 1H); 7.77-7.75 (d, *J*=8.8Hz, 1H); 4.81 (s, 2H); 4.76-4.74 (d, *J*=5.6Hz, 2H); 4.31-4.24 (m, 4H); 2.87 (s, 3H); 1.32-1.28 (t, *J*=7.2Hz, 6H)

^{13}C NMR (100MHz, $CDCl_3$): δ 205.8; 168.5 (2C); 154.2; 153.9; 131.3; 131.1; 129.9; 127.2; 127.1; 113.3; 112.3; 106.1; 67.0; 66.4; 61.6; 61.5; 35.2; 14.2 (2C)

IR (KBr): ν 1804; 1764; 1750; 1696; 1615; 1506; 1438; 1382; 1354; 1301; 1203; 1093; 1020; 832; 772; 720; 591; 436 cm^{-1}

Synthesis of ethyl 9-bromo-8-(2-ethoxy-2-oxoethoxy)-1-methylnaphtho[2,1-b]furan-2-carboxylate (73):

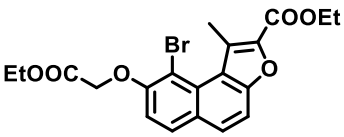

In a round bottom flask, Diethyl 2,2'-((1-acetyl-8-bromonaphthalene-2,7-diyl)bis (oxy))diacetate **(72)** (0.4g; 0.9mmol) was subjected to hydrolysis by adding 5% NaOH solution (5mL) and refluxing for 6h. The completion of reaction is marked by disappearance

of starting material on TLC. The reaction mixture is poured in water and acidified using dil. HCl. The precipitates formed after acidification are filtered, washed and dried to obtain white solid (0.33g; 0.83mmol) which is taken into a round bottom flask. To this flask, acetic anhydride (1.6mL; 16.6mmol) and freshly fused sodium acetate (0.5g; 6.2mmol) were added. The reaction mixture was heated to reflux for 12h. The reaction mixture was poured in water and extracted using ethyl acetate (3X50mL), separated organic layer was dried over anhy. Na_2SO_4 and concentrated. The residue obtained was dissolved in ethanol with a catalytic amount of *p*-TSA and allowed to stir at room temperature for 4h. The reaction mixture is then concentrated and subjected to column chromatography to obtain ethyl 9-bromo-8-(2-ethoxy-2-oxoethoxy)-1-methyl naphtho[2,1-b]furan-2-carboxylate **(73)** as pale yellow solid (0.19g; Yield 54%)

^{1}H NMR (400MHz, $CDCl_3$): δ 7.89-7.87 (d, *J*=8.8Hz, 1H); 7.76-7.73 (d, *J*=9.2Hz, 1H); 7.61-7.59 (d, *J*=8.8Hz, 1H); 7.19-7.17 (d, *J*=8.8Hz, 1H); 4.88 (s, 2H); 4.53-4.47 (q, *J*=7.2Hz, 2H); 4.35-4.30 (q, *J*=7.2Hz, 2H); 3.05 (s, 3H); 1.50-1.47 (t, *J*=7.2Hz, 3H); 1.36-1.32 (t, *J*=7.2Hz, 3H)

^{13}C NMR (100MHz, $CDCl_3$): δ 168.5; 160.4; 155.6; 154.7; 141.2; 131.4; 130.3; 129.6; 128.7; 128.5; 122.7; 112.8; 112.4; 106.2; 67.2; 61.7; 61.1; 18.5; 14.5; 14.2

IR (KBr): ν 2960; 2927; 1741; 1712; 1611; 1560; 1517; 1449; 1368; 1306; 1209; 1184; 1114; 1083; 1048; 822; 766; 618 cm^{-1}

2.2.2.5 Spectral Data:

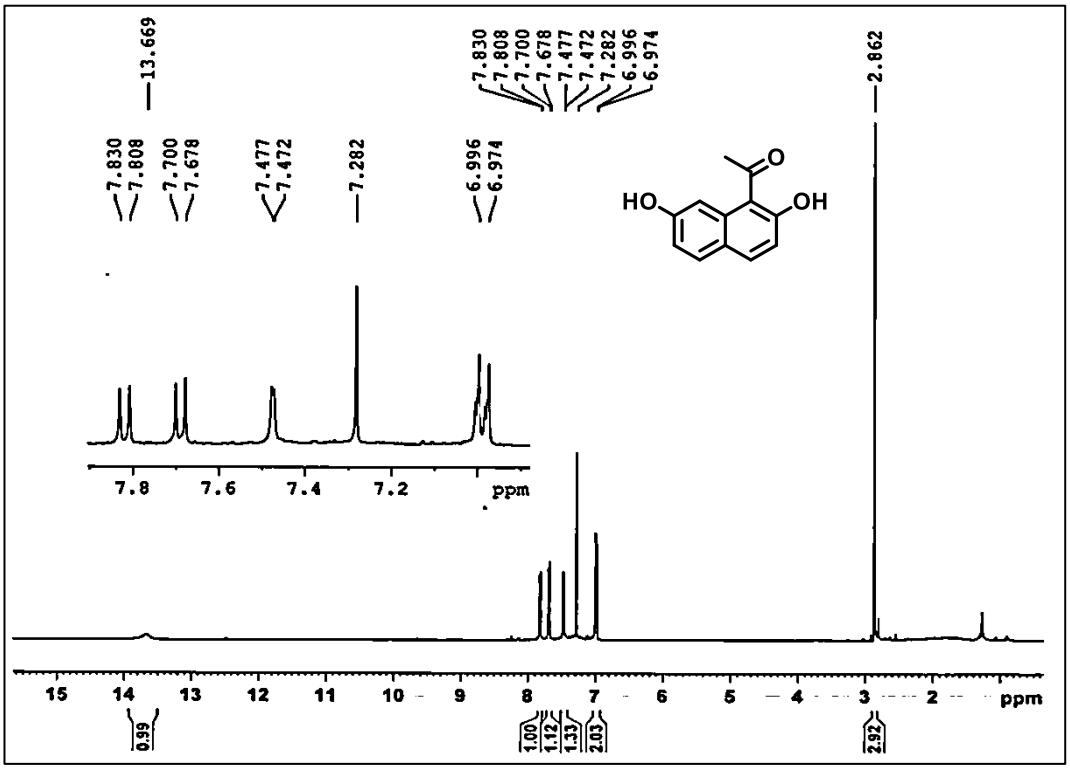

^{1}H NMR Spectra of compound **69** ($CDCl_3$, 400MHz)

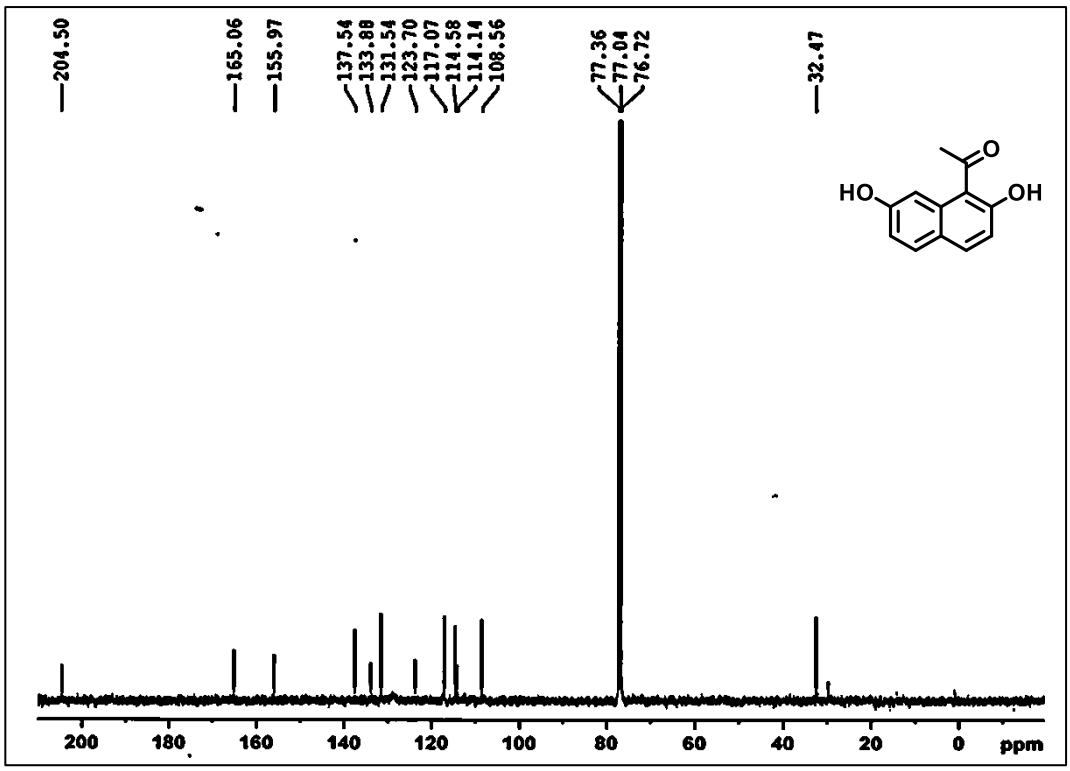

^{13}C NMR Spectra of compound **69** ($CDCl_3$, 100MHz)

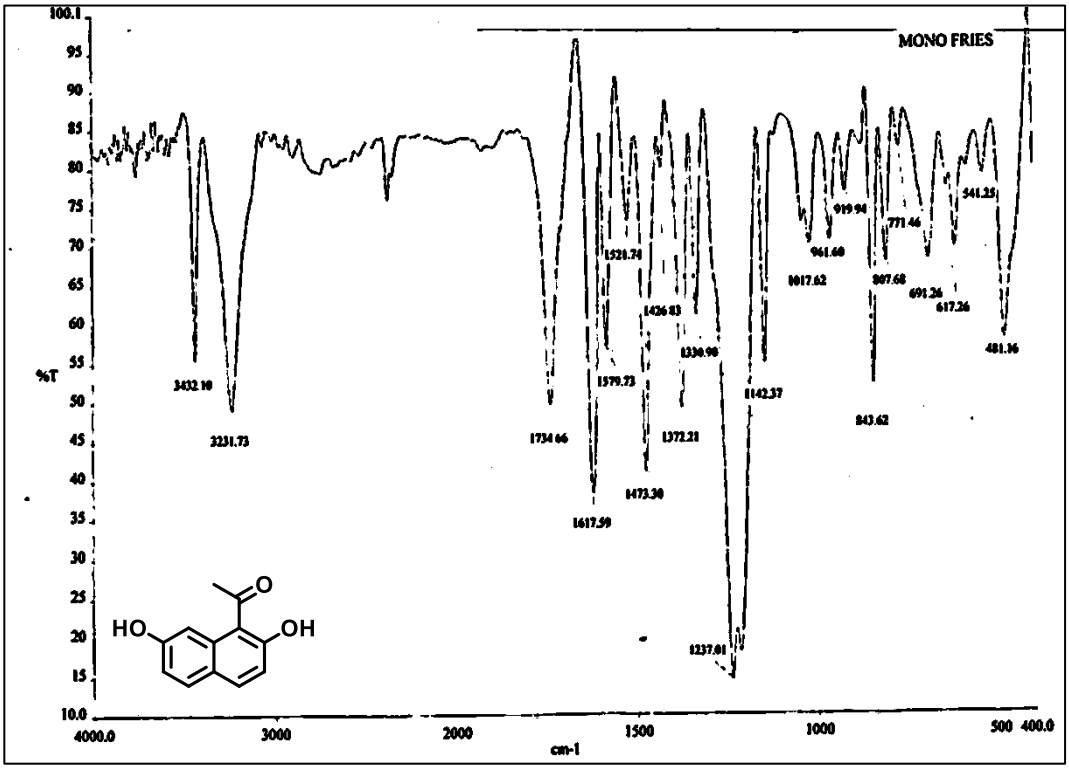

IR Spectra of compound **69**

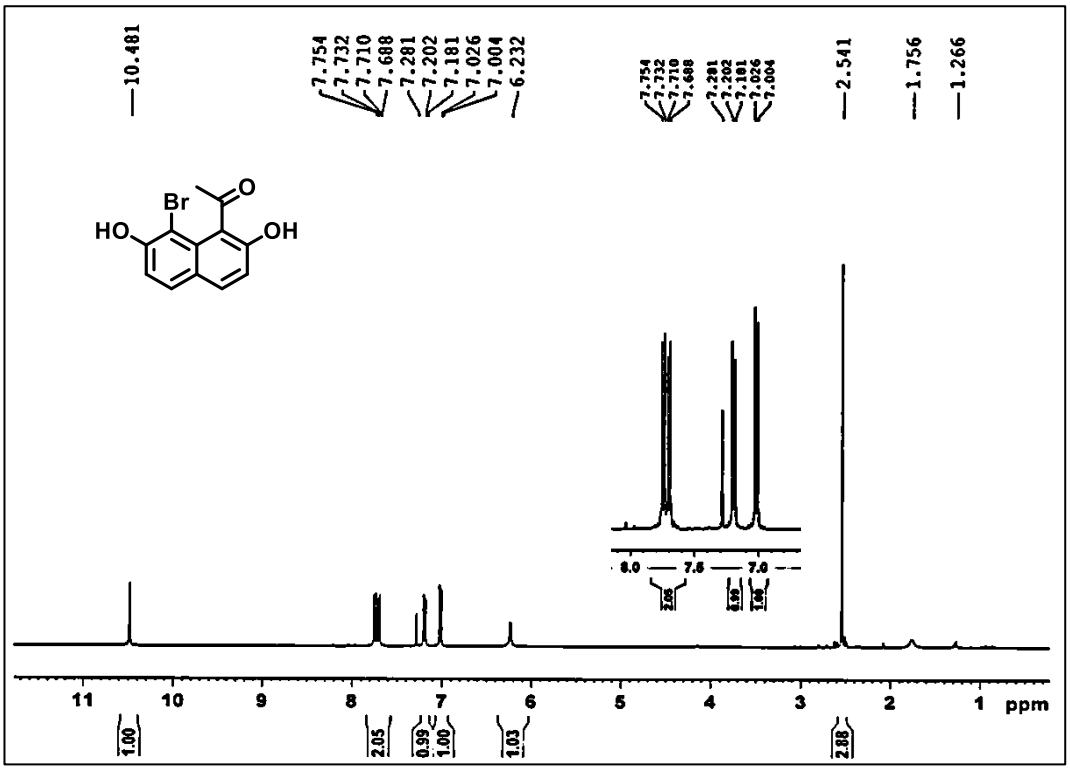

^{1}H NMR Spectra of compound **71** ($CDCl_3$, 400MHz)

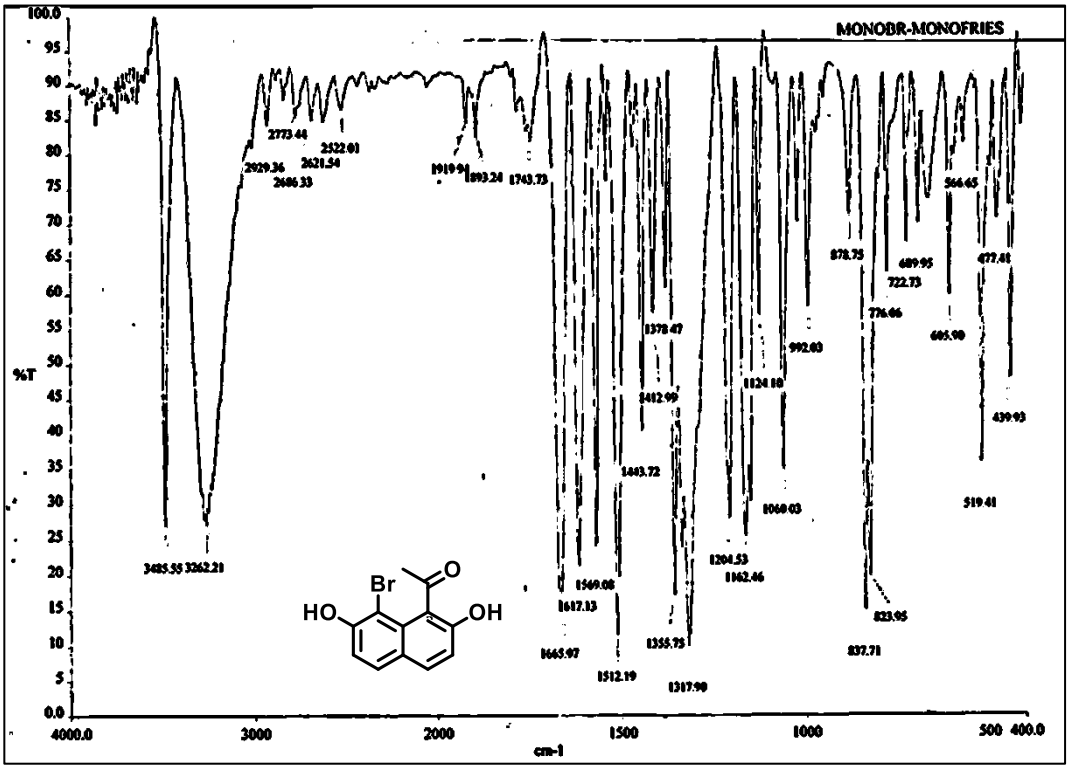

IR Spectra of compound **71**

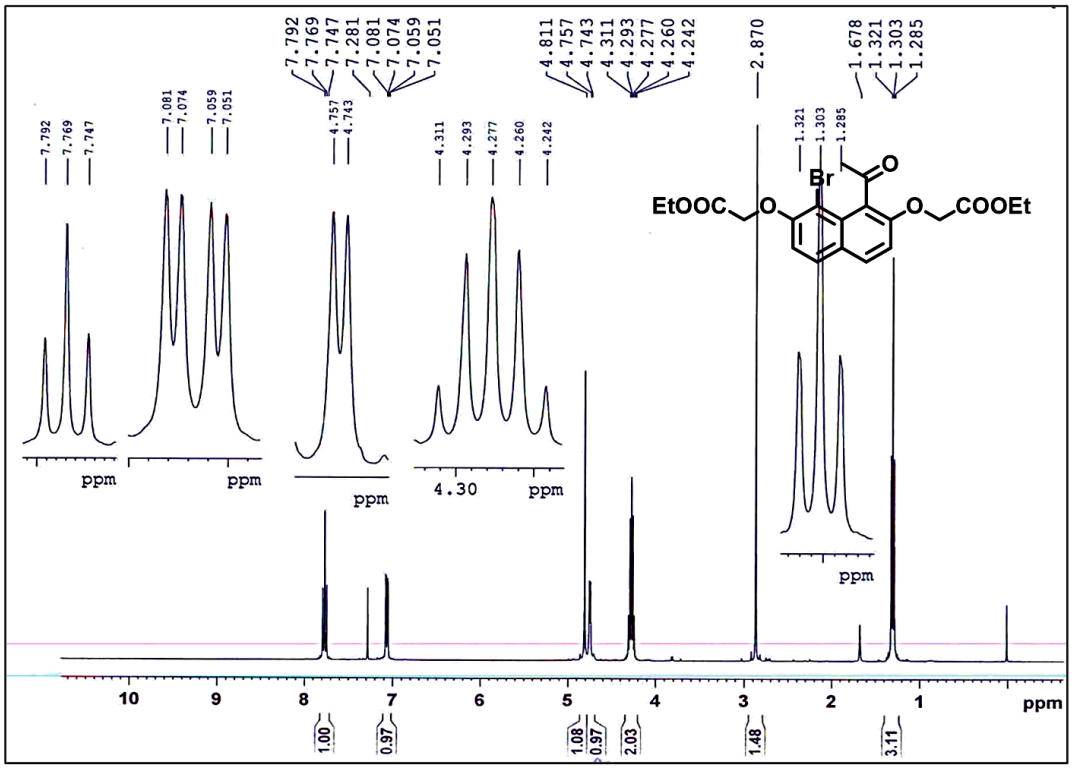

^{1}H NMR Spectra of compound **72** ($CDCl_3$, 400MHz)

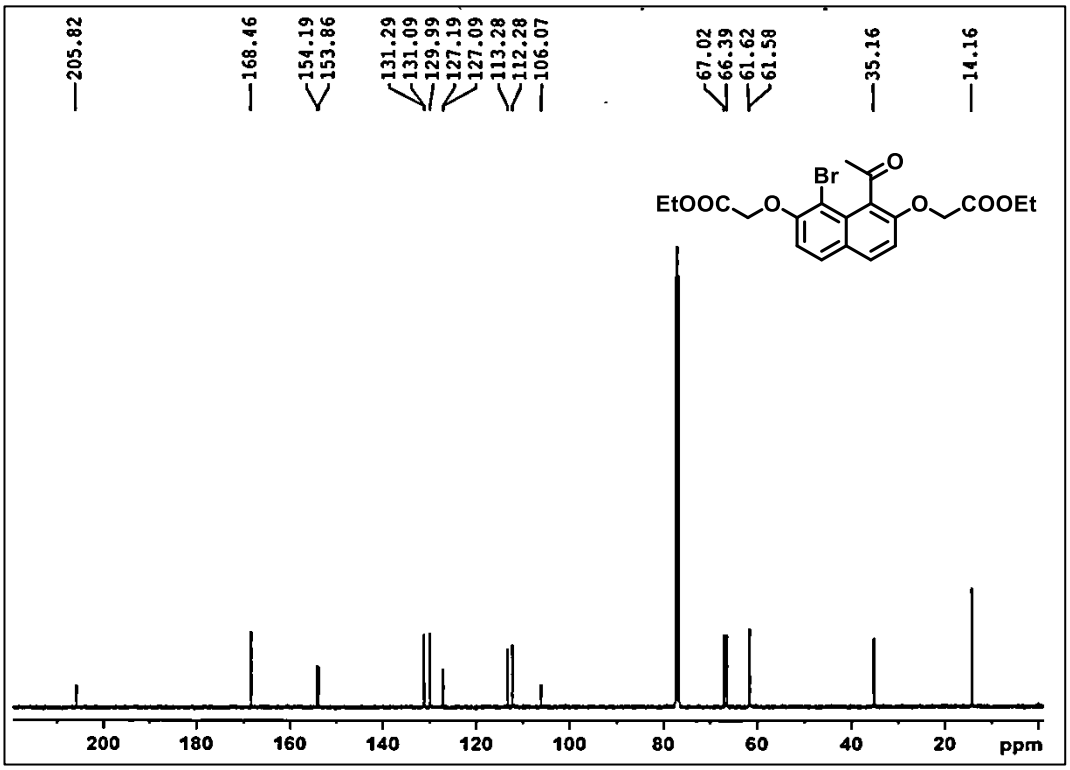

^{13}C NMR Spectra of compound **72** ($CDCl_3$, 100MHz)

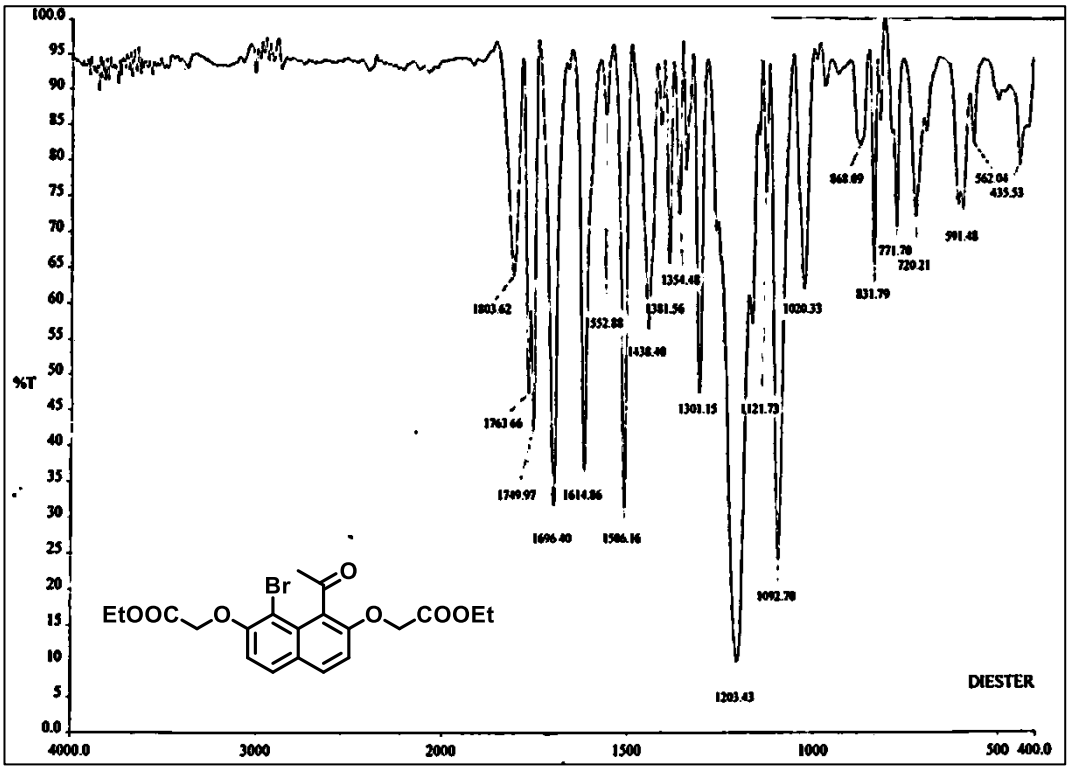

IR Spectra of compound **72**

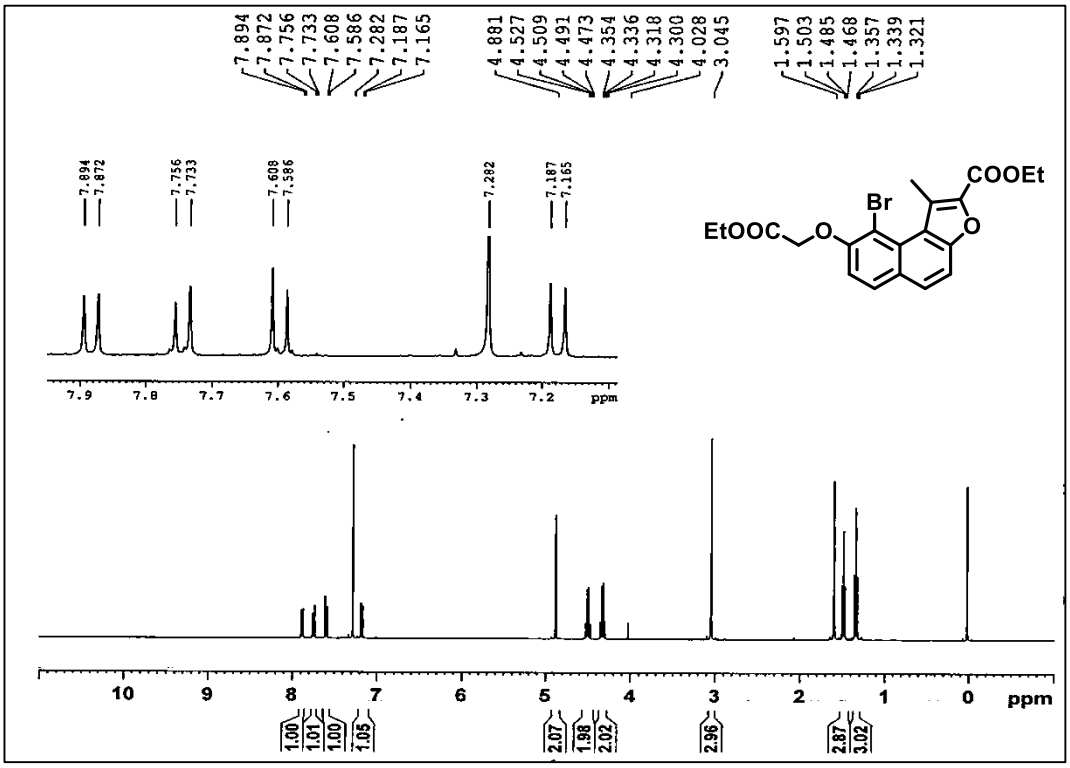

^{1}H NMR Spectra of compound **73** ($CDCl_3$, 400MHz)

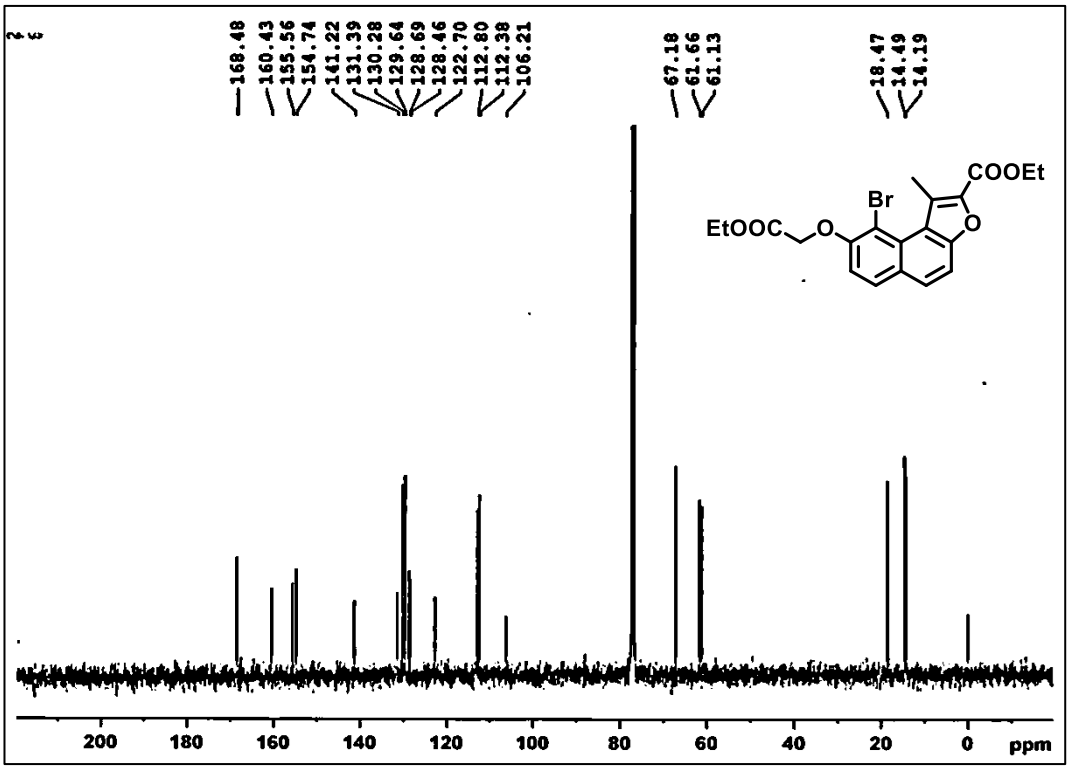

^{13}C NMR Spectra of compound **73** ($CDCl_3$, 100MHz)

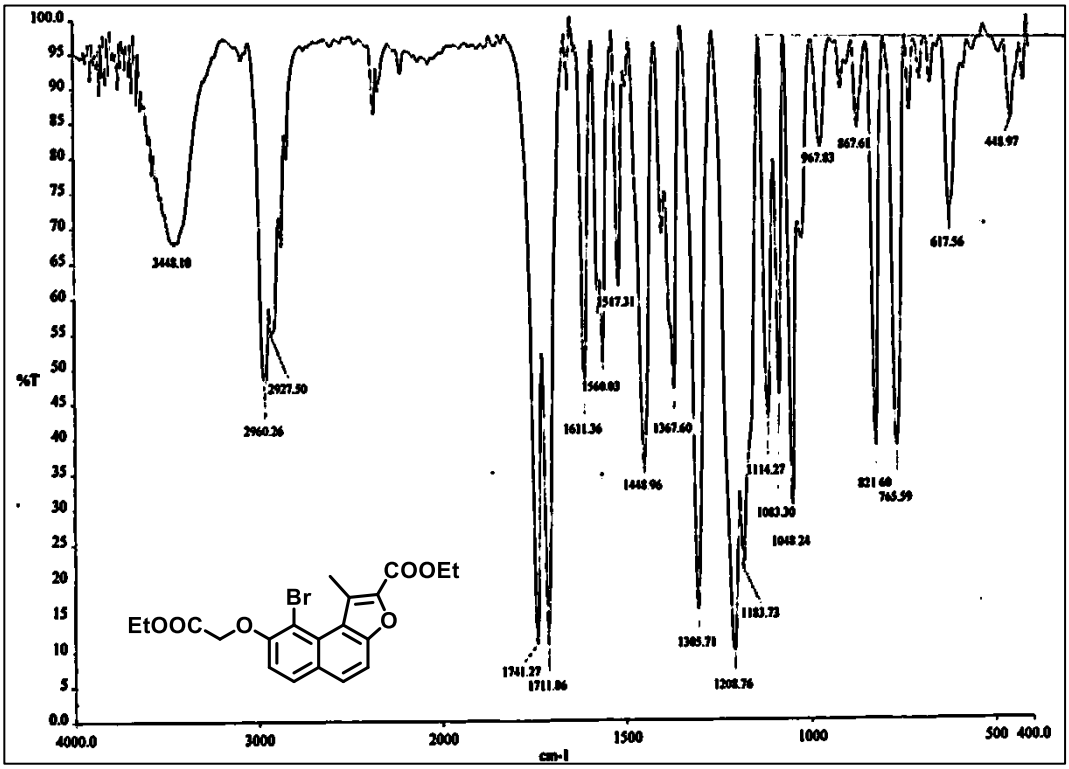

IR Spectra of compound **73**

2.2.2.6 Crystallographic Data:

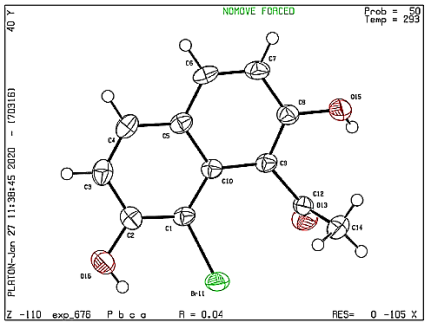

ORTEP diagram of compound 71
(50% probability factor for thermal ellipsoids)

Table 1 Crystal data and structure refinement for compound **71**

Empirical formula	$C_{12}H_9BrO_3$
Formula weight	281.10
Temperature/K	293(2)
Crystal system	orthorhombic
Space group	Pbca
a/Å	10.5125(4)
b/Å	11.5009(4)
c/Å	17.3089(6)
α/°	90.00
β/°	90.00
γ/°	90.00
Volume/$Å^3$	2092.69(12)
Z	8
ρcalcg/cm^3	1.784
μ/mm-1	5.274
F(000)	1120.0
Radiation	Cu Kα λ = 1.5418
2θ range for data collection/°	12.5 to 146.48
Index ranges	$-12 \leq h \leq 13$, $-14 \leq k \leq 6$, $-21 \leq l \leq 21$
Reflections collected	6757
Independent reflections	2085 [R_{int} = 0.0272, R_{sigma} = 0.0246]
Data/restraints/parameters	2085/0/148
Goodness-of-fit on F2	1.069
Final R indexes [I>=2σ (I)]	R_1 = 0.0365, wR_2 = 0.1031
Final R indexes [all data]	R_1 = 0.0393, wR_2 = 0.1059
Largest diff. peak/hole / e $Å^{-3}$	0.66/-0.57

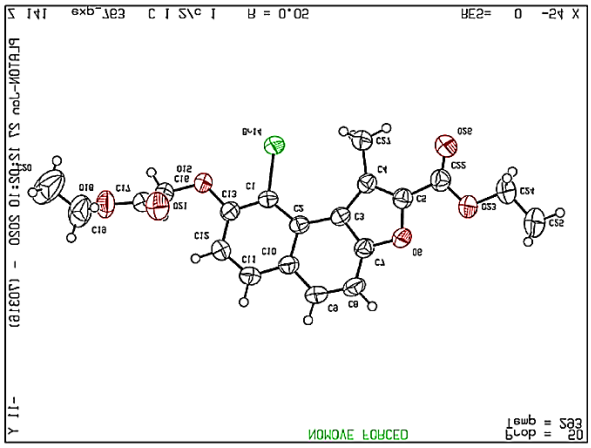

ORTEP diagram of compound 73 (CCDC No. 1851239)

(50% probability factor for thermal ellipsoids)

Table 2 Crystal data and structure refinement for compound 73.

Empirical formula	$C_{20}H_{19}BrO_6$
Formula weight	435.27
Temperature/K	293(2)
Crystal system	monoclinic
Space group	C2/c
a/Å	37.8285(10)
b/Å	4.41912(12)
c/Å	22.6934(6)
α/°	90
β/°	99.211(3)
γ/°	90
Volume/Å3	3744.71(17)
Z	8
ρcalcg/cm3	1.5440
μ/mm-1	3.297
F(000)	1773.5
Radiation	Cu Kα λ = 1.5418
2Θ range for data collection/°	7.9 to 146.5
Index ranges	$-46 \leq h \leq 46$, $-4 \leq k \leq 5$, $-28 \leq l \leq 28$
Reflections collected	22153
Independent reflections	3768 [R_{int} = 0.0374, R_{sigma} = 0.0256]
Data/restraints/parameters	3768/0/247
Goodness-of-fit on F2	1.042
Final R indexes [I>=2σ (I)]	R_1 = 0.0469, wR_2 = 0.1198
Final R indexes [all data]	R_1 = 0.0544, wR_2 = 0.1244
Largest diff. peak/hole / e $Å^{-3}$	0.92/-1.24

2.3 Section B: 4,5-Disubstituted Phenanthrenes:

2.3.1 Introduction:

Phenanthrene is the smallest angularly fused aromatic hydrocarbon which has been profoundly utilized in organic electronics[57,58] as well as medicinal chemistry.[59–61] Many methods for the synthesis of functionalized phenanthenes has been reported, but limited reports on the synthesis of sterically hindered phenanthrenes are known.[62] Such sterically hindered phenanthrenes are known to show optical isomerism if the substituents present at 4- and 5-positions are bulky or large enough to prevent rapid interconversion of the enantiomers through a planar transition state. These interactions appear to be more severe than the *peri* interactions in naphthalene which has been confirmed by thermochemical studies.[63,64] Therefore, for a given pair of substituents X, the internuclear distances for *peri* placed pairs would be greater than for *bay* placed pairs (Figure 13).

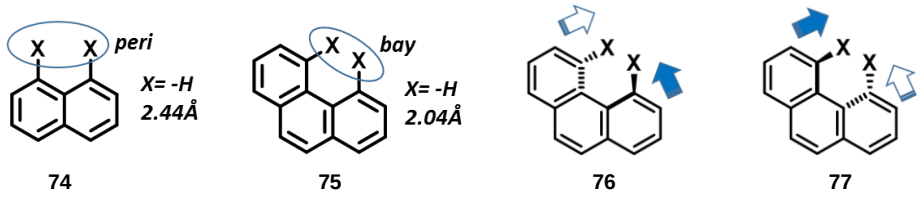

Figure 13 Showing the distance between *peri* and *bay* substitutents

Newmann *et al.* for the first time synthesized and partly resolved 4,5,8-trimethyl-l-phenanthryl acetic acid **(84)** (Scheme 13).

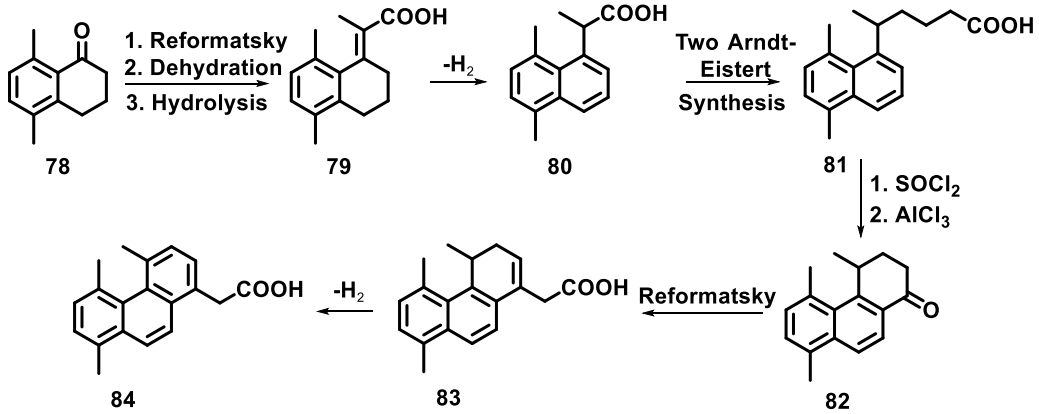

Scheme 13 Synthesis of 4,5,8-trimethyl-l-phenanthryl acetic acid (84)

The resolution of 4,5,8-trimethyl-l-phenanthryl acetic acid **(84)** was accomplished by recrystallization of the brucine salt. However, both the salt and the acid racemized rapidly in solution at room temperature concluding that the barrier to racemization was low.[65]

To determine the energy barrier for various 4,5-disubstituted phenanthrenes, Munday and Sutherland synthesized a series of 4,5-disubstituted phenanthrenes **(85-91)** bearing substituents containing prochiral protons. The interconversion of isomers was studied using NMR spectroscopy. Almost all the derivatives showed a complex splitting pattern in low temperature NMR for the diastereotopic protons (Table 1) proving the existence of these compounds in enantiomeric forms having the energy barrier of 9-25 kcal/mol.[66]

Table 3 Showing NMR data for temperature dependent signals for compounds 85-91

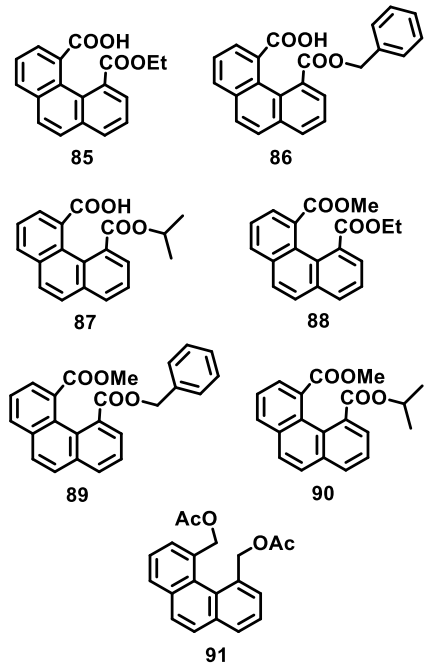

Compd.	Solvent	Temperature	System
85	Pyridine	-27	ABX_3
		+36	A_2X_3
86	Pyridine	-29	AB
		+55	A_2
87	Pyridine	-17	AX_3Y_3
		+54	AX_6
88	$CDCl_3$	-50	ABX_3
		+35	A_2X_3
89	$CDCl_3$	+35	A_2
90	$CDCl_3$	-43	AX_3Y_3
		+20	AX_6
91	$C_6D_5NO_2$	+35	AB
		+120	A_2

A similar comparison between the size of substituents at 4,5-position of phenanthrenes and barrier to racemization was reported by Mannschreck *et al.* They studied the diastereotopic methylene protons in these derivatives using Variable Temperature NMR spectroscopy

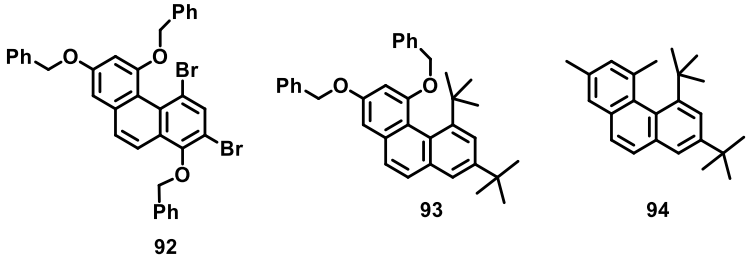

Figure 14 4,5-Disubstituted phenanthrenes having diastereotopic groups (92-94)

The signal for methylene protons of the benzyloxy group at the hindered position splits into an AB system. They concluded that the barriers depend upon the size of the groups R = CMe_3, Br, Me, Cl, OBz (Figure 14).[67]

The effect of additional substituents on the extent of distortion in such systems was determined for the first time by Armstrong *et al* who reported the SCXRD of 4,5-dimethyl phenanthrene **(95)** and its 3,6-substituted derivative **(96)**. The angle between the mean planes of the terminal rings in **95** was 27.9°[68] which increased to 29.2° in **96** which was attributed to the buttressing effect of the substituents at 3- and 6-positions. For the first time, the conformational enantiomers were separated by HPLC (Figure 15) using (+)-polytriphenylmethyl methacrylate coated silica as stationary phase at cryogenic temperatures (-70 to -80°C).[69]

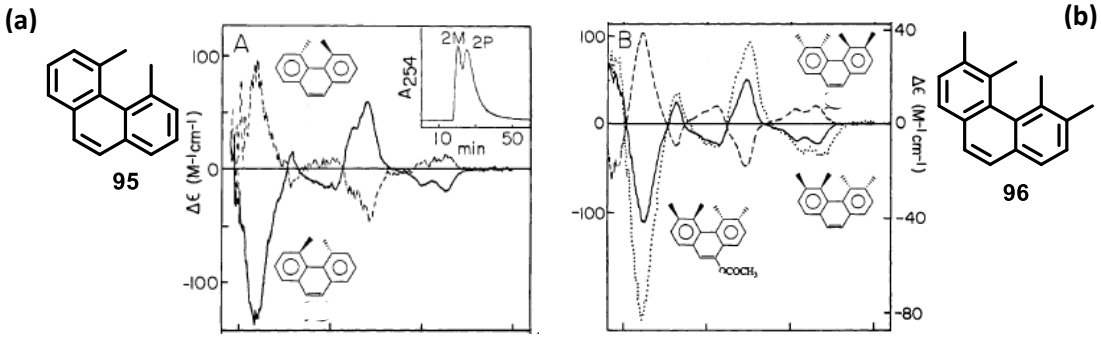

Figure 15 (a) CD spectra of 4,5-dimethyl phenanthrene (95) at -60°C and HPLC (insert) at -75°C (b) CD spectra of 3,4,5,6-tetramethyl phenanthrene (96) at 25°C

Having established that presence of additional functional groups at 3- and 6-position of 4,5-dimethyl phenanthrene motif leads to stabilization of the enantiomers, Sinnwell *et al.* synthesized 1- and 8-substituted derivatives of 4,5-dimethyl phenanthrene **(97)**. On comparing its values of ΔG with that of 4,5-dimethyl phenanthrene, they concluded that a decrease of ~10 kJ mol^{-1} was observed when the 1- and 8-substituents are removed.[70]

Gerkins compared SCXRD of methyl substituted at 2- and 7-position **(98)** as well as 3- and 6-position **(96)** of 4,5-dimethyl phenanthrene **(95)**. He found that the bay torsion angle C4-C12-C13-C5 is 32.4° in **(98)**, for **(96)** it is 31.5° and for **(95)** it is 32.9°. Hence, even though there was difference in the interplanar angle and ΔG values for these derivatives, the torsion along the *bay* region is similar in all the three cases suggesting that the placement of additional methyl groups in a 4,5-dimethylphenanthrene is of little importance in determining torsion angle.[71]

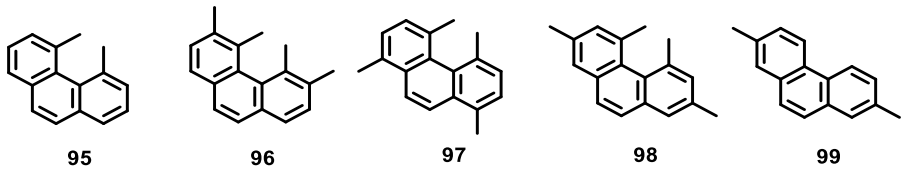

Figure 16 Various 4,5-dimethyl substituted phenanthrenes (95-99)

Later, they also reported that there was no evidence indicating disturbance of π-electron distribution along the C1/C2 and C2/C3 bonds, despite large deviations from planarity in the carbon skeleton of such molecules.[72]

The steric bulk in the *bay* region was further increased by replacing one of the methyl groups in tetramethyl phenanthrene with *tert*-butyl group utilizing the photochemical dehydrocyclization methodology by Vogtle *et al* (Scheme 14). The helical deformation of the aromatic carbon skeleton in the reported X-ray structure is found to be 36.6°.[73]

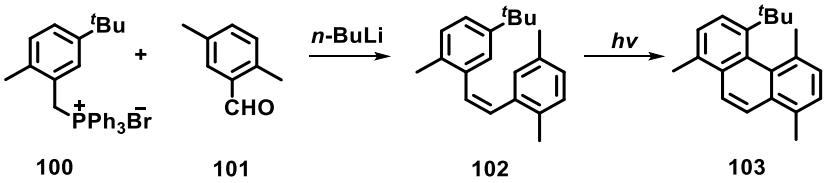

Scheme 14 Synthesis of 4,5-disubstituted phenanthrene using photocyclization

Sternhell *et al.* synthesized and studied the SCXRD of 4,5-difluoro **(104)**, chloro **(105)** and bromo **(106)** derivatives of phenanthrene (Figure 17).

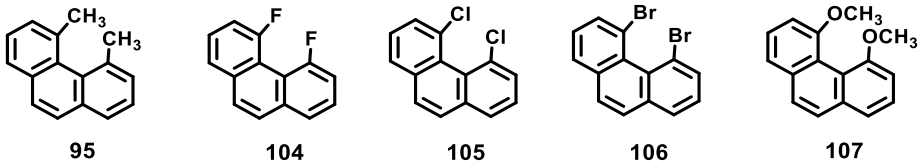

Figure 17 Comparison between 4,5-dihalo substituted phenanthrene (104-106) with 4,5-dimethyl (95) and 4,5-dimethoxy phenanthrene (107)

The interatomic distances between the two *bay* placed substituents of these derivatives was compared with 4,5-dimethyl phenanthrene **(95)** and unsubstituted phenanthrene. They concluded that the interatomic distances increase in the order: H (2.04Å) < CH_3 (2.33Å) < F (2.38Å) < Cl (3.10Å) < Br (3.29Å).[74,75] They also synthesized and studied 4,5-dimethoxy phenanthrene **(107)** and found that it is highly deformed, even more so than the analogous methyl **(95)** and chloro **(105)** compounds and nearly twice as much as the difluoro **(104)** compound.[76]

On the other hand 1,10-diiodo phenanthrene **(108)**, prepared for the first time by reacting I_2 with dilithiophenanthrene, has a twist angle 63° between the two iodine atoms.[77]

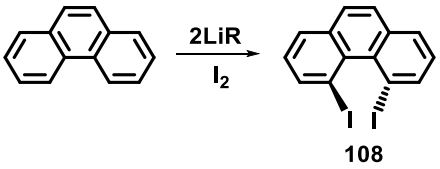

Scheme 15 Synthesis of 1,10-diiodo phenanthrene (108)

Thamattor *et al.* successfully carried out SCXRD for 4,5-dihalo phenanthrenes and compared the interplanar angles and torsional angles (Table 4).[75]

Table 4 A comparison of selected structural parameters in a series of known 4,5-dihalo phenanthrene derivatives

Compound	Angle between rings A and C	X···X distance	C4-C4'-C5'-C5 torsion angle	X-C4-C5-X torsion angle
104	16.779	2.381	19.954	43.273
105	32.282	3.097	37.738	69.980
106	28.510	3.277	32.800	74.700
108	29.451	3.610	33.716	78.611

The distortion of the phenanthrene framework was measured by either the angle between the mean planes of the terminal rings A and C, or the C4-C4'-C5'-C5 torsion angle which is largest for the dichloro derivative **(105)**, larger than that for dibromo **(106)** and diiodo **(108)**. Hence it was concluded that a combination of both size and electronegativity may account for 4,5-dichlorophenanthrene **(105)** showing the largest twist in the series of 4,5-dihalo phenanthrene compounds.[78]

To study the effect of steric interference on bond rotations of amide and ester groups, Kiefl *et al.* synthesized 4,5-substituted amide and ester derivatives of phenanthrene. The barrier to rotation along the Ar-C amide bond, Ar-C ester bond and C-N amide bond along with the barrier of helix inversion for these derivatives was determined (Figure 18).

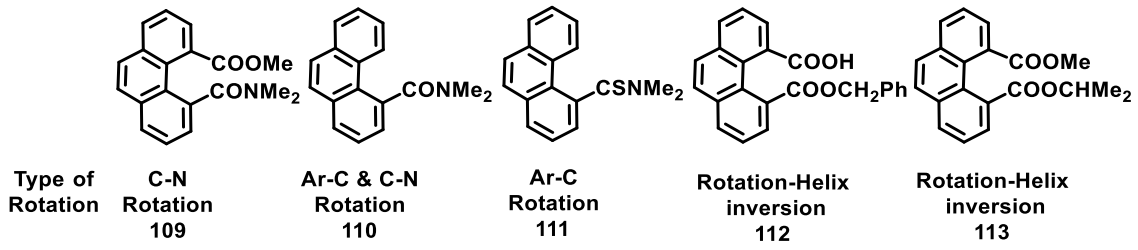

Figure 18 Showing the different type of rotations responsible for formation of enantiomers

Despite the large steric hindrance of the tightly interlocked substituents of these derivatives, chirality became visible only at temperatures below -60°C which was analysed by ^{1}H NMR spectroscopy.[79]

The first report for the synthesis of optically pure phenanthrenes was made by Yamaguchi *et al.* who had earlier synthesized optically pure 1,8-diadamantyl naphthalene ***(P)*-56**. Utilizing this chiral motifs, they synthesized 1,10-bis(1-adamantyl)phenanthrene **(121)** as pure enantiomers ***(P*** and ***M)*** enantiomers (Scheme 16).

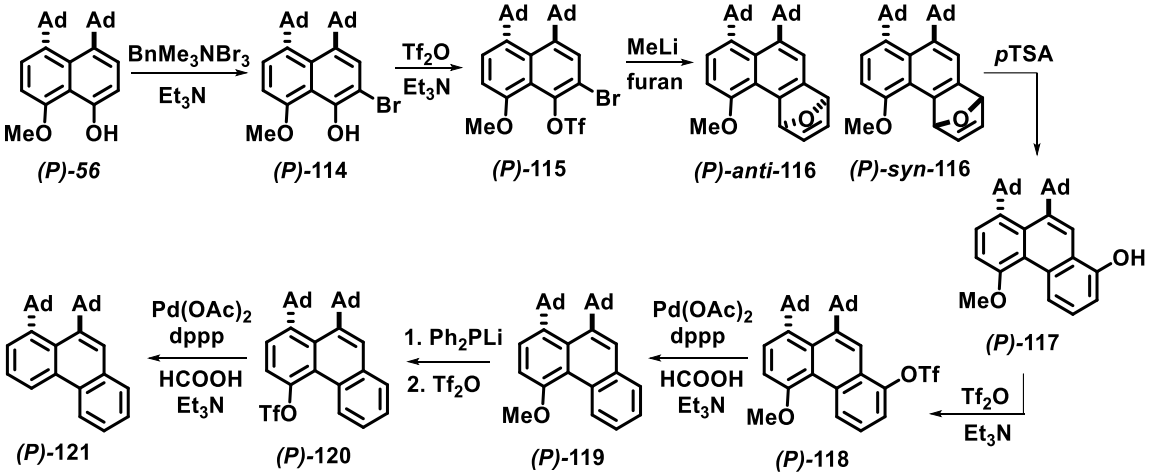

Scheme 16 Synthesis of optically pure 1,10-bis(1-adamantyl)phenanthrene (*P*)-121

SCXRD of **121** showed a dihedral angle of 76.0° along C11−C1−C10−C21. These optically pure derivatives can be exploited in the development of various chiral versions of aromatic compounds exhibiting notable functions.[43]

Based on the similarity between the basic structure of phenanthrene and 1,10-phenanthroline **(122)**, Rozen *et al.* synthesized its oxidized derivative 1,10-phenanthroline-*N*,*N*′-dioxide **(124)** using HOF-CH_3CN complex.

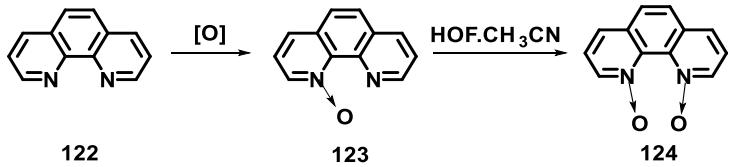

Scheme 17 Synthesis of 1,10-Phenanthroline-N,N'-dioxide (124)

This compound crystallized in $P2_1/c$ space group with two independent molecules in an asymmetric unit showing considerable distortion in the phenanthroline skeleton. The sum of the dihedral angles along the inner helical rim was found to be 60.1°.[80]

2.3.2 Results and Discussion:

2.3.2.1 Synthesis of 4 and 5-Disubstituted Phenanthrenes:

Phenanthrenes form an important class of compound owing to their occurrence in various natural products and alkaloids. Compounds having this structural motif also exhibit interesting biological properties.[81] Moreover, they are also very useful in material science because of their photoconductivity, photochemical and electroluminescent properties. Phenanthrenes also act as intermediates for the construction of higher members of PAHs of which helicenes are the most important class of compounds due to their numerous applications in opto-electronic devices and material sciences. Therefore, over the years, numerous synthetic routes have been developed in order to improve the efficiency of synthesis of phenanthrene skeleton. Among them, the preparation of stilbene followed by aryl–aryl coupling reactions are the most extensively studied approaches to afford the phenanthrene skeleton.

The oxidative photodehydrogenation of stilbene is an efficient method for the synthesis of phenanthrenes. Oxidative photocyclization methods have taken over non-photochemical methods due to its simplicity, ease of handling, tolerance to many functional groups and formation of a single regioisomer. The superiority of this method is predominantly seen during the synthesis of higher members of PAHs larger than phenanthrenes.[82] This method involves a two-step sequence beginning with the synthesis of stilbene derivatives using various reactions like Wittig, Grignard, Perkin, Heck, Knoevenagel *etc.* followed by intramolecular cyclization *via* radical mechanism to form the central ring of the phenanthrene core.

Our aim was to synthesize phenanthrene substituted with halogen group at 4th position and test if it caused the phenanthrene core to lose its planarity and show enantiomerism. The introduction of –Br atom was the substituent of choice due to its large size which would provide the steric bulk needed as well as presence of non-bonded electrons to study the electronic effects. The –Br group also proves to be important precursor for various chemical transformations and functional group interconversion. Summarizing all these benefits, we utilized the stilbene derivative obtained from carrying out Knoevenagel condensation between *p*-anisaldehyde **(125)** and benzyl cyanide **(126)**. The stilbene derivative **(127)** was ready converted into its corresponding phenanthrene derivative **(128)** by irradiating its solution in toluene using 250W HPMVL in presence of stoichiometric amounts of iodine as

oxidant and tetrahydrofuran as HI scavenger. 3-methoxyphenanthrene-9-carbonitrile **(128)** thus obtained, was subjected to deprotection using neutral conditions to obtain 3-hydroxyphenanthrene-9-carbonitrile **(129)** in good yield (more detailed discussion is included in Chapter-3).

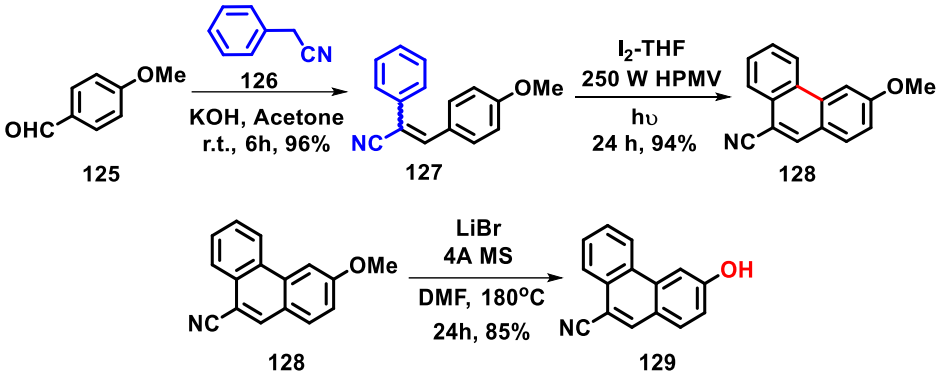

Scheme 18 Synthesis of 3-hydroxyphenanthrene-9-carbonitrile (129)

The 3-hydroxyphenanthrene-9-carbonitrile **(129)** was subjected to bromination using *N*-bromosuccinimide as the brominating agent in DCM to afford selective bromination to giving 4-bromo-3-hydroxyphenanthrene-9-carbonitrile **(130)** as the only product in good yield (Scheme 19).

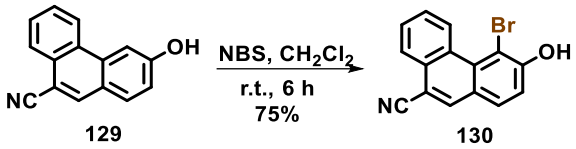

Scheme 19 Synthesis of 4-bromo-3-hydroxyphenanthrene-9-carbonitrile (130)

^{1}H NMR spectra clearly showed that bromination had occurred at the 4th position owing to the disappearance of its signal at **δ** 7.26. Hence we constructed a phenanthrene motif with –Br at 4th position and –H at 5th position. We wanted to compare and study the degree of deformity in this aromatic system with 4-bromo-5-substituted phenanthrenes. Various early investigations towards attempted synthesis of chiral phenanthrenes involved the presence of methyl substitution in the bay region due to various advantages like its effective large size, tolerance towards various chemical transformations and clear detection using ^{1}H NMR. This encouraged us to introduce –Me group at the 5th position of 4-bromo-3-hydroxyphenanthrene-9-carbonitrile **(130)**.

We modified our synthetic strategy by starting with mesitylene **(131)** as it has symmetrically substituted methyl groups. It was subjected to side chain bromination selectively giving 3,5-

dimethyl benzyl bromide **(132)** followed by its functional group interconversion to obtain 3,5-dimethyl benzonitrile **(133)** as the starting material for olefin synthesis. 3,5-dimethyl benzonitrile was then subjected to Knoevenagel condensation with *p*-anisaldehyde **(125)** to successfully obtain 2-(3,5-dimethylphenyl)-3-(4-methoxyphenyl)acrylonitrile **(134)** as a mixture of *E* and *Z* isomers in excellent yields (Scheme 20).

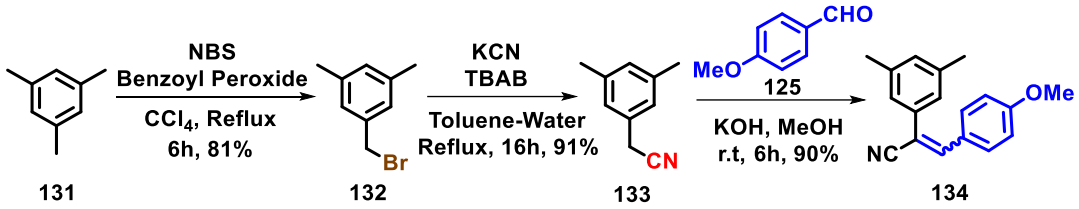

Scheme 20 Synthesis of 2-(3,5-dimethylphenyl)-3-(4-methoxyphenyl)acrylonitrile

The *E/Z* olefin mixture was collectively subjected to oxidative dehydrogenative photocyclization to afford 3-methoxy-5,7-dimethylphenanthrene-9-carbonitrile **(135)**. The formation of substituted phenanthrene was confirmed using ^{1}H NMR spectra which clearly showed the disappearance of olefinic protons as well as the appearance of two sharp singlets at **δ** 3.13 and 2.58 corresponding to the two aromatic methyl groups which could now be differentiated. The signal for the protons of one of the aromatic –Me group is deshielded as compared to the other due to the anisotropic effect of the phenanthrene nucleus owing to its position in the bay region. Hence, the signal at **δ** 3.13 corresponds to the –Me group at 5th position and that at **δ** 2.58 corresponds to the Ar –Me group at 7th position. The corresponding phenanthrol **(136)** was generated by the deprotection of –OMe using lithium bromide as lewis acid and heating the reaction to high temperature to access 3-hydroxy-5,7-dimethylphenanthrene-9-carbonitrile **(66)** in moderate yields (Scheme 21).

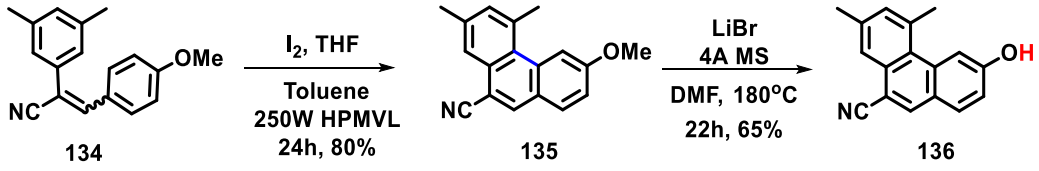

Scheme 21 Synthesis of 3-hydroxy-5,7-dimethylphenanthrene-9-carbonitrile (136)

^{1}H NMR spectra for 3-hydroxy-5,7-dimethylphenanthrene-9-carbonitrile **(136)** clearly showed the disappearance of the signal for the –OC*H*$_3$ protons and a broad singlet at **δ** 10.43 appears due to the –O*H* proton. This downfield signal suggests the possibility of intermolecular hydrogen bonding in this molecule which is an important factor affecting crystal packing. The tolerance of –CN group towards these reaction conditions was

confirmed by IR spectra which clearly showed a sharp band at 2229 cm^{-1} due to -C≡N stretching and a characteristic band at 3344 cm^{-1} for –O-H stretching supporting the effective deprotection of –OMe.

We attempted the bromination of 3-hydroxy-5,7-dimethylphenanthrene-9-carbonitrile **(136)** using NBS in dichloroethane and expected to give us our target molecule 4-bromo-3-hydroxy-5,7-dimethylphenanthrene-9-carbonitrile **(137)** but a mixture of 2-bromo-3-hydroxy-5,7-dimethyl phenanthrene-9-carbonitrile **(138)** and 2,4-dibromo-3-hydroxy-5,7-dimethylphenanthrene-9-carbonitrile **(139)** was obtained (Scheme 22). The formation of **138** and **139** lead to the conclusion that the first bromination occurred at the less hindered 2nd position and the addition of excess of brominating agent lead to second bromination at 4th position. This may be attributed to the fact that bromonium ion formed *in situ* is bulky in nature and hence it is unable to accommodate itself in the bay region due to the steric factors arising because of the presence of methyl group at 5th position.

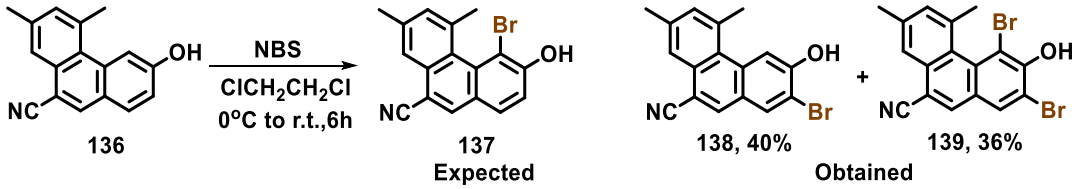

136 | 137 Expected | 138, 40% | 139, 36% Obtained

Scheme 22 Bromination of 3-hydroxy-5,7-dimethylphenanthrene-9-carbonitrile (136)

Our new strategy to access desired product **137** from the dibromo **139** was based on the expectation that the debromination of the dibrominated **139** would efficiently knock out the more accessible –Br at the 2nd position. With this aim, we subjected **139** to debromination using HBr and sodium sulphite (Scheme 23). To our surprise, 2-bromo-3-hydroxy-5,7-dimethylphenanthrene-9-carbonitrile **(138)** was the only product formed during the reaction.

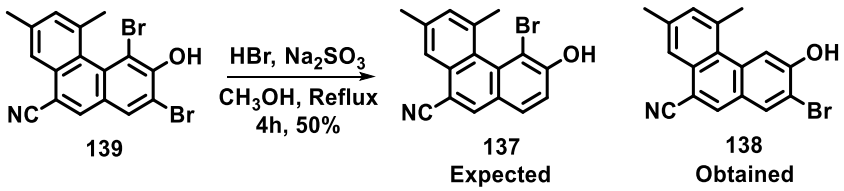

139 | 137 Expected | 138 Obtained

Scheme 23 Attempted alternate synthesis of 137

The mechanistic pathway for this reaction involves the formation of a carbocation which can form at 2nd (when –Br at 2nd position is knocked off) or 4th position (when –Br at 4th position is knocked off). The stability of the carbocation formed at 4th position, seems to be

higher than that formed from the carbocation at 2nd position. Also the debromination at 4th position may lead to strain relief in the molecule, favouring the formation of 2-bromo-3-hydroxy-5,7-dimethylphenanthrene-9-carbonitrile **(138)**.

The modulation of the size of the substituent at the 4th position was necessary to understand effective bulk required to undergo electrophilic substitution selectively at 4th position of a 5-methyl phenanthrene motif. So we investigated the introduction of a smaller halogen atom *ie.* –Cl at the 4th position of 3-hydroxy-5,7-dimethylphenanthrene-9-carbonitrile **(136)**. It was observed that chlorination of 3-hydroxy-5,7-dimethylphenanthrene-9-carbonitrile **(136)** indeed gave 4-chloro-3-hydroxy-5,7-dimethylphenanthrene-9-carbonitrile **(140)** as the only product where the chlorination occurred at 4th position selectively (Scheme 24) unlike bromination which gave a mixture of products.

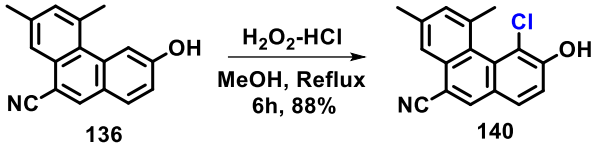

Scheme 24 Chlorination of 3-hydroxy-5,7-dimethylphenanthrene-9-carbonitrile (136)

This was confirmed by ^{1}H NMR spectra of 4-chloro-3-hydroxy-5,7-dimethylphenanthrene-9-carbonitrile **(140)** which showed a set of two doublets at **δ** 7.76 and 7.41 having a coupling constant of 8.4Hz corresponding to the *ortho* protons at 1st and 2nd position along with three clear singlets in the aromatic region. A broad singlet at **δ** 6.31 due to the phenolic –O-*H* is seen in the upfield region.

Having synthesized these molecules, we wanted to compare and study the degree of deformity in these aromatic systems. Preliminary use of NMR spectroscopy to detect presence of chiral isomers in these systems at ambient temperatures as well as low temperatures followed by the use of SCXRD to accurately determine the degree of non-planarity in these molecules was our prime objective.

2.3.2.2 NMR spectroscopy as a tool for detection of chirality:

One of the most exploited method for the determination of the presence of enantiomers is the use of NMR spectroscopy. It is a useful tool to examine chirality for molecules containing diastereotopic protons or group of protons. If the energy barrier separating the

two enantiomeric forms is of the order of 9-25 kcal/mol, the kinetics involved in the interconversion of the enantiomers can be studied using VT NMR.

As the halogenated derivatives synthesized during this work do not contain any diastereotopic group, they were converted into their *p*-bromo benzyl ether and the signal for the benzylic protons were closely examined for its diastereotopic nature. ^{1}H NMR for benzyl ether of 4-bromo-3-hydroxyphenanthrene-9-carbonitrile **(141)** (Scheme 25) clearly showed a sharp singlet at **δ** 5.33 showing no sign of enantiomerism on NMR scale(Figure 19). Had there been sufficient twist in the frame of phenanthrene, these two gem-dihydrogens would have become diastereotopic and would have split each other.

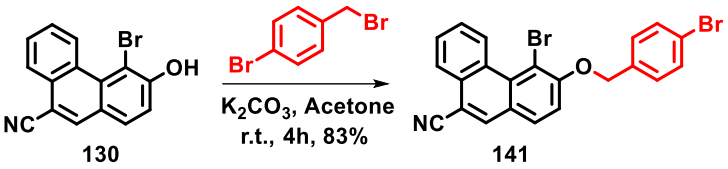

Scheme 25 Synthesis of *p*-bromo benzyl ether of 130

Figure 19 ^{1}H NMR (enlarged) for benzylic protons of 141

This was also confirmed by synthesizing its carbonate **(142)** with optically pure (-)-menthyl chloroformate (Scheme 26).

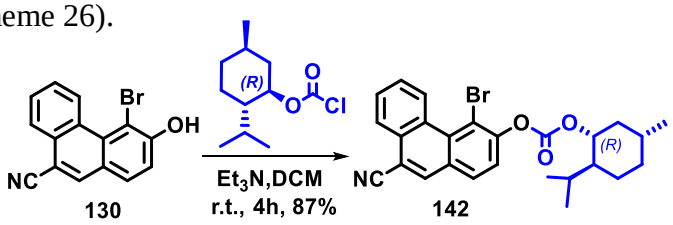

Scheme 26 Synthesis of menthyl carbonate of 130

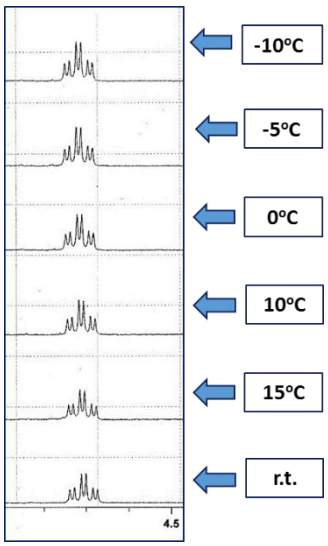

Figure 20 ^{1}H NMR spectra (enlarge) of compound 142 at various temperatures

The signal for the chiral centre was monitored for the presence of diastereomers at temperatures upto -20°C using VTNMR (Figure 20).

The analysis failed to show any change in the splitting pattern or chemical shift value for the proton at **δ** 4.73, suggesting that the steric bulk at the bay region is not large enough to render 4-bromo-3-hydroxyphenanthrene-9-carbonitrile chiral **(130)**.

Failing to synthesize 4-bromo-3-hydroxy-5,7-dimethylphenanthrene-9-carbonitrile **(137)**, we utilized the synthesized dibromo derivative **(139)** to analyse for the presence of enantiomers. Chiral menthyl carbonate derivative **(143)** (Scheme 27) was synthesized using similar procedure as before and NMR spectra was recorded. The ^{1}H NMR spectra at ambient temperature showed that the signal for the proton at the chiral centre of the auxiliary appeared as a d at **δ** 4.75 which significantly broadened at -15°C inferring that the interconversion of the diastereomers was slow but not slow enough to be detected even at this temperature (Figure 21).

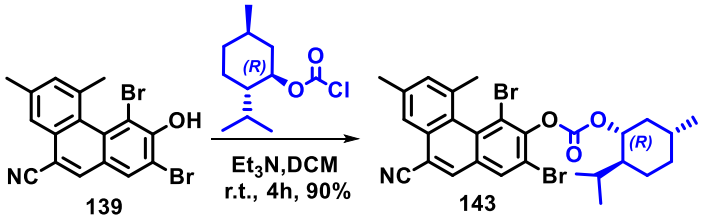

Scheme 27 Synthesis of menthyl carbonate of 139

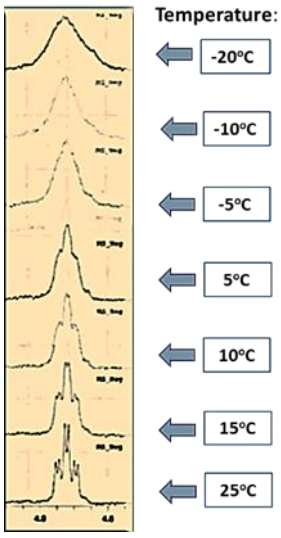

Figure 21 VT ^{1}H NMR Spectra (enlarge) of compound 143

The ^{1}H NMR for ether derivative **(144)** (Scheme 28) however showed the presence of two doublets at **δ** 5.29 and 5.11 having a coupling constant of 10.4Hz for the diastereotopic

protons of O-CH_2-C_6H_4Br (Figure 22) was in favour of 2,4-dibromo-3-hydroxy-5,7-dimethylphenanthrene-9-carbonitrile **(139)** being chiral.

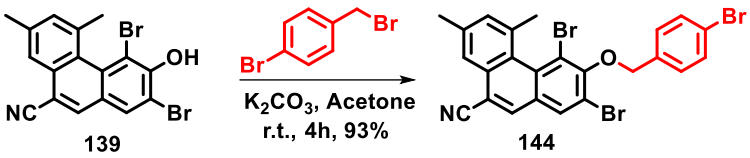

Scheme 28 Synthesis of *p*-bromo benzyl ether of 139

Figure 22 ^{1}H NMR (enlarged) for benzylic protons of 144

To prove that the bromine atom at 4th position is necessary to render the molecule non-planar, we analysed the ^{1}H NMR spectra of 2-bromo-3-((4-bromobenzyl)oxy)-5,7-dimethylphenanthrene-9-carbonitrile **(145)** (Scheme 29) which showed a sharp singlet of O-CH_2-C_6H_4Br at **δ** 5.36 (Figure 23).

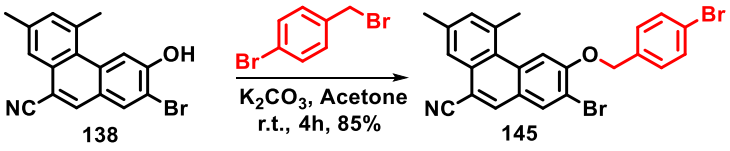

Scheme 29 Synthesis of *p*-bromo benzyl ether of 138

Figure 23 ^{1}H NMR (enlarged) for benzylic protons of 145

To further support the hypothesis that the diastereotopic protons appear as two doublets due to the twist in the molecule and not merely because of the difference in its chemical environment due to the slow bond rotation caused by the surrounding two bromine atoms, we synthesized 2,4-dibromo-3-hydroxyphenanthrene-9-carbonitrile **(146)** from 3-hydroxyphenanthrene-9-carbonitrile **(129)** by carrying out bromination with excess of NBS followed by synthesis of its ether derivative **(147)** with *p*-bromo benzyl bromide.

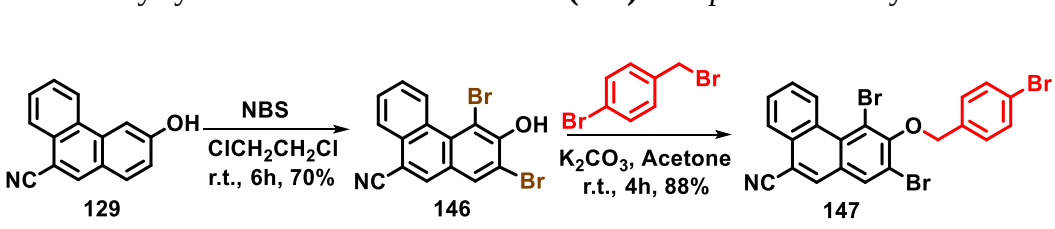

Scheme 30 Synthesis of *p*-bromo benzyl ether of 146

Figure 24 ^{1}H NMR (enlarged) for benzylic protons of 147

Supporting our assumption, the benzylic protons for this compound too appeared as sharp singlet at **δ** 5.18 (Figure 24) ruling out the possibility that the two bromine atoms at 2nd and

4th position create a difference in the chemical environment for the benzylic protons by causing slow rotation of bonds.

Hence, the introduction of methyl at 5th position and bromine at 4th position leads to sufficient steric bulk to render the phenanthrene chiral. The relatively less bulky, 4-chloro-3-hydroxy-5,7-dimethylphenanthrene-9-carbonitrile **(140)** was also converted into similar derivatives (**148** and **149**) (Scheme 31 & 32). The ^{1}H NMR spectra for chiral carbonate **(148)** showed an eight line signal for the proton attached to chiral centre at **δ** 4.73 as compared to conventional six line signal (Figure 25).

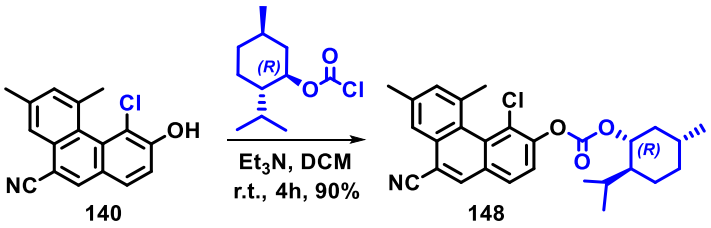

Scheme 31 Synthesis of menthyl carbonate of 140

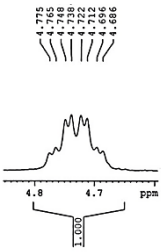

Figure 25 ^{1}H NMR (enlarged) for chiral centre of 148

The ^{1}H NMR for its *p*-bromo benzyl ether derivative **(149)** showed two doublets similar to that observed earlier in the dibromo derivative at **δ** 5.29 having *J*=12.4Hz (Figure 26).

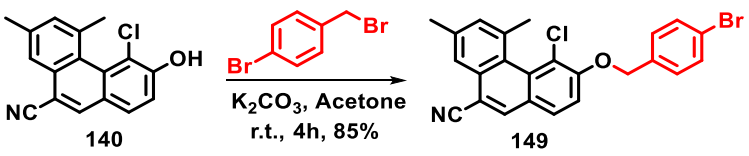

Scheme 32 Synthesis of *p*-bromo benzyl ether of 140

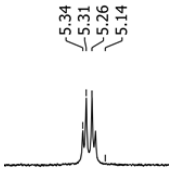

Figure 26 ^{1}H NMR (enlarged) for benzylic protons of 149

Hence, ^{1}H NMR clearly supports the possibility of 2,4-dibromo-3-hydroxyphenanthrene-9-carbonitrile **(139)** and 4-chloro-3-hydroxy-5,7-dimethylphenanthrene-9-carbonitrile **(140)** in two enantiomeric forms, following which we attempted crystallization for carrying out SCXRD to accurately determine the degree of non-planarity.

2.3.2.3 Single Crystal XRD to determine degree of non-planarity:

Crystals of **141** suitable for SCXRD were grown from a solution of ethyl acetate-petroleum ether by slow evaporation. It crystallizes out in Pī space group showing some degree of distortion from unsubstituted phenanthrene. The angle formed between the planes containing the two terminal rings (ring A and C) was found to be 12.04^o (Figure 27a). Not much distortion in the planarity aromatic rings making up the phenanthrene skeleton was

seen, leading us to analyse other modes of strain relief. A typical change in the bond lengths and bond angles was seen with the central B ring being the most distorted in nature. An increase in the bond lengths on the inner rim and its decrease on the outer rim are characteristic for molecules possessing helical shape. Such distortions are also seen in this molecule with the slight elongation in C4-C12 and C12-C13 bond lengths, 1.416 and 1.459Å respectively and compression of C1-C2 (1.367Å); C7-C8 (1.361Å) and C9-C10 (1.401Å). The bay substituents, -Br and -H are pushed out of the plane of the aromatic rings by a degree of 7.73^{o} and 2.18^{o} due to steric and electronic crowding created due to bulky –Br atom at 4th position. The introduction of –Br atom also leads to a change in crystal packing due to different non-covalent interactions between the molecules. An interesting intramolecular interaction between –Br and C(Ar) at 5th position is seen having a distance of 3.162Å (Figure 27b). This increase in the distance between bay placed pairs, leads to splaying of the bond angles C13-C12-C4: 127.03^{o} and C8-C14-C9:120.11^{o}. The dihedral angle along the inner rim was found to be 12.19^{o} (C4-C12-C13-C5).

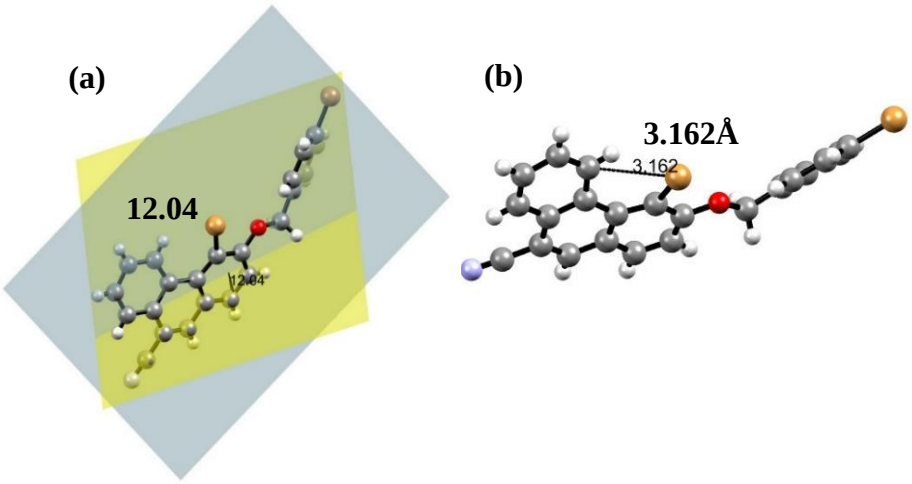

Figure 27 ORTEP of compound 141 showing (a) Interplanar angle between terminal rings (b) Intramolecular Br-C(Ar) short contact

Two molecules are oppositely oriented and held together by a Br-Br short contact of 3.52Å. Each of these oppositely oriented molecule does not undergo π-π stacking with each other, but with the molecules stacked directly above or below them leading to the formation of a column of molecules held together by alternating Br-Br short contact and π-stacking (Figure 28a). Such columns are held together by a lateral Br-H(Ar) and (Bn)Br-Br(Bn) interactions (Figure 28b). All these interactions lead to a uniform pattern of arrangement of molecules when viewed in a 3X3 packing (Figure 28c).

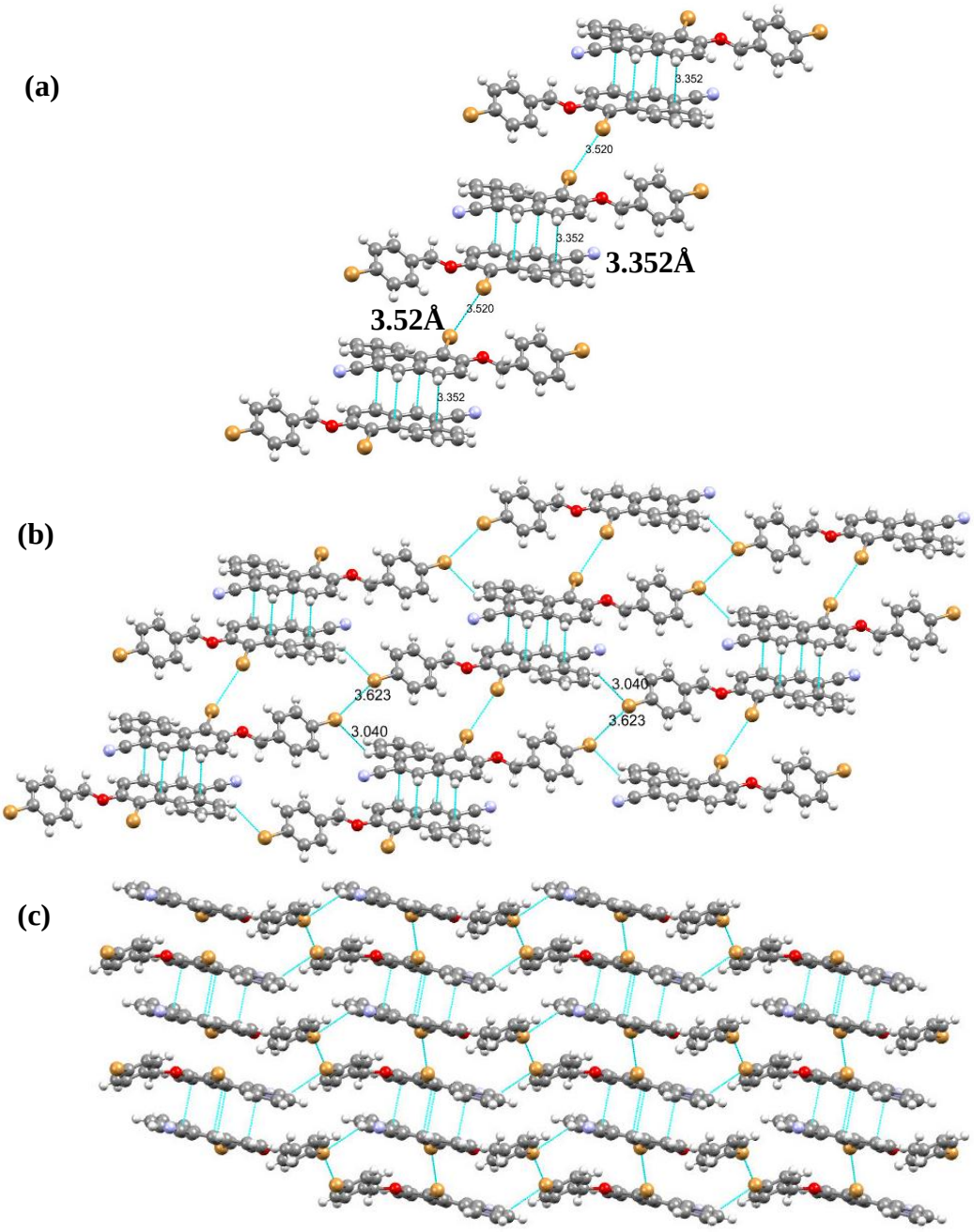

Figure 28 ORTEP diagram showing: (a) intramolecular Br-Br and π-stacking leading to columnar arrangement (b) lateral interactions that hold the columns together (c) 3X3 packing showing patterned arrangement

To study the effect of introduction of a –Me substituent at 4th position, we attempted crystallization of various derivatives of 2,4-dibromo-5,7-dimethylphenanthrene-9-carbonitrile **(139)**. In spite of extensive efforts, suitable crystals for SCXRD could not be obtained for any of the derivative of this compound as only amorphous solid fell out. However, the crystallization of benzyl ether derivative of 4-chloro-5,7-dimethylphenanthrene-9-carbonitrile **(149)** gave us crystals suitable for SCXRD. Crystals

suitable for SCXRD were obtained from its slow evaporation from a solution of ethyl acetate-petroleum ether. It crystallizes in P21/n space group and the interplanar angle between the two terminal rings of this phenanthrene system was 29.29^{o} (Figure 29a). An unusual Cl-C intramolecular H-bonding between the -Cl atom and aromatic C atom at 5th position is seen along with Cl-C(Me) interaction with the methyl carbon (3.23Å and 3.01Å respectively) (Figure 29b). The torsional angle along the inner rim was found to be 32.55^{o}.

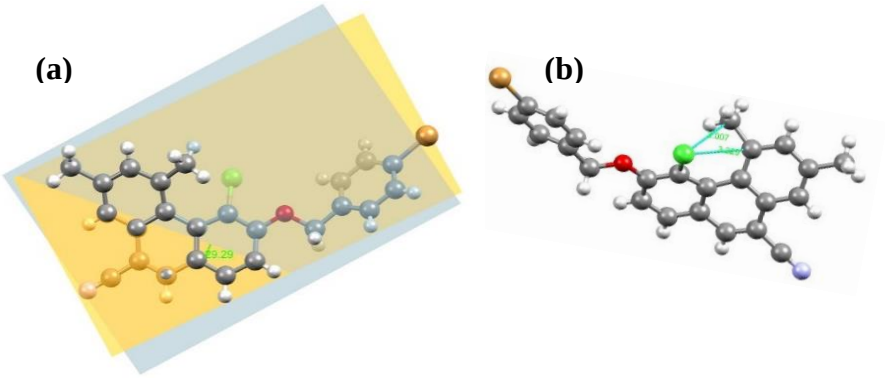

Figure 29 ORTEP diagram of compound 149 showing: (a) interplanar angle between the two terminal rings (b) intramolecular interactions

Two molecules are held together by a Cl-Cl short contact of 3.455Å and two Br-H(Me) bonds of 2.91Å each (Figure 30).

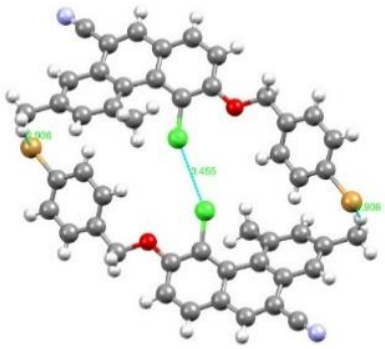

Figure 30 ORTEP diagram showing intermolecular Cl-Cl and Br-H(Me) short contact

Crystal packing in a 3X3 box shows that the molecules are arranged in zig-zag chains which are parallel to each other. Two chains are held together not by π-stacking which is usually seen for such molecules, but by Br-Br short contact between the bromine atoms of the pendent *p*-bromo benzyl group of neighboring molecules (3.302Å) and (Me)H-H(Me) short contact of 2.147Å (Figure 31).

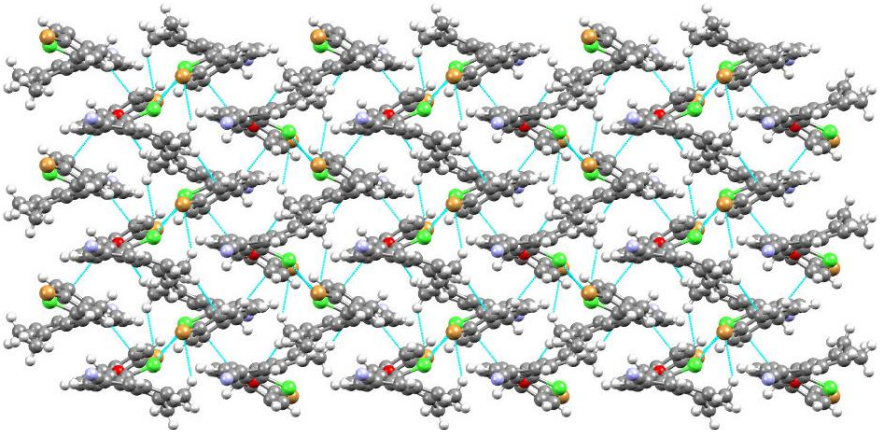

Figure 31 ORTEP diagram showing 3X3 packing having molecules arranged in parallel zig-zag chains

The distortion in the phenanthrene skeleton can be clearly seen in terms of discrepancies in the bond length and bond angles when compared to unsubstituted phenanthrene. The bond lengths along the inner rim are slightly elongated: C12-C13:1.460Å; C5-C13:1.418Å and the outer rim bond lengths are shortened: C1-C2:1.354Å; C9-C10: 1.339Å; C7-C8:1.368Å; with the central ring being the most distorted in nature. Deviations in the bond angles are also seen with the major distortion at C13-C12-C4:125.97^{o} (increase by 5.27^{o}) and C8-C14-C9:121.25^{o} (increase by 4.15^{o}). Due to the steric strain that develops in the bay region because of the presence of –Me group at 5th position and –Cl at 4th position, both the substituents are pushed out of the plane of the aromatic ring by 9.81^{o} and 13.4^{o} respectively.

Hence the strain in the molecules due to intramolecular crowding in the bay region is released not only by the distortion of the phenanthrene core but also by the mode of change in bond lengths, bond angles and out of the plane bending of the substituents. The chiral HPLC for these derivatives was attempted, but no separation could be observed even in cryogenic conditions. This led us to a conclusion that even though some of these derivatives **139** and **140** show the presence of enantiomers detectable by NMR spectroscopy, these enantiomers rapidly racemize at temperatures as low as -20^{o}C, making their resolution not possible.

2.3.2.4 Conclusion:

Various 4,5-substituted phenanthrene derivatives were synthesized and studied for their degree of non-planarity using different analytic tools such as NMR spectroscopy and SCXRD analysis. A derivative of phenanthrene, 4-bromo-3-hydroxyphenanthrene-9-carbonitrile **(130)**, possessing bulky –Br group at 4th position causes the molecule to deviate from planarity by 12.12^{o}. However, this twist in the molecule was found to be insufficient to cause enantiomerism at ambient conditions. Hence, the introduction of –Me group at the 5th position of the 4-bromo phenanthrene nucleus was carried out. We failed to synthesize 4-bromo-3-hydroxy-5,7-dimethylphenanthrene-9-carbonitrile **(137)**, but succeeded in synthesizing its dibromo derivative 2,4-dibromo-3-hydroxy-5,7-dimethylphenanthrene-9-carbonitrile **(139)**. It was then subjected to chiral carbonate formation by its reaction with (-)-menthylchloro formate. Low temperature NMR for this molecule **(143)** showed considerable broadening of the signal at the chiral center suggesting the slow interconversion of the enantiomers at a temperature of -20^{o}C. The presence of enantiomerism was also confirmed by synthesizing its ether derivative **(144)** with *p*-bromo benzyl bromide. The benzylic protons were found to be diastereotopic and appeared as a set of two doublets, proving the existence of 2,4-dibromo-3-hydroxy-5,7-dimethyl phenanthrene-9-carbonitrile **(139)** as enantiomers. The modulation of the substituent size led us to the synthesis of 4-chloro-3-hydroxy-5,7-dimethylphenanthrene-9-carbonitrile **(140)**. A similar observation was seen for its ether derivative **(148)** with *p*-bromo benzyl bromide, where a set of two doublets could be seen for the benzylic protons due to their diastereotopic nature. The SCXRD for this derivative was successful carried out and it showed an interplanar angle of 29.29^{o}. However, none of the synthesized derivatives showed two well resolved peaks in chiral HPLC confirming that the steric bulk due to substituents in the *bay* region is not enough for the molecules to separate at temperatures upto -20^{o}C. This motivated us to introduce a fourth benzene ring fused to the phenanthrene core prompting us to synthesize benzo[*c*]phnanthrenes.

2.3.2.5 Experimental Section:

Synthesis of 3,5-dimethylbenzyl bromide (132):

Mesitylene (1.0g; 8.32mmol), *N*-bromosuccinimide (1.33g; 7.49mmol) and benzoyl peroxide (0.1g; 0.42mmol) are added to 15 mL of carbon tetrachloride. This mixture is refluxed in a round-bottomed for 6h. The completion of the reaction can be seen from the precipitation of succinimide and confirmed by TLC. After the reaction is complete, the reaction mixture is cooled, filtered and washed with fresh carbon tetrachloride to remove succinimde which is a by-product of the reaction. The reaction mixture is then concentrated under vacuum. The residue is subjected to column chromatography which furnishes 3,5-dimethylbenzyl bromide as colourless viscous liquid which solidifies on cooling (1.0g; Yield: 81%; M.P. 40 °C).

^{1}H NMR ($CDCl_3$, 400MHz) δ 7.03 (s, 2H); 6.96 (s, 1H); 4.46 (s, 2H); 2.33 (s, 6H)

Synthesis of 3,5-dimethylbenzyl cyanide (133):

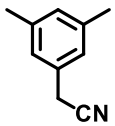

3,5-dimethylbenzyl bromide **(132)** (1.5g; 7.53mmol), potassium cyanide (0.59g; 9.05mmol) and tetrabutylammonium bromide (0.48g; 1.51mmol) are added to a mixture of toluene (18mL) and water (2mL). The reaction mixture is heated to 80^{o}C for 16h. The progress of the reaction is measured by TLC. After the completion of the reaction, the reaction mixture is allowed to cool and extracted using toluene (3 X 25mL). The combined organic layer is dried over Na_2SO_4 and concentrated under reduced pressure. The residue is subjected to column chromatography using petroleum ether to give 3,5-dimethylbenzyl cyanide as low melting colourless solid (1.00g; Yield 91%; M.P. 44^{o}C).

^{1}H NMR ($CDCl_3$, 400MHz) δ 6.99 (s, 1H); 6.97 (s, 2H); 3.69 (s, 2H); 2.35 (s, 6H)

Synthesis of 2-(3,5-dimethylphenyl)-3-(4-methoxyphenyl)acrylonitrile (134):

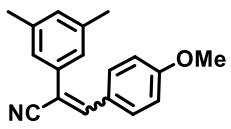

3,5-dimethylbenzyl cyanide **(133)** (1.02g; 7.03mmol), *p*-anisaldehyde (1.00g; 7.4mmol) and potassium hydroxide (0.31g; 7.73mmol) are added to 10mL dry methanol. The reaction is allowed to stir at room temperature for 6h. The proceeding of the reaction is seen by the formation of precipitates and completion is marked by the disappearance of the starting materials on TLC. The reaction mixture is then concentrated under reduced pressure and purified using column chromatography over silica gel to obtain 2-(3,5-dimethylphenyl)-3-(4-methoxyphenyl) acrylonitrile as pale yellow low melting solid (01.66g; Yield 90%; M.P. 50^{o}C)

^{1}H NMR (400MHz, $CDCl_3$): δ 7.91-7.89 (d, *J*=8.8Hz, 2H); 7.47 (s, 1H); 7.29 (s, 2H); 7.03 (s, 1H); 7.01-7.98 (d, *J*=8.8Hz, 2H); 3.89 (s, 3H); 2.39 (s, 6H)

^{13}C NMR (100MHz, $CDCl_3$): δ 161.3; 141.5; 138.7; 134.7; 131.1 (2C); 130.5; 126.7; 126.4; 123.6 (2C); 118.8; 114.4 (2C); 108.9; 55.4; 21.4 (2C)

IR (KBr): *ν* 3030, 2960, 2214, 2838, 2206, 1595, 1513, 1424, 1310, 1257, 1179, 1037, 847, 820, 689 cm^{-1}

Synthesis of 3-methoxy-5,7-dimethylphenanthrene-9-carbonitrile (135):

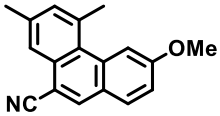

A solution of 2-(3,5-dimethylphenyl)-3-(4-methoxyphenyl) acrylonitrile **(134)** (1.0g; 3.8mmol), iodine (1.06g; 4.18mmol) and tetrahydrofuran (15.5mL; 190mmol) in 1200mL toluene was irradiated with 250W HPMVL for 24h. After the completion of the reaction (TLC), the organic layer was washed with saturated solution of $Na_2S_2O_3$ to remove excess of iodine. The organic layer was separated and washed with brine, concentrated under reduced pressure to obtain 3-methoxy-5,7-dimethylphenanthrene-9-carbonitrile as yellow solid (0.2g; Yield 80%; M.P. 90°C)

^{1}H NMR (400MHz, $CDCl_3$): δ 8.28 (s, 1H); 8.14 (s, 1H); 8.01 (s, 1H); 7.87-7.85 (d, *J*=8.8Hz, 1H); 7.42 (s, 1H); 7.30-7.27 (dd, *J*=8.8Hz, 1.6Hz, 1H); 4.03 (s, 3H); 3.13 (s, 3H); 2.58 (s, 3H)

^{13}C NMR (100MHz, $CDCl_3$): δ 159.9; 137.4; 135.8; 135.6; 134.8; 134.2; 131.1; 130.9; 127.2; 125.3; 124.4; 118.9; 115.6; 110.1; 106.9; 55.5; 27.1; 21.2

Mass (EI) *m/z*: 261 (M^+, 100%), 217 (12%), 98 (20%), 97 (17%), 83 (19%), 71 (29%), 69 (58%), 57 (42%), 55 (36%).

IR (KBr): 2215, 1611, 1521, 1451, 1352, 1274, 1226, 1128, 1032, 904, 842, 819, 622, 564 cm^{-1}

Synthesis of 3-hydroxy-5,7-dimethylphenanthrene-9-carbonitrile (136):

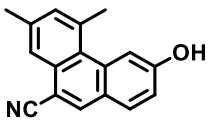

To a round bottom flask, was added 3-methoxy-5,7-dimethyl phenanthrene-9-carbonitrile **(135)** (0.7g; 2.68mmol), lithium bromide (0.37g, 4.30 mmol) in dimethylformamide (30 mL). To this solution was added 4Å molecular sieves (100% w/w) and stirred at room temperature for 15 mins, followed by heating in an oil bath to 180°C for 22 hours. The reaction mixture was then allowed to cool to room temperature and filtered to remove molecular sieves. Water was added to the reaction mixture and it was allowed to stir till solution becomes clear. It was extracted using ethyl acetate (3X50 mL). The combined organic layer was dried over sodium

sulfate and concentrated under reduced pressure. The concentrated mixture was purified on silica gel column using ethyl acetate and petroleum ether (2:3) to give 3-hydroxy-5,7-dimethylphenanthrene-9-carbonitrile (0.43g; Yield 65%; M.P. 210^{o}C) as pale yellow solid.

^{1}H NMR (400MHz, d_6-DMSO): δ 10. 43 (bs, 1H); 8.44 (s, 1H); 8.25 (s, 1H); 7.98-7.96 (d, *J*=8.4Hz, 1H); 7.78 (s, 1H); 7.44 (s, 1H); 7.24-7.21 (dd, *J*=8.4Hz, 1.6Hz, 1H); 3.37 (s, 3H); 3.00 (s, 3H)

^{13}C NMR (100MHz, d_6-DMSO): δ 159.2; 137.5; 136.9; 136.7; 134.8; 134.2; 132.3; 130.7; 126.8; 124.5; 123.6; 119.2; 117.4; 112.1; 104.9; 27.2; 21.2

Mass (EI) *m/z*: 247 (M^+, 100%), 246 (51%), 232 (24%), 230 (20%), 213 (10%)

IR (KBr): 3341, 2229, 1617, 1567, 1522, 1465, 1446, 1314, 1276, 1234, 1199, 904, 851, 818, 639 cm^{-1}

Synthesis of 2-bromo-3-hydroxy-5,7-dimethylphenanthrene-9-carbonitrile (138) and 2,4-dibromo-3-hydroxy-5,7-dimethylphenanthrene-9-carbonitrile (139):

To a solution of 3-hydroxy-5,7-dimethylphenanthrene-9-carbonitrile **(136)** (0.2g, 0.81mmol) in dichloroethane (10mL) was added *N*-bromosuccinimide (0.3g; 1.7mmol) portion wise three times at an interval of 15mins each at 0^{o}C. After the completion of the addition, the reaction mixture is allowed to stir at 0^{o}C for 6 hours. After the completion of the reaction, monitored by TLC which shows the disappearance of starting material and appearance of two spots of almost equal intensity. Both the spots were carefully separated by carrying out column chromatography on silica gel using a mixture of 10% ethyl acetate in petroleum ether. The non-polar spot that elutes out first from the column corresponds to 2,4-dibromo-3-hydroxy-5,7-dimethylphenanthrene-9-carbonitrile **(139)** (0.12g; Yield 36%) as brown solid and the relatively polar spot corresponds to 2-bromo-3-hydroxy-5,7-dimethylphenanthrene-9-carbonitrile **(138)** (0.1g; Yield 40%) as yellow solid.

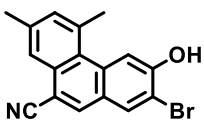

^{1}H NMR (400MHz, $CDCl_3$): δ 8.49 (s, 1H); 8.09 (s, 1H); 8.07 (s, 1H); 8.01 (s, 1H); 7.45 (s, 1H); 6.10 (bs, 1H); 3.10 (s, 3H); 2.58 (s, 3H)

IR (KBr): ν 3299, 2960, 2923, 2232, 1595, 1406, 1361, 1249, 1229, 1052, 905, 852, 623 cm^{-1}

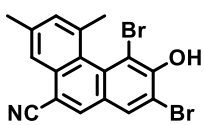

^{1}H NMR (400MHz, $CDCl_3$): δ 8.04 (s, 1H); 7.88 (s, 1H); 7.86 (s, 1H); 7.39 (s, 1H); 6.57 (bs, 1H); 2.71 (s, 3H); 2.59 (s, 3H)

Mass (EI) *m/z*: 407 (16%), 405 (40%), 403 (17%), 324 (26%), 245 (79%), 244 (91%), 230 (100%), 213 (39%)

Synthesis of 4-bromo-3-hydroxyphenanthrene-9-carbonitrile (130):

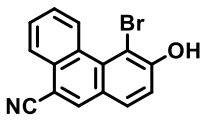

The same synthetic procedure involving the use of 3-hydroxy phenanthrene-9-carbonitrile **(129)** (0.1g; 0.46mmol) to obtain 4-bromo-3-hydroxyphenanthrene-9-carbonitrile **(130)** (0.1g; Yield 75%)

^{1}H NMR (400MHz, $CDCl_3$): δ 9.87-9.85 (d, *J*=8.4Hz, 1H); 8.35-8.33 (dd, *J*=8.4Hz, 1.6Hz 1H); 8.16 (s, 1H); 7.86-7.84 (d, *J*=8.8Hz, 1H); 7.83-7.74 (m, 2H); 7.48-7.46 (d, *J*=8.4Hz 1H); 6.74 (s, 1H)

IR (KBr): 3280, 2226, 1606, 1566, 1500, 1442, 1394, 1312, 1250, 1214, 1156, 869, 813, 761, 580 cm^{-1}

Mass (TOF ES) *m/z*: 320 ([M+Na],100%)

HRMS (ESI+): *m/z* Calculated for $C_{15}H_8ON^{79}BrNa$ 319.96820; Obtained 319.96815

Synthesis of 2,4-dibromo-3-hydroxyphenanthrene-9-carbonitrile (146):

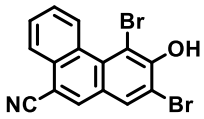

The same synthetic procedure involving the use of 3-hydroxy phenanthrene-9-carbonitrile **(129)** (0.1g; 0.46mmol) to obtain **(146)** (0.095g; Yield 70%)

^{1}H NMR (400MHz, $CDCl_3$): δ 9.89-9.87 (dd, *J*=8.4Hz, 1.2Hz, 1H); 8.36-8.33 (dd, *J*=8.0Hz, 1.2Hz 1H); 8.13 (s, 1H); 8.07 (s, 1H); 7.86-7.78 (m, 2H); 6.89 (bs, 1H)

^{13}C NMR (100MHz, $CDCl_3$): δ 151.5; 134.2; 133.3; 130.6; 130.3; 129.0; 127.0; 126.9; 126.1; 117.3; 110.9; 109.6; 109.3; 108.7; 106.5

IR (KBr): ν 3392, 2954, 2921, 2853, 2223, 1580, 1481, 1448, 1416, 1380, 1339, 1288, 1210, 1157, 894, 757, 719 cm^{-1}

Synthesis of 2-bromo-3-((4-bromobenzyl)oxy)-5,7-dimethylphenanthrene-9-carbonitrile (145):

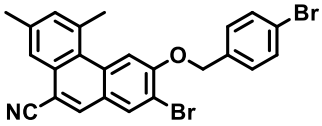

In a clean and dry round bottom flask, 2-bromo-3-hydroxy-5,7-dimethylphenanthrene-9-carbonitrile **(138)** (0.3g; 0.92mmol) was dissolved in 10mL of AR grade acetone. To this solution, *p*-bromo benzyl bromide (0.25g; 1.0mmol) and potassium carbonate (0.14g; 1.0mmol) are added in one portion. The reaction mixture is stoppered and allowed to stir at room temperature for 4 hours. The completion of the reaction is marked by the disappearance of the starting material on TLC. The reaction mixture is concentrated under reduced pressure to remove acetone and the residue is subjected to column chromatography on silica gel. The elution using 5% ethyl acetate-petroleum ether mixture afforded 2-bromo-3-((4-

bromobenzyl)oxy)-5,7-dimethylphenanthrene-9-carbonitrile **(145)** as colourless solid (0.39g; Yield 85%)

^{1}H NMR (400MHz, $CDCl_3$): δ 8.23 (s, 1H); 8.16 (s, 1H); 8.08 (s, 1H); 8.02 (s, 1H); 7.59-7.57 (d, *J*=8.8Hz, 2H); 7.44-7.42 (d, *J*=8.8Hz, 1H); 7.42 (s, 1H); 5.36 (s, 2H); 2.95 (s, 3H); 2.57 (s, 3H)

^{13}C NMR (100MHz, $CDCl_3$): δ 154.4; 142.4; 137.9; 135.3; 134.9; 134.7; 134.3; 133.6; 133.5; 132.0; 130.9; 128.5 (2C); 127.0; 126.5; 124.7; 122.2; 118.4; 112.7; 110.7; 108.7; 70.3; 26.9; 21.2

IR (KBr): ν 2956, 2915, 2850, 2214, 1610, 1595, 1508, 1487, 1446, 1388, 1353, 1291, 1246, 1214, 1066, 1033, 1007, 910, 853, 834, 804, 620, 475 cm^{-1}

Synthesis of 2,4-dibromo-3-((4-bromobenzyl)oxy)-5,7-dimethylphenanthrene-9-carbonitrile (144):

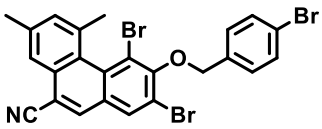

Similar synthetic procedure as above involving the use of 2,4-dibromo-3-hydroxy-5,7-dimethylphenanthrene-9-carbonitrile **(139)** (0.1g; 0.25mmol) to furnish 2,4-dibromo-3-((4-bromobenzyl)oxy)-5,7-dimethyl phenanthrene-9-carbonitrile **(144)** (0.13g; Yield 93%)

^{1}H NMR (400MHz, $CDCl_3$): δ 8.08 (s, 1H); 7.90 (s, 1H); 7.87 (s, 1H); 7.60-7.58 (d, *J*=8.8Hz, 2H); 7.56-7.54 (d, *J*=8.8Hz, 2H); 7.42 (s, 1H); 5.30-5.28 (d, *J*=10.4Hz,1H); 5.12-5.09 (d, *J*=10.4Hz, 1H); 2.71 (s, 3H); 2.60 (s, 3H)

^{13}C NMR (100MHz, $CDCl_3$): δ 153.8; 139.0; 137.2; 134.9; 133.2; 132.6; 132.4; 131.7 (2C); 131.5; 130.7; 130.2 (2C); 129.9; 127.8; 122.7; 122.1; 117.7; 117.3; 117.2; 110.5; 74.6; 24.5; 21.4

IR (KBr): ν 2956, 2917, 2221, 1605, 1568, 1487, 1446, 1376, 1306, 1213, 1196, 1067, 1012, 961, 891, 855, 808, 761, 640, 501 cm^{-1}

Synthesis of 4-bromo-3-((4-bromobenzyl)oxy)phenanthrene-9-carbonitrile (141):

Similar synthetic procedure as above involving the use of 4-bromo-3-hydroxy-5,7-dimethylphenanthrene-9-carbonitrile **(130)** (0.1g; 0.34mmol) to furnish 4-bromo-3-((4-bromobenzyl)oxy)phenanthrene-9-carbonitrile **(141)** (0.13g; Yield 83%) as colourless solid.

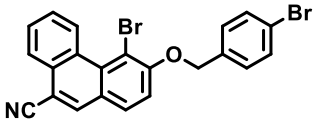

^{1}H NMR (400MHz, $CDCl_3$): δ 10.03-10.11 (m, 1H); 8.34-8.31 (dd, *J*=7.6Hz, 2.0Hz, 1H); 8.14 (s, 1H); 7.89-7.87 (d, *J*=8.8Hz,

1H); 7.83-7.74 (m, 2H); 7.59-7.57 (d, *J*=8.4Hz, 2H); 7.47-7.45 (d, *J*=8.8Hz, 2H); 7.38-7.36 (d, *J*=8.8Hz, 1H); 5.33 (s, 2H)

^{13}C NMR (100MHz, $CDCl_3$): δ 156.8; 135.4; 134.9; 132.1; 131.9 (2C); 130.6; 130.4; 129.6; 128.8 (2C); 128.7; 127.9; 126.9; 126.4; 125.8; 122.3; 117.8; 114.0; 109.6; 108.4; 71.1

IR (KBr): ν 2922, 2853, 2215, 1591, 1515, 1489, 1444, 1369, 1300, 1278, 1223, 1160, 1118, 1077, 1007, 889, 861, 801, 763 cm^{-1}

Synthesis of 2,4-dibromo-3-((4-bromobenzyl)oxy)phenanthrene-9-carbonitrile (147):

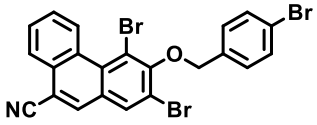

Similar synthetic procedure as above involving the use of 2,4-dibromo-3-hydroxy-5,7-dimethylphenanthrene-9-carbonitrile **(146)** (0.1g; 0.34mmol) to furnish 2,4-dibromo-3-((4-bromo benzyl)oxy)phenanthrene-9-carbonitrile **(147)** (0.14g; Yield 88%).

^{1}H NMR (400MHz, $CDCl_3$): δ 10.04-10.02 (m, 1H); 8.37-8.35 (dd, *J*=8.0Hz, 2.4Hz, 1H); 8.19 (s, 1H); 8.11 (s, 1H); 7.86-7.81 (m, 2H); 7.63-7.28 (m, 4H); 5.18 (s, 2H)

Synthesis of 4-chloro-3-hydroxy-5,7-dimethylphenanthrene-9-carbonitrile (140):

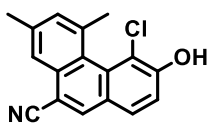

In a clean and dry round bottom flask, 3-hydroxy-5,7-dimethylphenanthrene-9-carbonitrile **(136)** (0.1g; 0.41mmol) was dissolved in 10mL of AR grade methanol. This solution was cooled to 0^{o}C using an ice bath and hydrogen peroxide (0.03mL; 0.45mmol) was added dropwise using an addition funnel over a period of half an hour. To this solution, conc. HCl (0.016mL; 0.45mmol) is added dropwise carefully with the reaction bath temperature maintained to 0^{o}C. After the addition, the reaction mixture is allowed to then stir at room temperature for 10 mins and then heated to reflux for 6 hours. The completion of the reaction is maked by the complete disappearance of the starting material. The reaction mixture is cooled and poured into cold water (25mL). The aqueous layer is extracted using ethyl acetate (3 X 25mL) and combined organic layers are collected, dried over anhy. Na_2SO_4. The organic layer is concentrated under reduced pressure to obtain residue which is subjected to column chromatography over silica gel using 5% ethyl acetate in petroleum ether to furnish 4-chloro-3-hydroxy-5,7-dimethylphenanthrene-9-carbonitrile **(140)** as a colourless solid (0.14g; Yield 88%).

^{1}H NMR (400MHz, $CDCl_3$): δ 7.99 (s, 1H); 7.87 (s, 1H); 7.78-7.75 (d, *J*=8.8Hz, 1H); 7.42-7.40 (d, *J*=8.8Hz, 1H); 7.39 (s, 1H); 6.31 (bs, 1H); 2.66 (s, 3H); 2.60 (s, 3H)

IR (KBr): ν 3427, 2923, 2854, 2214, 1598, 1550, 1505, 1442, 1408, 1305, 1246, 1192, 1065, 805, 780, 727 cm^{-1}

Synthesis of 3-((4-bromobenzyl)oxy)-4-chloro-5,7-dimethylphenanthrene-9-carbonitrile (149):

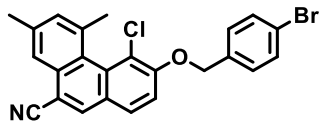

Similar synthetic procedure as above involving the use of 4-chloro-3-hydroxy-5,7-dimethylphenanthrene-9-carbonitrile **(140)** (0.1g; 0.36mmol) to furnish **(149)** (0.14g; Yield 85%) as colourless solid.

^{1}H NMR (400MHz, $CDCl_3$): δ 7.96 (s, 1H); 7.93 (s, 1H); 7.77-7.75 (d, *J*=8.4Hz, 1H); 7.56-7.54 (d, *J*=8.0Hz, 2H); 7.41-7.39 (d, *J*=8.0Hz, 2H); 7.36-7.34 (d, *J*=8.4Hz, 1H); 7.26 (s, 1H); 5.34-5.31 (d, *J*=11.6Hz, 1H); 5.26-5.23 (d, *J*=11.6Hz, 1H); 2.65 (s, 3H); 2.64 (s, 3H)

IR (KBr): ν 2957, 2924, 2854, 2219, 1594, 1544, 1506, 1438, 1409, 1377, 1284, 1157, 1076, 999, 803, 777, 468 cm^{-1}

Synthesis of 4-bromo-9-cyanophenanthren-3-yl((1*R*,2*S*,5*R*)-2-isopropyl-5-methyl cyclohexyl) carbonate (142):

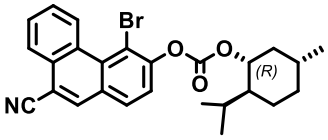

In a clean and dry round bottom flask, 4-bromo-3-hydroxyphenanthrene-9-carbonitrile **(130)** (0.2g; 0.67mmol) was dissolved in 10mL of AR grade MDC. The reaction mixture was cooled to 0°C using an ice bath. To this solution triethyl amine (0.12mL; 0.8mmol) was added followed by dropwise addition of (1*R*)-menthyl chloro formate (0.16mL; 0.74mmol) with vigourous stirring. The reaction mixture is allowed to stir at 0°C for 10 mins and then at room temperature for 4 hours. After the completion of the reaction (monitored by TLC), the reaction mixture is concentrated and subjected to purification by column chromatography on silica gel giving **(142)** as a colourless solid (0.28g; Yield 87%)

^{1}H NMR (400MHz, $CDCl_3$): δ 10.07-10.05 (dd, *J*=8.8Hz, 1.2Hz, 1H); 8.38-8.36 (dd, *J*=7.6Hz, 1.6Hz, 1H); 8.23 (s, 1H); 7.98-7.96 (d, *J*=8.8Hz, 1H); 7.87-7.78 (m, 2H); 7.60-7.58 (d, *J*=8.8Hz, 1H); 4.76-4.69 (dt, *J*=10.8Hz, 4.4Hz, 1H); 2.27-2.24 (m, 1H); 2.20-2.15 (m, 1H); 1.80-1.73 (m, 2H); 1.61-1.54 (m, 2H); 1.29-1.15 (m, 1H); 1.14-1.11 (m, 1H); 1.01-1.00 (d, *J*=1.6Hz, 3H); 1.99-1.98 (d, *J*=1.6Hz, 3H); 0.97-0.96 (m, 1H); 0.91-0.89 (d, *J*=6.8Hz, 3H)

^{13}C NMR (100MHz, $CDCl_3$): δ 152.3; 150.5; 135.0; 131.6; 130.5; 130.4; 130.0; 129.8; 128.9; 127.5; 127.0; 126.0; 122.7; 117.3; 114.5; 110.7; 80.7; 47.0; 40.6; 34.0; 31.5; 26.3; 23.4; 22.0; 20.7; 16.4

IR (KBr): ν 2957, 2923, 2869, 2226, 1758, 1492, 1451, 1370, 1276, 1228, 1149, 1075, 952, 916, 764, 711 cm^{-1}

Synthesis of 2,4-dibromo-9-cyano-5,7-dimethylphenanthren-3-yl ((1*R*,2*S*,5*R*)-2-isopropyl-5-methylcyclohexyl) carbonate (143):

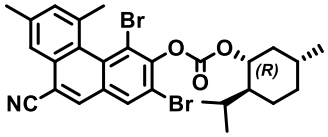

Similar synthetic procedure as above involving the use of 2,4-dibromo-3-hydroxy-5,7-dimethylphenanthrene-9-carbonitrile **(139)** (0.1g; 0.25mmol) to furnish **(143)** (0.13g; Yield 90%)

^{1}H NMR (400MHz, $CDCl_3$): δ 8.13-8.10 (dd, *J*=10.8Hz, 1.2Hz, 1H); 7.97-7.92 (d, *J*=18.4Hz, 1H); 7.92-7.88 (d, *J*=16.8Hz, 1H); 7.43 (s, 1H); 4.78-4.71 (dt, *J*=10.4Hz, 4.4Hz, 1H); 2.79-2.71 (m, 4H); 2.61 (s, 2H); 2.28-2.15 (m, 2H); 1.78-1.73 (m, 2H); 1.56-1.54 (m, 2H); 1.30-1.20 (m, 1H); 1.14-1.11 (m, 1H); 0.99-0.97 (d, *J*=7.2Hz, 6H); 0.93-0.92 (m, 1H); 0.93-0.86 (dd, *J*=14.6Hz, 7.6Hz, 3H)

Synthesis of 4-chloro-9-cyano-5,7-dimethylphenanthren-3-yl ((1*R*,2*S*,5*R*)-2-isopropyl-5-methylcyclohexyl) carbonate (148):

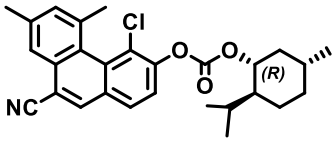

Similar synthetic procedure as above involving the use of 4-chloro-3-hydroxy-5,7-dimethylphenanthrene-9-carbonitrile **(140)** (0.1g; 0.36mmol) to furnish 4-chloro-9-cyano-5,7-dimethylphenanthren-3-yl ((1*R*,2*S*,5*R*)-2-isopropyl-5-methylcyclohexyl) carbonate **(148)** (0.15g; Yield 90%)

^{1}H NMR (400MHz, $CDCl_3$): δ 8.03 (s, 1H); 7.89 (s, 1H); 7.85-7.83 (d, *J*=8.4Hz, 1H); 7.56-7.53 (dd, *J*=8.4Hz, 3.6Hz, 1H); 7.43 (s, 1H); 4.78-4.69 (m, 1H); 2.68-2. (d, *J*=4.8Hz, 3H); 2.60 (s, 3H); 2.26-2.18 (m, 1H); 2.16-2.11 (m, 1H); 1.75-1.73 (m, 2H); 1.58-1.52 (m, 2H); 1.27-1.21 (m, 2H); 1.14-1.10 (m, 1H); 0.99-0.97 (d, *J*=6.4Hz, 6H); 0.93-0.84 (d, *J*=6.8Hz, 3H)

IR (KBr): ν 2956, 2921, 2852, 2223, 1756, 1608, 1455, 1374, 1286, 1232, 1180, 1075, 959, 891, 773 cm^{-1}

2.3.2.6 Spectral Data:

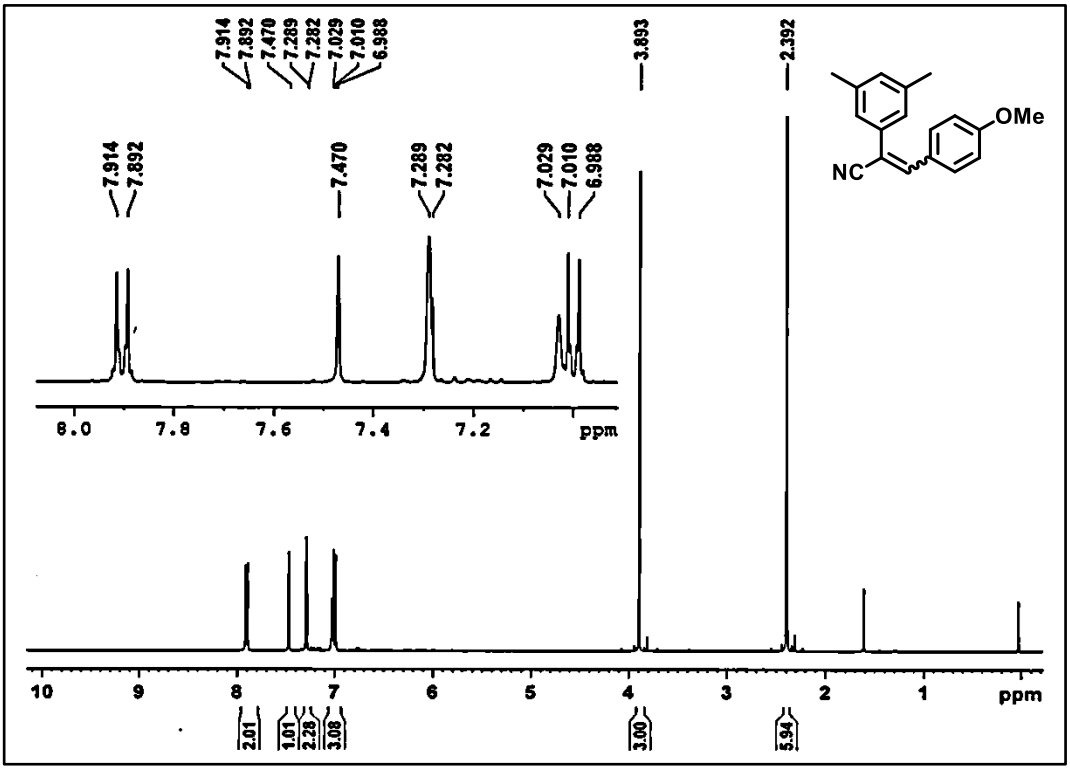

^{1}H NMR Spectra of compound **134** ($CDCl_3$, 400MHz)

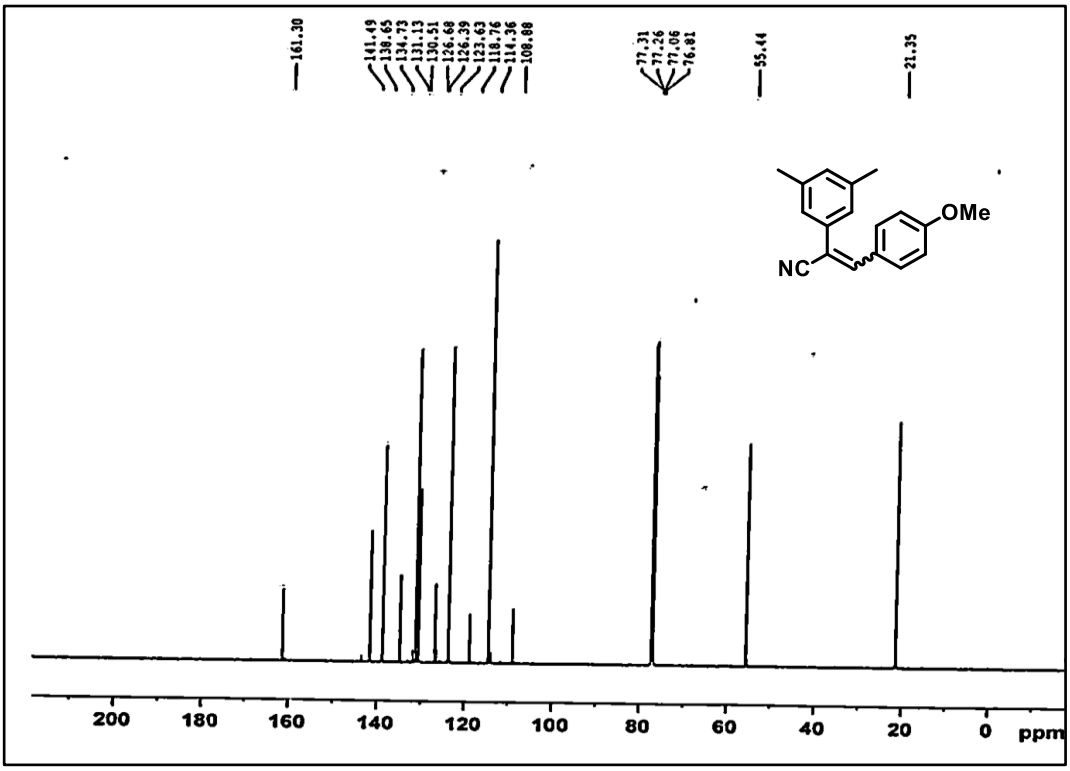

^{13}C NMR Spectra of compound **134** ($CDCl_3$, 100MHz)

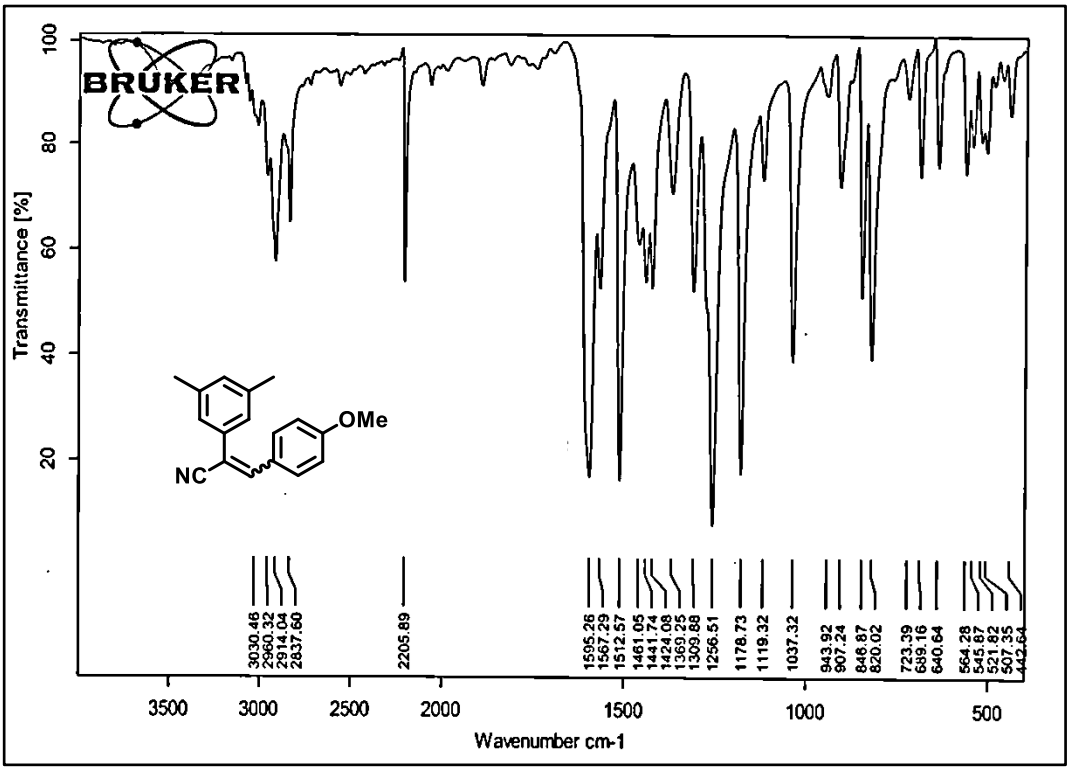

IR Spectra of compound **134**

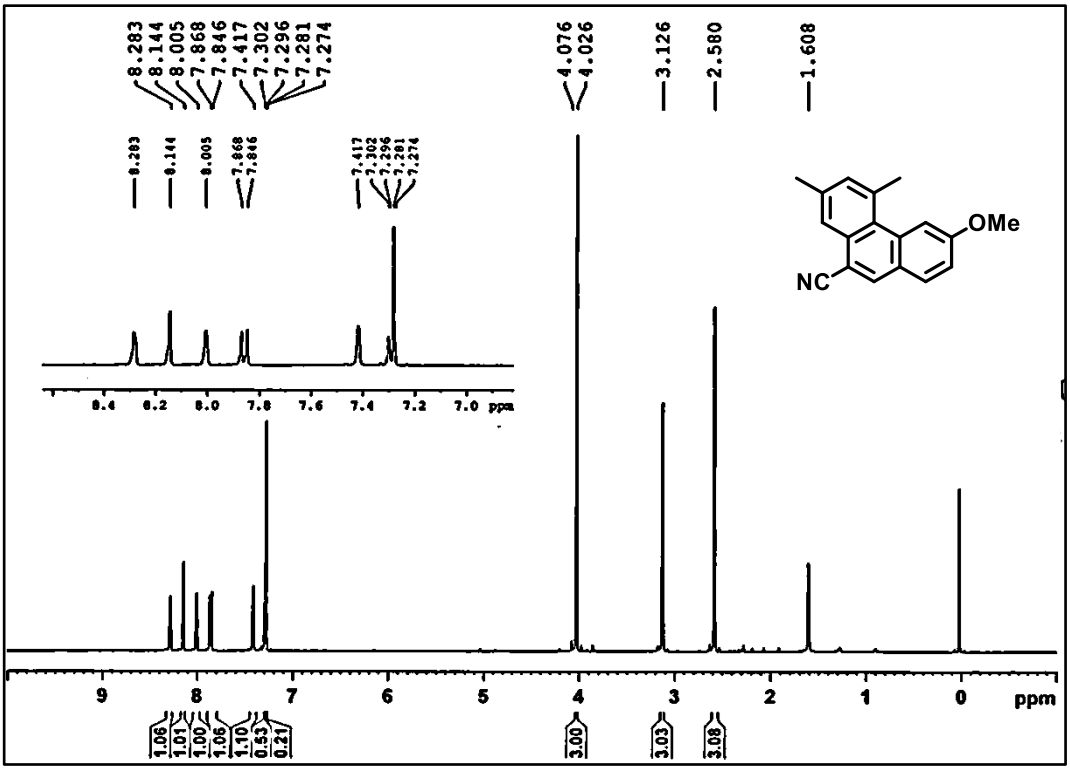

^{1}H NMR Spectra of compound **135** ($CDCl_3$, 400MHz)

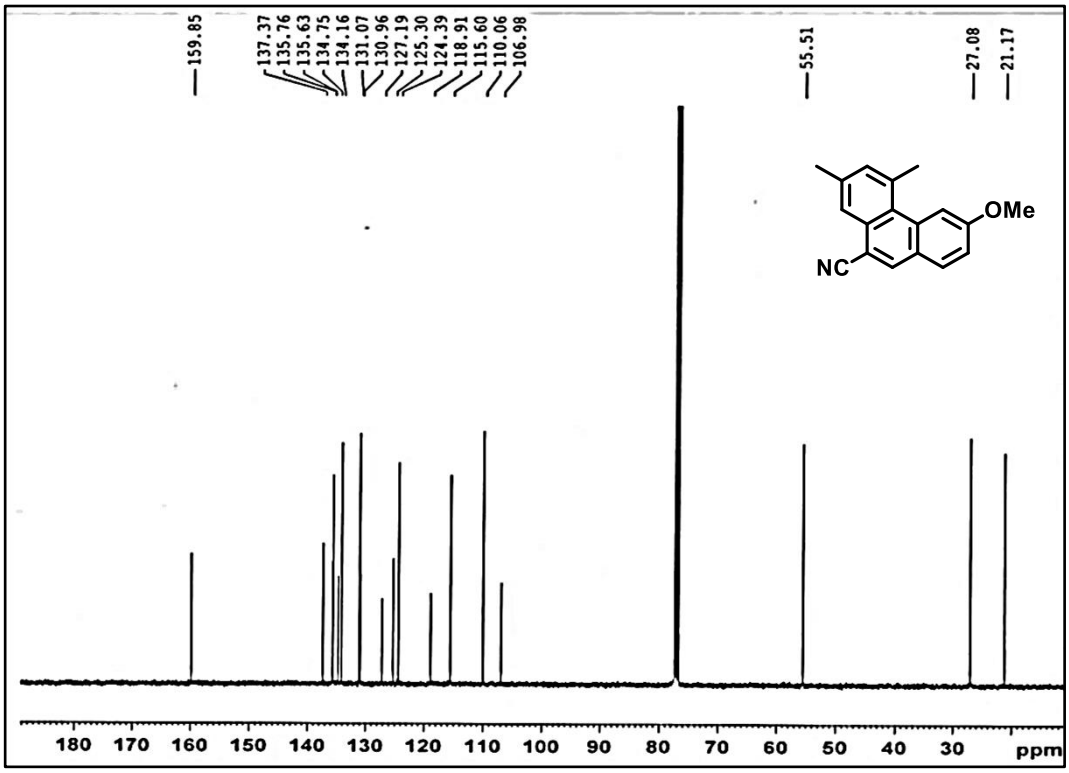

^{13}C NMR Spectra of compound **135** ($CDCl_3$, 100MHz)

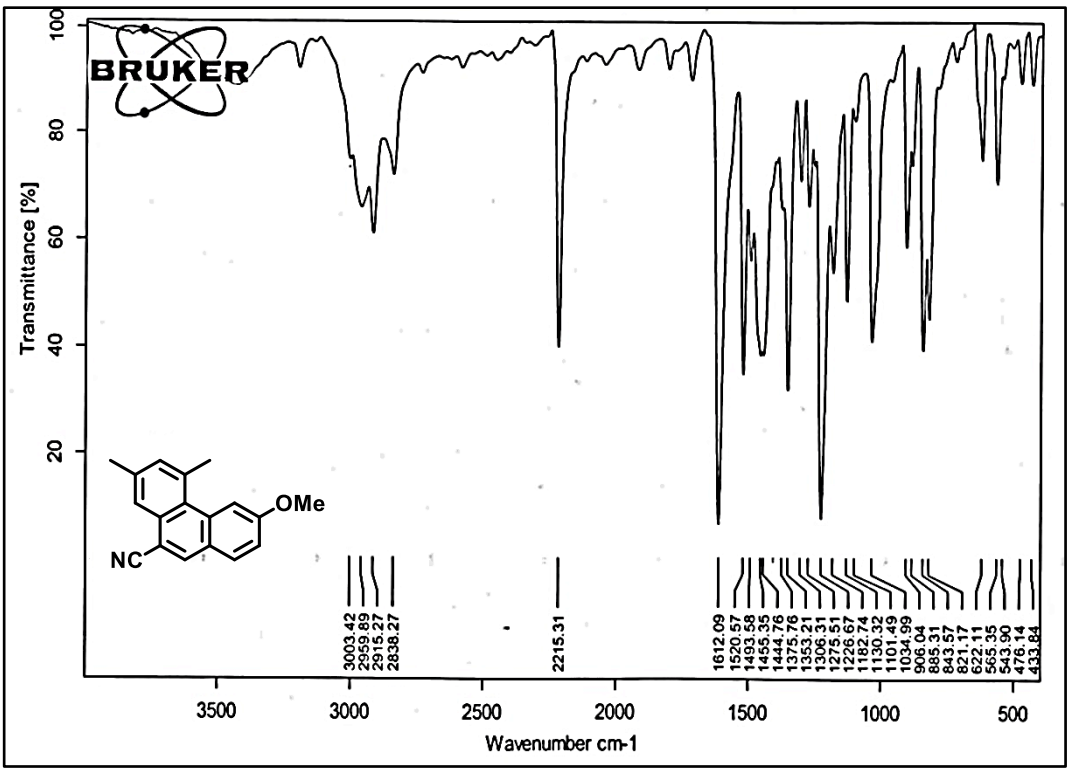

IR Spectra of compound **135**

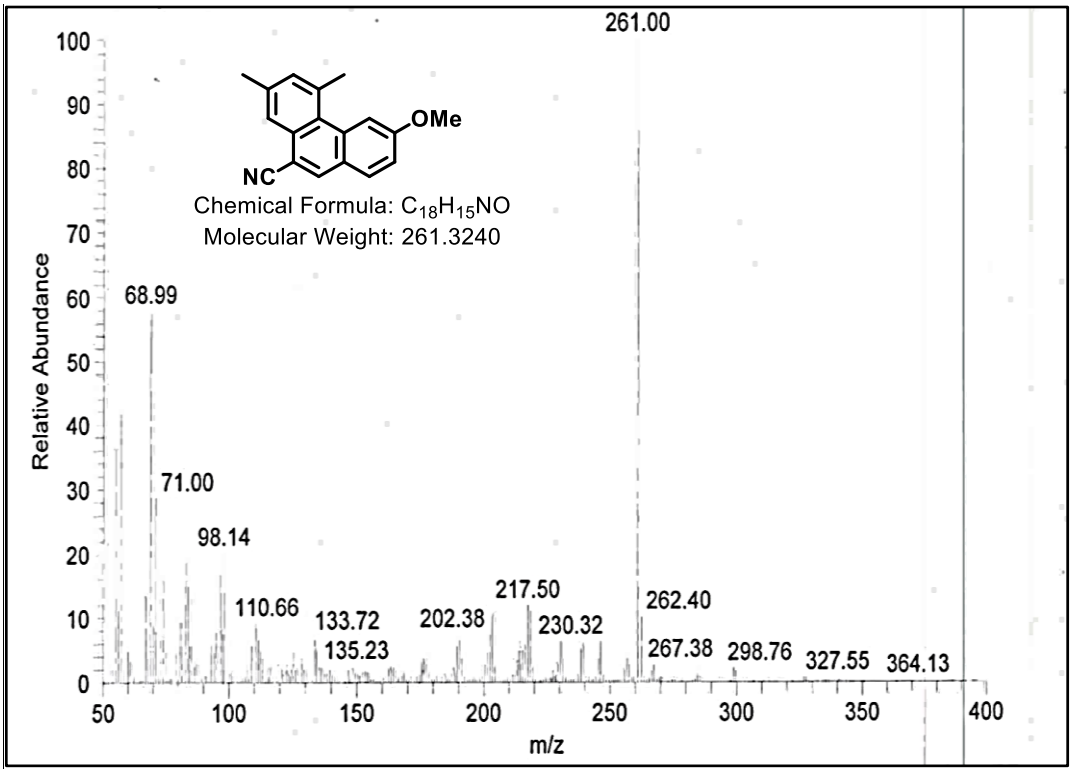

Mass Spectra of compound **135**

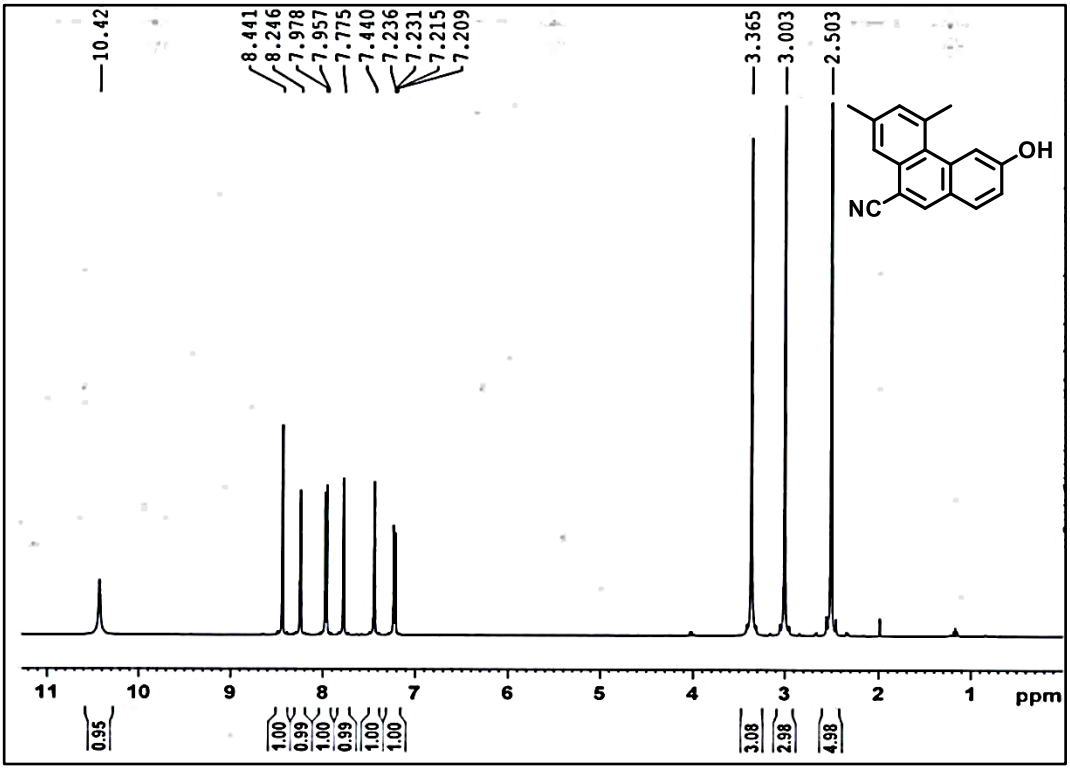

^{1}H NMR Spectra of compound **136** (d_6-DMSO, 400MHz)

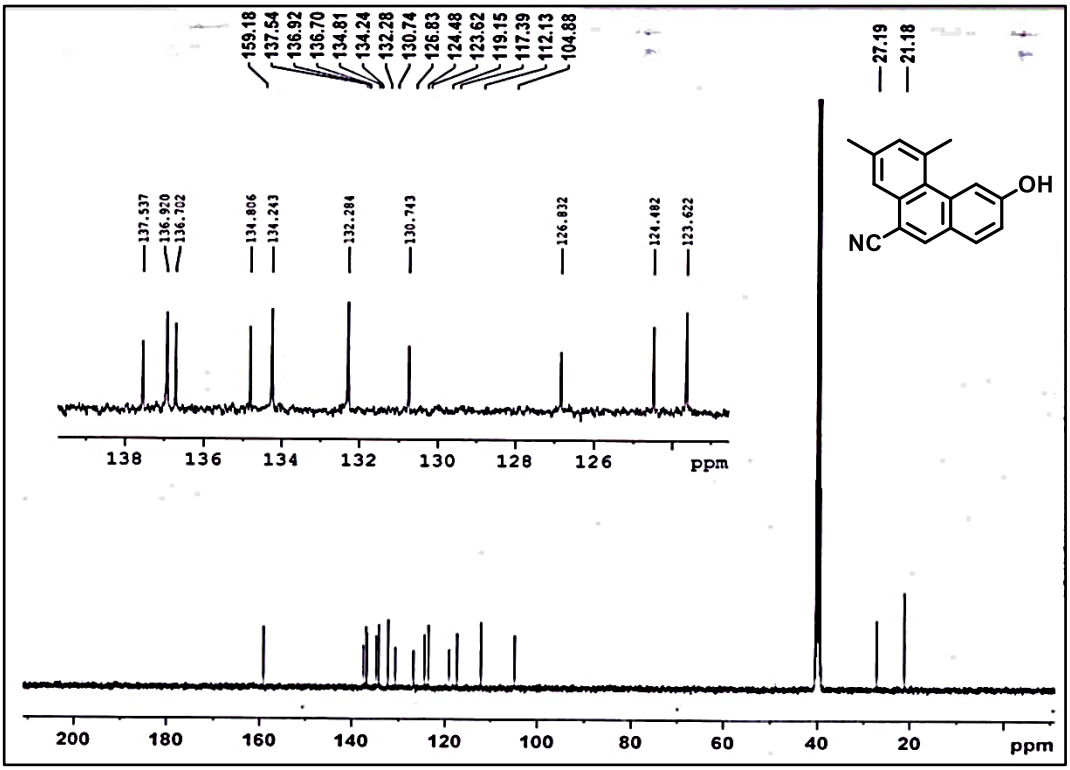

^{13}C NMR Spectra of compound **136** (d_6-DMSO, 100MHz)

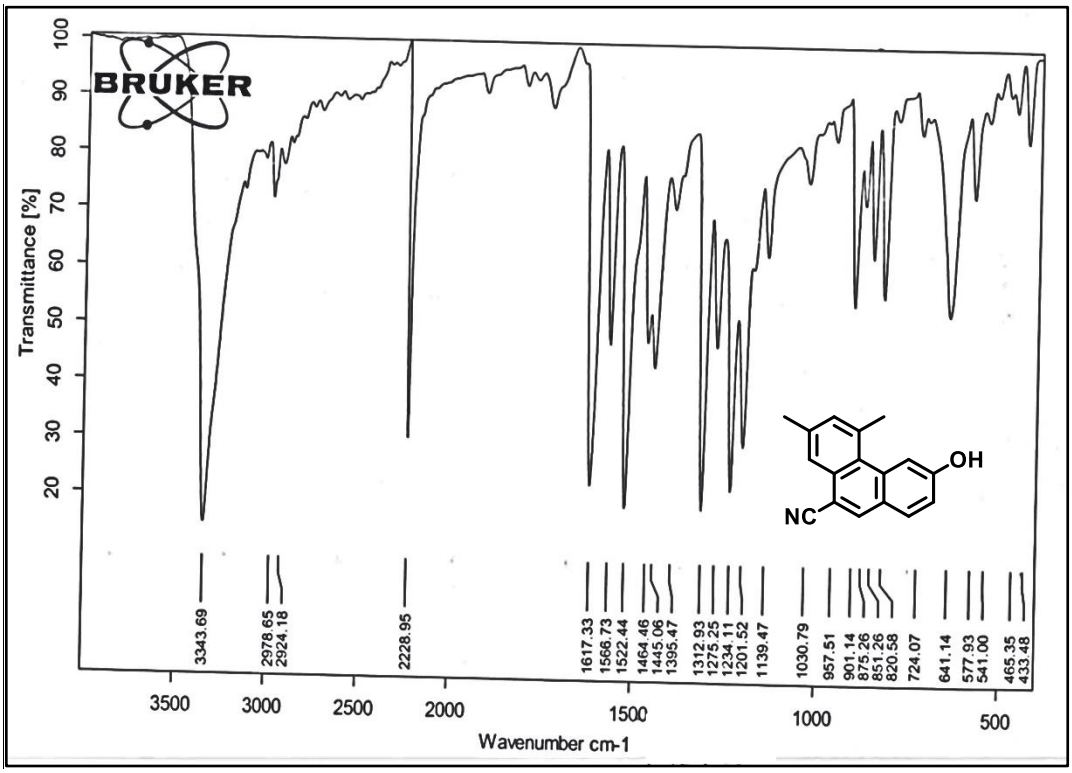

IR Spectra of compound **136**

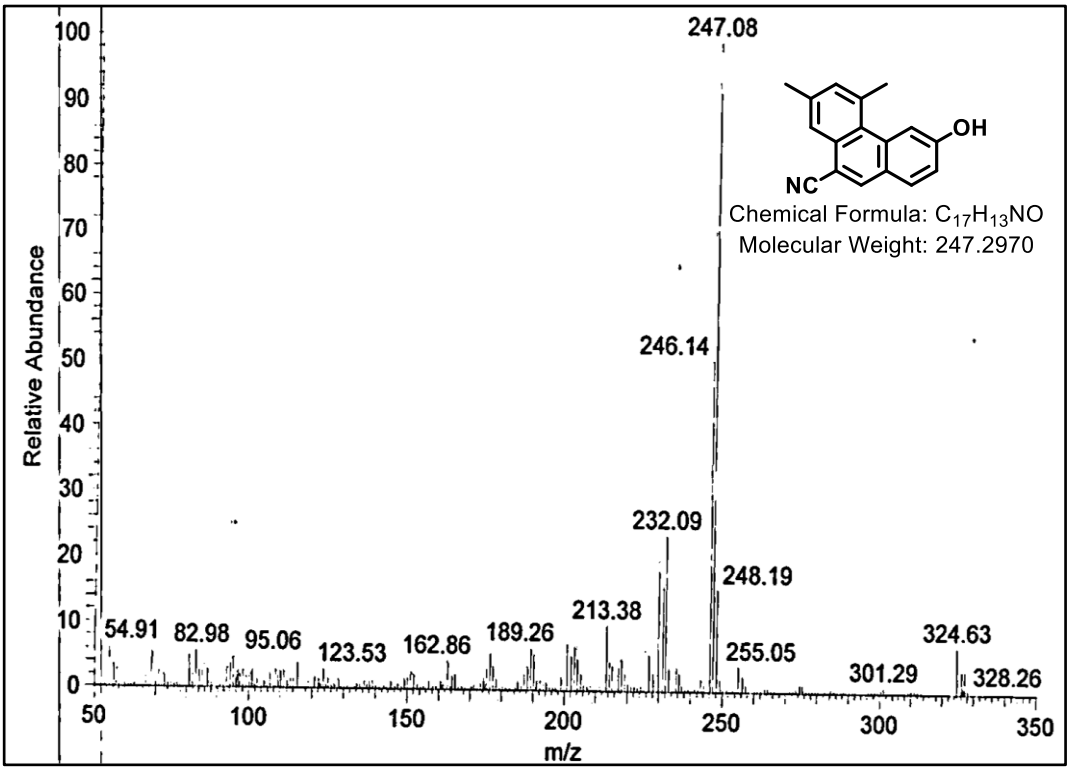

Mass Spectra of compound **136**

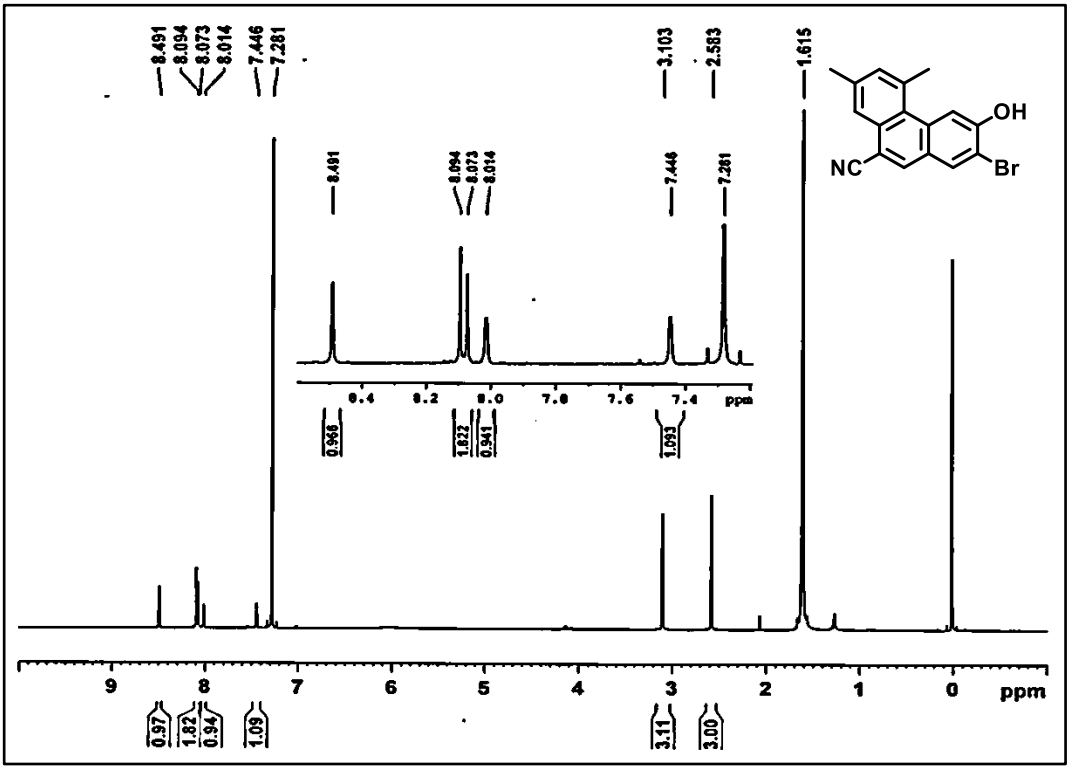

^{1}H NMR Spectra of compound **138** ($CDCl_3$, 400MHz)

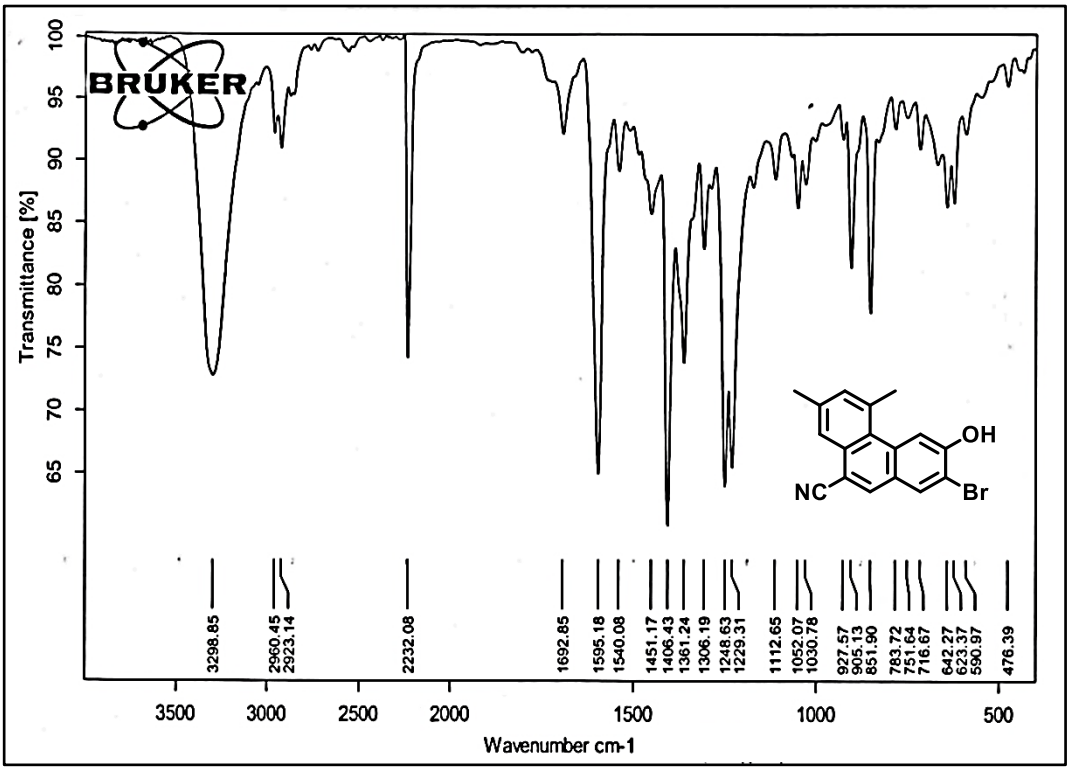

IR Spectra of compound **138**

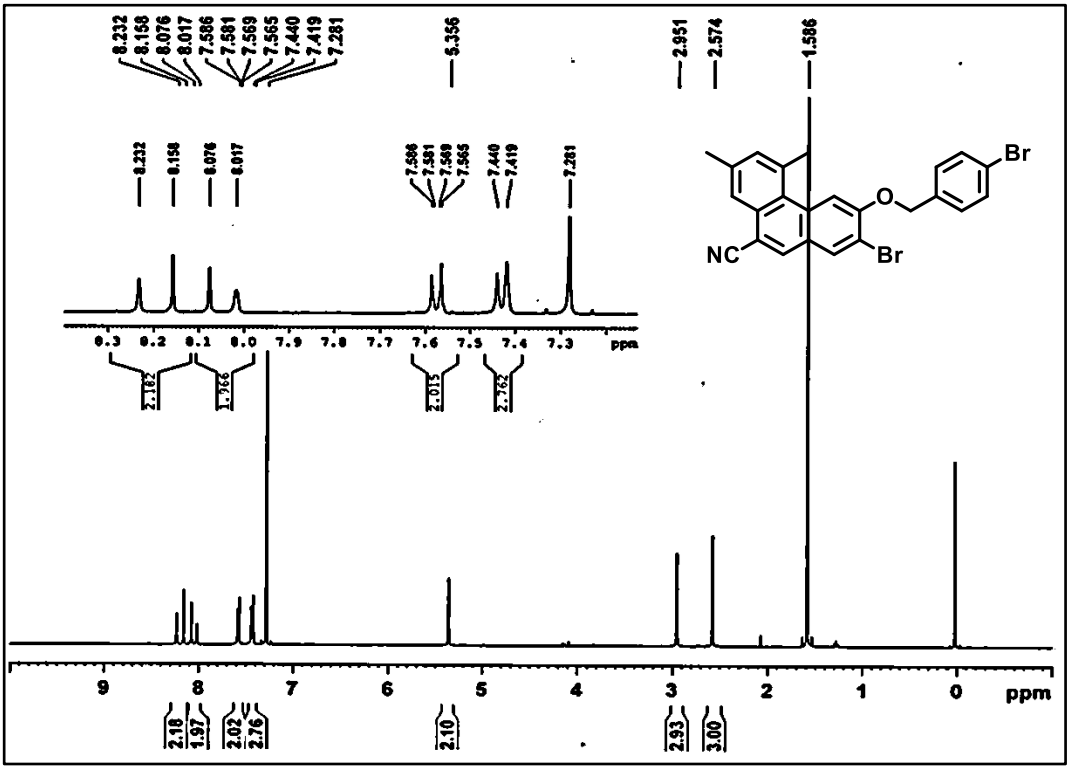

^{1}H NMR Spectra of compound **145** ($CDCl_3$, 400MHz)

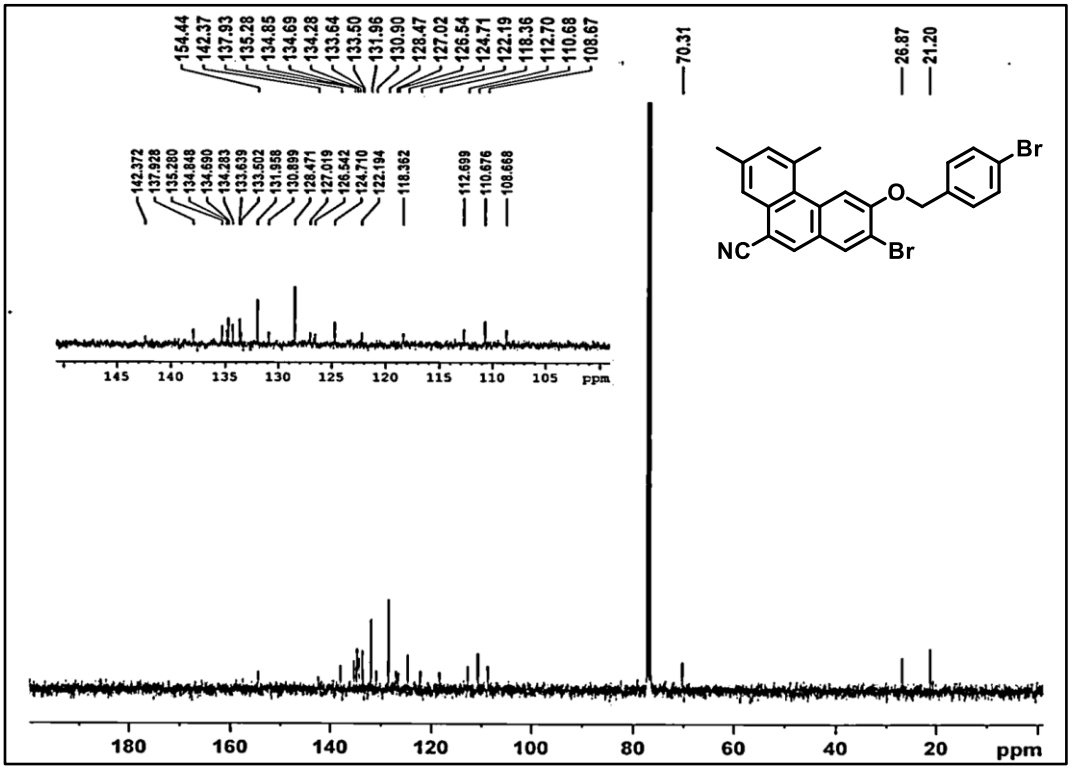

^{13}C NMR Spectra of compound **145** ($CDCl_3$, 400MHz)

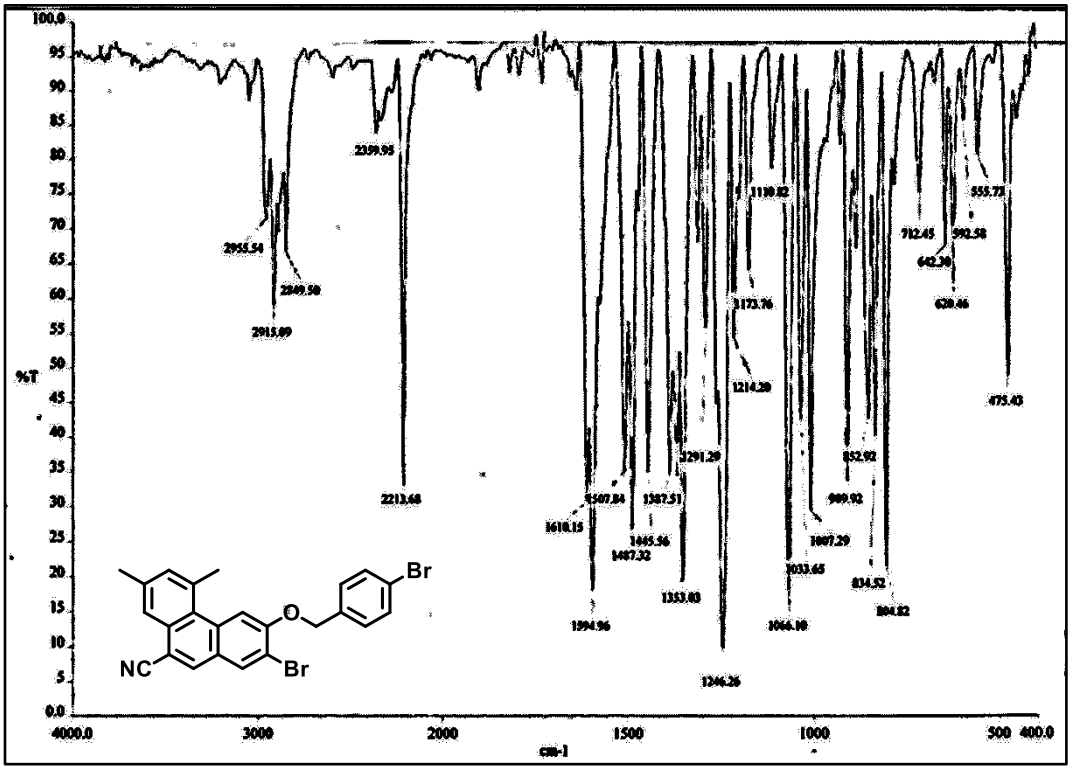

IR Spectra of compound **145**

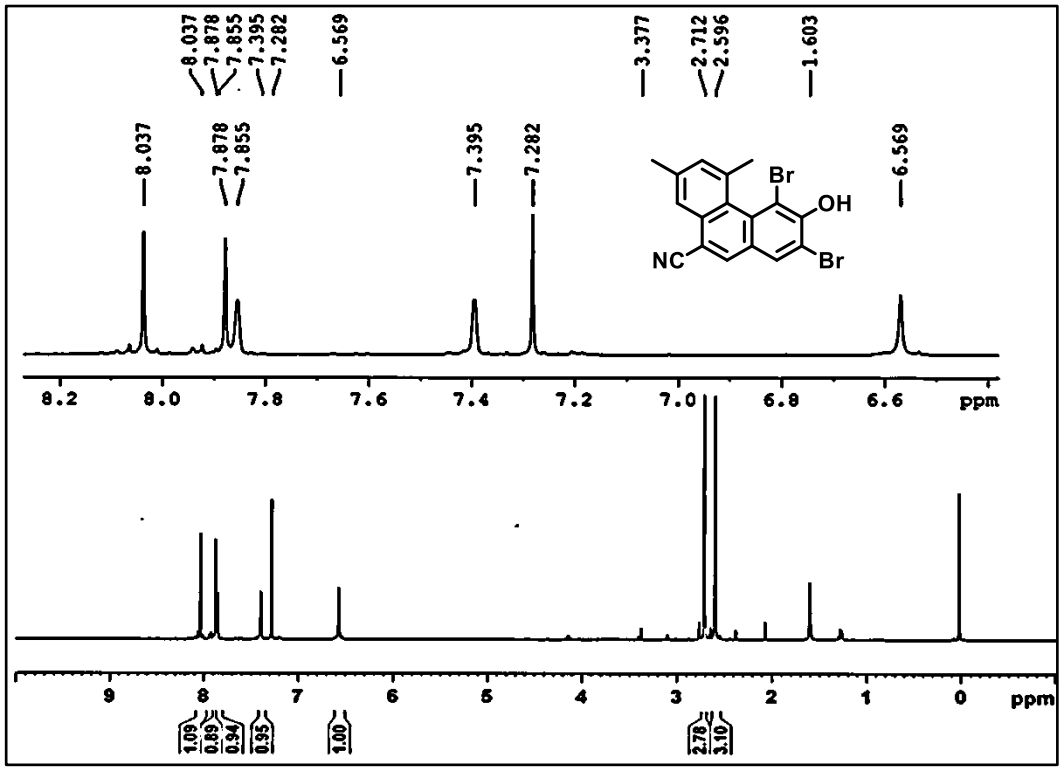

^{1}H NMR Spectra of compound **139** ($CDCl_3$, 400MHz)

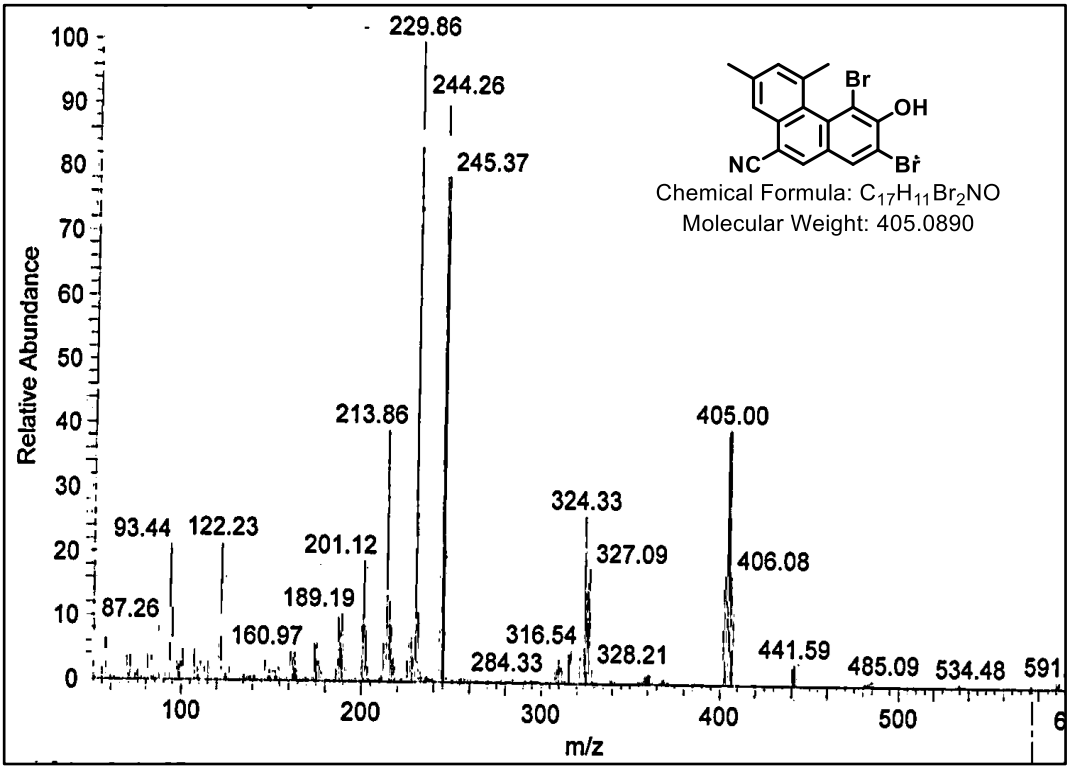

Mass Spectra of compound **139**

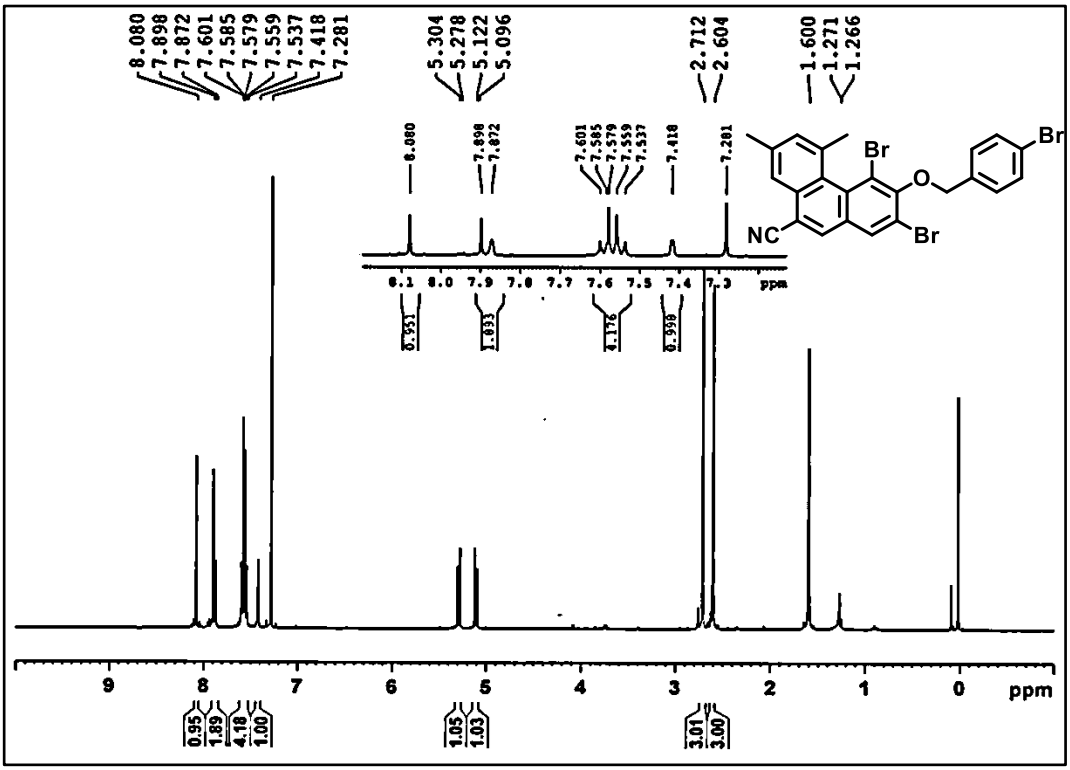

^{1}H NMR Spectra of compound **144** ($CDCl_3$, 400MHz)

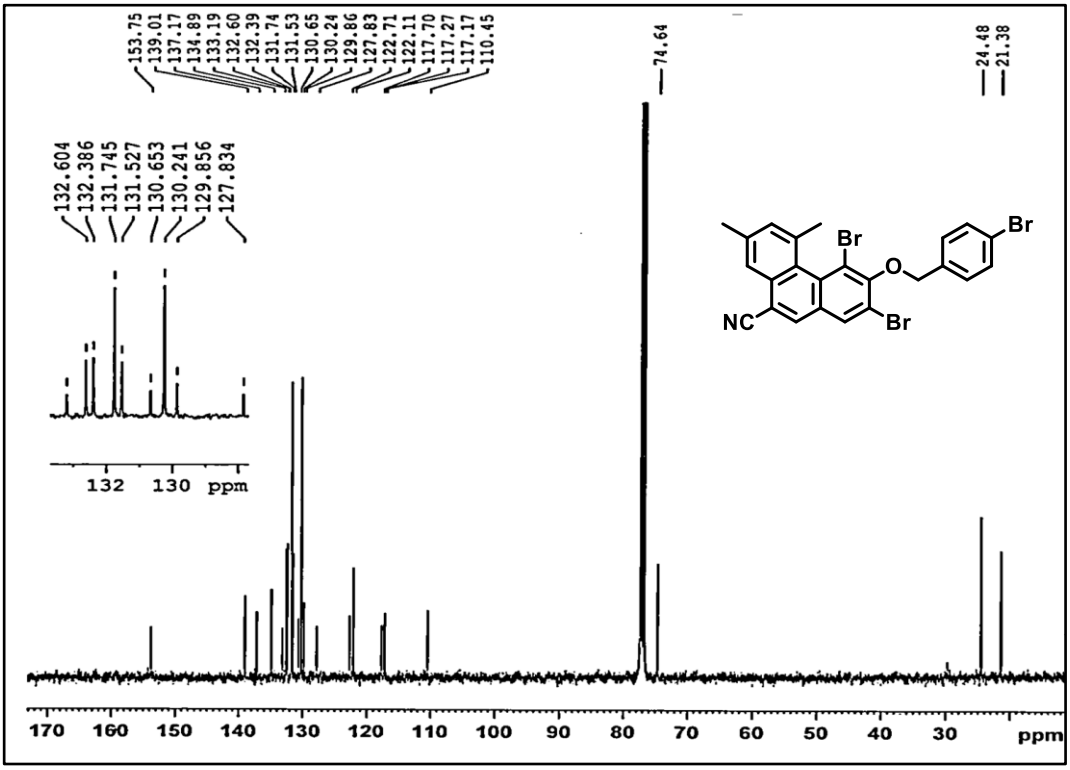

^{13}C NMR Spectra of compound **144** ($CDCl_3$, 100MHz)

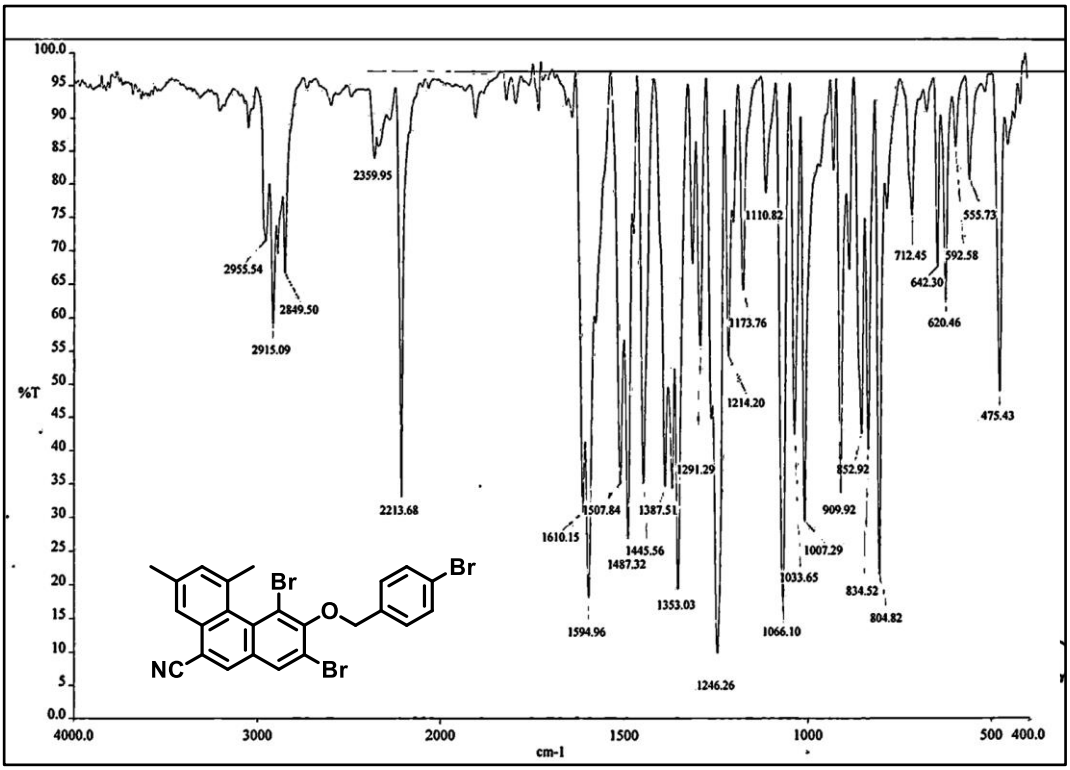

IR Spectra of compound **144**

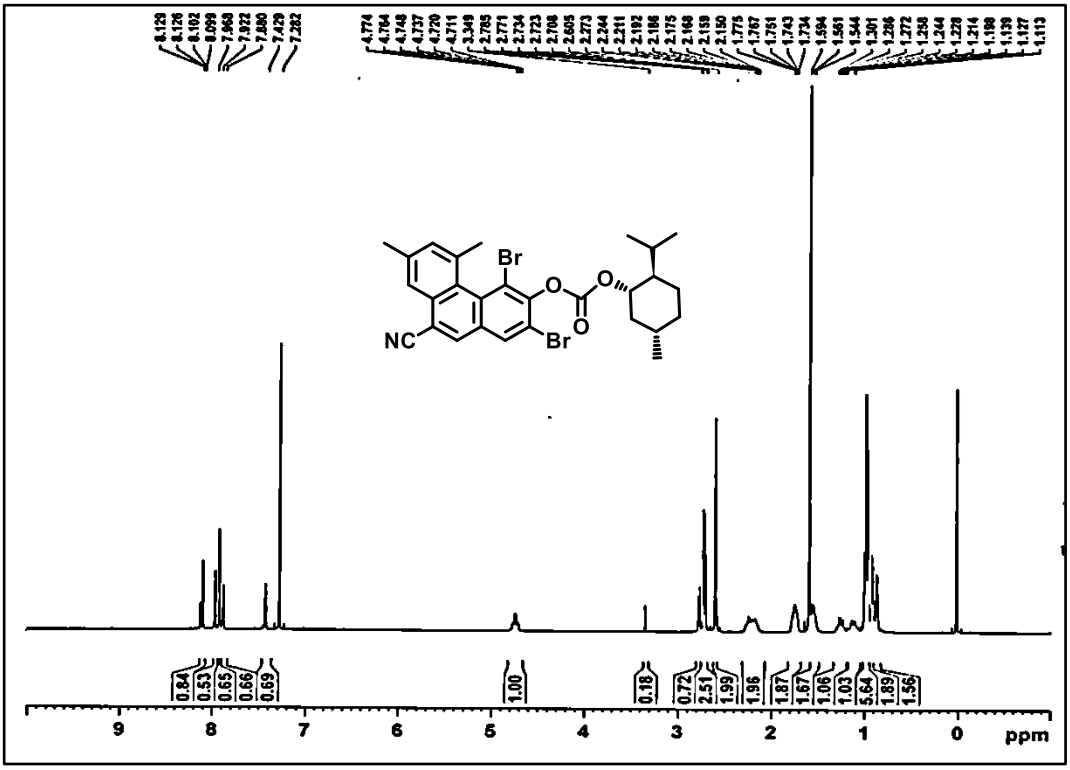

^{1}H NMR Spectra of compound **143** ($CDCl_3$, 400MHz)

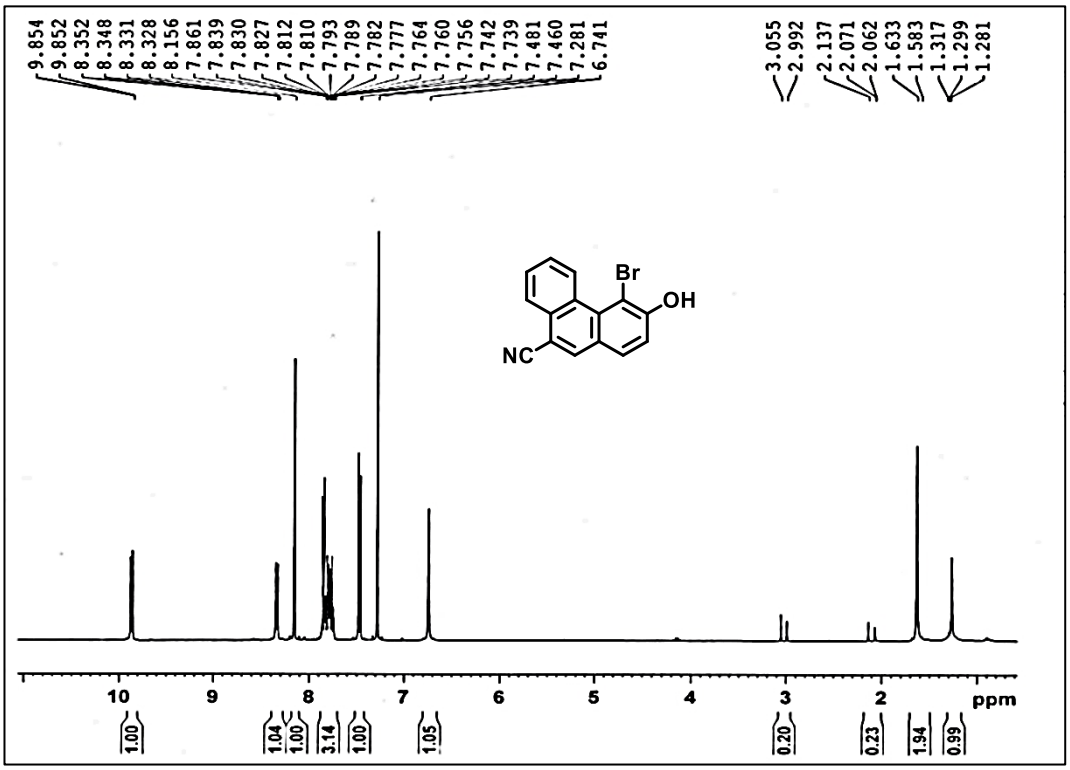

^{1}H NMR Spectra of compound **130** ($CDCl_3$, 400MHz)

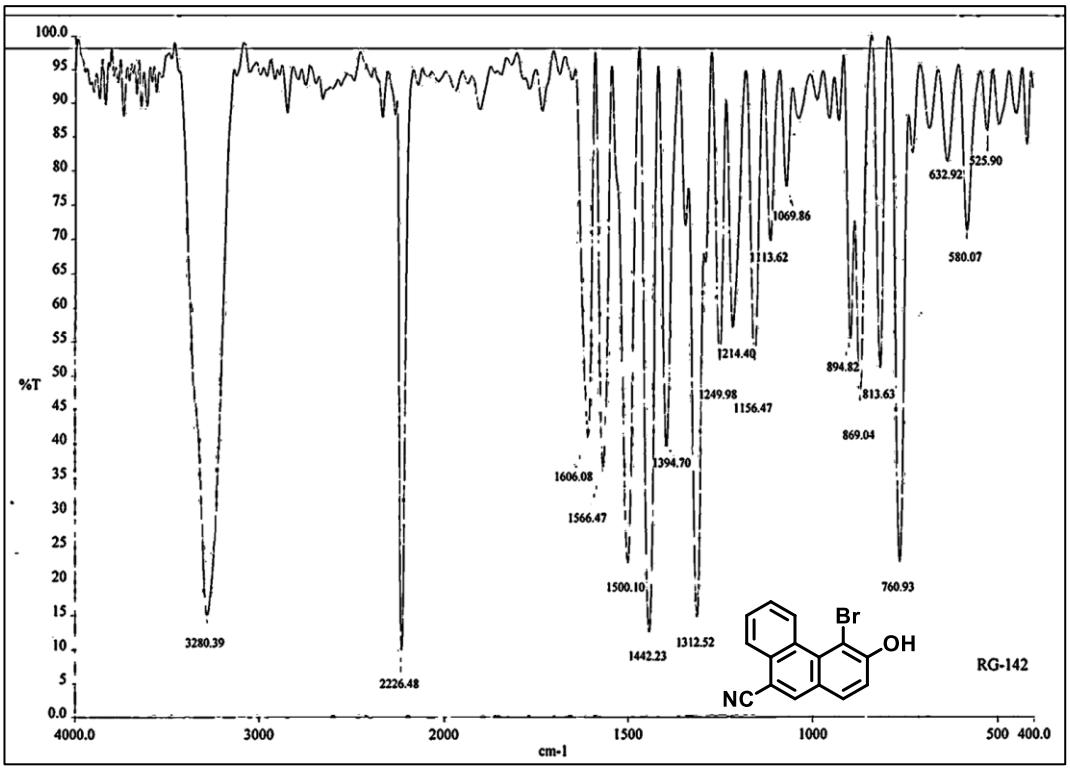

IR Spectra of compound **130**

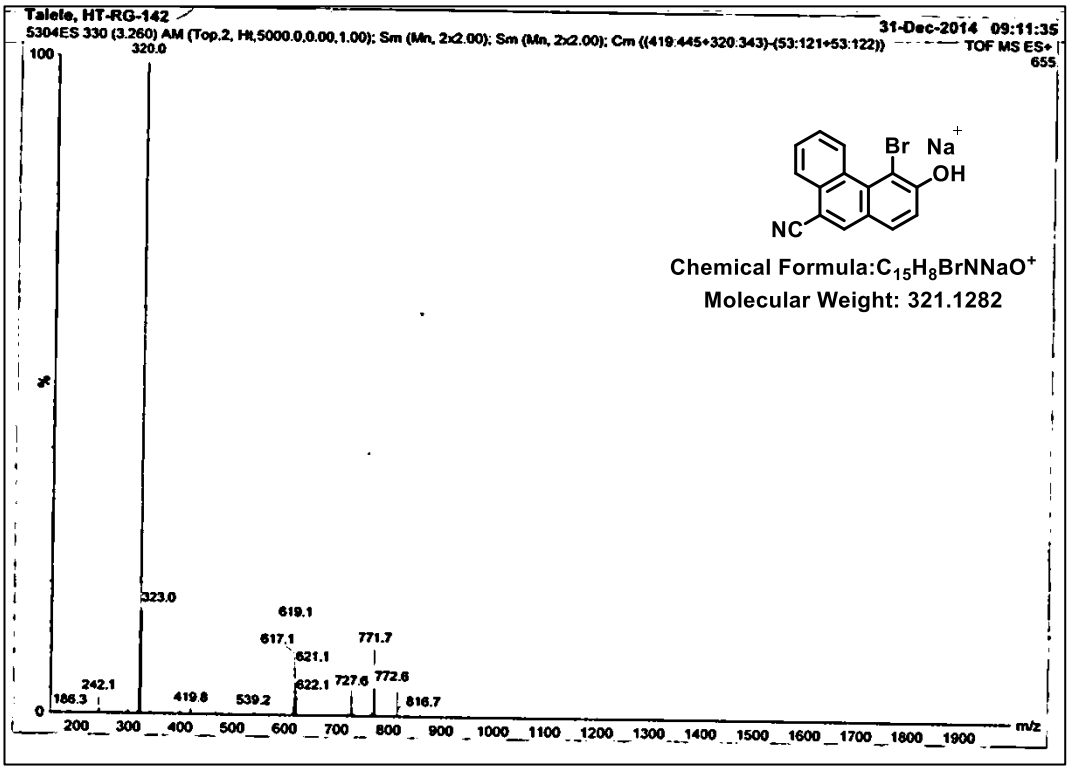

Mass Spectra of compound **130**

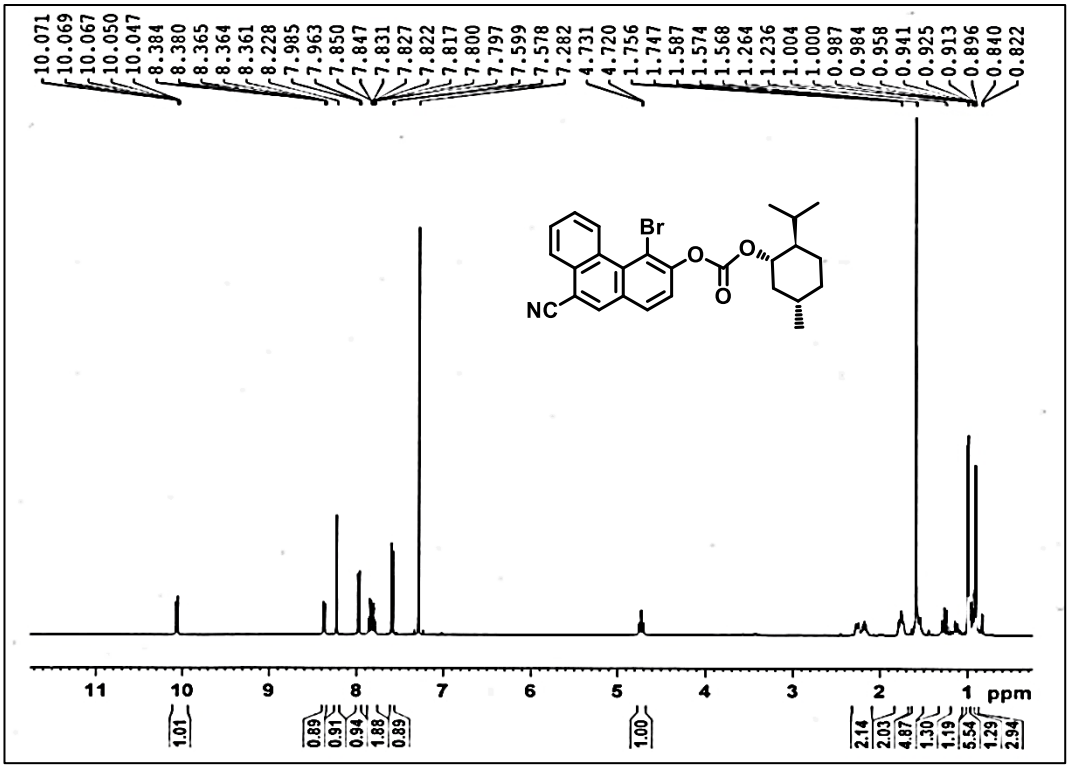

^{1}H NMR Spectra of compound **142** ($CDCl_3$, 400MHz)

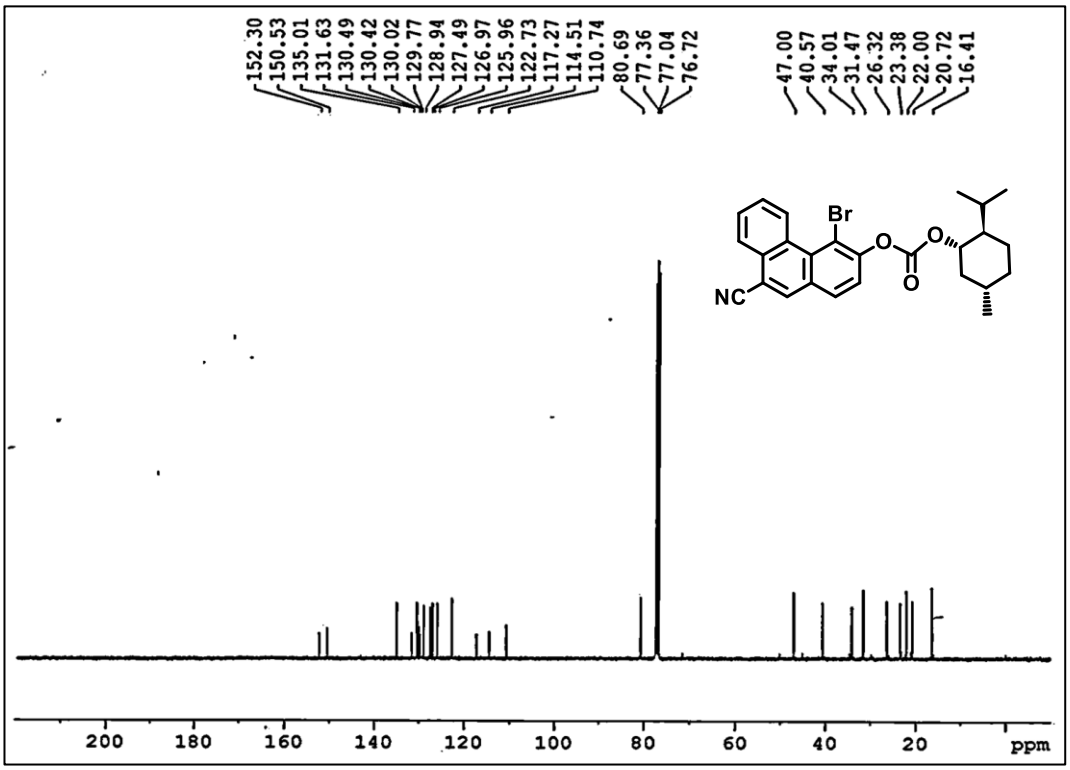

^{13}C NMR Spectra of compound **142** ($CDCl_3$, 100MHz)

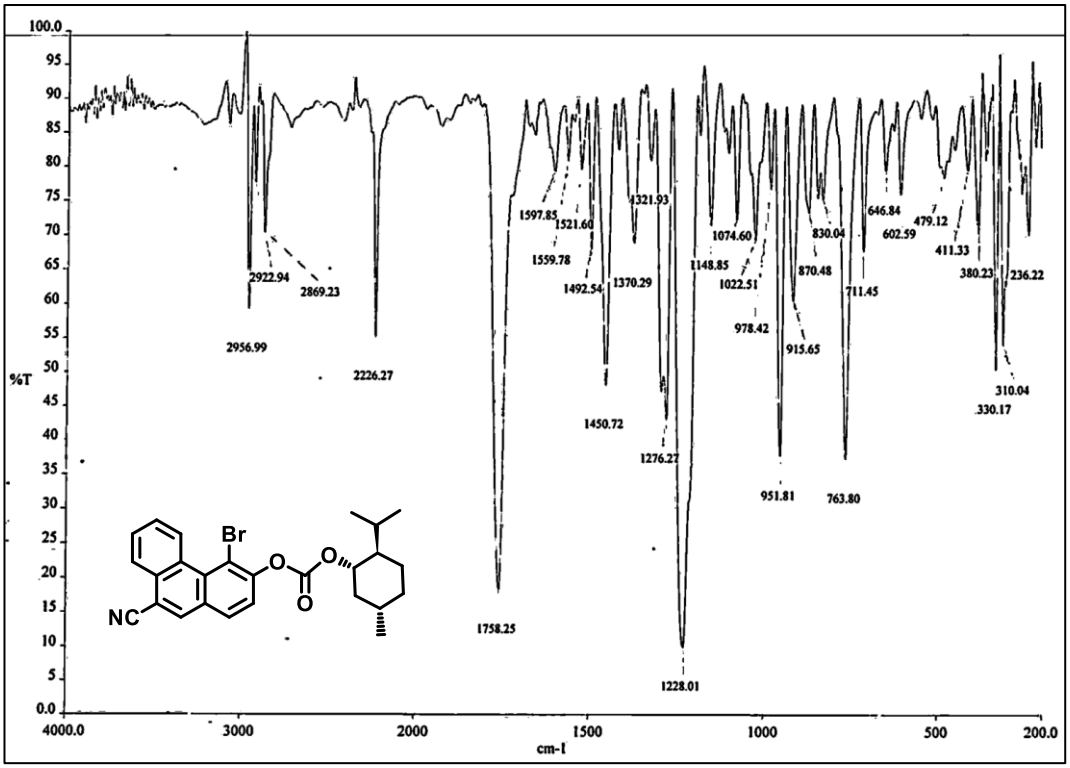

IR Spectra of compound **142**

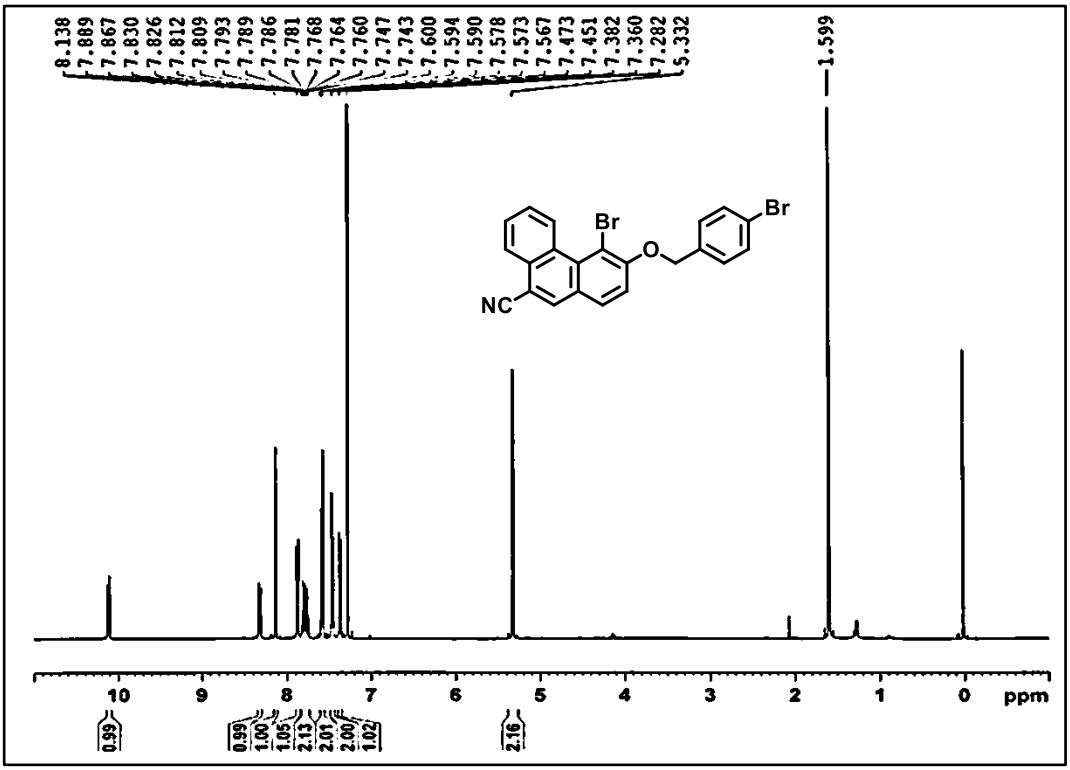

^{1}H NMR Spectra of compound **141** ($CDCl_3$, 400MHz)

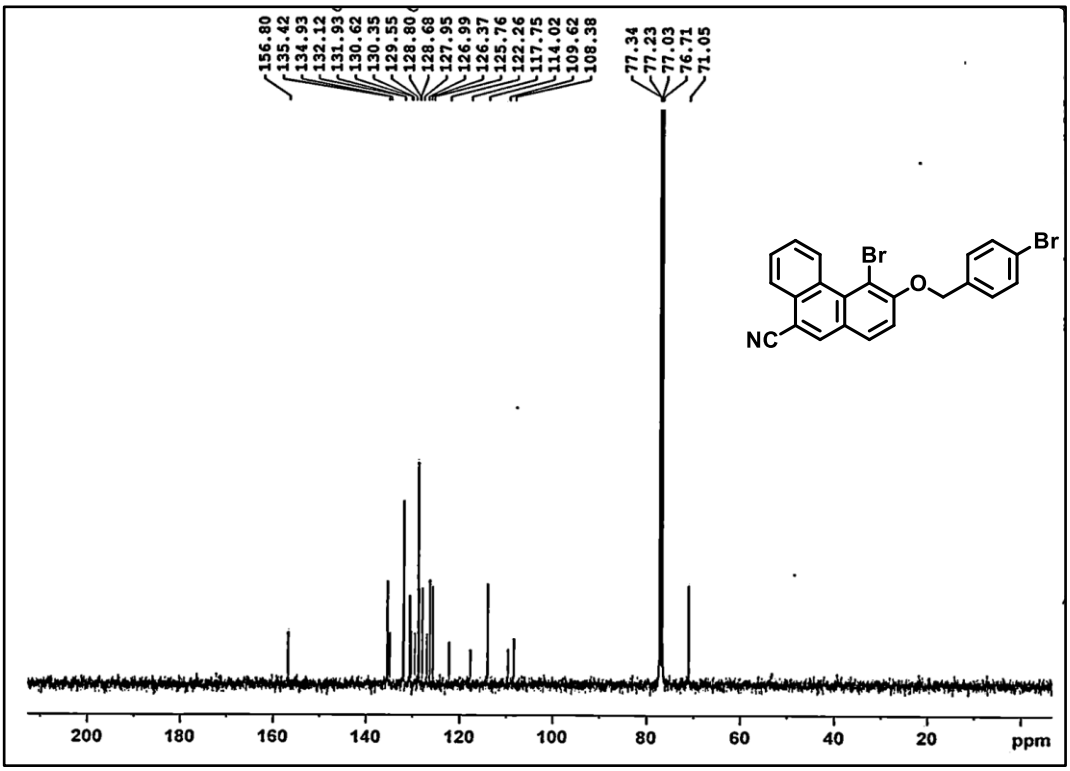

^{13}C NMR Spectra of compound **141** ($CDCl_3$, 100MHz)

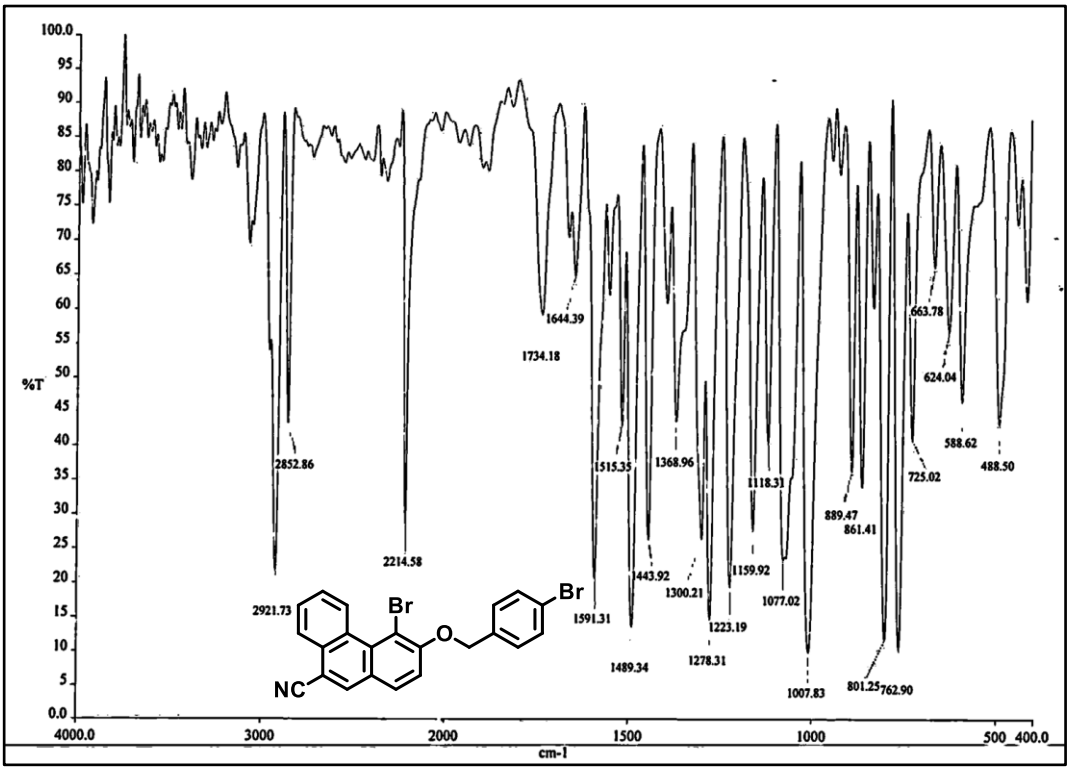

IR Spectra of compound **141**

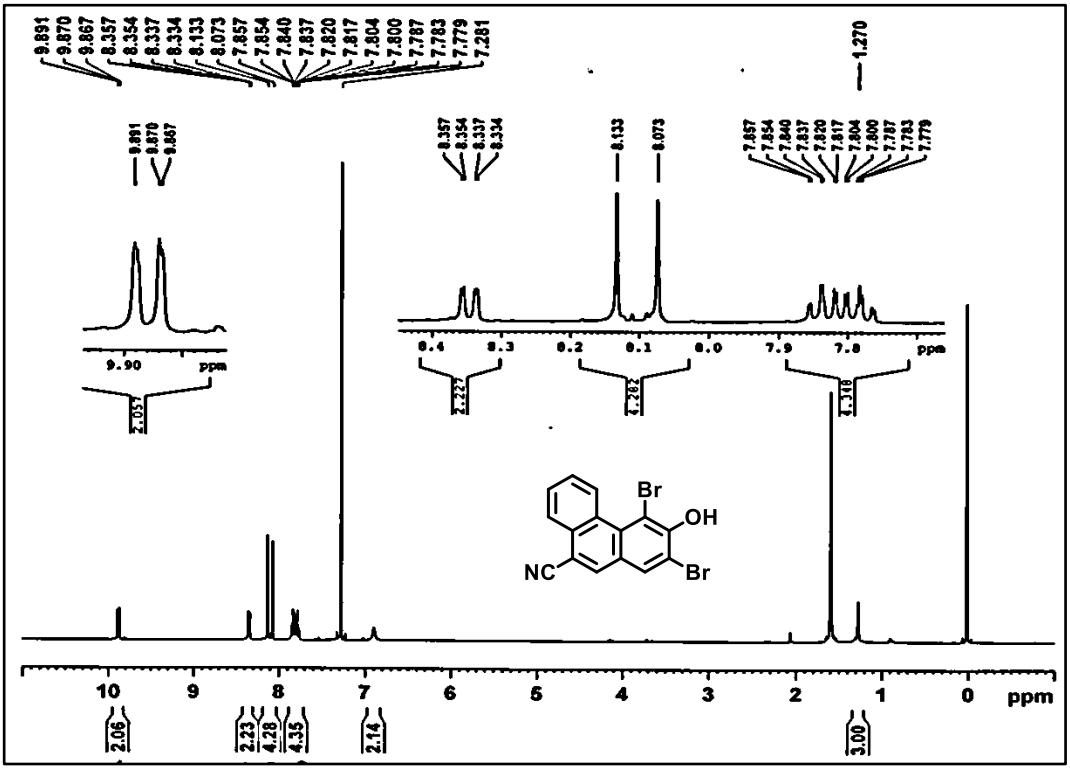

^{1}H NMR Spectra of compound **146** ($CDCl_3$, 400MHz)

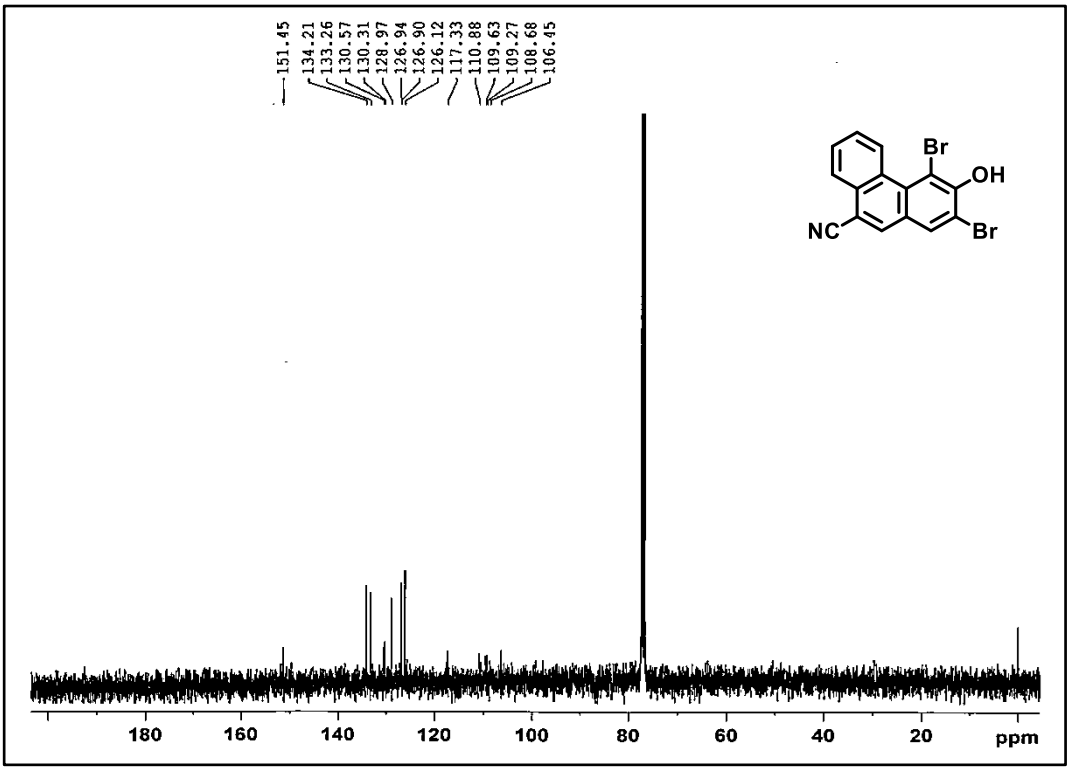

^{13}C NMR Spectra of compound **146** ($CDCl_3$, 100MHz)

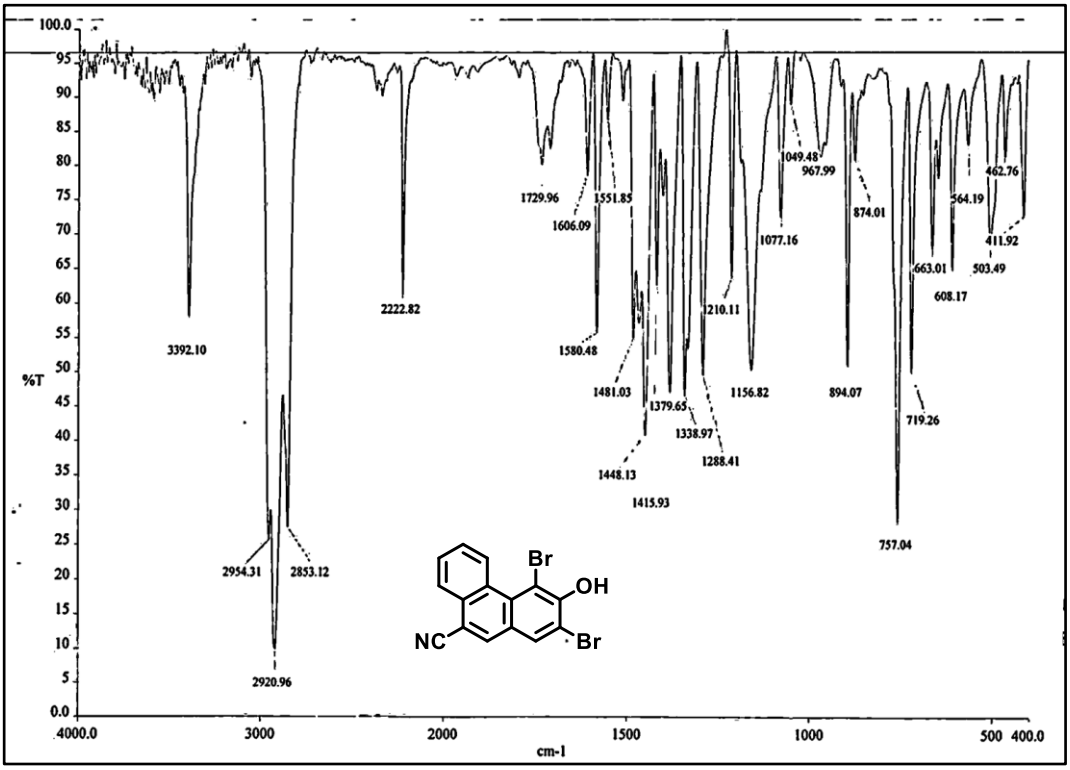

IR Spectra of compound **146**

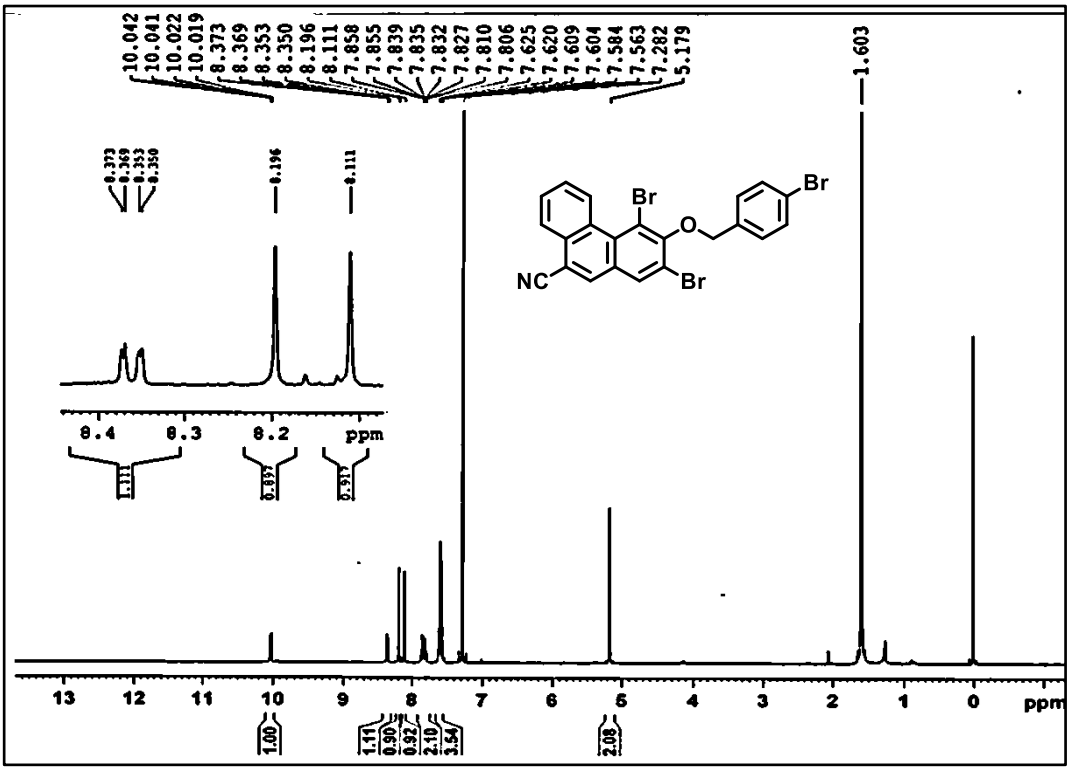

^{1}H NMR Spectra of compound **147** ($CDCl_3$, 400MHz)

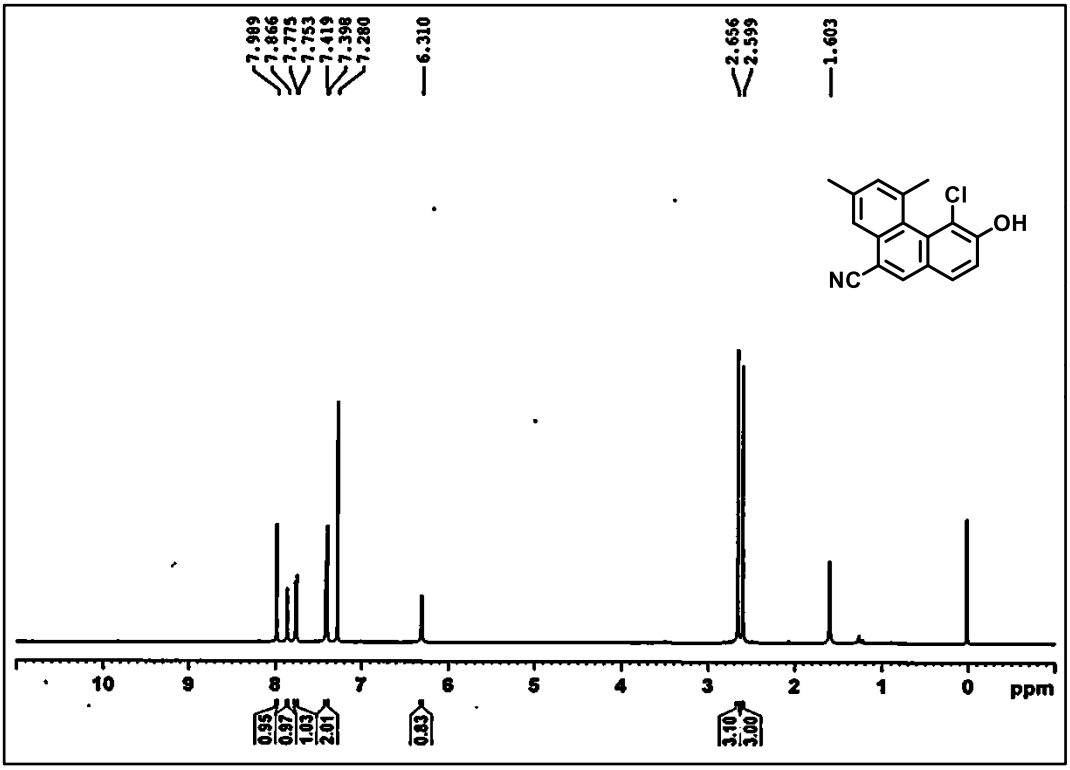

^{1}H NMR Spectra of compound **140** ($CDCl_3$, 400MHz)

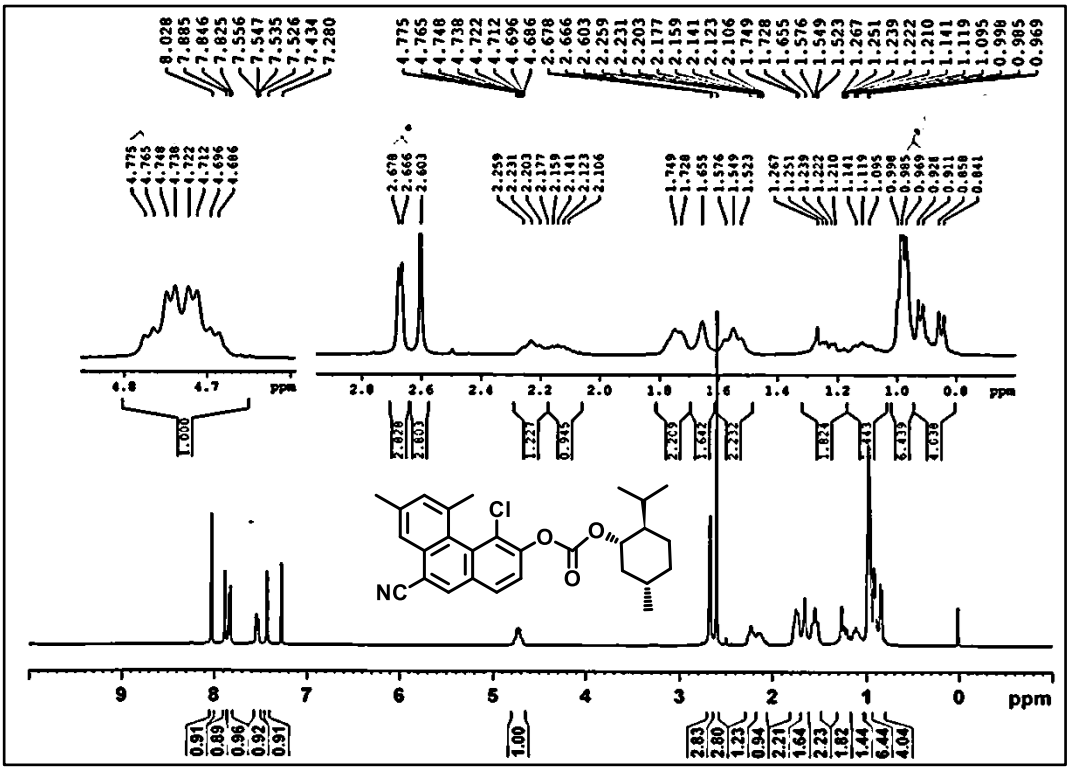

^{1}H NMR Spectra of compound **148** ($CDCl_3$, 400MHz)

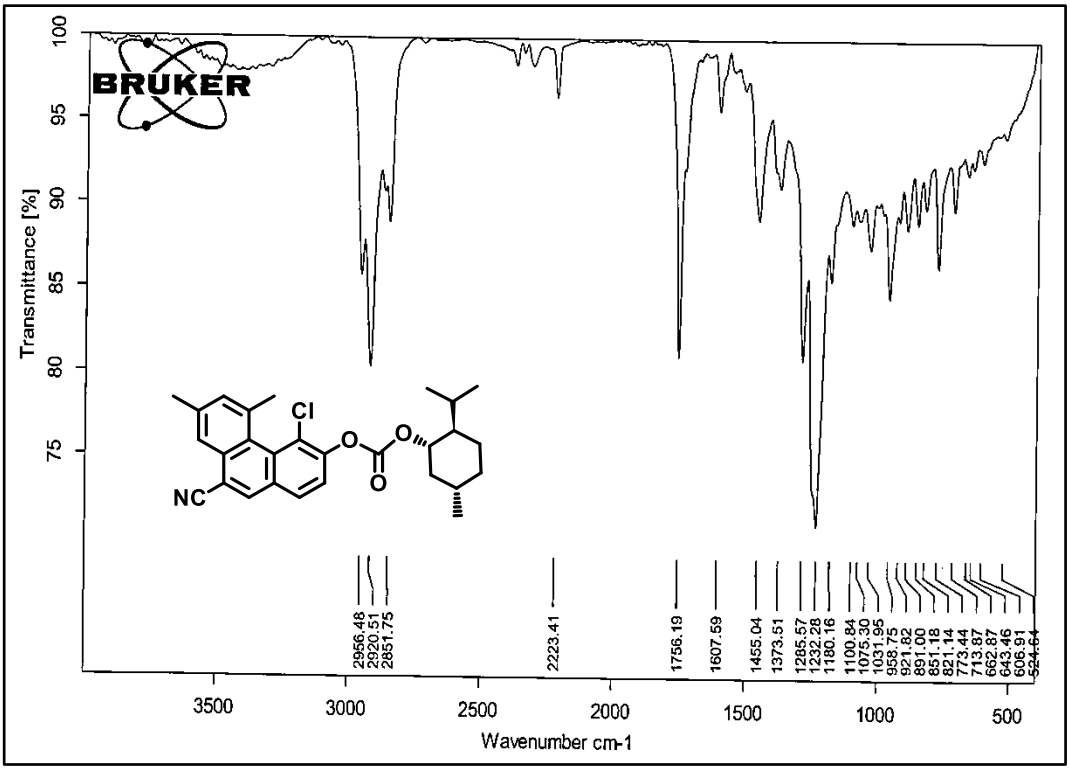

IR Spectra of compound **148**

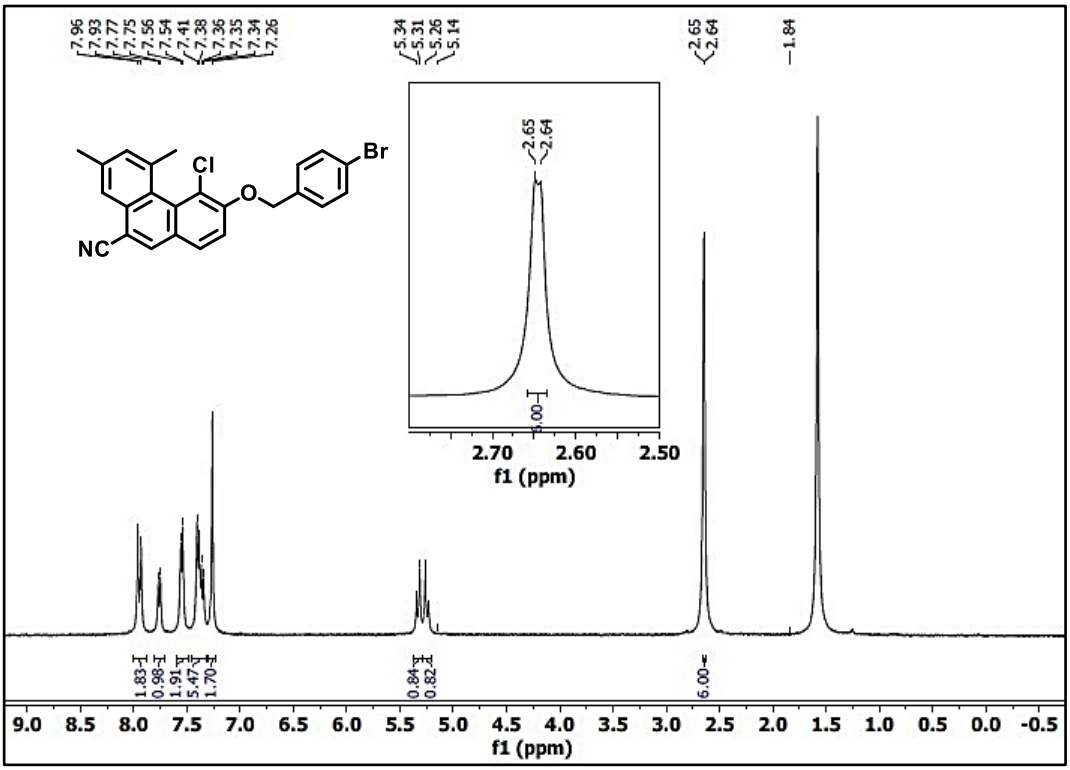

^{1}H NMR Spectra of compound **149** ($CDCl_3$, 400MHz)

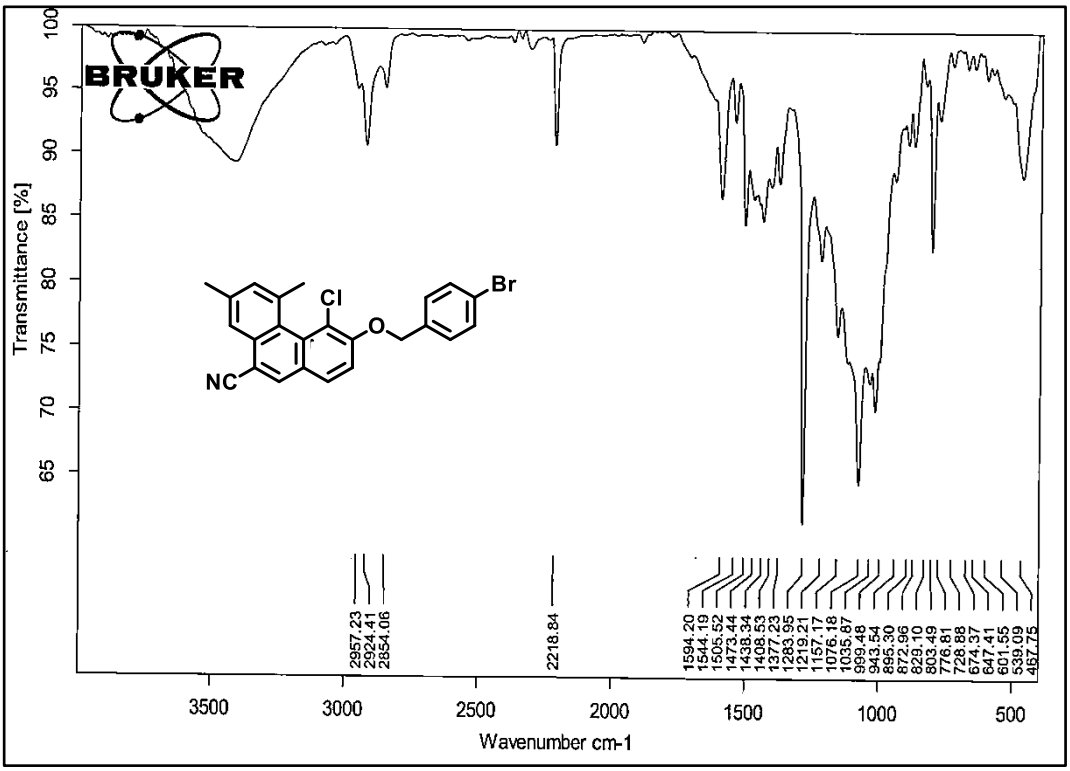

IR Spectra of compound **149**

2.3.2.7 Crystallographic Data:

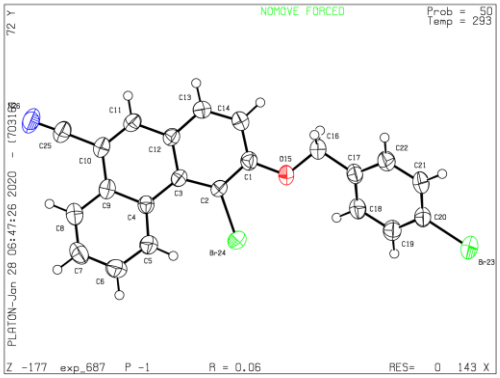

ORTEP diagram of compound 141
(50% probability factor for thermal ellipsoids)

Table 5 Crystal data and structure refinement for compound 141

Empirical formula	$C_{22}H_{13}Br_2NO$
Formula weight	467.15
Temperature/K	293(2)
Crystal system	triclinic
Space group	P-1
a/Å	7.3545(4)
b/Å	9.2747(5)
c/Å	13.2980(6)
α/°	86.318(4)
β/°	84.581(4)
γ/°	79.772(4)
Volume/$Å^3$	887.62(7)
Z	2
ρcalcg/cm^3	1.748
μ/mm^{-1}	5.873
F(000)	460.0
Radiation	Cu Kα (λ = 1.5418)
2Θ range for data collection/°	6.68 to 146.5
Index ranges	$-9 \leq h \leq 6$, $-11 \leq k \leq 11$, $-16 \leq l \leq 16$
Reflections collected	5570
Independent reflections	3246 [R_{int} = 0.0315, R_{sigma} = 0.0412]
Data/restraints/parameters	3246/0/235
Goodness-of-fit on F2	1.029
Final R indexes [I>=2σ (I)]	R_1 = 0.0557, wR_2 = 0.1501
Final R indexes [all data]	R_1 = 0.0614, wR_2 = 0.1581
Largest diff. peak/hole / e $Å^{-3}$	1.73/-1.42

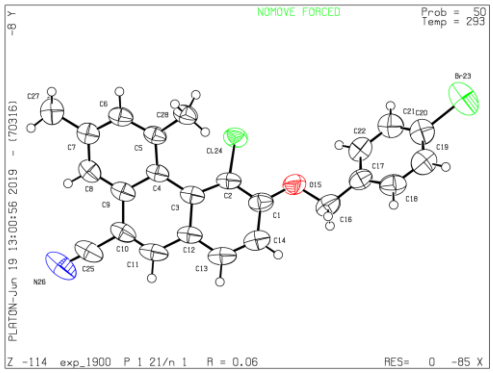

ORTEP diagram of compound 149 (CCDC No. 1935202)

(50% probability factor for thermal ellipsoids)

Table 6 Crystal data and structure refinement for compound 149

Empirical formula	$C_{24}H_{17}BrClNO$
Formula weight	450.75
Temperature/K	293(2)
Crystal system	monoclinic
Space group	P21/n
a/Å	16.2427(12)
b/Å	7.4032(4)
c/Å	17.2525(10)
α/°	90.00
β/°	105.439(7)
γ/°	90.00
Volume/Å^3	1999.7(2)
Z	4
ρcalcg/cm^3	1.497
μ/mm-1	2.204
F(000)	912.0
Radiation	MoKα (λ = 0.71073)
2Θ range for data collection/°	6.08 to 57.82
Index ranges	$-20 \leq h \leq 21$, $-9 \leq k \leq 9$, $-23 \leq l \leq 23$
Reflections collected	22245
Independent reflections	4816 [R_{int} = 0.0709, R_{sigma} = 0.0784]
Data/restraints/parameters	4816/0/255
Goodness-of-fit on F2	1.009
Final R indexes [I>=2σ (I)]	R_1 = 0.0607, wR_2 = 0.1097
Final R indexes [all data]	R_1 = 0.1594, wR_2 = 0.1404
Largest diff. peak/hole / e Å^{-3}	0.39/-0.48

2.4 Section C: 1-Substituted Benzo[*c*]phenanthrenes:

2.4.1 Introduction:

Distortion in PAHs containing a highly hindered *peri*, *bay* or *fjord* region is known in literature to cause change in electronic and molecular properties of a compound *e.g.* acceleration of DNA alkylation by nonplanar PAHs producing a higher adenine/guanine adduct ratio as compared to planar ones.[83–85] Although benzo[*c*]phenanthrene (B[*c*]Ph) had been described in literature as early as the 20th century by Weitzenbock and co-workers, as well as by Mayer and Oppenheimer,[86–88] the isolation of the first B[*c*]Ph was not confirmed until the early 1930s when Cook and Heweit reinvestigated their work.[89]

Parent B[*c*]Ph is the smallest PAH with a *fjord* region. Single crystal XRD investigation has demonstrated that the rings of the B[*c*]Ph are folded having a dihedral angle of 27^{o} between the terminal rings and the distance between carbons 1 and 12 is 3.0Å instead of 2.1Å, the distance expected if the molecule was planar.[90] Steric interference due to substituents on the carbons at positions 1 and 12 lead to the increased deformation of the rings which would affect the physical and chemical properties of B[*c*]Ph. B[*c*]Ph **(150)** is known to show biological activity such as carcinogenic,[91] mutagenic[92] and antiproliferative activity.[93] Structure-activity relationship shows that the 3-, 4-, 5-, and 6-methylated derivatives **(153-156)** were found to be tumorigenic in mouse skin, but the 1- and 2-methyl derivatives **(151 & 152)** were reported to be less active than the parent (B[*c*]Ph) (Figure 1).[94] However, only a few compounds of 1-substituted and 1,12-disubstituted B[*c*]Ph derivatives have been studied because of their unavailability due to difficulties in synthesis.

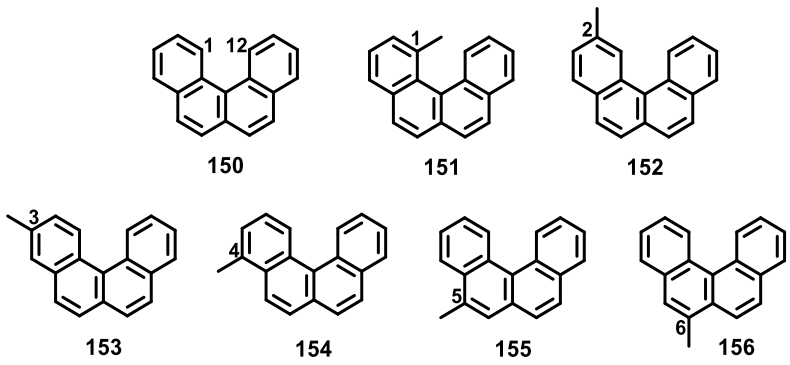

Figure 32 Showing B[*c*]Ph and its methylated derivatives

The first unambiguous synthesis of a 1-substituted B[*c*]Ph derivative, was reported by Newman *et al.* by synthesizing l-methylbenzo[*c*]phenanthrene-l-acetic acid **(162)** (Scheme

33).[95,96] Its attempted resolution using *l*-menthol resulted in the isolation of an isomer having a specific rotation of +1.0° to +2.3°, which gradually disappeared on standing due to rapid interconversion of the enantiomers in solution.

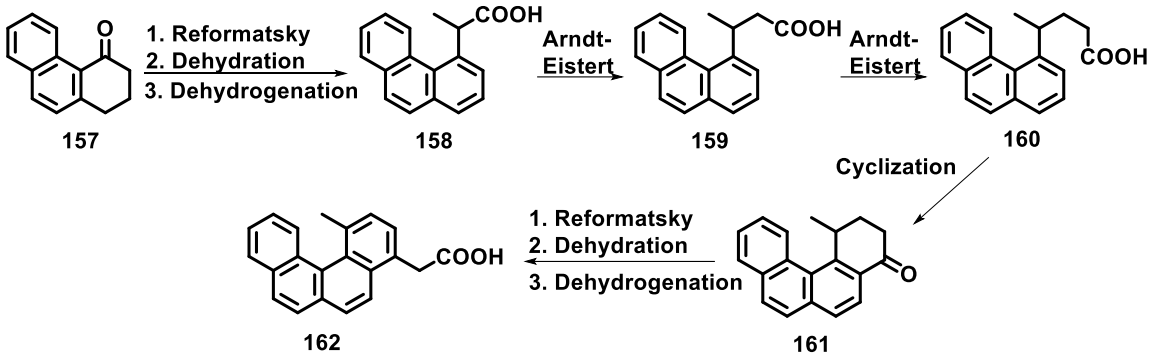

Scheme 33 Synthesis of l-methylbenzo[*c*]phenanthrene-l-acetic acid (162)

Laksham *et al* later synthesized 1,4-dimethylbenzo[*c*]phenanthrol **(167)** (Scheme 34) and carried out its SCXRD showing an interplanar angle of 37° between the terminal rings. The presence of methyl group at 1 and 4 position induced non-planarity in the molecule resulting in *P* and *M* enantiomers. However the separation of enantiomers of **167** was unsuccessful.[97]

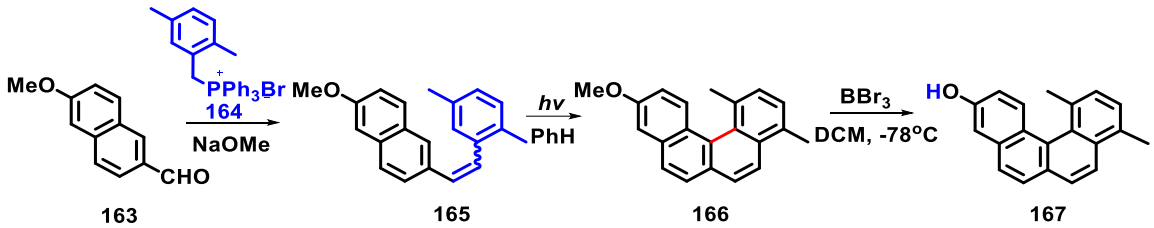

Scheme 34 Synthesis of 1,4-dimethylbenzo[*c*]phenanthrol (167)

The same authors also synthesized fluorine substituted B[*c*]Ph (Scheme 35) and studied its SCXRD which showed an interplanar angle of 34° between the terminal rings. They compared the tumorigenic activity of 1-fluoro and 2-fluoro B[*c*]Ph with unsubstituted B[*c*]Ph. They concluded that 1-fluoro B[*c*]Ph exhibit enhanced tumorigenicity due to enhanced molecular distortion,[98] but the 2-fluoro derivative which is almost planar was found to be less active.[99]

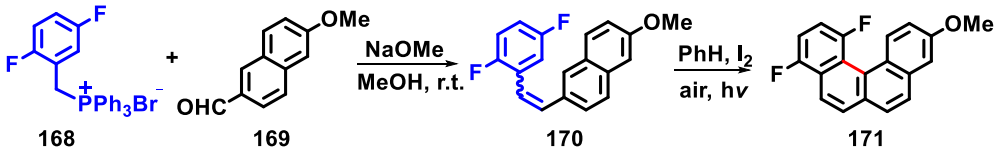

Scheme 35 Synthesis of 1,4-difluoro B[*c*]Ph derivative (171)

The synthesis of 1-bromo B[*c*]Ph was important as it could be useful as an intermediate in the preparation of a number of 1-substituted B[*c*]Ph derivatives as well as in the synthesis of higher members of helicenes like hepta-, octa-, nona- or decahelicenes.[100] The first unambiguous synthesis of highly strained 1-bromo B[*c*]Ph **(179)** (Scheme 36) was carried out by Newman *et al.* in 1959.[101]

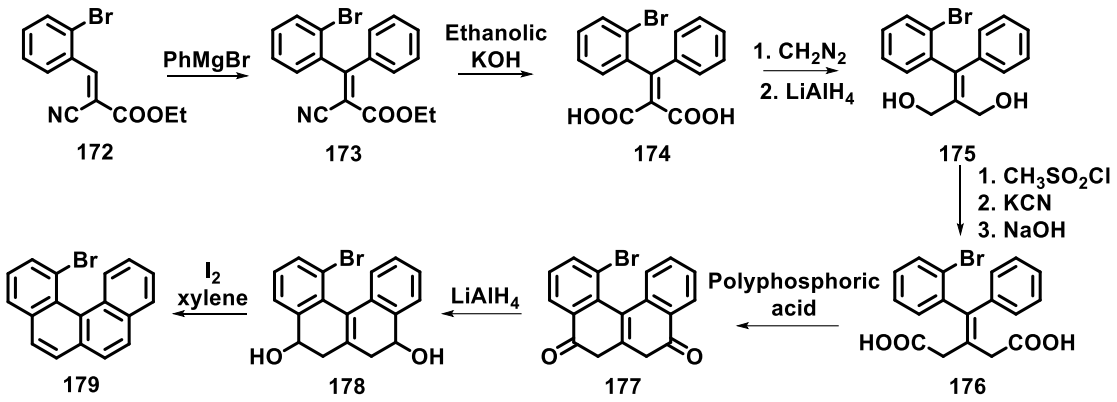

Scheme 36 Synthesis of 1-bromo B[*c*]Ph (179)

None of the 1-substitued B[*c*]Ph derivatives could be successfully resolved due to low barrier of racemization facilitating rapid interconversion of the enantiomers in solution. In order to prepare compounds which are stable at room temperature in their optically pure forms, Newman *et al.* synthesized 1,12-dimethyl B[*c*]Ph **(186)** (Scheme 37).[96]

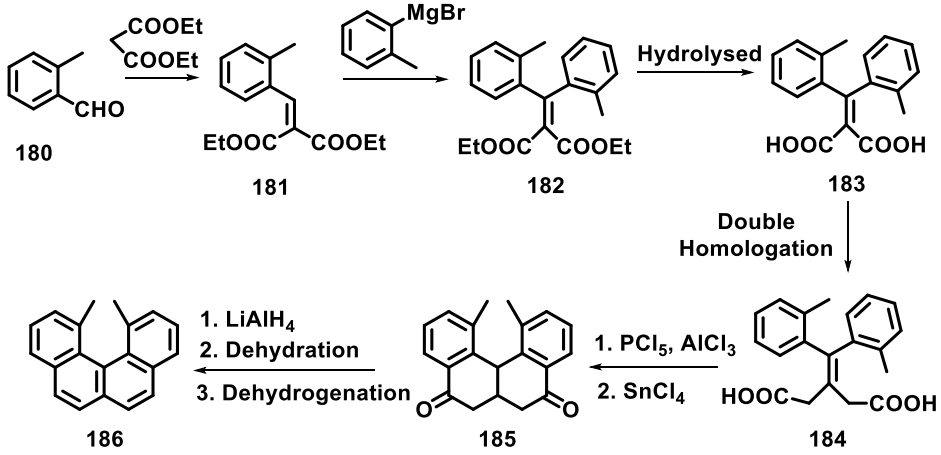

Scheme 37 Synthesis of 1,12-dimethyl B[*c*]Ph (186)

The resolution of 1,12-dimethyl B[*c*]Ph **(186)** was successfully achieved by synthesizing its acid derivative, l,12-dimethylbenzo[*c*]phenanthrene-5-acetic acid **(191)** (Scheme 38) which was partly resolved by forming a salt with cinchonidine. The enantiomers thus obtained were optically stable at ambient as well as temperatures as high as 300°C after which the compound started undergoing decomposition.[102]

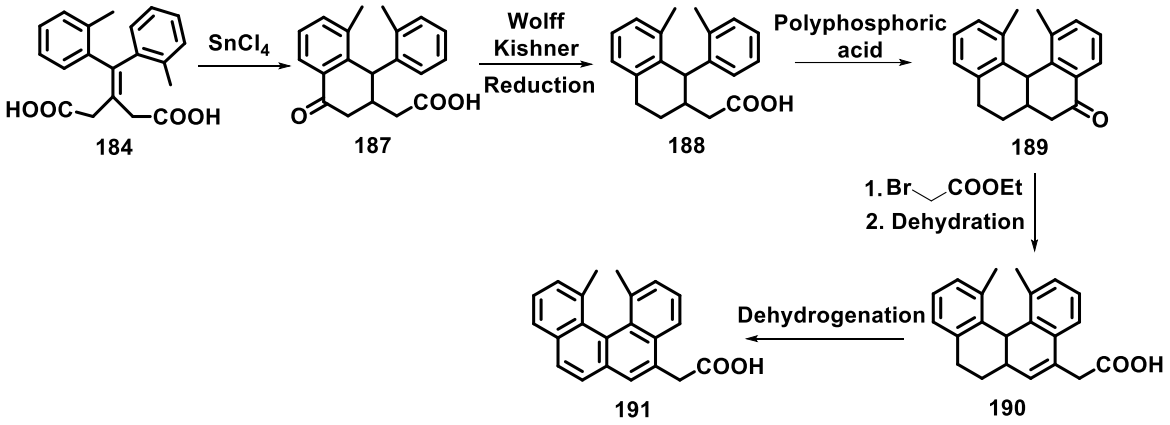

Scheme 38 **Synthesis of 1,12-dimethylbenzo[*c*]phenanthrene-5-acetic acid (191)**

Although the synthesis of optically active l,12-dimethylB[*c*]Ph-5-acetic acid **(191)** was successfully carried out, the overall yield of the compound was poor. Yamaguchi *et al.* were the first to report multi-gram synthesis of 1,12-dimethylB[*c*]Ph-5,8-dicarboxylic acid **(192)**. Its enantiomers (*M*)-(+)-**192**/(*P*)-(-)-**192** were obtained in optically pure forms using (-)-quinine as resolving agent, followed by repeated recrystallization[103] (Scheme 39).

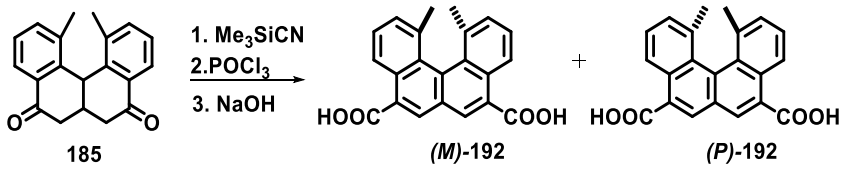

Scheme 39 **Synthesis of 1,12-dimethylB[*c*]Ph-5,8-dicarboxylic acid (192)**

Since repeated crystallization proved to be a tedious process, a different strategy involving diastereomer formation was utilized for its resolution. *Rac*-**192** was treated with optically pure *d*-(-)-camphorsultam giving diastereomers **(193)** which were separated easily by chromatography (Scheme 40).

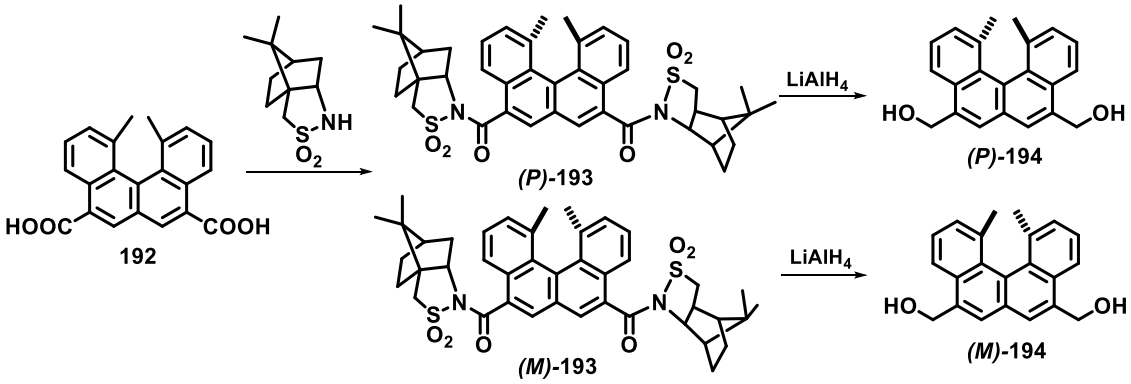

Scheme 40 **Resolution of 1,12-dimethylB[*c*]Ph-5,8-dicarboxylic acid (192)**

The chiral auxiliary was effectively cleaved using $LiAlH_4$ giving enantiopure **194** (Scheme 40). Since both the enantiomers were accessible in large quantities, 1,12-dimethylbenzo[*c*]phenanthrene-5,8-dicarboxylic acid **(192)** proved to be an attractive chiral bifunctional building block.[102]

A series of optically active cyclic anyhydrides **(197)**[104] and macrocyclic amides **(195,196)** (Figure 33) consisting of this chiral unit were synthesized and utilized as chiral Langmuir-Blodgett films by Feng and co-workers. An optically active LB film based on helical chirality was produced for the first time and the properties of the chiral LB film were studied.[105,106]

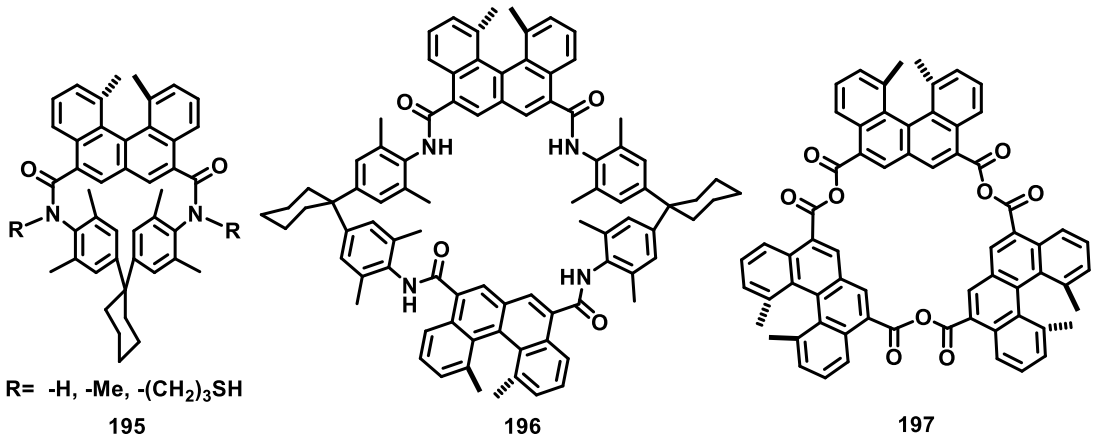

Figure 33 Some representative cyclic anhydride (197) and macrocyclic amides (195 & 196) possessing chiral 1,12-dimethylbenzo[*c*]phenanthrene-5,8-dicarboxylate unit

Various optically active cyclic polyamines **(201)**, polyimines **(200)** and macrocyclic alkynes **(204)** containing this chiral motif were reported by Yamaguchi *et al.*[107]

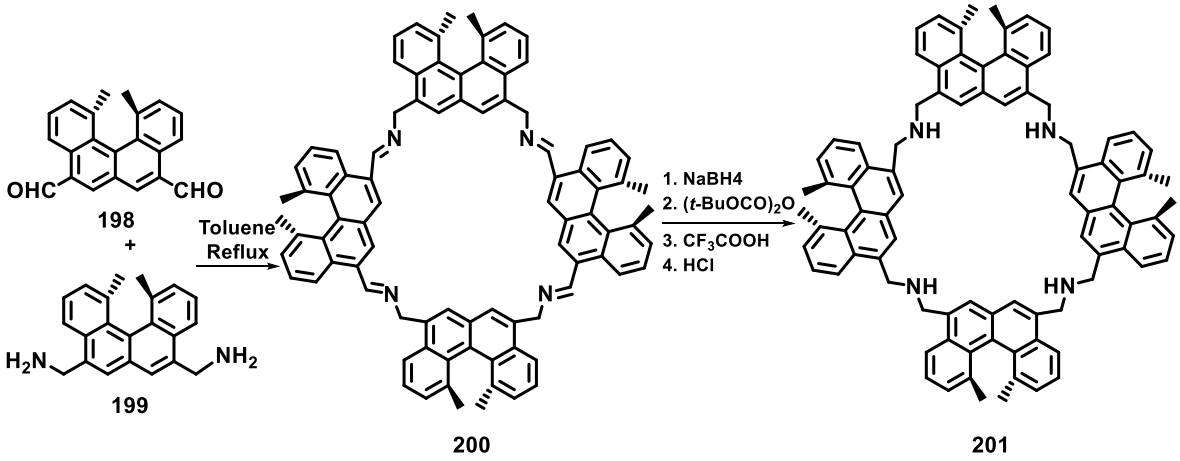

Scheme 41 Synthesis of optically active cyclic polyamines (201) and polyimines (200) bearing chiral 1,12-dimethylbenzo[*c*]phenanthrene unit

These macrocyclic alkynes underwent aggregation in organic solvents due to π-π interactions. It was found that the homo-aggregation of the (*M,M,M*)-**201** isomer turned out to be stronger than the hetero-aggregation between the (*M,M,M*)-isomer and the (*P,P,P*)-isomer.[108–110] Such type of chiral recognition due to supramolecular interactions between the molecules of same chirality is important in molecular biology.

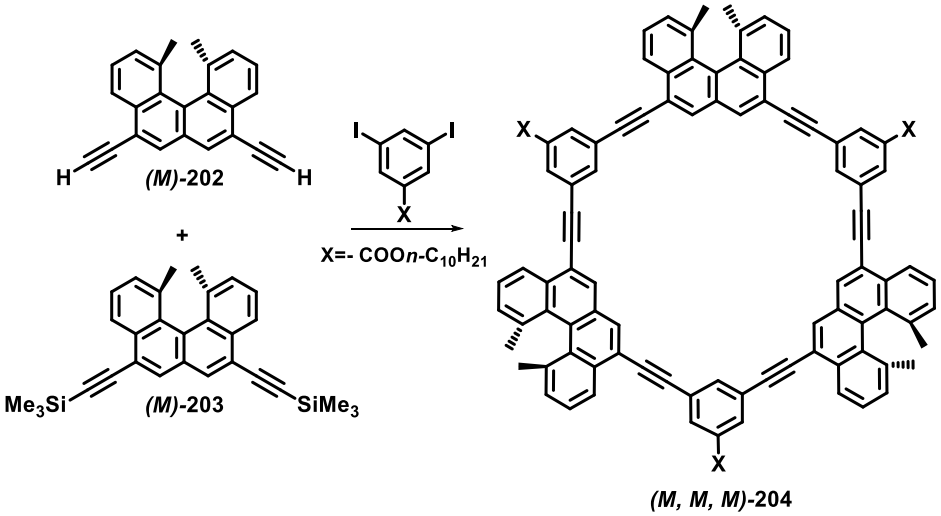

Scheme 42 Synthesis of optically active macrocyclic alkynes *(M,M,M)*-204 bearing chiral 1,12-dimethyl benzo[*c*]phenanthrene unit

Inspired from Kartz who prepared a bis[5]helicenediol ligand ([5]HELOL) and utilized it as a catalyst in asymmetric addition of diethylzinc to aldehydes,[111] Kabuto *et al.* synthesized bihelicenol based on 1,12-dimethyl B[*c*]Ph motif.

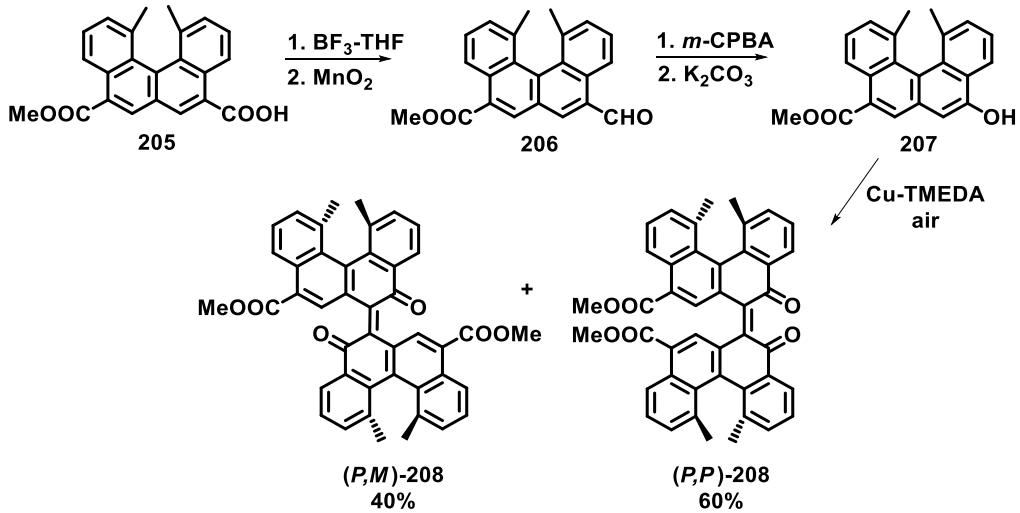

Scheme 43 Asymmetric coupling of 207

They expecting it to form a larger chiral pocket at the catalytic metal center, and hence act as a better ligand for such transformations. Interestingly, the formation of the homo coupling

of (*P*)-**207** predominates slightly over the hetero coupling (Scheme 43). Such chiral recognition of helicenes favoring the molecules of the same helicity has been proved to be beneficial in various applications.[112]

As 1,12-dimethyl B[*c*]Ph quickly become an interesting motif for various applications, its functionalization was necessary. Hence, Yamaguchi *et al* carried out nitration of 1,12-dimethylbenzo[*c*]phenanthrene-5,8-dinitrile **(209)** giving 4,9-dinitro **(210)**, 2,9-dinitro **(211)**, 2,11-dinitro **(212)** and 2,4,9,11-tetranitro **(213)** helicenes depending on the reaction conditions (Scheme 44). These electron-deficient helicenes formed charge-transfer complexes with pyrene and other electron rich donors in the solution as well as in solid state.[104,113]

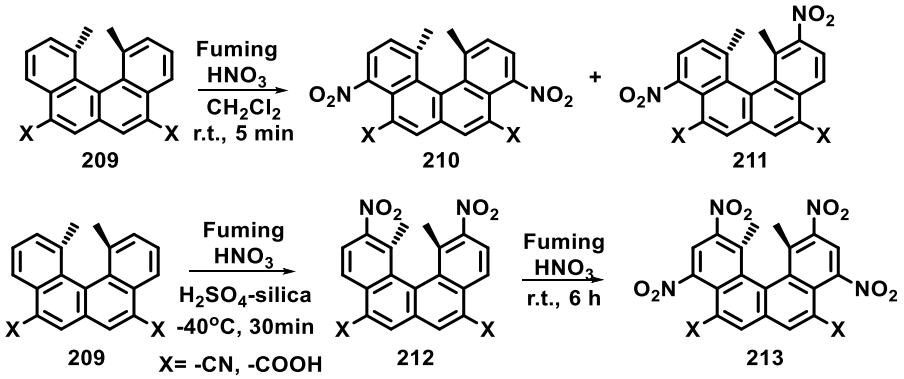

Scheme 44 Nitration of 1,12-dimethylB[*c*]Ph-5,8-dicarboxylic acid or dinitrile (209)

As 1,12-dimethyl B[*c*]Ph skeleton proved to be of great importance and utility in various fields of chemistry as well as biology, owing to its non-planarity because of the presence of bulky methyl substituents in the *fjord* region, the need to study the effect of bulkier groups at 1 and 12 position of the B[*c*]Ph core was necessary. Yamaguchi *et al.* synthesized and resolved 1,12-diethyl B[*c*]Ph **(217)** and 1,12-diisopropyl B[*c*]Ph **(218)** derivatives (Scheme 45) and compared them with 1,12-dimethyl derivatives synthesized earlier. Contrary to the expectation that replacing the 1,12-dimethyl group with diethyl or diisopropyl groups would increase the strain of the helicene ring system, the diisopropyl derivative was less strained than the dimethyl derivative.[114] This was due to the rotation around the C(1α)–C(1) bond as well as the anti-periplanar arrangements of the C(1α)–H bond and C(12α)–H bond in **218** appear to have contributed to decrease repulsions of the isopropyl group, hence, leading to decrease in the effective size of the isopropyl group.

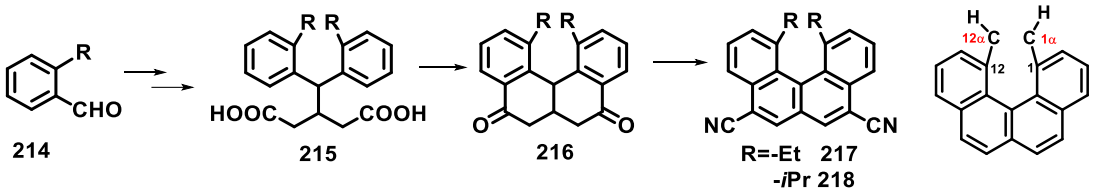

Scheme 45 **Synthesis of 1,12-dialkyl B[*c*]Ph derivatives (217 & 218)**

Later, 1-fluoro-12-methyl B[*c*]Ph **(225)** was synthesized (Scheme 46) in 39% yield and for the first time the energy of activation as well as entropy for racemization of a compound which owes its asymmetry to intramolecular overcrowding had been determined.[115] The resolution for **225** was carried out by its crystallization with optically active optically α-(2,4,5,7-tetranitro-9-fluorenylidene aminooxy)propionic acid (TAPA) which had been earlier reported for the resolution of various polycyclic aromatic hydrocarbons.[116]

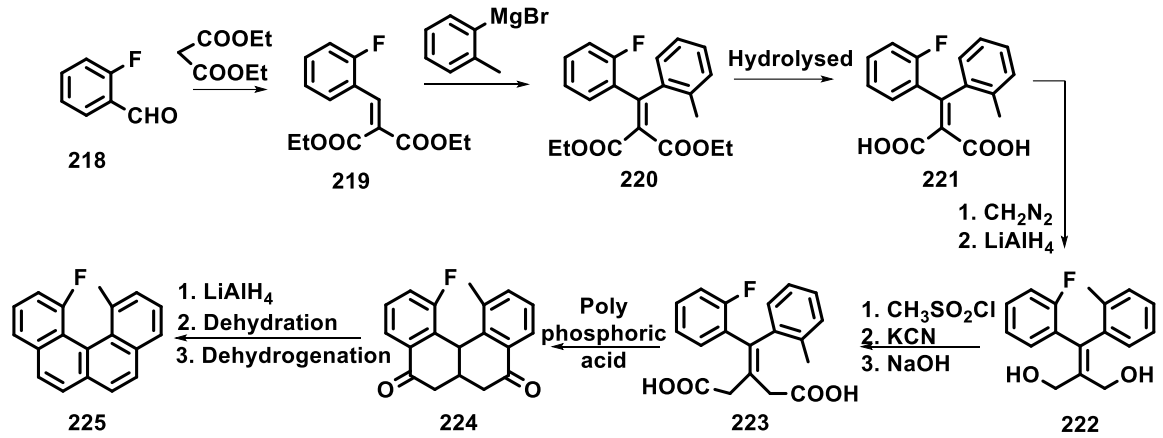

Scheme 46 **Synthesis of 1-fluoro-12-methyl B[*c*]Ph (225)**

Kemp and Meson later reported the resolution and circular dichroism as well as electronic absorption spectra of 1-fluoro-12-methyl B[*c*]Ph **(225)** and compared the results with the theoretical rotational and dipole strengths of the lower-energy π-π* transitions of the optical isomers of B[*c*]Ph which indicated that (+)-l-fluoro-12-methyl B[*c*]Ph has the stereochemical form of a segment of a right-handed helix.[117]

The first synthesis of methyl substituted B[*c*]Ph by the mode of photocyclization was reported by Nagel *et al.* in 1977 (Scheme 47). This method was found to have distinct advantages over the earlier reported methods[118–121] since naphthylstyrenes could be readily prepared in good to excellent yields *via* Wittig, Heck or Grignard reactions in a single step. Since this procedure had been utilized earlier in the preparation of phenanthrenes with large variety of substituents, the synthesis of similarly substituted B[*c*]Ph by this route seemed feasible.[122]

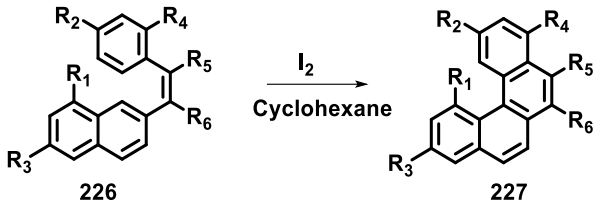

Scheme 47 Synthesis of substituted B[*c*]Ph *via* photocyclization of styrenes

Recently, pyrene fused B[*c*]Ph derivatives have been reported by Yamato *et al.* They have developed two types of new pyrene-cored blue-light emitting B[*c*]Ph **(228 & 229)** *via* intramolecular photocyclisation (Figure 34). Such helical molecules exhibit bright fluorescent emissions both solution and the solid state, ranging from deep-blue to sky-blue in the visible regions, making them potential candidates for several important applications in modern electronic and optoelectronic devices, such as blue emitters in OLEDs.[123]

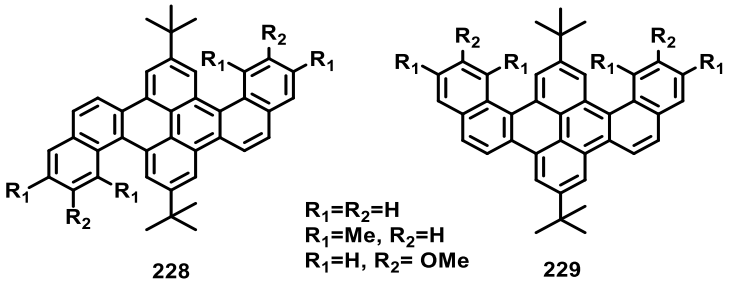

Figure 34 Pyrene fused B[*c*]Ph (228 & 229) *via* photocyclization of styrenes

The photophysical and electrochemical properties of these compounds were fully examined in solution and in thin films.[124]

2.4.2 Results and Discussion:

2.4.2.1 Synthesis of 1-Substituted Benzo[*c*]phenanthrenes:

It can be seen then that the steric interference of the carbon (and hydrogen) atoms at positions 1 and 12 alters the properties of B[*c*]Ph considerably. Only a few compounds containing substituents at the desired 1-position have been studied, however, the main problem has been their unavailability due to difficulties in synthesis. The introduction of various groups at the 1- and 12 -positions results in steric hindrance causing greater non-planarity of the aromatic system. Since, 1,12-disubstituted B[*c*]Ph have been well studied and applied in various fields of chemistry, it was of great interest to us to devise a synthetic route to access B[*c*]Ph derivatives containing functional groups at 1-position. Since 1-substituted B[*c*]Ph have not been well explored to study the effect of skeletal deformation on physical and chemical properties, we undertook this objective. These molecules would offer a method of studying not only the effect of steric interference due to a single substituent in the *fjord* region on the aromatic ring system but also the effect of functional groups themselves. Methyl group was the substituent of choice as it remains intact during a large variety of chemical reactions and also provides clear signals in NMR spectra required to observe the presence (or absence) of enantiomerism. Since many methylated derivatives of B[*c*]Ph were already reported in literature, we selected 1,3-dimethyl B[*c*]Ph skeleton having an additional methyl group at 3rd position which was not yet explored. The presence or absence of -CN group along with its variation in position was also studied to provide a fundamental understanding of the complex molecular assemblies.

Many synthetic routes towards synthesis of B[*c*]Ph involve cross-coupling reactions and in some cases metal catalyzed cycloisomerization. These methodologies however suffer from many disadvantages like use of expensive metal salts, involvement of a number of steps, poor to moderate yields *etc.* Since photocyclization of stilbene derivatives had been widely employed for the synthesis of phenanthrene core but relatively less utilized for the synthesis of B[*c*]Ph, our synthetic approach was based on using this strategy to synthesize 1-substituted B[*c*]Ph derivatives.

To obtain 1,3-dimethyl B[*c*]Ph skeleton, mesitylene was the reagent of choice due to symmetrically placed methyl groups and easy commercial availability. Mesitylene **(131)** was subjected to side chain bromination with *N*-bromosuccinimide in presence of catalytic amounts of benzoyl peroxide which acts as a radical initiator in CCl_4. The reaction mixture

was irradiated with light from a tungsten lamp, to give us 3,5-dimethyl benzyl bromide **(132)** in 81% yield. It was then subjected to Kornblum oxidation to give the corresponding aldehyde **230** in moderate yield (Scheme 48).

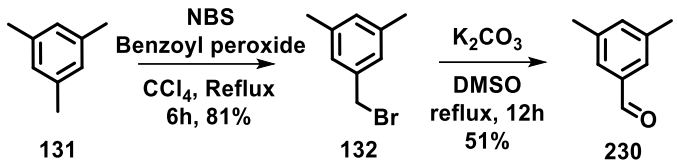

Scheme 48 Synthesis of 3,5-dimethylbenzaldehyde (230)

To obtain the coupling partner for olefin synthesis using Wittig reaction, we started with commercially available 2-methyl naphthalene **(231)** and subjected it to side chain bromination using the same procedure mentioned above. The obtained 2-bromomethylnaphthalene **(232)**, was then subjected to Wittig salt formation by reaction with triphenyl phosphine and refluxing it in xylene (Scheme 49). The Wittig salt **233** readily precipitated out which was then filtered and dried.

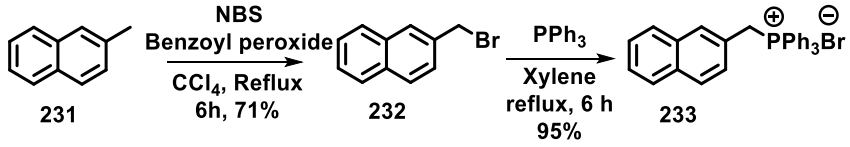

Scheme 49 Synthesis of Wittig salt from 2-methyl naphthalene (233)

The synthesized Wittig salt **233** was then subjected to Wittig reaction with 3,5-dimethyl benzaldehyde **230** in presence of freshly prepared sodium methoxide as base in dry methanol to give the olefin **234** in good yield. The olefin was then subjected to photocyclization using stoichiometric amount of iodine as an oxidant and tetrahydrofuran as HI quencher in toluene and irradiating the reaction mixture with 250W HPMVL for 24 hours (Scheme 50).

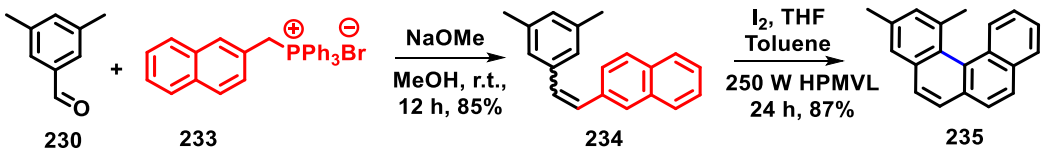

Scheme 50 Synthesis of 1,3-dimethylbenzo[*c*]phenanthrene (235)

The photocyclized product **235** was the only product formed during the reaction in excellent yield. This was confirmed by carrying out ^{1}H NMR of the crude mixture after photocyclization which did not show any traces of side products. ^{1}H NMR spectra of 1,3-dimethylB[*c*]Ph **(235)**, recorded after column purification, showed disappearance of the

olefinic protons and the differentiation of the two aromatic –CH_3 groups which resonated as a sharp singlet at **δ** 2.39 in olefin **234** now appeared as two separate singlets at **δ** 2.63 and 2.43 in **235**. This difference in the chemical shift values for the two methyl groups arises due to the presence of one of the –CH_3 groups at 1-position of the B[*c*]Ph skeleton which falls in the deshielding zone due to the terminal aromatic ring causing its signal to shift downfield relative to the other present at 3-position which is unaffected by such environment. This can also be seen in ^{13}C NMR spectra which clearly shows two peaks in the aliphatic region at **δ** 21.46 and 24.88.

As –CN group is well studied for a wide variety of functional group interconversions, changes in electronic properties of molecule and its ability to drive self-assemblies in many organic systems due to potential hydrogen bonding abilities, lead us to introduce –CN group in this 1,3-dimethyl B[*c*]Ph skeleton. We slightly modified our strategy by synthesizing 2-(3,5-dimethylphenyl)acetonitrile **(236)** from 1-(bromomethyl)-3,5-dimethylbenzene **(132)** and hence introducing –CN group at an early stage of synthesis (Scheme 51). 2-(3,5-dimethylphenyl)acetonitrile **(236)** was characterized by ^{1}H NMR spectroscopy which showed a sharp singlet for the benzylic protons at **δ** 3.69 which appeared at **δ** 4.46 in 1-(bromomethyl)-3,5-dimethylbenzene **(132)** which was in accordance with the reported values. This upfield shift is attributed to the electron withdrawing nature of –CN group. 2-Naphthaldehyde **(237)** which was the coupling partner required for olefin synthesis was obtained by oxidation of 2-bromomethylnaphthalene **(232)**. The ^{1}H NMR of the synthesized 2-naphthaldehyde showed disappearance of the benzylic protons which appeared at **δ** 4.89 for 2-bromomethylnaphthalene **(232)**.

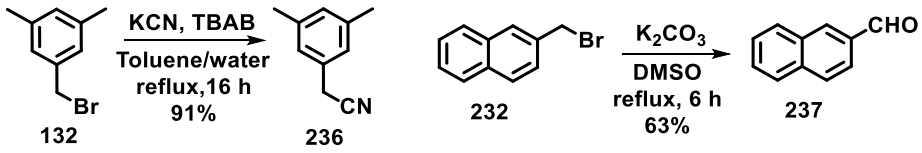

Scheme 51 Synthesis of the olefinic partners 2-(3,5-dimethylphenyl)acetonitrile (236) and 2-naphthaldehyde (237)

Having synthesized **236** and **237**, they were subjected to Knoevenagel condensation in presence on potassium hydroxide as base in methanol at room temperature to give olefin **238**. The olefinic mixture was subjected to photocyclization using similar conditions mentioned before giving product **239** in excellent yield (Scheme 52), which was purified by column chromatography on silica gel (5% ethyl acetate-petroleum ether).

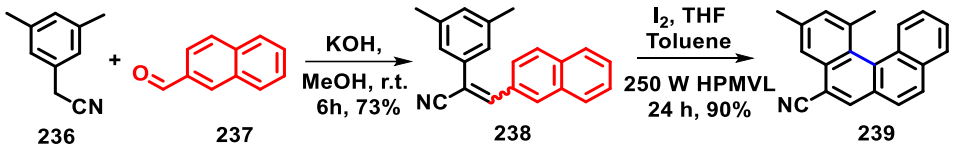

Scheme 52 Synthesis of 1,3-dimethylbenzo[*c*]phenanthrene-5-carbonitrile (239)

^{1}H NMR spectra for 1,3-dimethylbenzo[*c*]phenanthrene-5-carbonitrile **(239)** showed two distinct singlets at **δ** 2.36 and 2.66 for the two –C*H*$_3$ groups. A characteristic singlet corresponding to the proton next to –CN group (6-position) can be seen in the downfield region at **δ** 8.23. The tolerance of –CN group towards photocyclization was also proved by IR spectroscopy which showed a sharp band at 2217 cm^{-1} assigned to –C≡N stretching frequency.

The photochromic and opto-electronic properties of a molecule are not only affected by the nature of substituent present in the molecule but also upon its site of attachment. The position of -CN group on a molecular scaffold is known to play a crucial role not only in the crystallization pattern and crystal packing but also drives the phenomena of molecular recognition. Although a large amount of literature can be found on the effect of different substituents in a molecule, studies on the effect of position of the substituents on its properties is relatively rare. Hence, our target was to synthesize compound **242** which is a positional isomer of 1,3-dimethyl B[*c*]Ph-5-carbonitrile **(239)** and compare their properties. A similar retrosynthetic scheme was designed, by simply changing the coupling partners. 2-bromomethyl naphthalene **(232)** was converted into its corresponding nitrile derivative **(240)** by reaction with KCN in refluxing toluene-water mixture in good yield. The 2-(naphthalen-2-yl)acetonitrile **(240)** synthesized was then subjected to Knoevenagel condensation with 3,5-dimethyl benzaldehyde **(230)** under similar conditions to afford olefin **241** in moderate yield which was photocyclized using similar conditions to get our target molecule 1,3-dimethylnenzo[*c*]phenanthrene-6-carbonitrile **(242)** as the only product in good yield (Scheme 53).

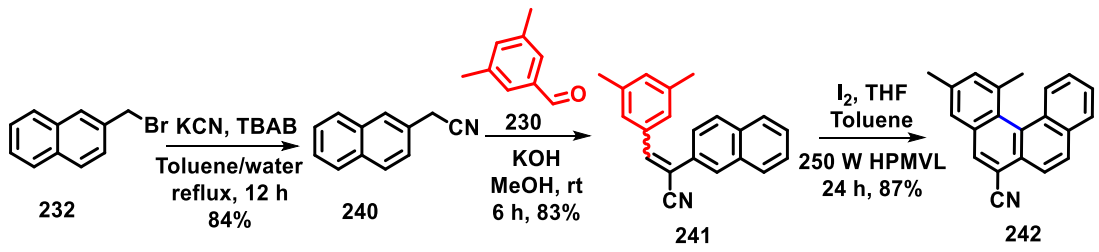

Scheme 53 Synthesis of 1,3-dimethylbenzo[*c*]phenanthrene-6-carbonitrile (242)

The formation of 1,3-dimethylbenzo[*c*]phenanthrene-6-carbonitrile **(242)** was confirmed by recording its ^{1}H NMR spectra which was quite similar to that of 1,3-dimethylbenzo[*c*]phenanthrene-5-carbonitrile **(239)** with only a slight difference in the chemical shift values. However, a downfield doublet signal is seen for **242** at **δ** 8.264 which corresponds to the proton of ring C near to –CN group (7-position) which has shifted downfield due to the electronic effect of –CN group present in its vicinity.

In order to increase the steric bulk at the 1-position of B[*c*]Ph moiety, we planned to introduce a halogen atom in the *fjord* region. Halogen atoms are Lewis acidic in nature having a positive electrostatic potential and often undergo highly directional interactions with electron rich atoms. Such interactions favor the organization of π-conjugated molecules which is of great importance in organic electronic applications. Bromo group was the substituent of choice due to its large size and ease to undergo facile functional group interconversion broadening the scope to access a wide variety of 1-substituted B[*c*]Ph derivatives as well as its utility as an intermediate for the synthesis of higher members of helicenes (hepta-, octa-, nona- or decahelicene). Thorough study of previously reported routes to B[*c*]Ph having bulky substituents at 1-position revealed that certain requirements should be met in order to achieve its successful synthesis: (1) the steric hindrance in the molecule should be introduced stepwise and not all at once, (2) the bulky group should be introduced early in the course of synthesis, (3) reactions that might involve attack on the substituent, such as very strongly alkaline reactions, high temperatures or reactions involving reactive metals should be avoided.

Hence, the synthesis of 1-bromo B[*c*]Ph was not only challenging, but the curiosity to study and compare its properties with our previously synthesized molecules was the driving force for us to take up this objective. A modification to our previously reported synthetic scheme was necessary by replacing the 1,3-dimethyl benzyl bromide moiety with bromo substituted benzyl bromide. 1-bromo-3-(bromomethyl)benzene scaffold with 4-position blocked by some substituent was the synthon required to effectively drive the photocyclization of the olefin to the desired position giving our target molecule. Hence, *p*-bromo anisol **243** was the reagent of choice due to the presence of $–OCH_3$ group which being *ortho* directing, facilitates the functionalization of the molecule at desired position as well as proves to be a good handle for accessing –OH group which can be utilized for its resolution.

We subjected *p*-bromo anisol **243** to bromomethylation using paraformaldehyde and HBr in refluxing acetic acid to get **244** in 85% yield. The formation of **244** was confirmed by ^{1}H NMR spectra which clearly showed the appearance of a sharp singlet for two protons at **δ** 4.49. 4-bromo-2-(bromomethyl)-1-methoxybenzene **(244)** was then subjected to Kornblum oxidation to obtain the corresponding aldehyde **245** in moderate yield. The disappearance of the benzylic protons and appearance of a sharp singlet in the downfield region at **δ** 10.39 confirmed the formation of the molecule. 5-bromo-2-methoxybenzaldehyde **(245)** was then subjected to Knoevenagel condensation with previously synthesized 2-(naphthalen-2-yl)acetonitrile **(240)** under similar conditions to obtain the corresponding olefin **(246)** in good yield (Scheme 54).

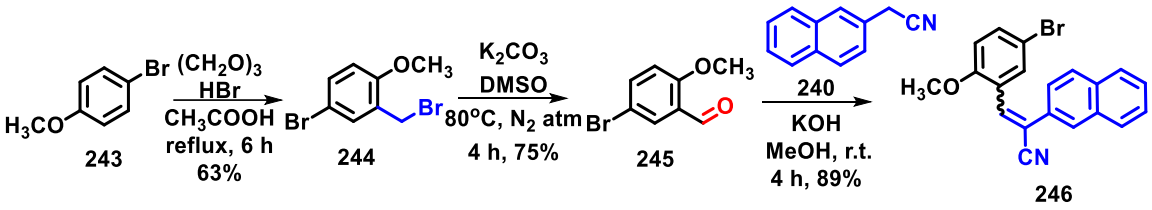

Scheme 54 Synthesis of olefin (246)

The synthesized olefinic mixture of *E/Z* isomers was subjected to oxidative dehydrogenative photocyclization using iodine-THF system in toluene which was irradiated with 250W HPMVL. Even after repeated efforts to modify this strategy by changing to 125W HPMVL and varying the reaction time, our target molecule was not formed. A large number of spots could be visualized in the TLC for the reaction mixture. However, a single prominent spot could be seen which was isolated by column chromatography followed by repeated crystallization. ^{1}H NMR analysis for this compound showed the presence of 10 aromatic protons and 3 aliphatic protons. The signal at **δ** 4.12 for three protons corresponded to the –OC*H*$_3$ group which survived the photocyclization. The presence of 10 aromatic protons clearly indicated the loss of –Br group during the course of photocyclization. So we modified our reaction conditions and used cyclohexene as the oxidant and cyclohexane as the solvent of choice and irradiated the olefin mixture with 125W HPMVL for a period of 22 hours (Scheme 55). This condition lead to the complete disappearance of the starting material and formation of three compounds, one of which matched with the debrominated product **(248)** formed previously. Purification by carefully carrying out column chromatography on silica gel gave us two new compounds which were characterized using ^{1}H NMR. One of the two compounds was relatively non-polar and highly fluorescent in

nature. The ^{1}H NMR spectra of this compound however showed the presence of only 8 aromatic protons and 3 aliphatic protons. The sharp signal at **δ** 4.03 is for –OC*H*$_3$ protons supports the presence of methoxy group in this compound. However, the signals in the aromatic region were simplified in pattern showing a sharp singlet at **δ** 8.45 assigned to the proton present on the carbon atom next to –CN group and a set of 4 doublets, two doublet of doublets and a multiplet which can appear only when a bond between C1 and C12 is present leading to the formation of a benzo[*ghi*]fluoranthrene type derivative **(249)**. Such derivatives of B[*c*]Ph are reported in literature but under Flash Vacuum Pyrolysis (FVP) which requires very high temperatures. However, their formation during photocyclization has not been reported. The HRMS spectra for this compound was recorded to confirm the structure of this compound. The HRMS spectra was in accordance with the exact mass of 3-methoxybenzo[*ghi*]fluoranthene-1-carbonitrile **(249)** confirming its formation during the process of photocyclization. The other compound was pale yellow in colour and ^{1}H NMR showed the presence of 9 aromatic protons and a singlet for three protons at **δ** 4.12. The signal for the proton closest to –CN group is shifted downfield at **δ** 8.82. This matched with expected structure of target molecule 1-bromo-4-methoxybenzo[*c*]phenanthrene-6-carbonitrile **(247)**, which was also confirmed by HRMS analysis.

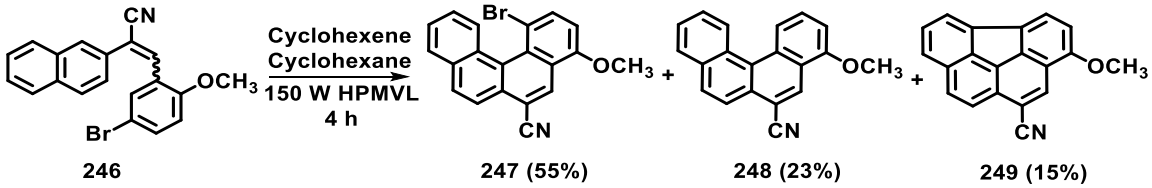

246 247 (55%) 248 (23%) 249 (15%)

Scheme 55 Photocyclization of 3-(5-bromo-2-methoxyphenyl)-2-(naphthalen-2-yl)acrylonitrile (246)

Having succeeded in the synthesis of 1-bromo-4-methoxybenzo[*c*]phenanthrene-6-carbonitrile **(247)**, we extended our study towards analyzing the effect due to change in the position of –CN group. Focusing on our next target where the –CN group is present at 5-position, we synthesized 2-(5-bromo-2-methoxyphenyl)acetonitrile **(250)** from previously synthesized 4-bromo-2-(bromomethyl)-1-methoxybenzene **(244)** using standard conditions involving the use of potassium cyanide. It was then subjected to Knoevenagel condensation with previously synthesized 2-naphthaldehyde **(237)** under similar conditions to obtain the corresponding olefin **(251)** in good yield. The photocyclization of this olefinic mixture under similar conditions involving the use of cyclohexene in cyclohexane was carried out giving us our desired target 1-bromo-4-methoxybenzo[*c*]phenanthrene-5-carbonitrile **(252)**

in moderate yield with almost equivalent amount of debrominated 4-methoxyB[*c*]Ph-5-carbonitrile **(253)** being formed (Scheme 56). This can be attributed to the presence of –Br group at the sterically hindered position, which may facilitate its easy loss during photocyclization.

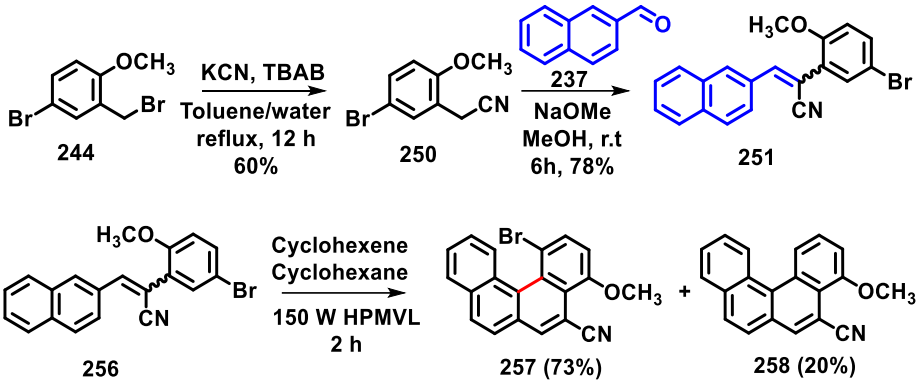

Scheme 56 Synthesis of 1-bromo-4-methoxyB[*c*]Ph-5-carbonitrile (257)

A similar strategy to obtain 1-bromo-4-methoxybenzo[*c*]phenanthrene lacking a –CN group was followed involving Wittig reaction between (5-bromo-2-methoxybenzyl)triphenyl phosphonium bromide **(259)** and 2-naphthaldehyde **(237)**. The olefin **260** was photocyclized under similar conditions to obtain a mixture of products.

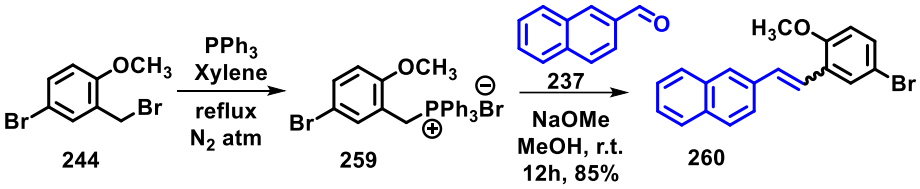

Scheme 57 Synthesis of olefin 260

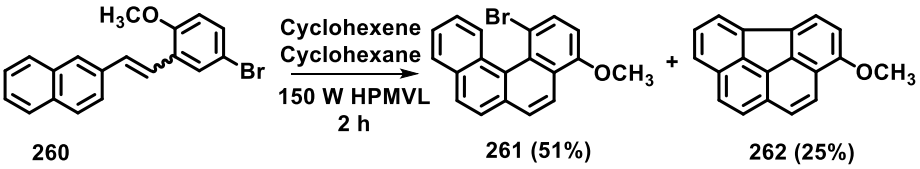

Scheme 58 Synthesis of 1-bromo-4-methoxybenzo[*c*]phenanthrene (261)

The careful isolation of the compounds showed the successful formation of 1-bromo-4-methoxybenzo[*c*]phenanthrene **(261)**.

2.4.2.2 Single Crystal XRD to determine degree of non-planarity:

Upon synthesis of 1,3-dimethylbenzo[*c*]phenanthrene-5-carbonitrile **(239)**, analysis of its solid state structure was undertaken. Single crystal X-ray quality crystals were obtained by

slow evaporation of the compound from a mixture of hexane-ethyl acetate. Single crystal X-ray diffraction analysis showed that the crystals adopted a chiral space group of $P2_12_12_1$. It also depicts the twisted helical shape adopted by the molecule with an angle of 41.81° seen between the planes defined by the terminal aromatic rings (Figure 35a) as compared to 51.2° for [5]helicene and 27° for unsubstituted B[*c*]Ph. The interplanar angle between the plane containing atoms 1, 2, 3, 4, 17 and 18 constituting ring A and atoms 17, 18, 5, 6, 15, 16 constituting ring B is found to be 13.53° while that between ring B and C is 14.57° whereas for ring C and D it is found to be 13.71°. Torsional angle along the inner rim is found to be 52.24° (C1-C17-C15-C13: 30.79° and C17-C15-C13-C12: 21.45°).

The distance between C12 and C22(Me) was found to be 2.974 Å and that between C12 and C1 is 3.153Å leading to overcrowding in the *fjord* region causing distortion from planarity of the B[*c*]Ph core (Figure 35b). The molecular geometry is distorted due to the shortening and lengthening of C-C bonds. The bonds along the inner rim are lengthened namely C13-C15, C15-C17 and C17-C11 is 1.441, 1.458, 1.441Å. It is interesting to note that in the peripheral rim, C14-C8, C7-C16, C16-C6 and C5-C18 have bond length 1.403, 1.419, 1.417 and 1.438 respectively, and are significantly shorter than the normal C-C bond length. It can be seen that the two terminal rings are bent out of plane in the opposite direction with respect to the mean plane of the central rings.

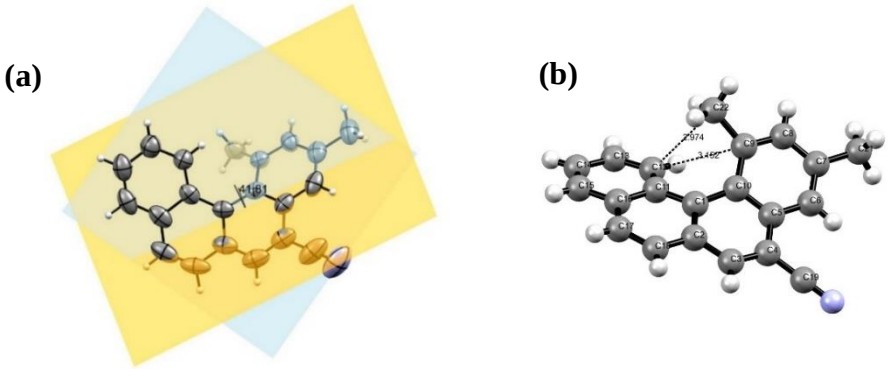

Figure 35 ORTEP diagram showing (a) interplanar angle (b) interatomic distances between C1-C12 and C12-C22 placed in *fjord* region

Molecules held together by a C-N···H-Ar bond (2.695Å) due to strong hydrogen bonding between –CN group at 5th position and peripheral hydrogen at 6th position which plays a crucial role in the formation of supramolecular assembly (Figure 36a). These interactions lead to the formation of a zig zag orientation of molecules with every alternate molecule being stacked on one another due to π-π stacking having a distance of 3.472Å between the centroids of the two central benzene rings. These sections of highly ordered arrangement of

molecules is repeated throughout the crystal packing with each section being held to the other by (CH_3)H-H(CH_3) short contact of 2.366Å (Figure 36b).

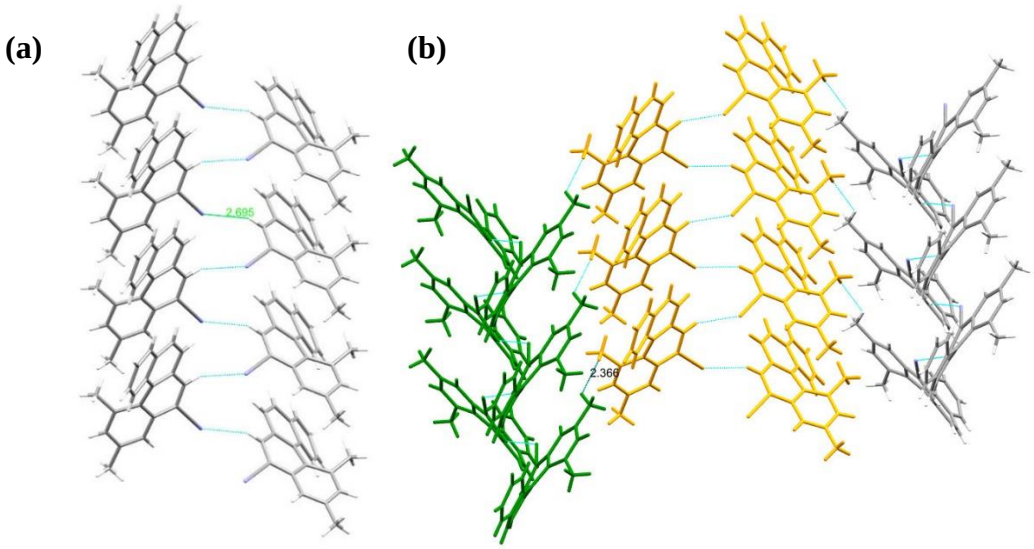

Figure 36 Showing (a) repeating unit formed by stacks of molecules held together by CN-H bonds (b) three repeating units shown with three different colours (green, orange and grey) are held together by (Me)H-H(Me) short contact seen along b-axis

It was expected that change in the position of –CN from 5th to 6th position, should not cause any significant changes in the crystal structure. But the SCXRD structure for 1,3-dimethylbenzo[*c*]phenanthrene-6-carbonitrile **(242)** showed the molecule crystallizes out in Pī space group with two molecules occupying a unit cell (Figure 37b). The angle formed between the planes containing terminal rings was reduced slightly to 37.85^o (Figure 37a). The interplanar angle between the rings A and B increased slightly to 14.07^o whereas that between B & C as well as C & D reduced slightly to 13.85^o and 10.87^o respectively.

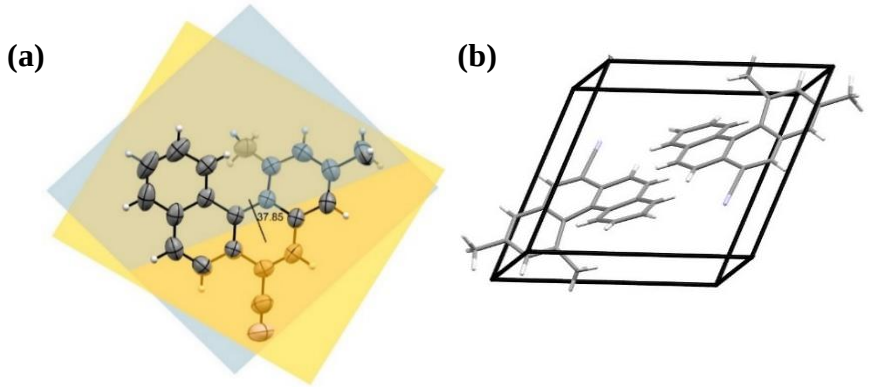

Figure 37 ORTEP diagram showing (a) interplanar angle between terminal rings (b) unit cell showing presence of two molecules

The sum of the torsional angles along the inner rim was also reduced to 49.04° (C1-C17-C15-C13: 32.40° and C17-C15-C13-C12: 16.64°). The change in the position of –CN group significantly changes the interactions between the molecules. The –CN group present at 6th position undergoes intermolecular hydrogen bonding, not with the neighbouring hydrogen (5-position), but with the aromatic hydrogen present at 2nd position. Such intermolecular bonding of the order of 2.763Å leads to the formation of a linear chain like structure and two such chains are held together by π-π stacking (3.439Å) (Figure 38).

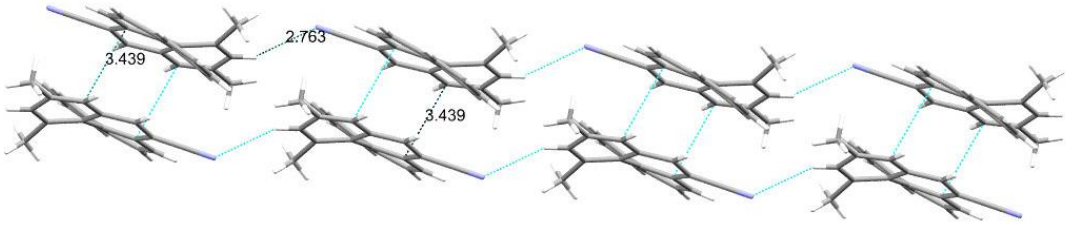

Figure 38 Showing linear chains formed by CN-H(Ar) bonding and π-π stacking

These linear chains of molecules forming a repeating unit are held together by (Me)H-H(Me) type of short contact (2.448Å) leading to the formation of a 2D network of linearly arranged molecules (Figure 39). 3X3 packing of the molecule showed a well-defined regular arrangement of molecules (Figure 40).

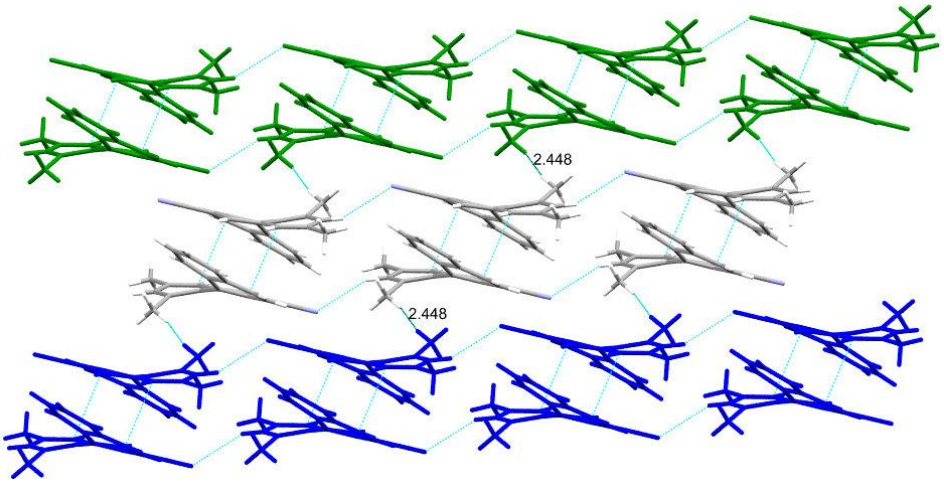

Figure 39 A 2D network of molecules formed by linear repeating units (shown in different colours of green, grey and blue)

Hence by changing the position of the substituent (-CN) in the molecule, the compounds crystallized in different space group. Also the intermolecular interactions were quite different and hence the arrangement of molecules in the crystal lattice was significantly different. These results were then compared to that of 1,3-dimethyl B[*c*]Ph **(235)** where no –CN group is present.

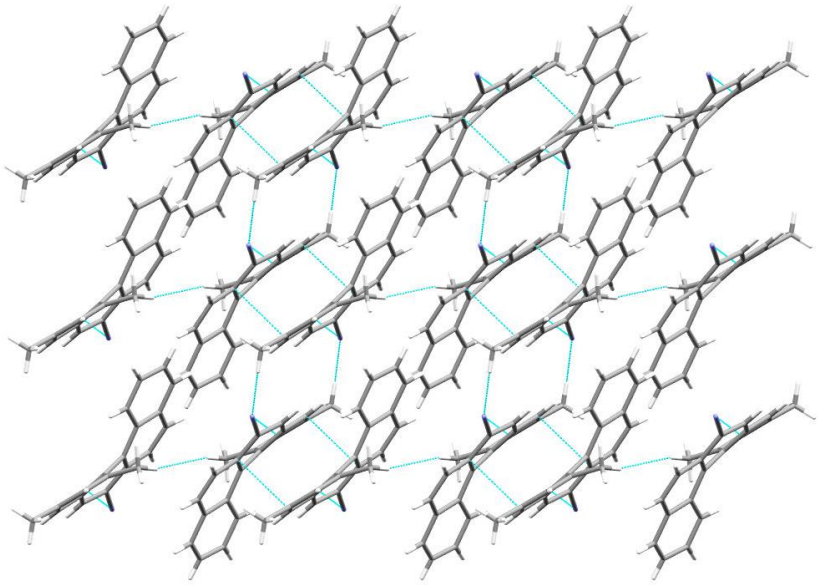

Figure 40 3X3 packing viewed along the b-axis showing systematic packing of molecules

Crystals suitable for SCXRD of 1,3-dimethyl B[*c*]Ph **(235)** were grown from a slow evaporating mixture of ethyl acetate-hexane. It crystallizes out in $Pn2_1a$ space group where one unit cell consists of four molecules (Figure 41a). The angle formed between the planes containing terminal aromatic rings (A & D) is further reduced to 36.72° (Figure 41b) and hence each ring of the B[*c*]Ph skeleton is deformed to a lesser extent. The sum of the torsional angles along the inner rim is further reduced to 47.08°.

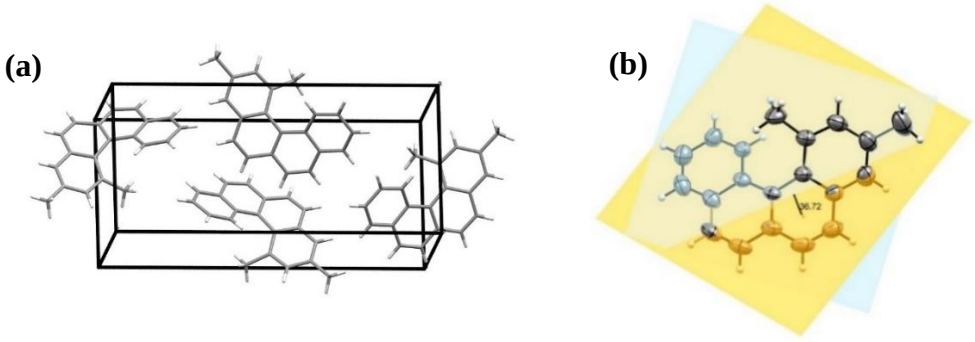

Figure 41 ORTEP diagram showing (a) asymmetric unit cell consisting of four molecules (b) the interplanar angle between two terminal rings

No hydrogen bonding is seen due to the lack of –CN group which is known to participate in such non-covalent interactions. However, a number of (Ar)H-C(Ar) interactions are seen which hold the molecules in a regular arrangement. The aromatic proton present at the 6th position undergoes C-H interaction with the C12 and C13 carbon atoms whereas the proton at 7th position is involved in similar interaction with C15 giving rise to a zig-zag arrangement of molecules (Figure 42).

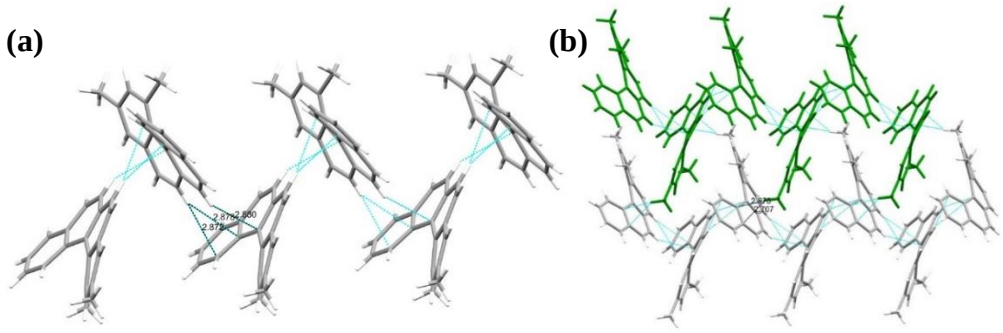

Figure 42 Showing (a) zig-zag chains formed due to C-H(Ar) interactions (b) different chains (shown with green and grey) held together by C-H(Me) interaction

These zig-zag chains are held together by another set of C-H interactions between the H of the outer methyl group present at the 3rd position and aromatic C13 and C14 (Figure 43).

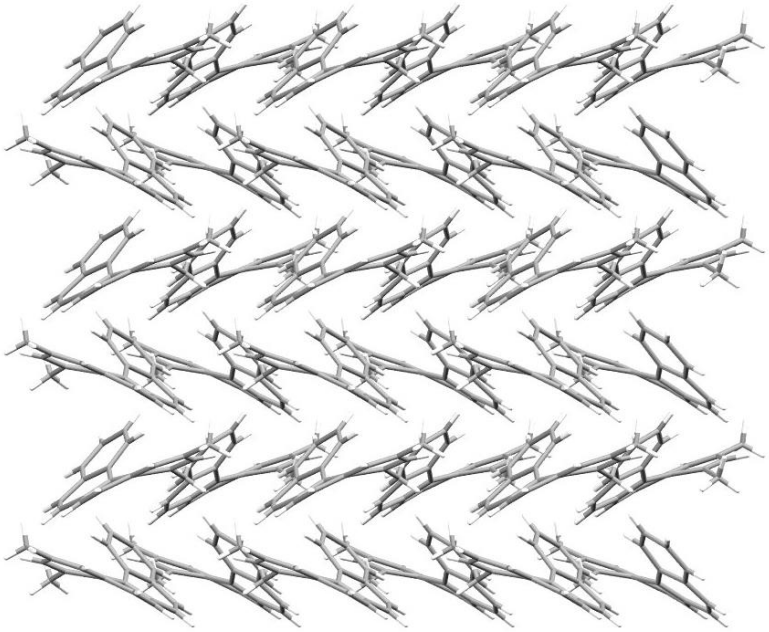

Figure 43 3X3 crystal packing viewed along c-axis

The introduction of –Br atom at the 1st position of B[*c*]Ph motif was expected to show a greater degree of distortion as compared to 1,3-dimethyl B[*c*]Ph systems. To closely analyze the degree of deformation of the molecule from planarity and to study the effect of change in the position of –CN group along the C5 and C6 carbon atoms of ring B, we subjected all the three derivatives namely 1-bromo-4-methoxyB[*c*]Ph-6-carbonitrile **(247)**, 1-bromo-4-methoxyB[*c*]Ph-5-carbonitrile **(257)** and 1-bromo-4-methoxyB[*c*]Ph **(261)** to SCXRD analysis.

A comparative study for all the three molecules showed that both the derivatives of 1-bromo B[*c*]Ph possessing –CN group **(247** & **257)** crystallized in the same space group *ie.* P21/c whereas the derivative lacking –CN group **(261)** crystallized in Pna21. Supporting our expectations, the interplanar angle between the terminal rings A and D in these molecules was slightly greater when compared to their 1-methyl substituted analogues. A comparative data for the degree of deformity and change in torsional angles is summarized in Table 7.

Table 7 Comparison of structural features for 1-bromo B[*c*]Ph derivatives

		1-Br5CN B[*c*]Ph	1-Br6CN B[*c*]Ph	1-Br B[*c*]Ph
		Compound 247	Compound 257	Compound 261
Space group		P21/c	P21/c	Pna21
Interplanar angles	A & B	13.86°	11.27°	14.33°
	B & C	16.33°	13.77°	13.83°
	C & D	13.00°	13.70°	12.34°
	A & D	42.55°	38.66°	40.04°
Torsional Angle	C1-C17-C15-C13	33.97°	28.31°	30.21°
	C17-C15-C13-C12	16.98°	19.81°	19.15°
	Sum	50.95°	48.12°	49.36°

A unit cell for each of the derivative accommodates four molecules. The steric strain in the molecule is relieved primarily by distortion of the aromatic rings (Figure 44) as well as out-of-the-plane bending of the –Br atom.

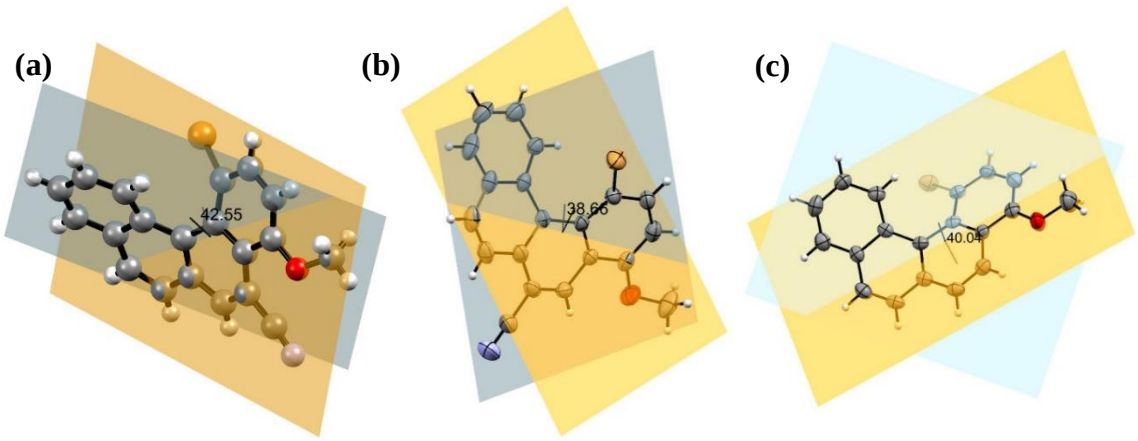

Figure 44 ORTEP diagram showing a comparison of inter-planar angle for (a) 1-Br5CN B[*c*]Ph (247) (b) 1-Br6CN B[*c*]Ph (257) (c) 1-Br B[*c*]Ph (261)

All the three derivatives show changes in the bond lengths where the bonds along the inner rim are slightly lengthened while those on the outer rim are shortened which is a characteristic for molecules adopting a helical topology. A pair of intramolecular hydrogen

bonding between –Br atom and C12 as well as C13 is observed for all the three derivatives (Figure 45), but the crystal packing differs greatly due to other non-covalent interactions present in the molecules.

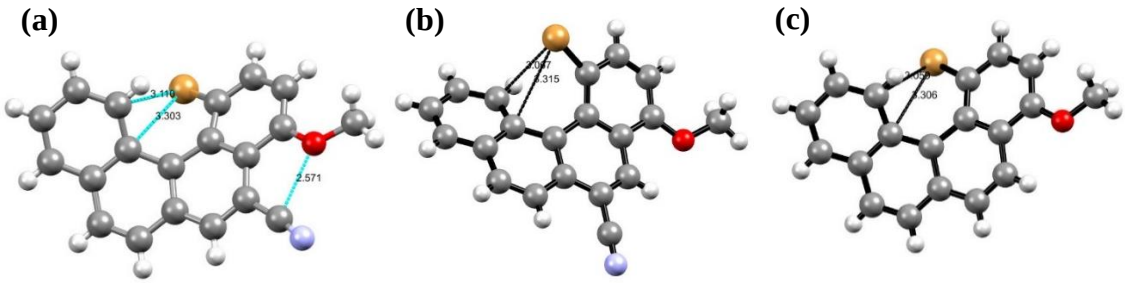

Figure 45 ORTEP diagram showing Br-C13 and Br-C12 intramolecular hydrogen bonding for (a) 1-Br5CN B[*c*]Ph (247) (b) 1-Br6CN B[*c*]Ph (257) (c) 1-Br B[*c*]Ph (261)

For 1-bromo-4-methoxyB[*c*]Ph-5-carbonitrile **(257)**, an additional (Me)O-C(N) bonding is seen (Figure 46a) which is found absent in the other two derivatives. Three molecules are held together by an intermolecular hydrogen bonding between Br-C16 of 3.546Å and a short contact C10-H(C8) of 2.876Å forming a continuous columnar arrangement of molecules (Figure 46b).

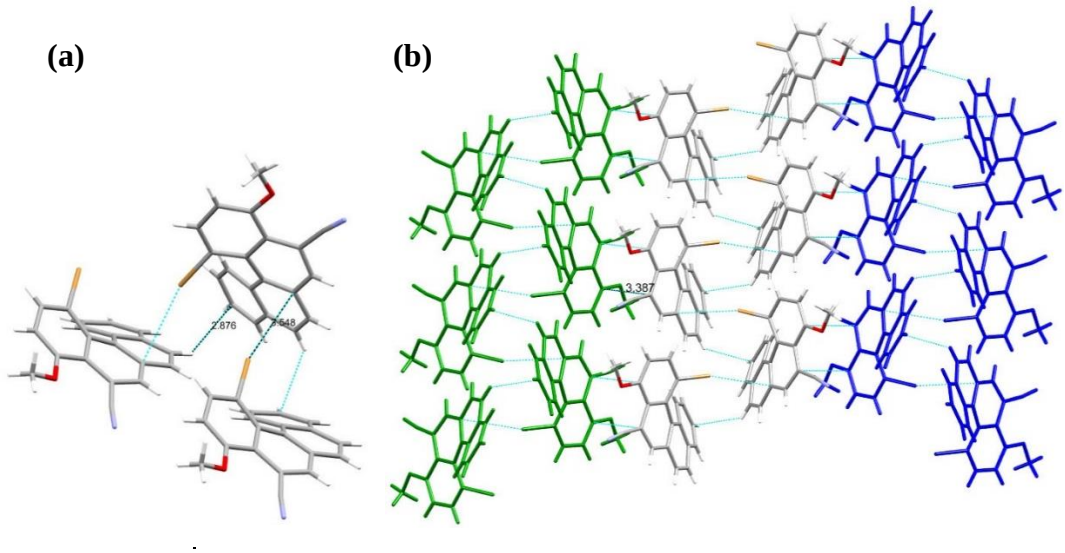

Figure 46 Crystal structure showing non-covalent interactions (a) holding three molecules together forming columns (b) columns (shown with blue, green and grey) being held together leading to a 2D regular arrangement

These columns of molecules are held with each other by π-π stacking between the aromatic rings of the B[*c*]Ph system. The presence of –OMe at C4 renders the carbon atom as electron rich site whereas, –CN at C5 makes the carbon atom electron deficient and hence creating environments ideal for such non-covalent interactions (Figure 47).

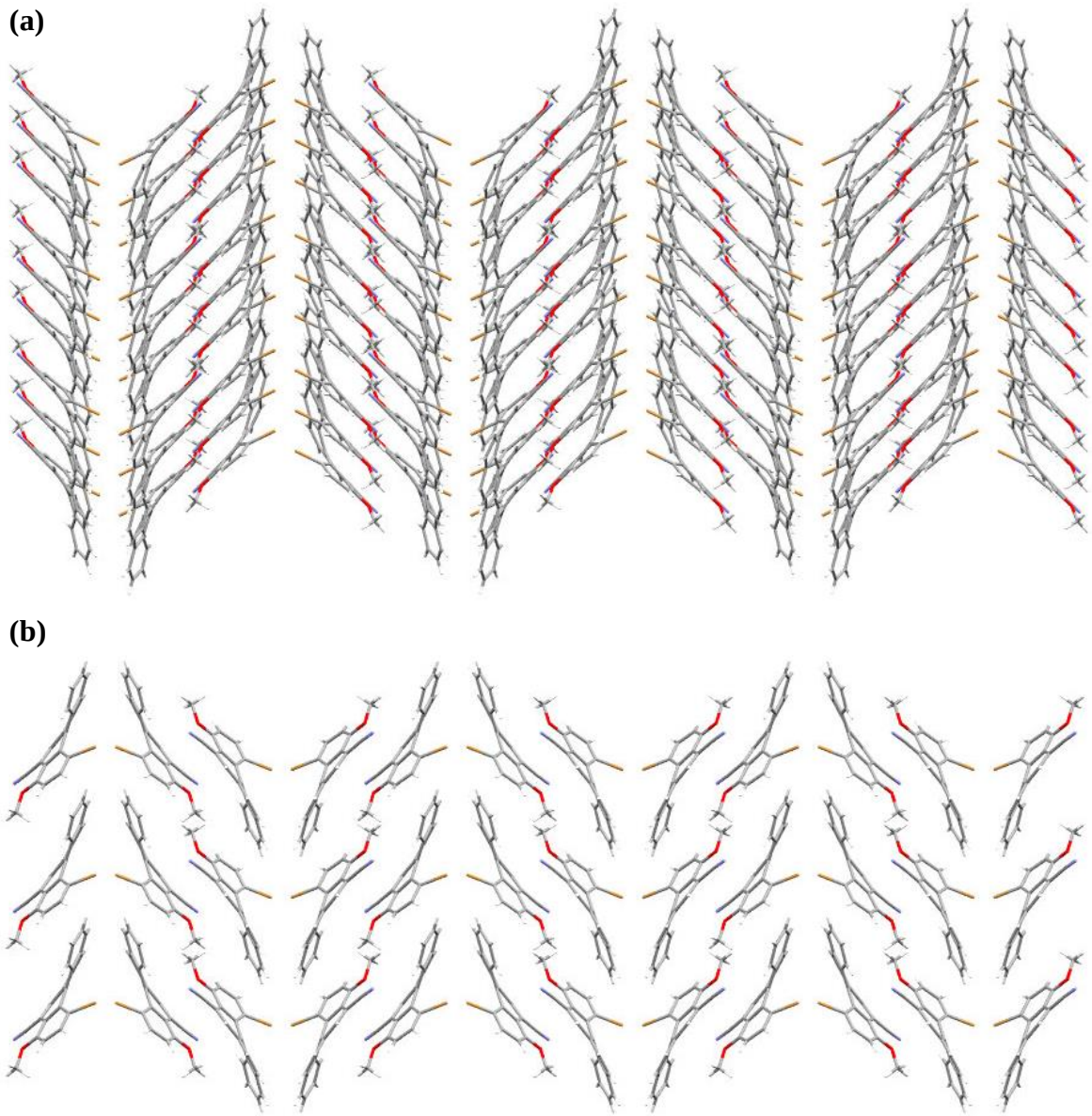

Figure 47 3X3 packing in 1-bromo-4-methoxyB[*c*]Ph-5-carbonitrile (257) viewed along (a) A-axis and (b) C-axis

However, in 1-bromo-4-methoxybenzo[*c*]phenanthrene-6-carbonitrile **(247)**, two individual molecules are held together by Br-Br short contact of 3.633Å forming a repeating unit which are arranged in a 2D plane supported by (C)N-H(C10) short contact of 2.55Å (Figure 48a). These planes of molecules are held together by (Me)H-C bonds leading to the formation of a 3D network of regularly arranged molecules (Figure 48b).

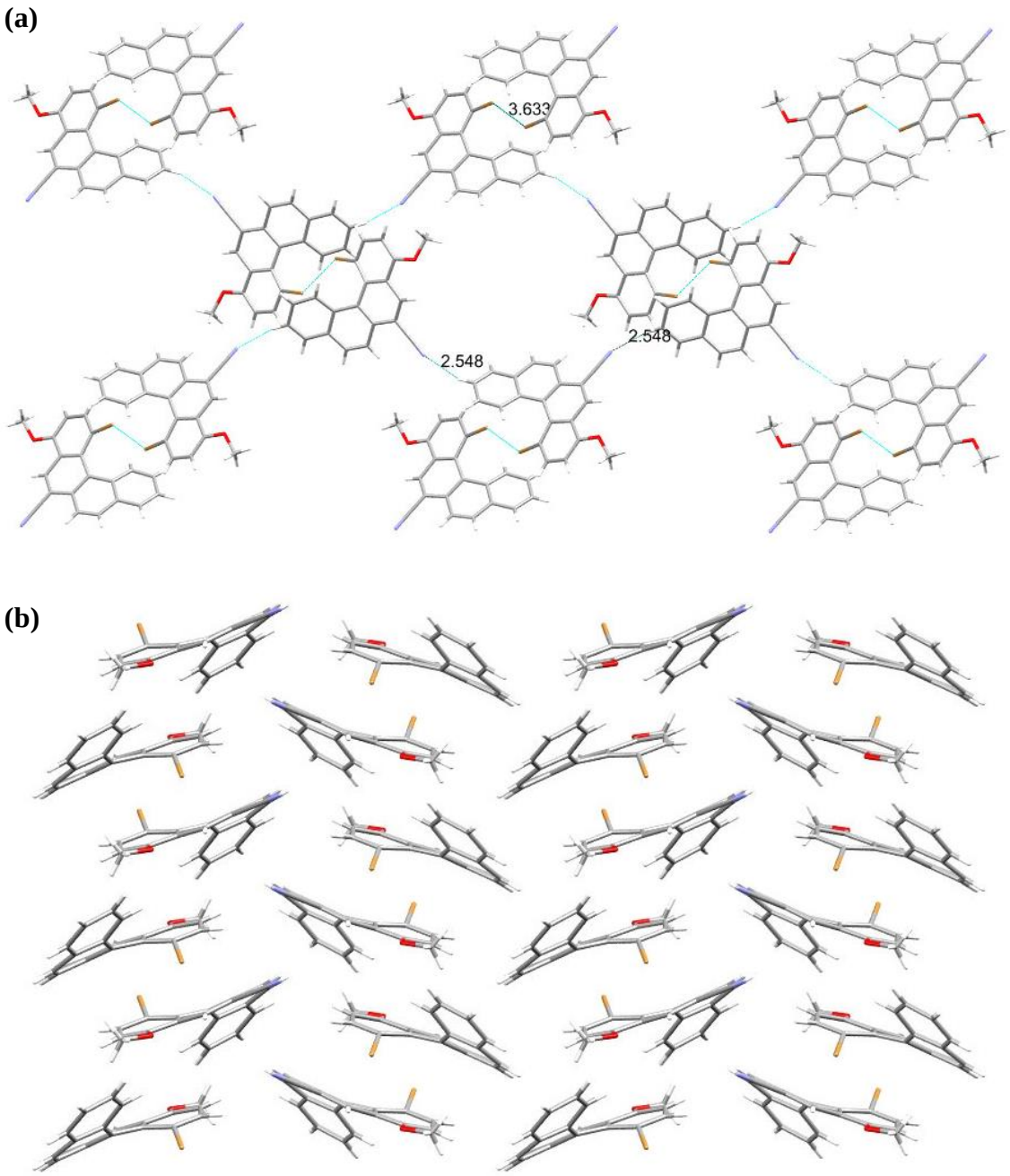

Figure 48 (a) Various non-covalent interactions holding molecules together in a plane (b) 3X3 packing viewed along A-axis

The absence of –CN group diminishes the Br-Br interactions, and now the (Ar)C-H interactions are more pronounced. Molecules are linearly held together in the form of a long chain by Br-C7 intermolecular hydrogen bonding. These linear chains are held together in a parallel arrangement by (C7)H-C15 short contact of 2.85Å (Figure 49a). A 3D 3X3 packing shows that the molecules are arranged in an ordered manner forming parallel zig zag chains (Figure 49b).

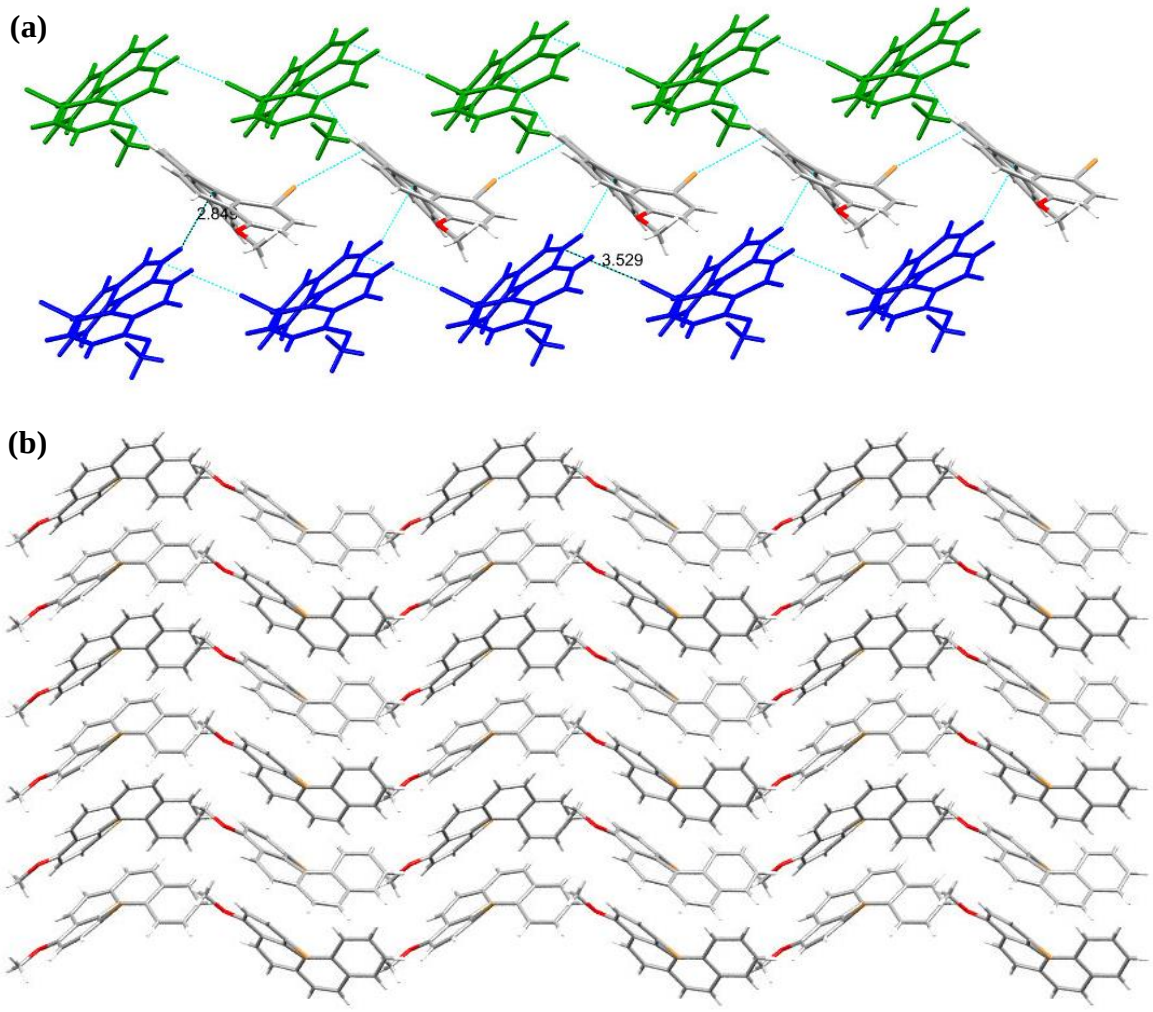

Figure 49 (a) Intermolecular contacts holding chains together (b) 3X3 packing viewed along B-axis

Hence, two positional isomers having –CN group present at C5 or C6 atoms on ring B for 1,3-dimethyl B[*c*]Ph and 1-bromo B[*c*]Ph skeleton have been analyzed for their crystal packing. The structural features in these cyano substituted derivative have been compared with its unsubstituted analogues. It was concluded that the crystal packing is strikingly different in all the derivatives under study.

2.4.2.3 Chiral HPLC Analysis:

Having observed the degree of deformity in all the six synthesized derivatives of B[*c*]Ph and the mode of steric strain relief using SCXRD, our next objective was to prove the existence of these molecules in two enantiomeric forms namely *P* and *M*. Unsubstituted B[*c*]Ph itself shows molecular distortions, but its resolution into enantiopure entities has not been possible due to its fast rate of racemization at room temperature. This rate of

enantiomer interconversion is highly influenced by the presence of substituents in the *fjord* region. Greater the size of the substituent, larger will be the barrier to racemization and hence the enantiomers will be more configurationally stable leading to effective resolution. Although limited reports on the synthesis of 1-substituted B[*c*]Ph derivatives are known, its separation by chemical or chromatographic methods is an area unexplored. Chiral HPLC is a technique well employed for the resolution of enantiomers for molecules having high barrier to interconversion (60-100 $kJmol^{-1}$). This analytical tool has been the analysis of choice due to its accurate and precise measurements, requirement of small quantities of sample for analysis and the presence of small amount of impurities generally do not interfere with the analysis results.

The synthesized 1,3-dimethyl B[*c*]Ph-5-carbonitrile **(239)** was subjected to chiral HPLC on Chiralcel OD-H column, IPA (10%) in hexane was used as the mobile phase maintaining a flow rate of 1mL/min and analyzing the output using a UV-detector. The HPLC analysis for this sample at room temperature gave a single broad peak (Figure 50a) indicating that the enantiomers of this compound underwent rapid interconversion in solution state at room temperature. The broad nature of the peak encouraged us to carry out the analysis in cryogenic conditions of 0°C. Surprisingly, at this temperature we could obtain some separation of the peak and three notches could be seen, two of them corresponding to the enantiomers separated by a slight broadened peak. This broad peak may be attributed to the racemic compound formed due to on-column isomerization or interconversion of the two enantiomers. The process of interconversion of the enantiomers was more pronounced when HPLC analysis was performed at room temperature, leading to the amalgamation of all the three peaks into a single broad peak. As temperature for the analysis was reduced to 0°C, this isomerization of the enantiomers becomes slow and some separation can be seen (Figure 50b). This was possible because the rate of racemization probably became slower as compared to the time required for the chiral stationary phase to distinguish between the enantiomers giving us some extent of separation. This encouraged us to further lower the temperature for HPLC analysis to -20°C. To our delight, two sharp peaks with almost baseline separation was successfully achieved (Figure 50c). Hence we could conclude that at -20°C, the racemization within the solution has almost been paused at equilibrium, leading to effective separation of the enantiomers at this temperature.

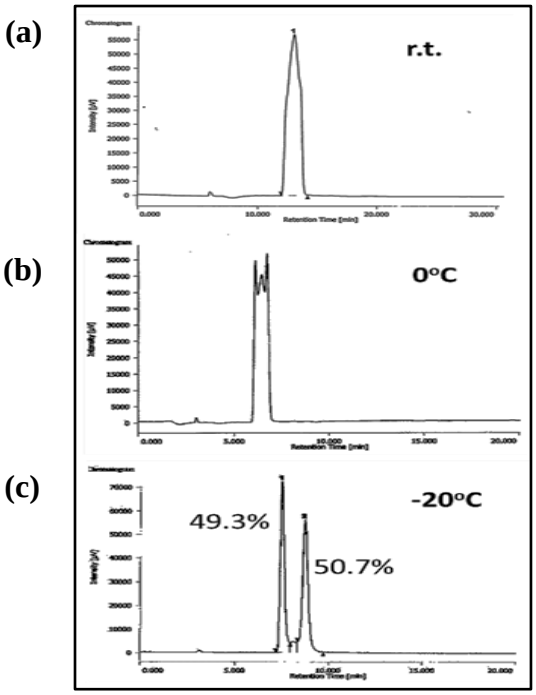

Figure 50 HPLC chromatogram of 1,3-dimethylbenzo[*c*]phenanthrene-5-carbonitrile at (a) r.t. (b) 0°C (c) -20°C

Similar observation was made for 1,3-dimethyl B[*c*]Ph where resolution could only be obtained at temperatures of -20°C (Figure 51).

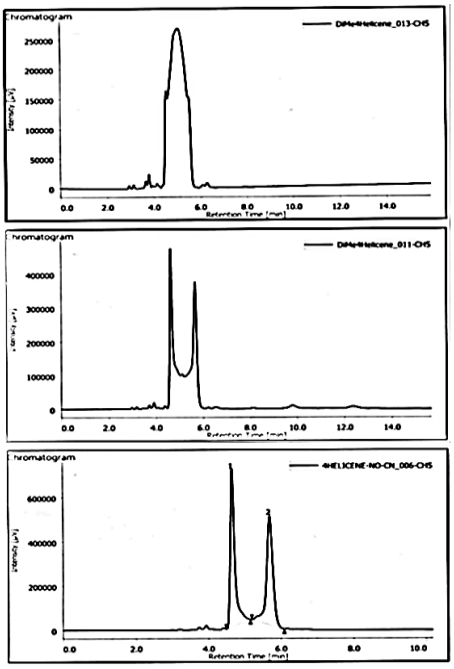

Figure 51 HPLC chromatogram of 1,3-dimethylB[*c*]Ph at (a) r.t. (b) 0°C (c) -20°C

Hence such dynamic temperature dependent HPLC can be utilized for the precise and accurate investigation of kinetic study of interconversion of enantiomers and can be an additional tool powerful for supplementary support towards results from other analytical analysis.

Similarly, 1-bromo-4-methoxy B[*c*]Ph-6-carbonitrile **(247)** was also subjected to chiral HPLC on Chiralcel OD-H at room temperature using 10% IPA in hexane as the mobile phase and 1mL/min flow rate. The chromatogram for this compound showed two sharp well resolved peaks corresponding to its two enantiomers being stable at room temperature (Figure 52). Hence, the rate of interconversion of the enantiomers for this derivative of B[*c*]Ph is slow or the barrier to racemization is high enough to prevent interconversion of the enantiomers at room temperature.

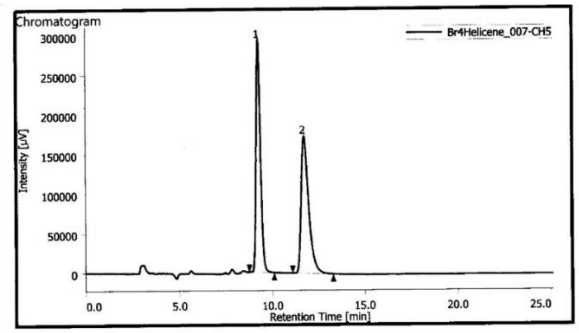

Peak Information

#	Peak Name	CH	tR [min]	Area [μV·sec]	Height [μV]	Area%	Height%	Quantity	NTP	Resolution	Symmetry Factor	Warning
1	Unknown	5	9.240	4870240	294838	49.993	62.980	N/A	7412	4.353	1.207	
2	Unknown	5	11.707	4871664	173306	50.007	37.020	N/A	4387	N/A	1.597	

Figure 52 HPLC chromatogram of 1-bromo-4-methoxybenzo[*c*]phenanthrene-6-carbonitrile at r.t.

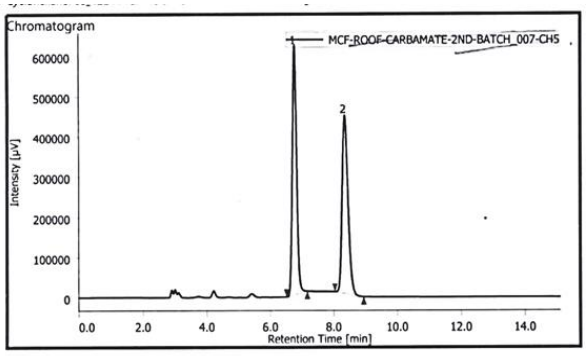

Peak Information

#	Peak Name	CH	tR [min]	Area [μV·sec]	Height [μV]	Area%	Height%	Quantity	NTP	Resolution	Symmetry Factor	Warning
1	Unknown	5	6.760	5774233	619383	50.345	58.399	N/A	12582	5.475	1.131	
2	Unknown	5	8.340	5695171	441229	49.655	41.601	N/A	9763	N/A	1.287	

Figure 53 HPLC chromatogram of 1-bromo-4-methoxybenzo[*c*]phenanthrene at r.t.

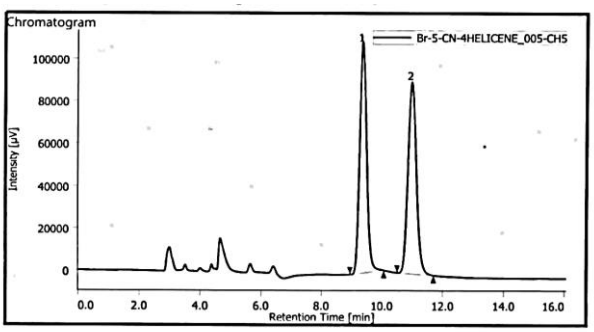

Peak Information

#	Peak Name	CH	tR [min]	Area [μV sec]	Height [μV]	Area%	Height%	Quantity	NTP	Resolution	Symmetry Factor	Warning
1	Unknown	5	9.353	1739972	108947	50.091	54.634	N/A	8192	3.543	1.180	
2	Unknown	5	10.967	1733645	90467	49.909	45.366	N/A	7703	N/A	1.154	

Figure 54 HPLC chromatogram of 1-bromo-4-methoxybenzo[*c*]phenanthrene-5-carbonitrile at r.t.

Thus, these derivatives have sufficient bulk at 1-position of the B[*c*]Ph skeleton which not only render them chiral, but also make them ideal candidates for attempting resolution to obtain optically pure enantiomers.

2.4.2.4 Chiral Crystals: Absolute Asymmetric Synthesis:

Chiral recognition of molecules due to intermolecular interactions is of utmost importance in material sciences. PAHs have proved to be an important scaffold in the research on supramolecular chirality of self-assembled systems. Such assemblies of PAHs with helically aligned sp^2-carbons is of particular interest due to their unique applications as optical materials. Apart from their fascinating inherent chiro-optic properties, their self-assemblies may represent new structures with novel properties. They also readily undergo π-π stacking which is one of the most important forms of noncovalent interactions determining if a system can perform self-assembly or not. They also absorb strongly in UV−Vis region, which allows their chiral assemblies to be easily characterized with CD spectra and other analytical tools.

Spontaneous Deracemization:

When racemic compounds are subjected to crystallization without the addition of external chiral moieties, they may crystallize as (i) *racemate* where both the enantiomers are present in the same crystal, (ii) as *pseudoracemate* in which both the enantiomers are present in equal amounts but in a non-ordered arrangement, (iii) *conglomerate* where each crystal contains only one of the enantiomers leading to spontaneous resolution. Most of the organic compounds crystallize as racemates with only 5-10% of them crystallizing as

conglomerates. A distinct advantage of racemates crystallizing as conglomerates is their ability to form enantiomorphous crystals. These enantiopure crystals usually differ in morphology, leading to their separating by hand picking each crystal itself. This eliminates the use of expensive reagents employed for resolution along with additional steps of bond making and breaking. Hence formation of conglomerates and their resolution by crystallization has gained tremendous interest as a mode for resolution of racemates.

However, all these approaches for resolution of enantiomers by crystallization, leads to ideally a maximum yield of 50%. Sometimes, it is possible to racemize the other isomer in a separate loop, and reinjecting the racemized mixture in the resolution process repeatedly. Starting from the solution of the racemic mixture, a flux of energy is applied to the system in the form of temperature gradient, ultrasound, grinding *etc*. The solution remains racemic in composition at all time during the process of deracemization until one of the two solid enantiomers completely disappears. Resolution by this method leads to complete conversion of the racemate to one enantiomer leading to possibility of 100% theoretical yield and is termed as *'Spontaneous Deracemization'*.[125]

Although a few molecules have been reported in literature to undergo such spontaneous deracemization, a prerequisite for such type of resolution is the presence of a certain extent of molecular flexibility and the compound should form a solid conglomerate. Also the ability of the molecule to undergo various non-covalent interactions such as hydrogen bonding, π-π stacking *etc*. influences the symmetry of crystals. For such mode of resolution, the rate of racemization in the solution phase should be fairly larger than the rate of crystal growth. Smaller helicenes like B[*c*]Ph are reported to undergo racemization upon heating in solution where the enantiomers undergo rapid interconversion *via* a planar transition state. The slow growth of one primary enantiopure crystal allows either enrichment of that enantiomer or leads to crystallization of the entire sample as single enantiomer. The difference in the melting point of the racemic sample and enantiopure compound facilitates the crystallization of one enantiomer over its crystallization in racemic form leading to enrichment of one of the enantiomers.[126]

2.4.2.4.1 SCXRD as a tool for detecting spontaneous resolution:

The most suitable method to determine if such spontaneous deracemization has taken place is by single crystal X-ray diffraction studies along with CD spectroscopy. 1,3-

Dimethylbenzo[*c*]phenanthrene-5-carbonitrile **(239)** was subjected to crystallization in various solvent systems. Majority of the solvent systems investigated like hexane-methanol, tetrahydrofuran, dimethyl sulphoxide, hexane-chloroform etc. did not give crystals suitable for carrying out SCXRD. However, thin needle like crystals were obtained from a mixture of hexane-ethyl acetate or hexane-acetone. A systematic methodology was developed using accurately weighed samples (100 mg) and subjecting them to crystallization in the same solvent system with different ratios of hexane and ethyl acetate/acetone under refluxing conditions. Slow evaporation from a mixture of hexane (2 mL) and ethyl acetate (3 mL)/acetone (2 mL) lead to formation of needle shape crystals within a few hours.

A close examination of the SCXRD structure of crystals obtained from hexane-ethyl acetate mixture showed that the compound crystallized in a chiral $P2_12_12_1$ space group with four molecules present in a unit cell. All the four molecules present in a unit cell possessed the same configuration. A preliminary examination of the Flack parameter in Olex2 showed a value of -6.2 which lead us to believe that the configuration of these molecules was (*P*). A number of crystals were randomly selected from the same batch as well as the crystals obtained from evaporation of the mother liquor. To our delight, all the crystals analyzed, crystallized in the same chiral space group having molecules with a single configuration namely (*P*). To check the reproducibility of this observation, other 06 number batches were subjected to similar crystallization conditions. The crystals obtained were analyzed and the observation were in agreement with the earlier one (Table 8).

Table 8 Comparison of SCXRD data for compound 239 from same batch

	Exp-1241	**Exp-1574**	**Exp-1698**
space_group_name	P 21 21 21	P 21 21 21	P 21 21 21
space_group_crystal_system	orthorhombic	orthorhombic	orthorhombic
space_group_name_Hall	P 2ac 2ab	P 2ac 2ab	P 2ac 2ab
cell_length_a	5.8560(12)	5.819(2)	5.834(2)
cell_length_b	11.369(3)	11.327(5)	22.543(6)
cell_length_c	22.613(6)	22.483(11)	11.322(3)
cell_angle_alpha	90	90	90
cell_angle_beta	90	90	90
cell_angle_gamma	90	90	90
cell_volume	1505.6(6)	1481.9(12)	1489.0(8)
cell_formula_units_Z	4	4	4
cell_measurement_theta_max	69.9870	69.9870	18.4490
cell_measurement_theta_min	3.4620	3.4620	3.8530
exptl_crystal_density_diffrn	1.246	1.261	1.2550

exptl_crystal_F_000	596	592.2257	592.2257
refine_ls_abs_structure_Flack	-5(10)	-24.3(11)	-3(5)
diffrn_reflns_limit_h_max	6	7	7
diffrn_reflns_limit_h_min	-7	-7	-7
diffrn_reflns_limit_k_max	12	15	30
diffrn_reflns_limit_k_min	-15	-15	-29
diffrn_reflns_limit_l_max	21	29	15
diffrn_reflns_limit_l_min	-30	-29	-15
R-factor(%)	8.18	13.63	12.57

Table 9 Comparison of SCXRD data for compound 239 from various batches

	Exp-1979	**Exp-1992**	**Exp-2039**
space_group_name	P 21 21 21	P 21 21 21	P 21 21 21
space_group_crystal_system	orthorhombic	orthorhombic	orthorhombic
space_group_name_Hall	P 2ac 2ab	P 2ac 2ab	P 2ac 2ab
cell_length_a	5.8269(13)	5.8266(14)	5.8621(7)
cell_length_b	11.332(2)	11.353(3)	11.4080(12)
cell_length_c	22.530(3)	22.535(5)	22.649(3)
cell_angle_alpha	90	90	90
cell_angle_beta	90	90	90
cell_angle_gamma	90	90	90
cell_volume	1487.6(5)	1490.7(6)	1514.6(3)
cell_formula_units_Z	4	4	4
cell_measurement_theta_max	18.2720	18.4450	20.8570
cell_measurement_theta_min	3.6100	3.9480	3.9800
exptl_crystal_density_diffrn	1.2561	1.2535	1.243
exptl_crystal_F_000	592.2257	592.2257	600
refine_ls_abs_structure_Flack	-15.1(13)	0(24)	-5.8(10)
diffrn_reflns_limit_h_max	7	7	7
diffrn_reflns_limit_h_min	-7	-7	-8
diffrn_reflns_limit_k_max	15	15	15
diffrn_reflns_limit_k_min	-14	-15	-15
diffrn_reflns_limit_l_max	30	29	29
diffrn_reflns_limit_l_min	-30	-29	-29
R-factor(%)	11.26	12.08	8.44

Hence, 1,3-dimethylB[*c*]Ph-5-carbonitrile **(239)** undergoes spontaneous deracemization, where one enantiomer crystallizes out and the solution or mother liquor racemizes at room temperature. These crystals were subjected to specific optical rotation measurements which was expected to show some value due to the presence of a single enantiomer obtained by spontaneous deracemization. But no specific optical rotation could be observed in the experimental conditions of 25ºC. This could be attributed to the possibility of rapid racemization of the molecules in solution state at this temperature but its enantiopure nature

is confirmed in the solid state in the form of crystals. Hence we resorted to solid state analysis which could prove the chiral nature of the crystallized compound.

In a similar set of experiment involving the use of hexane-acetone (1:1) as the solvent for crystallization, pale yellow coloured needles were obtained which were also subjected to SCXRD. The crystals not only possessed similar physical morphology but also crystallizes in the same chiral space group namely $P2_12_12_1$. The unit cell showed the presence of 4 molecules all having the same helical configuration. However, the flack parameter was positive (18.1). When the configuration of the molecules was inverted, the flack parameter reduced greatly -13.3 concluding that the configuration of these set of crystals was different than that obtained from hexane-ethyl acetate. The reproducibility of such spontaneous deracemization has been observed by repeatedly carrying out SCXRD of randomly picked crystals and the results are summarized in Table 10.

Table 10 Comparison of SCXRD data for compound 239 from hexane-acetone

	Exp-1533	**Exp-1537**	**Exp-1551**
space_group_name	P 21 21 21	P 21 21 21	P 21 21 21
space_group_crystal_system	orthorhombic	orthorhombic	orthorhombic
space_group_name_Hall	P 2ac 2ab	P 2ac 2ab	P 2ac 2ab
cell_length_a	5.8266(17)	5.8337(17)	5.8268(11)
cell_length_b	11.338(4)	11.345(3)	11.313(3)
cell_length_c	22.560(9)	22.590(5)	22.506(3)
cell_angle_alpha	90	90.00	90.00
cell_angle_beta	90	90.00	90.00
cell_angle_gamma	90	90.00	90.00
cell_volume	1490.3(9)	1495.1(7)	1483.6(5)
cell_formula_units_Z	4	4	4
cell_measurement_theta_max	18.3770	18.1240	20.9750
cell_measurement_theta_min	4.0080	4.0110	3.8840
exptl_crystal_density_diffrn	1.2539	1.250	1.260
exptl_crystal_F_000	592.2257	546	592
refine_ls_abs_structure_Flack	-13.1(18)	-10(10)	-10(10)
diffrn_reflns_limit_h_max	7	7	6
diffrn_reflns_limit_h_min	-7	-7	-7
diffrn_reflns_limit_k_max	7	6	14
diffrn_reflns_limit_k_min	-15	-14	-13
diffrn_reflns_limit_l_max	28	28	30
diffrn_reflns_limit_l_min	-16	-12	-28
R-factor(%)	8.06	5.36	6.81

2.4.2.4.2 Solid State Circular Dichroism:

Solid state CD was the analysis of choice as the solution state can be avoided where we believe the molecules undergo racemization and also it can be used for the determination of absolute configuration of organic molecules. Solid state CD however has less applications in the field of organic chemistry and its use has been mainly restricted to the analysis of metal complexes and some organic derivatives like benzamides.

A solid state CD analysis for the crystals obtained from hexane-ethyl acetate mixture was carried out. The CD spectra obtained was a bisignate with a curve at higher wavelength being positive and that at lower wavelength being negative. The sign pattern of the CD curve reflects the clockwise skew sense of the molecules present in the crystals obtained from hexane-ethyl acetate mixture. Hence, the absolute configuration obtained from solid state CD was assigned as "*P*" which is in agreement with that assigned using the Flack parameter.

A similar analysis for the crystals obtained from hexane-acetone was carried out. We expected these crystals to possess (*M*) absolute configuration which was confirmed by carrying out its solid state CD. The solid state CD showed an almost equal and opposite bisignate curve, confirming that these crystals constituted the other isomer namely *M*.

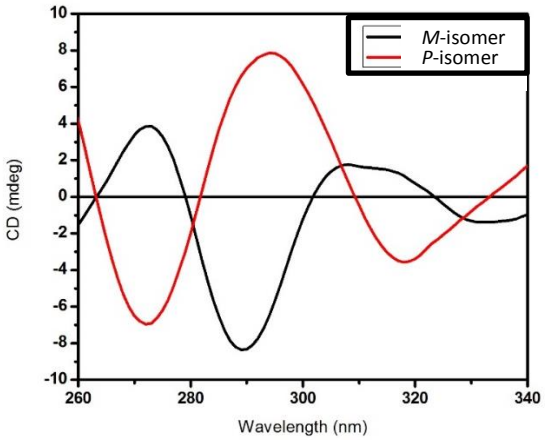

Figure 55 Solid state CD spectra of both the isomers

As these molecules undergo rapid racemization in solution state, the optical rotation for this compound was not obtained and hence these enantiomers could only be characterized using SCXRD and solid state CD measurements.

However, when the functional isomer of 1,3-dimethylB[*c*]Ph-5-carbonitrile **(239)** namely 1,3-dimethylB[*c*]Ph-6-carbonitrile **(242)** was subjected to similar crystallization in various solvent conditions, we invariably obtained racemic crystals. This proves that even a slight

modification in the structure of a compound (change in the position of functional group) can affect its ability to undergo spontaneous deracemization. On the other hand, 1,3-dimethylB[*c*]Ph **(235)** which lacks –CN group also failed to undergo spontaneous deracemization. This can be attributed to the fact that the lack of –CN group which is an efficient hydrogen bond acceptor, leads to loss in secondary interactions failing to form a supramolecular assembly required for self-recognition of the isomers.

To confirm this hypothesis, the 1-bromoB[*c*]Ph derivatives were also subjected to a similar study. 1-BromoB[*c*]Ph **(261)** and 1-bromoB[*c*]Ph-6-carbonitrile **(247)** were structurally similar to 1,3-dimethylB[*c*]Ph **(235)** and 1,3-dimethylB[*c*]Ph-6-carbonitrile **(242)** possessing the absence of –CN group or presence of –CN group at the 6th position respectively. Similar to earlier observations, both the 1-bromoB[*c*]Ph **(261** & **247)** derivatives failed to show the phenomena of spontaneous deracemization. This confirmed our assumption, that the position of –CN on the molecular scaffold plays an important role in determining whether the molecule undergoes spontaneous resolution or not. However, we expected that 1-bromoB[*c*]Ph-5-carbonitrile **(257)** which is similar to 1,3-dimethylB[*c*]Ph-5-carbonitrile **(239)** would be effective in forming supramolecular assemblies due to similar positioning of the –CN group which plays a vital role in molecular recognition. However, 1-bromoB[*c*]Ph-5-carbonitrile **(257)** also failed to undergo spontaneous deracemization. This can attributed to the replacement of –Me group by –Br at the 1st position which causes a loss in the non-covalent interactions needed for such recognition. Also the electronic factors that cause the 1-bromoB[*c*]Ph-5-carbonitrile **(257)** to be stable at room temperature lead to a decrease in the rate of racemization in the solution state. Hence, the rate of racemization required to maintain the solution in its racemic form is slow in 1-bromoB[*c*]Ph-5-carbonitrile **(257)** and both the isomers crystallize out at the same time to maintain the equilibrium of the solution. Hence, the phenomena of spontaneous resolution is very selective to the nature and position of functional groups present in a molecule.

2.4.2.5 Conclusion:

Various 1-substituted benzo[*c*]phenanthrenes (B[*c*]Ph) have been synthesized in the present study. We have introduced –Me group or –Br group at 1st position of the B[*c*]Ph skeleton and studied the structural changes occurring in the molecule due to the introduction of –CN group. The –CN group is introduced either at the 5th position or 6th position of the 1-substituted B[*c*]Ph skeleton and the results are compared to the corresponding derivatives without the –CN group. Three 1-methylB[*c*]Ph derivatives were synthesized as a single product in good yields. However, the synthesis of 1-bromoB[*c*]Ph was difficult due to the presence of labile –Br group which was lost during the process of photocyclization of the stilbene derivatives. The formation of a benzo[*ghi*]fluoranthene type of molecule which has been reported under drastic conditions of Flash Vacuum Pyrolysis (FVP), has been reported for the first time during the process of photocyclization. All the six molecules synthesized were subjected to SCXRD analysis to compare various structural features and the degree of distortion with 1-bromo-4-methoxyB[*c*]Ph-5-carbonitrile **(257)** showing maximum distortion (42.55^{o}). The three 1-methylB[*c*]Ph derivatives could be separated using chiral HPLC at cryogenic temperature of -20^{o}C whereas the 1-bromoB[*c*]Ph derivatives were found to show stable enantiomers at room temperature making them ideal candidates for resolution. Among all the six derivatives synthesized, only 1,3-dimethyl B[*c*]Ph-5-carbonitrile **(239)** was observed to undergo spontaneous deracemization. A mixture of hexane-ethyl acetate or hexane-acetone gave crystals of opposite configuration (*P* and *M* respectively). This was proved by carrying out SCXRD as well as solid state CD for the crystals due to rapid racemization in the solution phase. Such meticulous study proves the sensitivity of molecular recognition and formation of supramolecular assemblies which depend greatly, not only on the nature of functional groups, but also their position on the aromatic scaffold.

2.4.2.6 Experimental Section:

Synthesis of 1-(bromomethyl)-3,5-dimethylbenzene (132):

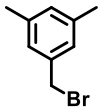

Mesitylene **(131)** (1.0g; 8.32mmol), *N*-bromosuccinimide (1.33g; 7.49mmol) and benzoyl peroxide (0.1g; 0.42mmol) are added to 15 mL of carbon tetrachloride. This mixture is refluxed in a round-bottomed for 6h. The completion of the reaction can be seen from the precipitation of succinimide and confirmed by TLC. After the reaction is complete, the reaction mixture is cooled, filtered and washed with fresh carbon tetrachloride to remove succinimde which is a byproduct of the reaction. The reaction mixture is then concentrated under vacuum. The residue is subjected to column chromatography which furnishes 3,5-dimethylbenzyl bromide **(132)** as colourless viscous liquid which solidifies when kept in the refridgerator (1.0g; Yield: 81%; M.P. 40 °C).

^{1}H NMR ($CDCl_3$, 400MHz) δ 7.03 (s, 2H); 6.96 (s, 1H); 4.46 (s, 2H); 2.33 (s, 6H)

Synthesis of 3,5-dimethylbenzaldehyde (230):

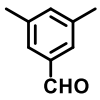

3,5-dimethylbenzyl bromide **(132)** (0.5g; 2.5mmol) was dissolved in 5mL acetic acid. To this, a solution of hexamethylenetetraamine (0.7g; 5.0mmol) in 5mL water is added and the reaction is heated to refluxed under nitrogen atmosphere for 4h. The reaction mixture was cooled to room temperature and 10mL of conc. HCl was added and the reaction was heated at 80^{o}C for 12h. After the completion of reaction (TLC), the mixture was poured in cold water and extracted with ethyl acetate (4 X 20 mL). The combined organic layers were dried over Na_2SO_4 and concentrated. The residue was chromatographed over SiO_2 column using petroleum ether to obtain 3,5-dimethyl benzaldehyde **(230)** as a viscous colourless liquid (0.68g; Yield 51%).

^{1}H NMR ($CDCl_3$, 400MHz) δ 7.76 (s, 2H); 7.27 (s, 1H); 2.40 (s, 6H)

Synthesis of 3,5-dimethylbenzyl cyanide (236):

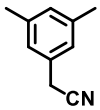

3,5-dimethylbenzyl bromide **(132)** (1.5g; 7.53mmol), potassium cyanide (0.59g; 9.05mmol) and tetrabutylammonium bromide (0.48g; 1.51mmol) are added to a mixture of toluene (18mL) and water (2mL). The reaction mixture is heated to 80^{o}C for 16h. The progress of the reaction is measured by TLC. After the completion of the reaction, the reaction mixture is allowed to cool and extracted using toluene (3 X 25mL). The combined organic layer is dried over Na_2SO_4 and concentrated under reduced pressure. The residue is subjected to column chromatography using petroleum ether to give 3,5-

dimethylbenzyl cyanide **(236)** as low melting colourless solid (1.00g; Yield 91%; M.P. 44°C).

^{1}H NMR ($CDCl_3$, 400MHz) δ 6.99 (s, 1H); 6.97 (s, 2H); 3.69 (s, 2H); 2.35 (s, 6H)

Synthesis of 2-bromomethyl naphthalene (232):

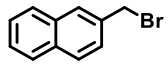

2-Methylnaphthalene **(231)** (2.0g; 14.1mmol) is dissolved in 15 mL of carbon tetrachloride and is treated with *N*-bromosuccinimide (2.63g; 14.4mmol) and benzoyl peroxide (0.17g; 0.69mmol). This mixture is refluxed in a round-bottomed for 6h. The completion of the reaction can be seen from the precipitation of succinimide and confirmed by TLC. After the reaction is complete, the reaction mixture is cooled, filtered and washed with fresh carbon tetrachloride to remove succinimde which is a byproduct of the reaction. The reaction mixture is then concentrated under vacuum. The residue is subjected to crystallization in ethanol which furnishes white crystals of 2-bromomethyl naphthalene **(232)** (2.20g; Yield: 71%; M.P. 53 °C)

^{1}H NMR ($CDCl_3$, 400MHz) δ 8.37-8.35 (d, *J*=8.4Hz, 1H); 7.86-7.84 (d, *J*=8.0Hz, 1H); 7.84-7.81 (d, *J*=8.4Hz, 2H); 7.66-7.62 (m, 1H); 7.59-7.57 (m, 1H); 7.56-7.54 (d, *J*=8.4Hz, 1H); 7.28 (s, 1H); 4.89 (s, 2H)

Synthesis of 2-napthaldehyde (237):

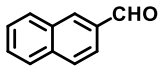

2-Bromomethyl naphthalene **(232)** (0.5g; 2.3mmol) was dissolved in 10 mL AR grade Dimethyl sulfoxide. To this solution, potassium carbonate (0.6g; 4.5mmol) is added and the reaction is heated to 80-90°C under nitrogen atmosphere for 6h. The reaction mixture was cooled to room temperature and 50mL of ice-cold water was added. The mixture was then transferred to a separating funnel and extracted with ethyl acetate (4 X 20 mL). The combined organic layers were dried over Na_2SO_4 and concentrated. The residue was chromatographed over SiO_2 column using petroleum ether to obtain 2-napthaldehyde **(237)** as a low melting colourless solid (0.22g; Yield 63%; M.P. 59°C).

^{1}H NMR ($CDCl_3$, 400MHz) δ 7.92-7.87 (m, 4H); 7.54-7.52 (m, 2H); 7.50-7.47 (dd, *J*=8.8Hz, 1.6Hz, 1H); 4.17 (s, 1H)

Synthesis of 2-naphthyl acetonitrile (240):

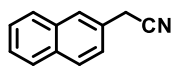

2-(Bromomethyl)naphthalene **(232)** (0.30g; 1.36mmol) is dissolved in 9mL toluene to which a solution of potassium cyanide (0.11g; 1.63mmol) and

tetrabutylammonium bromide (0.09g; 0.27mmol) in 1 mL water is added. The reaction mixture is heated to 80°C for 12h. The progress of the reaction is measured by TLC. After the completion of the reaction, the reaction mixture is allowed to cool and extracted using toluene (3 X 25mL). The combined organic layer is dried over Na_2SO_4 and concentrated under reduced pressure. The residue is subjected to column chromatography using 5% ethyl acetate in petroleum ether to give 2-naphthyl acetonitrile **(240)** as colourless crystalline solid (0.19g; Yield 84%; M.P. 60°C).

^{1}H NMR ($CDCl_3$, 400MHz) ***δ*** 7.90-7.85 (m, 4H); 7.57-7.52 (m, 2H); 7.42-7.40 (dd, *J*=8.4Hz, 1.6Hz, 1H); 3.95 (s, 2H)

Synthesis of 4-bromo-2-(bromomethyl)-1-methoxy benzene (244):

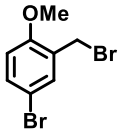

A mixture of 4-bromo anisole **(243)** (2.0g; 10.7 mmol) and paraformaldehyde (0.35g; 11.7 mmol) in 10 mL of glacial acetic acid was taken in a two necked round bottom flask which was heated to 80°C till the solution becomes clear. At the same temperature, 48% HBr solution (2.7mL; 16.0mmol) is added dropwise using an addition funnel over a period of 20mins. The reaction mixture was refluxed at 80°C for 6h. After the completion of the reaction (monitored by TLC) the reaction mixture is poured into 100 mL of water. This aqueous layer is then basified using $NaHCO_3$ till effervescence are observed followed by its extraction in ethyl acetate. The organic layer is separated, dried over sodium sulfate and concentrated under reduced pressure. The residue obtained is subjected to column chromatography over silica gel to get 4-bromo-2-(bromomethyl)-1-methoxy benzene **(244)** as colourless low melting solid (1.9g; Yield 63%; M.P. 58°C).

^{1}H NMR ($CDCl_3$, 400MHz) ***δ*** 7.46 (s, 1H); 7.41-7.39 (d, *J*=8.4Hz, 1H); 6.78-6.76 (d, *J*=8.4Hz, 1H); 4.50 (s, 2H); 3.89 (s, 3H)

Synthesis of 5-bromo-2-methoxybenzaldehyde (245):

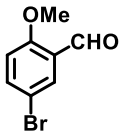

4-Bromo-2-bromomethylbenzyl bromide **(244)** (0.25g; 0.9mmol) and potassium carbonate (0.24g; 1.8mmol) were taken DMSO (5mL) in a round bottom flask. The mixture was stirred at a temperature of 120-130°C for 4h under N_2 atmosphere. After disappearance of starting material (TLC), the mixture was cooled to room temperature and 50mL of ice-cold water and was allowed to stir at room temperature till the solution became clear. The mixture was then transferred to a separating funnel and extracted with ethyl acetate (20 mL × 4). The combined organic layers were dried

over Na_2SO_4 and concentrated. The residue was chromatographed over SiO_2 column using petroleum ether to obtain 5-bromo-2-methoxybenzaldehyde **(245)** as a colourless solid (0.16g; Yield 75%; M.P. 118°C).

^{1}H NMR ($CDCl_3$, 400MHz) δ 10.39 (s, 1H); 7.93-7.92 (d, *J*=1.2Hz, 1H); 7.66-7.63 (dd, *J*=8.8Hz, 2.4Hz, 1H); 6.92-6.90 (d, *J*=8.8Hz, 1H); 3.94 (s, 3H)

Synthesis of 5-bromo-2-methoxybenzonitrile (250):

4-bromo-2-(bromomethyl)-1-methoxybenzene **(244)** (0.25g; 0.9mmol), potassium cyanide (0.07g; 1.07mmol) and tetrabutylammonium bromide (0.06g; 0.18mmol) are dissolved in 10 ml of toluene-water mixture (9:1). The reaction mixture is heated to 80°C for 12h. The progress of the reaction is measured by TLC. After the completion of the reaction, the reaction mixture is allowed to cool and extracted using toluene (3 X 25mL). The combined organic layer is dried over Na2SO4 and concentrated under reduced pressure. The residue is subjected to column chromatography using 2% ethyl acetate in petroleum ether to give 5-bromo-2-methoxybenzonitrile **(250)** as colourless crystalline solid (0.13g; Yield 60%; M.P. 62°C).

^{1}H NMR ($CDCl_3$, 400MHz) δ 7.50-7.49 (d, *J*=1.6Hz, 1H); 7.45-7.42 (dd, *J*=8.8Hz, 1.6Hz, 1H); 6.80-6.78 (d, *J*=8.8Hz, 1H); 3.87 (s, 3H); 3.68 (s, 2H)

Synthesis of 2-(3,5-dimethylphenyl)-3-(naphthalen-2-yl)acrylonitrile (238):

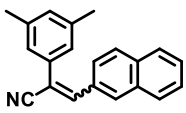

3,5-dimethylbenzyl cyanide **(236)** (0.16g; 1.09mmol), 2-napthaldehyde **(237)** (0.17g; 1.09mmol) and potassium hydroxide (0.13g; 2.20mmol) are added to 10mL dry methanol. The reaction is allowed to stir at room temperature for 6h. The proceeding of the reaction is seen by the formation of precipitates and completion is marked by the disappearance of the starting materials on TLC. The reaction mixture is then concentrated under reduced pressure and purified using column chromatography over silica gel to obtain 2-(3,5-dimethylphenyl)-3-(naphthalen-2-yl)acrylonitrile **(238)** as pale yellow low melting solid (0.23g; Yield 73%)

^{1}H NMR ($CDCl_3$, 400MHz) δ 8.31 (s, 1H); 8.13-8.11 (dd, *J*=8.8Hz, 1.6Hz, 1H); 7.95-7.88 (m, 3H); 7.70 (s, 1H); 7.60-7.55 (m, 2H); 7.37 (s, 2H); 7.08 (s, 1H); 2.42 (s, 6H)

^{13}C NMR ($CDCl_3$, 100MHz) δ 141.9; 138.8 (2C); 134.5; 134.0; 133.1; 131.4; 130.9; 130.4; 128.8; 128.7; 127.8; 127.6; 126.8; 125.3; 123.9 (2C); 118.5; 111.7; 21.4 (2C)

IR (KBr) ν 3056; 3012; 2955; 2917; 2864; 2212; 1604; 1462; 1374; 1274; 1127; 1038; 916; 847; 819; 751; 687; 648; 479

Synthesis of 2-(3,5-dimethylphenyl)-2-(naphthalen-2-yl)acrylonitrile (241):

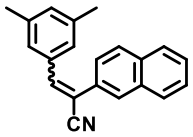

2-naphthyl acetonitrile **(240)** (0.3g; 1.79mmol), 3,5-dimethyl benzaldehyde **(230)** (0.27g; 1.97mmol) and potassium hydroxide (0.2g; 3.60mmol) are added to 10mL dry methanol. The reaction is allowed to stir at room temperature for 6h. The proceeding of the reaction is seen by the formation of precipitates and completion is marked by the disappearance of the starting materials on TLC. The reaction mixture is then concentrated under reduced pressure and purified using column chromatography over silica gel to obtain 3-(3,5-dimethylphenyl)-2-(naphthalen-2-yl)acrylonitrile **(241)** as pale yellow low melting solid (0.42g; Yield 83%)

^{1}H NMR ($CDCl_3$, 400MHz) δ 8.19-8.18 (d, *J*=1.6Hz, 1H); 7.95-7.94 (m, 1H); 7.93-7.91 (d, *J*=8.4Hz, 1H); 7.89-7.87 (m, 1H); 7.79-7.76 (dd, *J*=8.8Hz, 2.0Hz, 1H); 7.65 (s, 1H); 7.59 (s, 2H); 7.57-7.55 (m, 2H); 7.12 (s, 1H); 2.42 (s, 6H)

^{13}C NMR ($CDCl_3$, 100MHz) δ 142.8; 138.8; 133.9; 133.6; 133.5; 132.6 (2C); 132.2; 129.1; 128.7; 127.9 (2C); 127.4; 127.2; 127.1; 126.4; 122.8; 118.4; 111.4; 21.5 (2C)

IR (KBr) ν 3052; 2943; 2914; 2857; 2209; 1590; 1508; 1460; 1374; 1344; 1296; 1274; 1126; 1029; 945; 918; 881; 849; 808; 743; 687; 479

Synthesis of 2-(3,5-dimethylphenyl)-3-(naphthalen-2-yl)acrylonitrile (238):

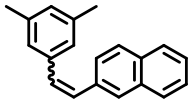

3,5-dimethylbenzyl bromide **(132)** (1.0g; 5.03mmol) and triphenyl phosphine (1.32g; 5.03mmol) were refluxed in 15mL xylene. The completion of the reaction is marked by the precipitation of the corresponding Wittig salt and disappearance of the starting material (TLC). The reaction mixture is filtered, washed with fresh xylene and the residue is dried to obtain (3,5-dimethylbenzyl) triphenylphosphonium bromide as colourless powder. In a round bottom flask, a solution of sodium (0.03g; 0.96mmol) in dry methanol (5mL) is added dropwise to a suspension of 2-naphthaldehyde **(237)** (0.1g; 0.64mmol) and (3,5-dimethylbenzyl triphenyl phosphonium bromide (0.25g; 0.64mmol) in 5mL dry methanol. The addition is done over a period of 0.5h after which, the reaction is allowed to stir at room temperature for 12h till no starting material is seen on TLC. The reaction mixture is then concentrated under vacuum and poured onto cold water. The aqueous layer is extracted using ethyl acetate (3 X 25mL), dried over Na_2SO_4 and concentrated under reduced pressure. The residue obtained is subjected to column chromatography on silica gel using 2% ethyl acetate in

petroleum ether to obtain 2-(3,5-dimethylstyryl)naphthalene **(238)** as white solid (0.14g; Yield 85%)

^{1}H NMR ($CDCl_3$, 400MHz) δ 7.87-7.83 (m, 4H); 7.78-7.76 (dd, *J*=8.8Hz, 1.6Hz, 1H); 7.53-7.45 (m, 2H); 7.32-7.27 (d, *J*=16.4Hz, 1H); 7.23 (s, 2H); 7.23-7.19 (d, *J*=16.0Hz, 1H); 6.97 (s, 1H); 2.39 (s, 6H)

^{13}C NMR ($CDCl_3$, 100MHz) δ 138.4 (2C); 137.5; 135.3; 133.9; 133.2; 129.7; 129.5; 128.6; 128.5; 128.2; 127.9; 126.7; 126.5; 126.0; 124.7 (2C); 123.8; 21.5 (2C)

IR (KBr) ν 3051; 3016; 2918; 2853; 1624; 1593; 1506; 1457; 1387; 1365; 1038; 1015; 966; 890; 852; 816; 751; 691; 481

Synthesis of 2-(5-bromo-2-methoxyphenyl)-3-(naphthalen-2-yl) acrylonitrile (251):

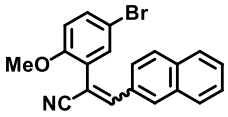

Similar synthetic procedure; but using 5-bromo-2-methoxybenzonitrile **(250)** (0.15g; 0.66mmol), 2-napthaldehyde **(237)** (0.11g; 0.66mmol) to obtain 2-(5-bromo-2-methoxyphenyl)-3-(naphthalen-2-yl) acrylonitrile **(251)** as pale yellow solid (0.19g; Yield 78%)

^{1}H NMR ($CDCl_3$, 400MHz) δ 8.29 (s, 1H); 8.12-8.01 (dd, *J*=8.4Hz, 2.0Hz, 1H); 7.95-7.93 (d, *J*=8.4Hz, 1H); 7.93-7.92 (d, *J*=2.4Hz, 1H); 7.90-7.88 (dd, *J*=7.6Hz, 2.0Hz, 1H); 7.60-7.58 (dd, *J*=7.6Hz, 2.4Hz, 1H); 7.58 (s, 1H); 7.57-7.54 (m, 2H); 7.52-7.49 (dd, *J*=8.8Hz, 2.4Hz, 1H); 6.90-6.88 (d, *J*=8.8Hz, 1H); 3.95 (s, 3H)

^{13}C NMR ($CDCl_3$, 100MHz) δ 156.2; 146.9; 134.2; 133.1 (2C); 132.4; 131.2; 130.6; 128.8; 128.7; 127.8; 127.7; 126.8; 126.7; 125.3; 117.8; 113.2; 113.1; 107.5; 56.1

IR (KBr) ν 3077; 3051; 3016; 2964; 2943; 2910; 2843; 2204; 1594; 1486; 1381; 1359; 1258; 1217; 1187; 1142; 1026; 932; 868; 799; 735; 650; 623; 467

Synthesis of 3-(5-bromo-2-methoxyphenyl)-2-(naphthalen-2-yl) acrylonitrile (246):

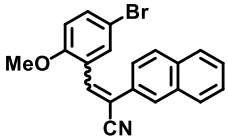

Similar synthetic procedure; but using 2-naphthyl acetonitrile **(240)** (0.11g; 0.61mmol), 5-bromo-2-methoxybenzaldehyde **(245)** (0.13g; 0.61mmol) to obtain 3-(5-bromo-2-methoxyphenyl)-2-(naphthalene-2-yl)acrylonitrile **(246)** as pale yellow solid (0.21g; Yield 89%)

^{1}H NMR ($CDCl_3$, 400MHz) δ 8.27-8.26 (d, *J*=2.4Hz, 1H); 8.20-8.19 (d, *J*=1.2Hz, 1H); 7.98 (s, 1H); 7.95-7.94 (m, 1H); 7.93-7.90 (d, *J*=8.4Hz, 1H); 7.89-7.87 (m, 1H); 7.80-7.78 (dd, *J*=8.4Hz, 2.0Hz, 1H); 7.57-7.52 (m, 3H); 6.87-6.85 (d, *J*=8.4Hz, 1H); 3.92 (s, 3H)

^{13}C NMR ($CDCl_3$, 100MHz) δ 156.9; 135.6; 134.3; 133.4; 133.2; 131.5; 131.0; 128.9; 128.5; 127.7; 127.1; 127.0; 126.4; 124.9; 122.6; 117.6; 113.1; 112.4; 55.9

IR (KBr) ν 3110; 3052; 3014; 2946; 2917; 2844; 2222; 1590; 1484; 1397; 1368; 1314; 1255; 1177; 1012; 947; 887; 851; 801; 739; 607; 532; 469

Synthesis of 2-(5-bromo-2-methoxystyryl) naphthalene (260):

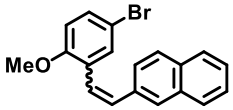

Similar synthetic procedure; but using (5-bromo-2-methoxybenzyl)triphenylphosphonium bromide **(259)** (which is prepared from 4-bromo-2-(bromomethyl)-1-methoxy benzene **(244)**) (0.22g; 0.41mmol), 2-naphthaldehyde **(237)** (0.064g; 0.41mmol) to obtain 2-(5-bromo-2-methoxystyryl) naphthalene **(260)** as pale yellow solid (0.12g; Yield 85%)

^{1}H NMR ($CDCl_3$, 400MHz) ***δ*** 7.87-7.80 (m, 4H); 7.77-7.75 (dd, *J*=7.6Hz, 2.4Hz, 2H); 7.74-7.70 (m, 3H); 7.64-7.62 (d, *J*=8.4Hz, 1H); 7.53-7.42 (m, 5H); 7.35-7.30 (m, 3H); 7.28-7.26 (d, *J*=7.6Hz, 1H); 6.83-6.80 (d, *J*=8.8Hz, 1H); 6.80-6.78 (d, *J*=8.8Hz, 1H); 6.79-6.77 (d, *J*=9.6Hz, 1H); 6.87-6.64 (d, *J*=12.4Hz, 1H); 3.90 (s, 3H); 3.78 (s, 3H)

IR (KBr) ν 3055; 3013; 2988; 2957; 2931; 2897; 2832; 1587; 1480; 1457; 1401; 1282; 1247; 1175; 1119; 1030; 963; 903; 864; 810; 750; 622; 481

Synthesis of 1,3-dimethylbenzo[*c*]phenanthrene-5-carbonitrile (239):

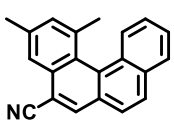

A solution of 2-(3,5-dimethylphenyl)-3-(naphthalen-2-yl)acrylonitrile **(238)** (0.225g; 0.8mmol), iodine (0.22g; 0.88mmol) and tetrahydrofuran (3.2mL; 40mmol) in 650mL toluene was irradiated with 250W HPMVL for 24h. After the completion of the reaction (TLC), the organic layer was washed with saturated solution of $Na_2S_2O_3$ to remove excess of iodine. The organic layer was separated and washed with brine, concentrated under reduced pressure to obtain 1,3-dimethylbenzo[*c*] phenanthrene-5-carbonitrile **(239)** as yellow solid (0.2g; Yield 90%)

^{1}H NMR ($CDCl_3$, 400MHz) ***δ*** 8.23 (s, 1H); 8.06 (s, 1H); 8.02-7.98 (d, *J*=12.0Hz, 1H); 7.67-7.60 (m, 2H); 7.48 (s, 1H); 2.66 (s, 3H); 2.36 (s, 3H)

^{13}C NMR ($CDCl_3$, 100MHz) ***δ*** 137.7; 136.4; 133.8; 133.4; 132.9; 131.6; 130.4; 130.2; 129.6; 129.2; 128.1; 127.6; 127.4; 127.2; 125.7; 125.4; 122.4; 118.4; 108.9; 24.7; 21.5

IR (KBr) ν 3052; 2965; 2922; 2862; 2217; 1609; 1444; 1372; 1234; 1110; 1032; 912; 854; 817; 669; 645; 584; 434

Synthesis of 1,3-dimethylbenzo[*c*]phenanthrene-6-carbonitrile (242):

Similar procedure; but using 3-(3,5-dimethylphenyl)-2-(naphthalen-2-yl)acrylonitrile **(241)** (0.3g; 1.06mmol) to obtain **242** as pale yellow solid (0.29g; Yield 87%)

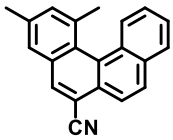

^{1}H NMR ($CDCl_3$, 400MHz) δ 8.28 (s, 1H); 8.28-8.25 (d, J=8.8Hz, 1H); 8.11-8.09 (d, *J*=8.8Hz, 1H); 8.07-8.05 (dd, *J*=8.4Hz, 1.6Hz, 1H); 8.02-7.99 (dd, *J*=8.4Hz, 1.6Hz, 1H); 7.69 (s, 1H); 7.68-7.60 (m, 2H); 7.53 (s, 1H); 2.64 (s, 3H); 2.37 (s, 3H)

^{13}C NMR ($CDCl_3$, 100MHz) δ 137.1; 136.3; 135.4 (2C); 134.8 (2C); 132.6; 132.5; 130.1; 129.9; 129.3; 128.7; 127.9; 126.8; 125.9; 125.8; 122.7; 118.4; 109.6; 24.7; 21.4

IR (KBr) ν 3052; 2950; 2916; 2860; 2218; 1608; 1503; 1445; 1415; 1377; 1336; 1256; 1030; 895; 848; 819; 755; 688; 608; 581; 501; 443

Synthesis of 1,3-dimethylbenzo[*c*]phenanthrene (235):

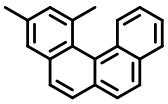

Similar synthetic procedure; but using 2-(3,5-dimethylstyryl)naphthalene **(234)** (0.11g; 0.43mmol) to obtain 1,3-dimethylbenzo[*c*]phenanthrene **(235)** as pale yellow solid (0.10g; Yield 87%)

^{1}H NMR ($CDCl_3$, 400MHz) δ 8.08-8.06 (m, 1H); 8.03-8.01 (m, 1H); 7.97-7.95 (d, *J*=8.4Hz, 1H); 7.88-7.86 (d, *J*=8.4Hz, 1H); 7.82-7.80 (d, *J*=8.4Hz, 1H); 7.76-7.74 (d, *J*=8.4Hz, 1H); 7.67 (s, 1H); 7.61-7.57 (m, 2H); 7.41 (s, 1H); 2.63 (s, 3H); 2.43 (s, 3H)

^{13}C NMR ($CDCl_3$, 100MHz) δ 135.8; 135.7; 134.6; 132.4; 131.7; 131.5; 130.5; 130.3; 127.9; 127.6; 127.5; 127.4; 127.1; 126.3; 126.0; 125.6; 125.3; 124.9; 24.9; 21.5

IR (KBr) ν 3045; 3015; 2952; 2918; 2857; 1605; 1479; 1438; 1378; 1264; 1214; 1031; 855; 829; 794; 749; 670; 585; 523; 436

Synthesis of 1-bromo-4-methoxybenzo[*c*]phenanthrene-5-carbonitrile (257):

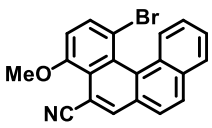

A solution of 2-(5-bromo-2-methoxyphenyl)-3-(naphthalen-2-yl) acrylonitrile **(251)** (0.14g; 0.39mmol), and cyclohexene (0.4mL; 3.9mmol) in 300mL cyclohexane was irradiated with 125W HPMVL for 4h. The organic layer was concentrated under reduced pressure to obtain 1-bromo-4-methoxybenzo[*c*]phenanthrene-5-carbonitrile **(257)** as yellow solid (0.1g; Yield 73%)

^{1}H NMR ($CDCl_3$, 400MHz) δ 8.34 (s, 1H); 8.28-8.26 (dd, *J*=8.4Hz, 1.6Hz, 1H); 8.08-8.06 (d, *J*=8.4Hz, 1H); 8.04-8.02 (dd, *J*=8.4Hz, 1.6Hz, 1H); 7.94-7.92 (d, *J*=8.4Hz, 1H); 7.85-7.83 (d, *J*=8.8Hz, 1H); 7.72-7.68 (m, 1H); 7.66-7.62 (m, 1H); 7.08-7.06 (d, *J*=8.4Hz, 1H); 4.18 (s, 3H)

Synthesis of 1-bromo-4-methoxybenzo[*c*]phenanthrene-6-carbonitrile (257):

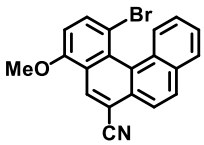

Similar synthetic procedure; but using 3-(5-bromo-2-methoxyphenyl)-2-(naphthalene-2-yl) acrylonitrile **(246)** (0.15g; 0.41mmol) to obtain 1-bromo-4-methoxybenzo[*c*]phenanthrene-6-carbonitrile **(257)** as yellow solid (0.082g; Yield 55%)

^{1}H NMR ($CDCl_3$, 400MHz) δ 8.82 (s, 1H); 8.26-8.24 (d, *J*=8.8Hz, 1H); 8.25-8.23 (dd, *J*=8.8Hz, 1.2Hz, 1H); 8.15-8.13 (d, *J*=8.8Hz, 1H); 8.06-8.04 (dd, *J*=8.4Hz, 1.2Hz, 1H); 7.98-7.96 (d, *J*=8.4Hz, 1H); 7.71-7.67 (m, 1H); 7.66-7.62 (m, 1H); 7.02-7.00 (d, *J*=8.8Hz, 1H); 4.12 (s, 3H)

IR (KBr) ν 3068; 3004; 2967; 2932; 2897; 2834; 2224; 1581; 1552; 1470; 1416; 1349; 1329; 1305; 1281; 1252; 1160; 1072; 990; 905; 817; 759; 684; 550; 496

Synthesis of 1-bromo-4-methoxybenzo[*c*]phenanthrene (261):

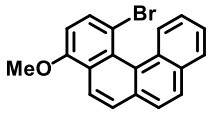

Similar synthetic procedure; but using 2-(5-bromo-2-methoxystyryl) naphthalene **(260)** (0.2g; 0.59mmol) to obtain 1-bromo-4-methoxybenzo[*c*]phenanthrene **(261)** as yellow solid (0.1g; Yield 51%)

^{1}H NMR ($CDCl_3$, 400MHz) δ 8.36-8.34 (d, *J*=8.4Hz, 1H); 8.34-8.32 (dd, *J*=8.8Hz, 2.0Hz, 1H); 8.01-7.99 (m, 2H); 7.87-7.85 (d, *J*=8.4Hz, 1H); 7.86-7.84 (d, *J*=8.0Hz, 1H); 7.85-7.83 (d, *J*=8.4Hz, 1H); 7.62-7.60 (m, 2H); 6.97-6.95 (d, *J*=8.4Hz, 1H); 4.11 (s, 3H)

IR (KBr) ν 3046; 3004; 2953; 2928; 2859; 2833; 1589; 1482; 1455; 1408; 1356; 1321; 1281; 1243; 1125; 1070; 835; 794; 762; 668; 501

Spectral data of 3-methoxybenzo[*ghi*]fluoranthene-1-carbonitrile (249):

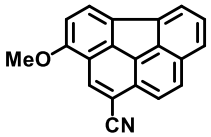

^{1}H NMR ($CDCl_3$, 400MHz) δ 8.45 (s, 1H); 7.98-7.96 (d, *J*=9.2Hz, 1H); 7.84-7.81 (d, *J*=9.2Hz, 1H); 7.53-7.47 (m, 1H); 7.47-7.45 (dd, *J*=7.6Hz, 1.2Hz, 1H); 7.13-7.11 (d, *J*=8.8Hz, 1H); 7.07-7.05 (dd, *J*=7.6Hz, 1.2Hz, 1H); 6.93-6.91 (d, *J*=8.4Hz, 1H); 4.03 (s, 3H)

Spectral data of 4-methoxybenzo[*c*]phenanthrene-6-carbonitrile (248):

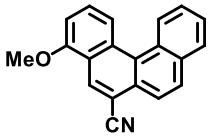

^{1}H NMR ($CDCl_3$, 400MHz) δ 9.07-9.05 (m, 1H); 8.92 (s, 1H); 8.67-8.65 (dd, *J*=8.4Hz, 1.6Hz, 1H); 8.27-8.24 (dd, *J*=8.8Hz, 1.6Hz, 1H); 8.08-8.06 (dd, *J*=8.0Hz, 1.6Hz, 1H); 8.06-8.04 (d, *J*=8.8Hz, 1H); 7.76-7.74 (dd, *J*=8.0Hz, 1.6Hz, 1H); 7.72-7.68 (m, 2H); 7.09-7.08 (d, *J*=7.6Hz, 1H); 4.12 (s, 3H)

2.4.2.7 Spectral Data:

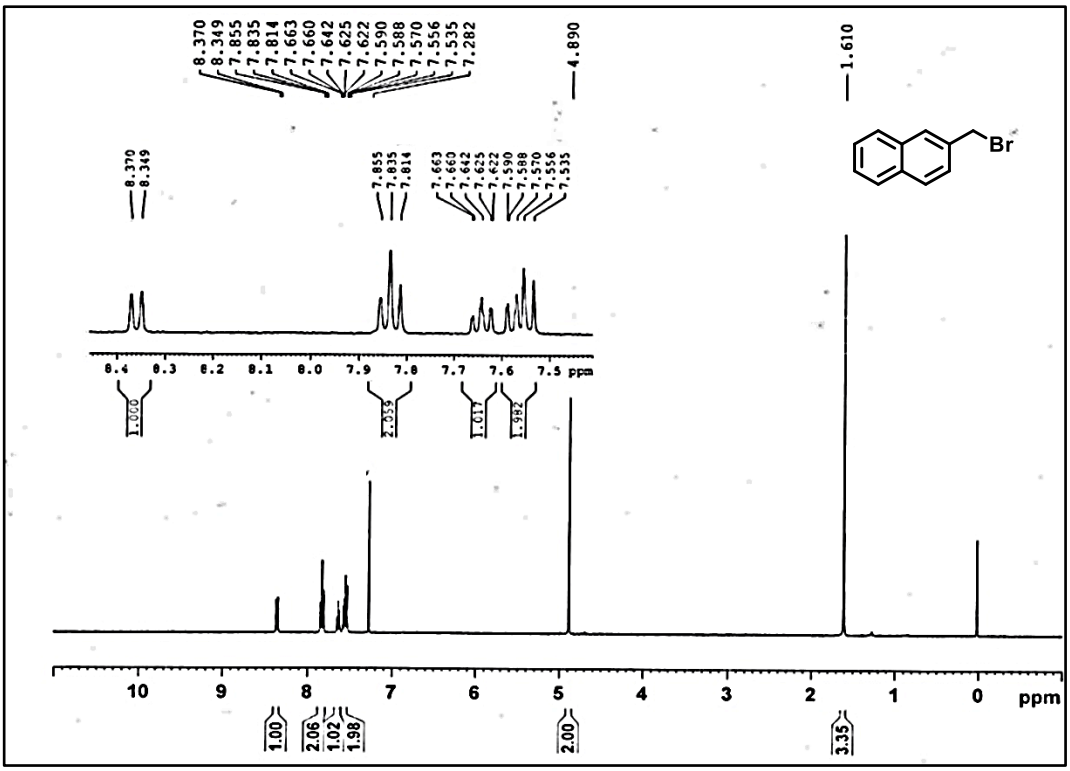

^{1}H NMR Spectra of compound **232** ($CDCl_3$, 400MHz)

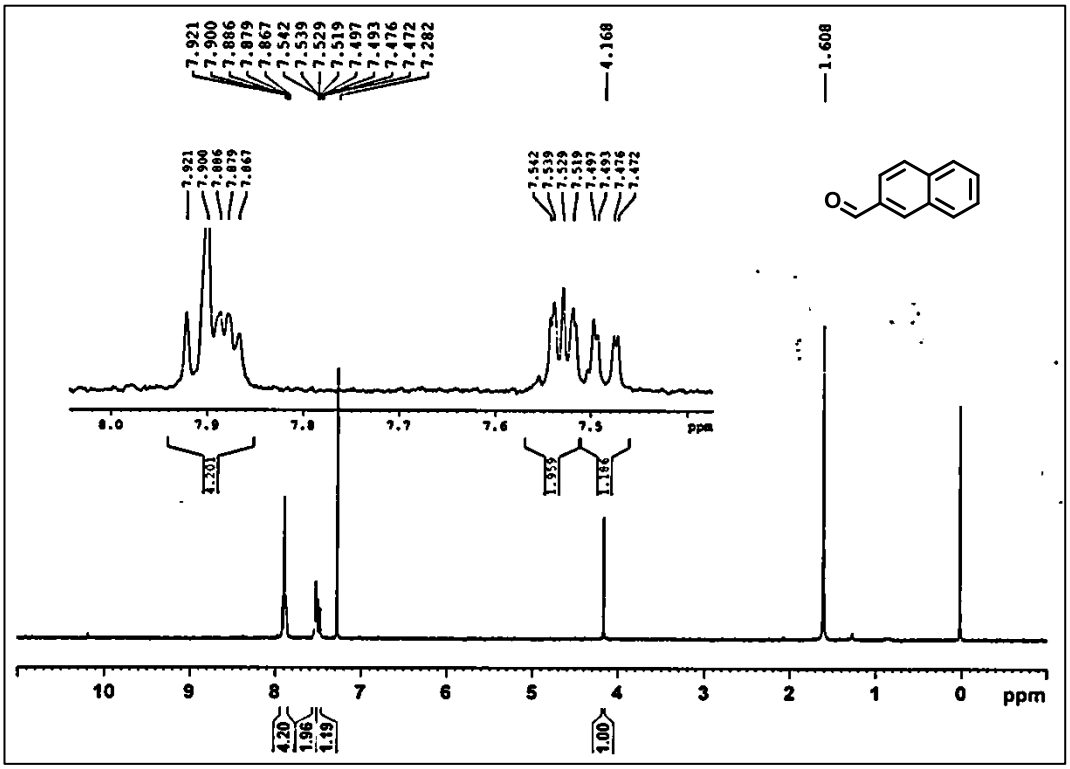

^{1}H NMR Spectra of compound **237** ($CDCl_3$, 400MHz)

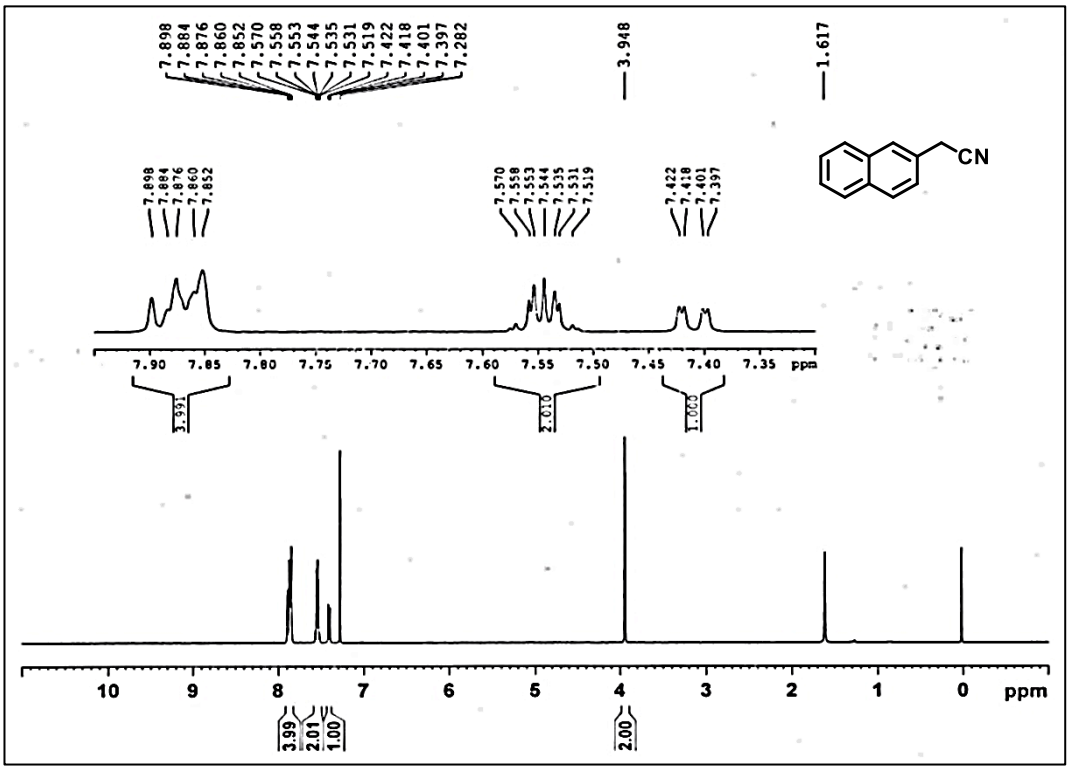

^{1}H NMR Spectra of compound **240** ($CDCl_3$, 400MHz)

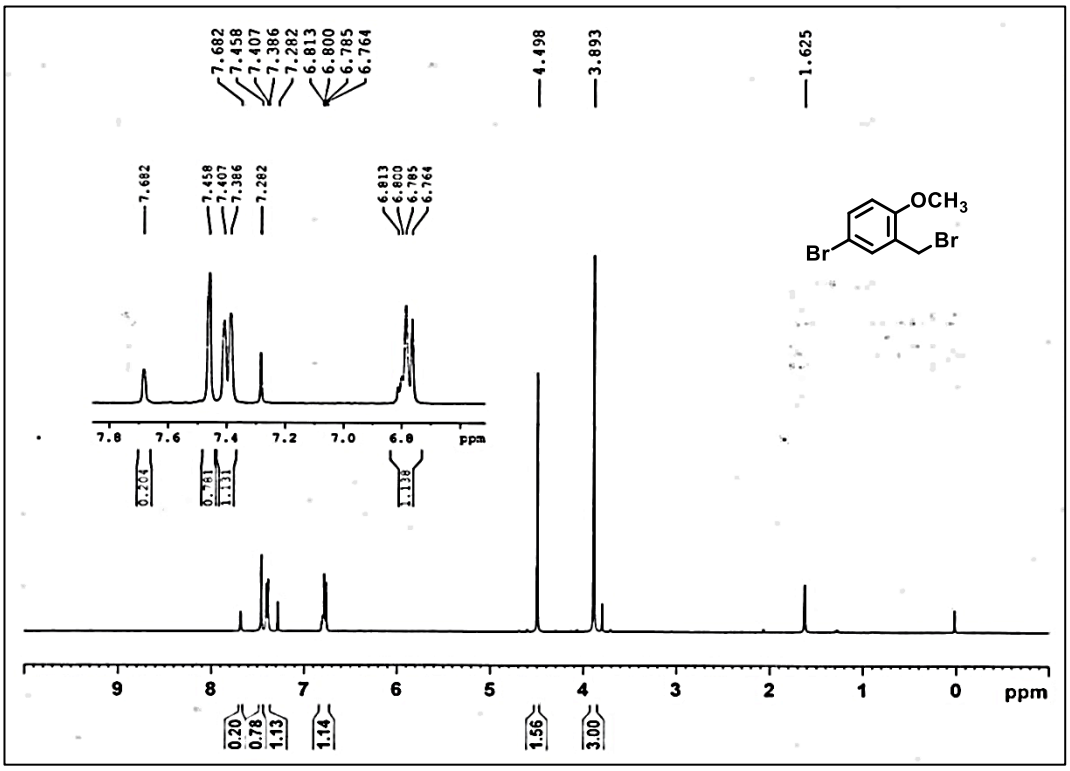

^{1}H NMR Spectra of compound **244** ($CDCl_3$, 400MHz)

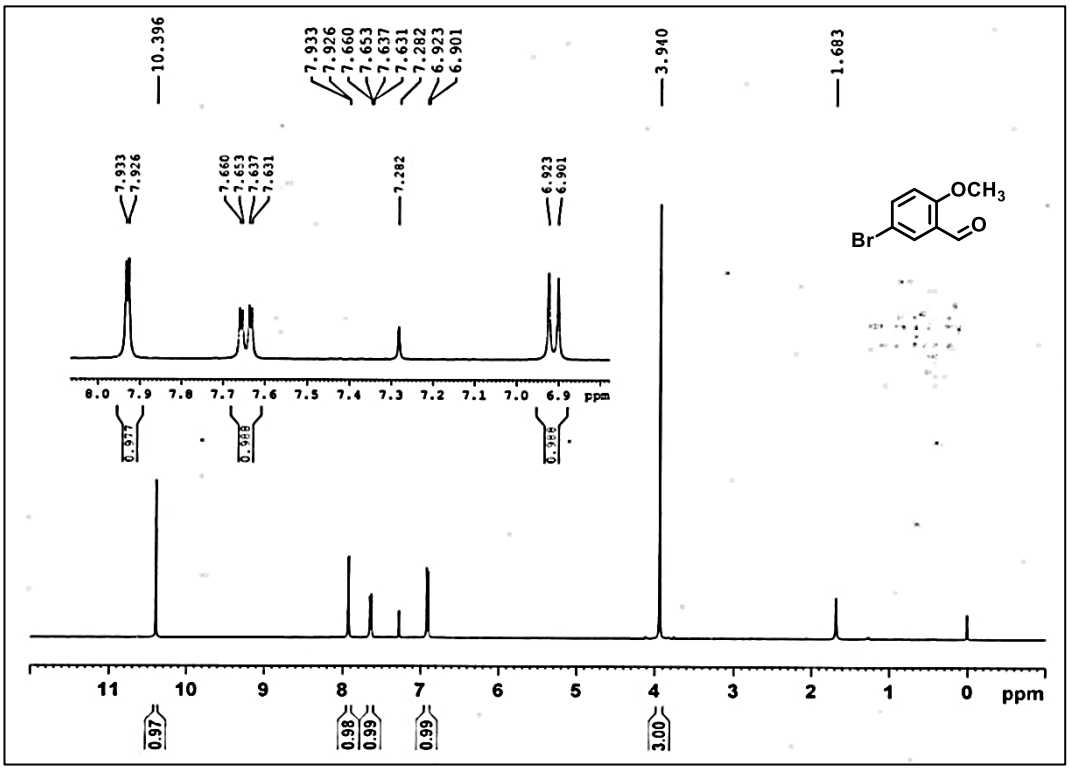

^{1}H NMR Spectra of compound **245** ($CDCl_3$, 400MHz)

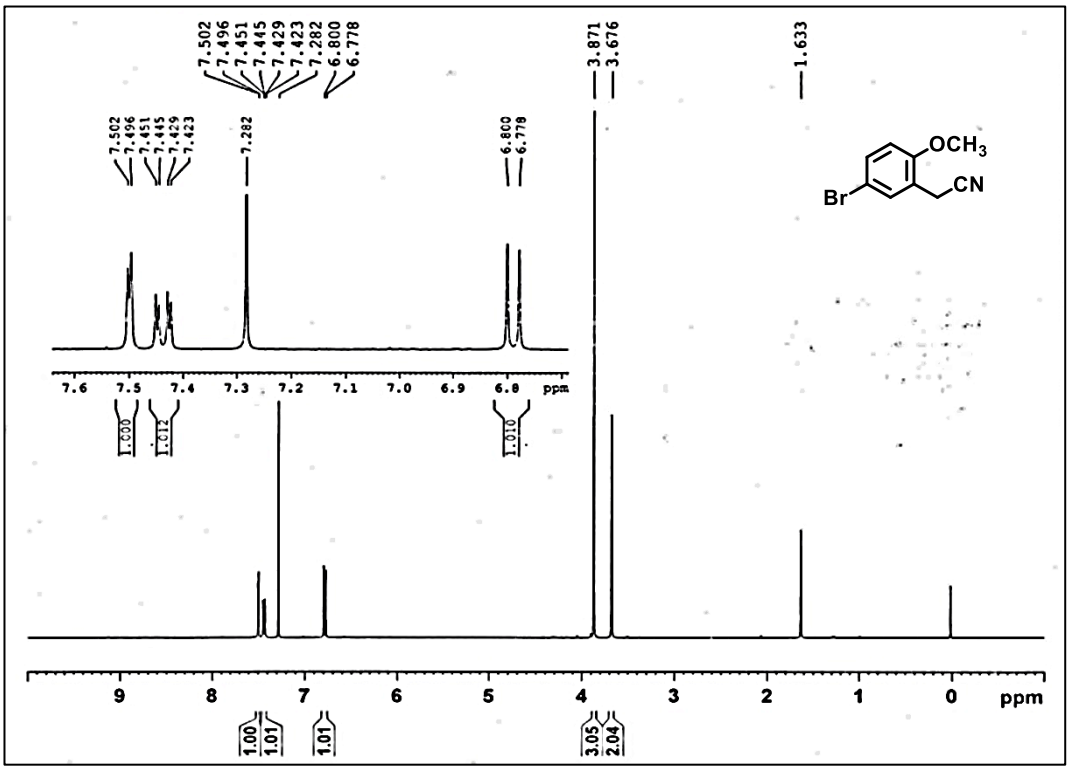

^{1}H NMR Spectra of compound **250** ($CDCl_3$, 400MHz)

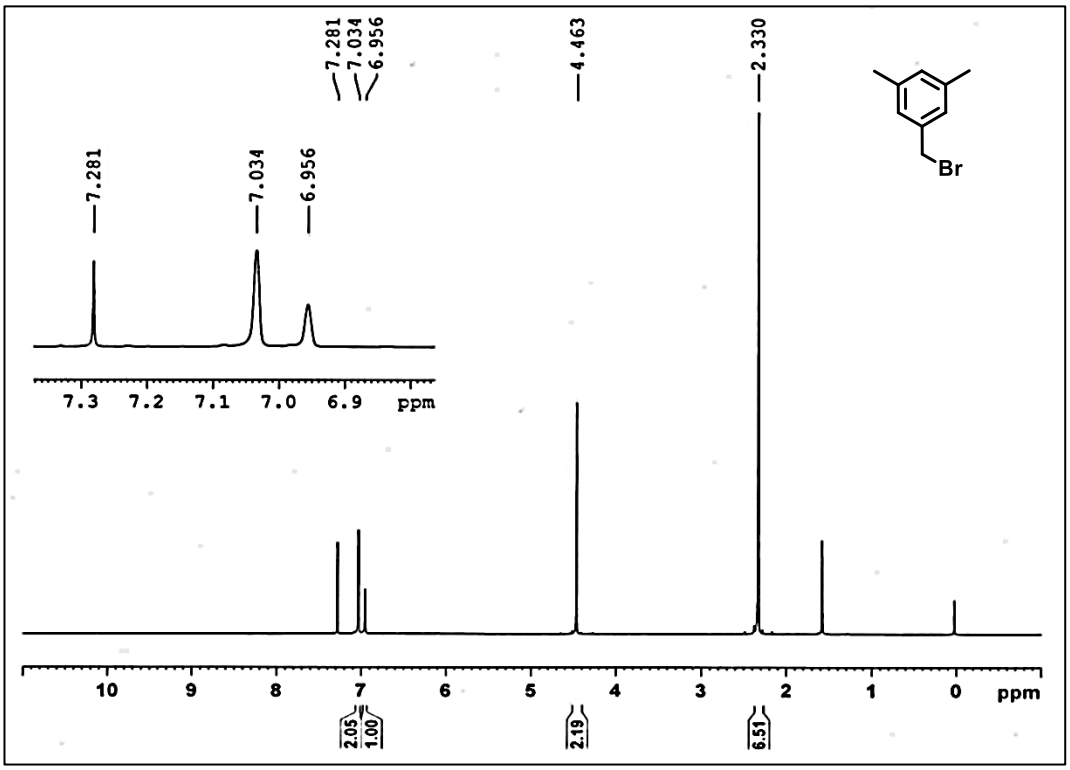

^{1}H NMR Spectra of compound **132** ($CDCl_3$, 400MHz)

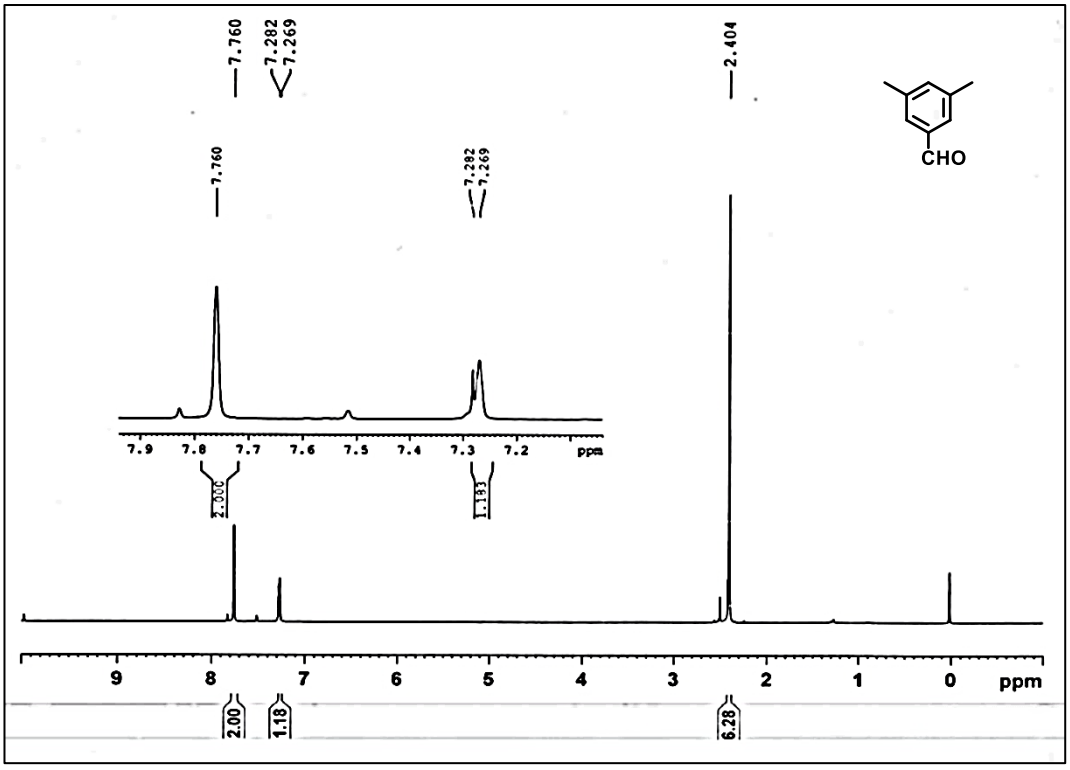

^{1}H NMR Spectra of compound **230** ($CDCl_3$, 400MHz)

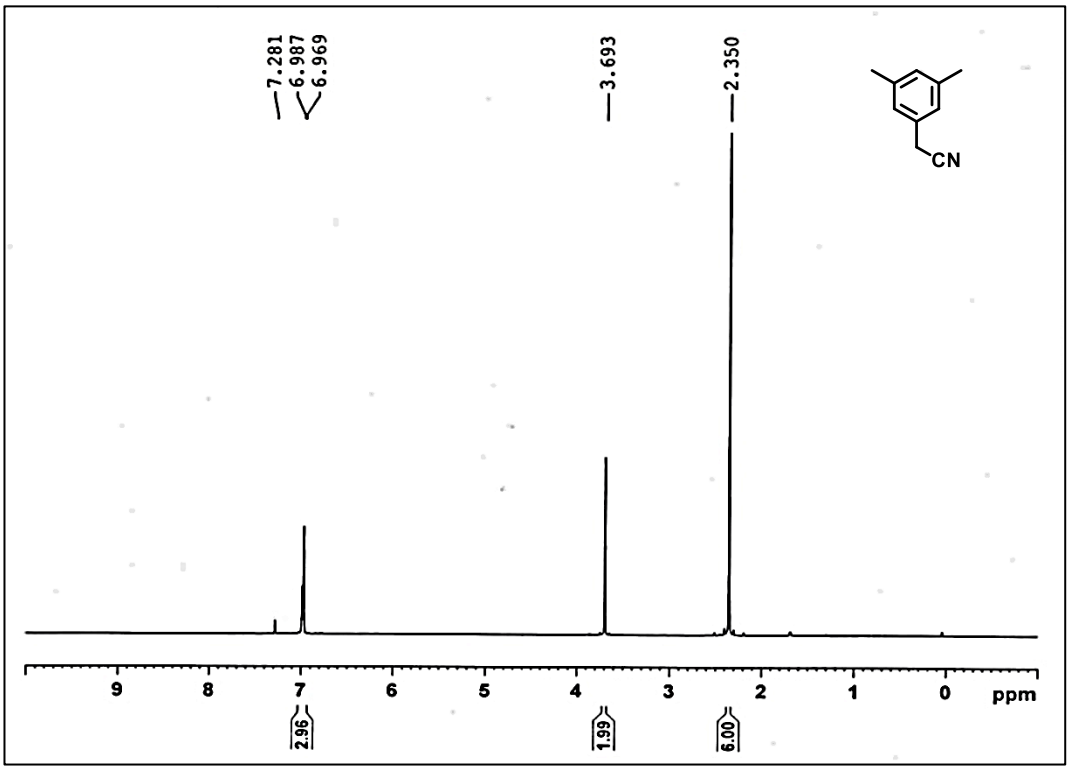

^{1}H NMR Spectra of compound **236** ($CDCl_3$, 400MHz)

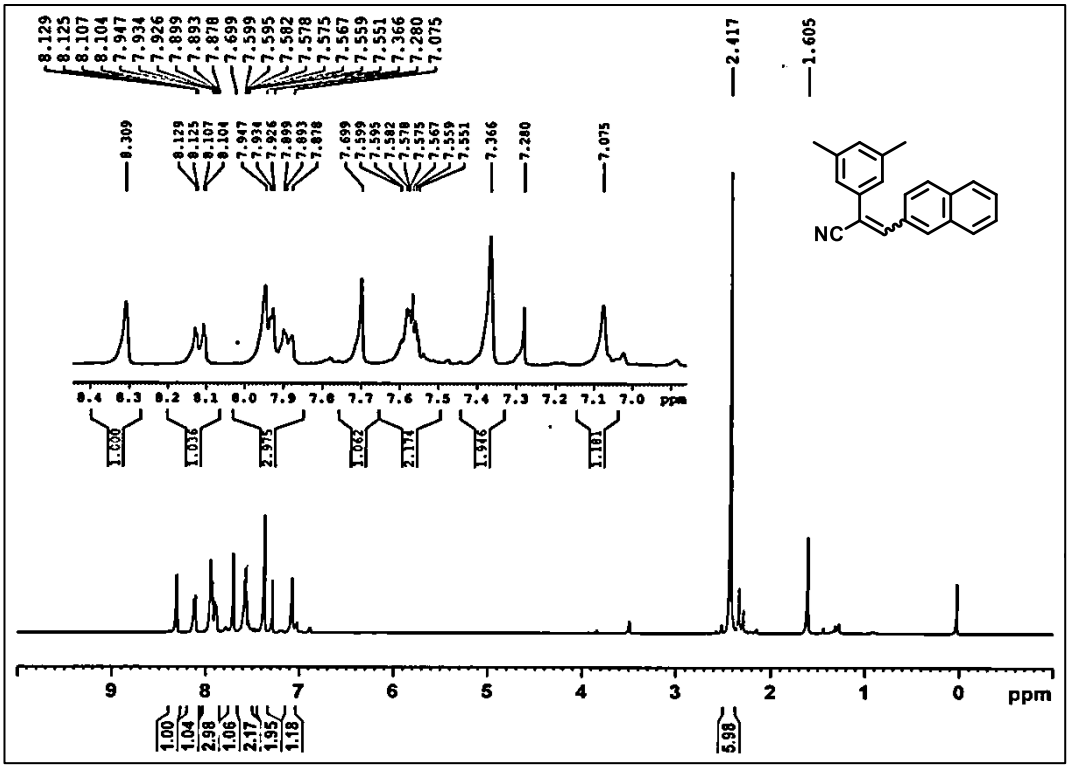

^{1}H NMR Spectra of compound **238** ($CDCl_3$, 400MHz)

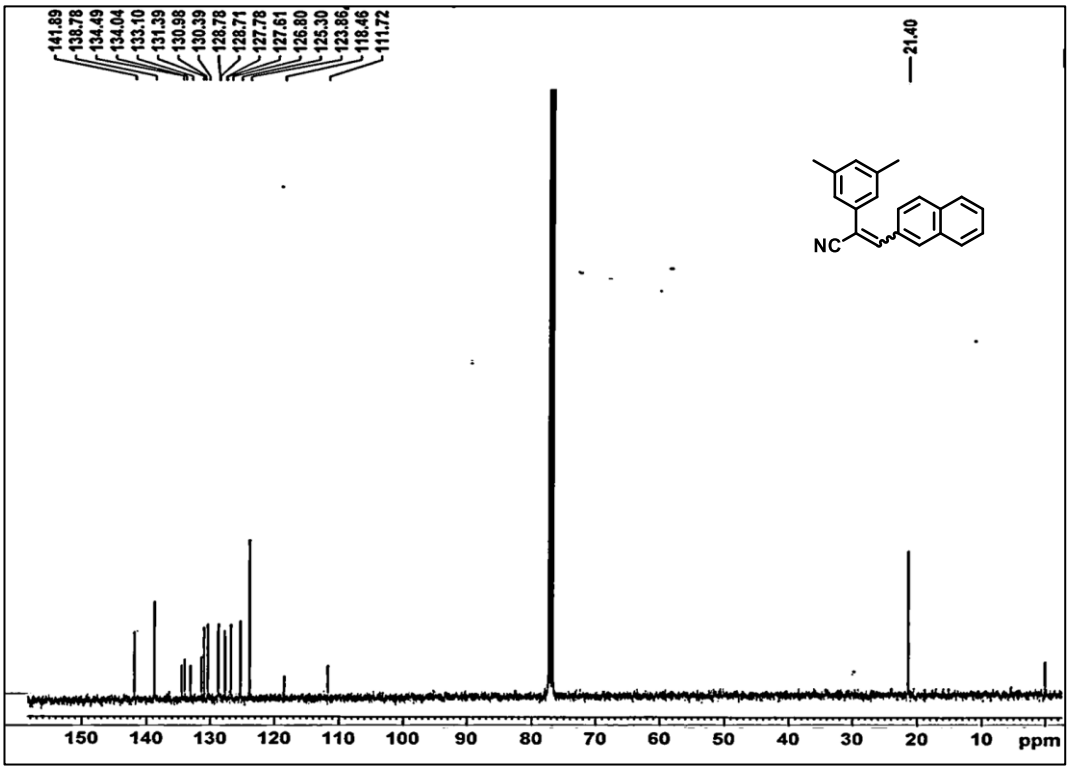

^{13}C NMR Spectra of compound **238** ($CDCl_3$, 100MHz)

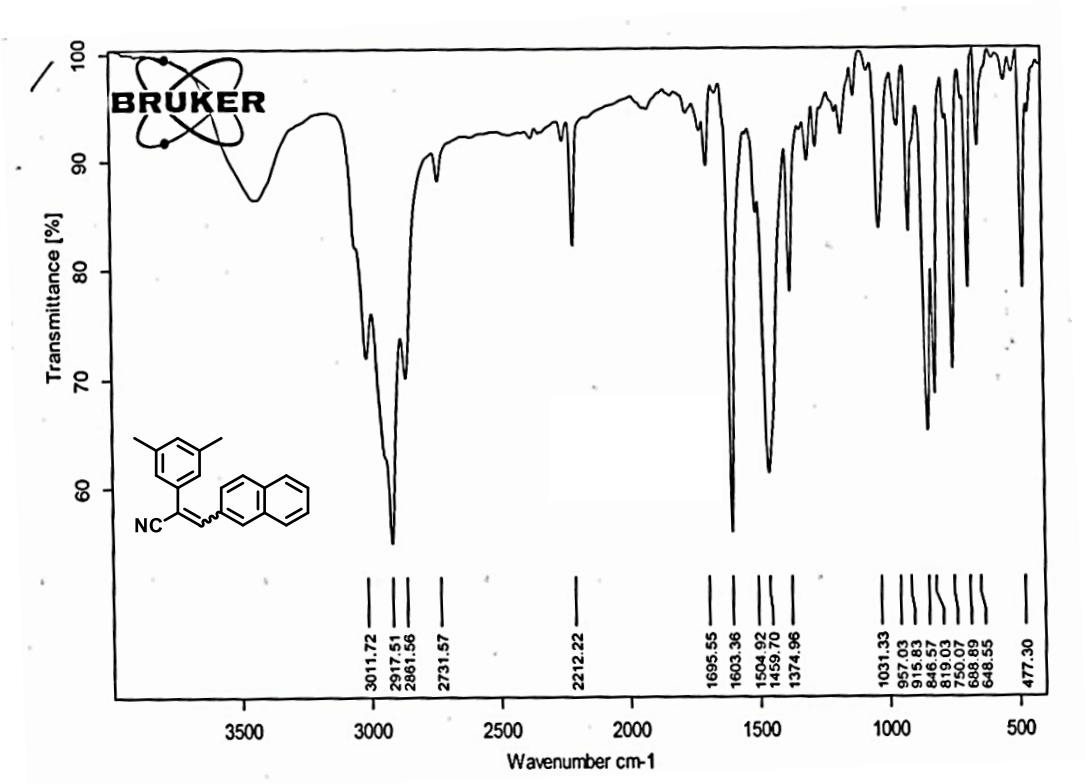

IR Spectra of compound **238**

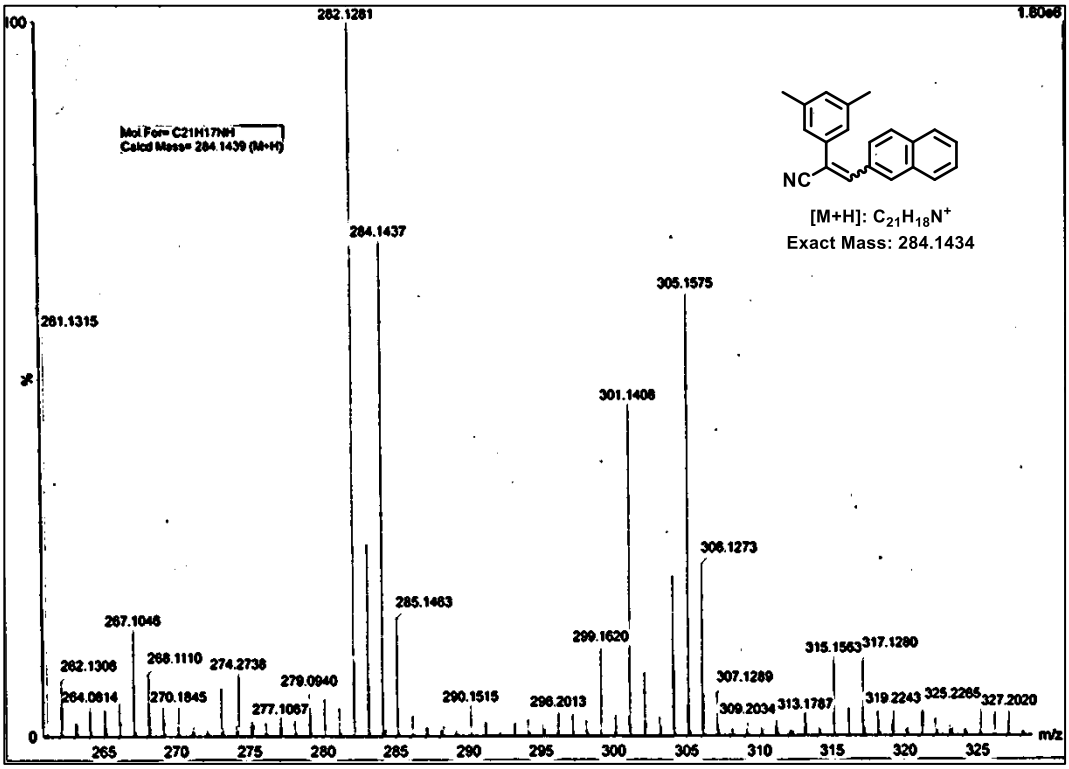

HRMS Spectra of compound **238**

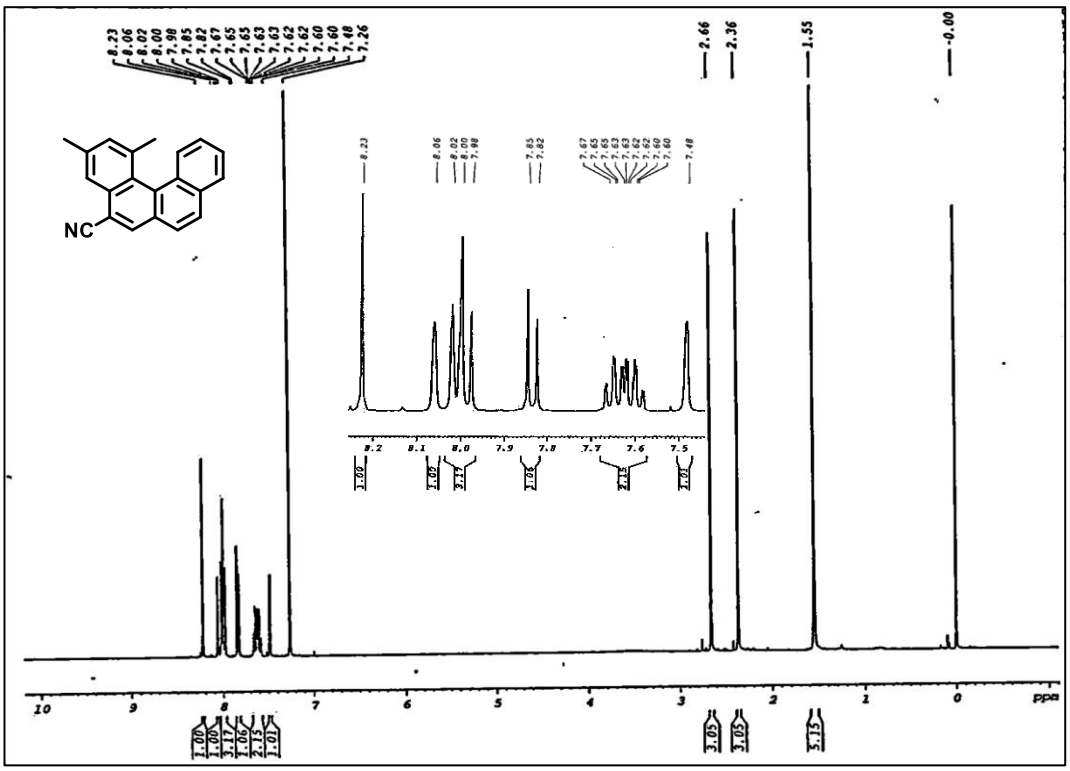

^{1}H NMR Spectra of compound **239** ($CDCl_3$, 400MHz)

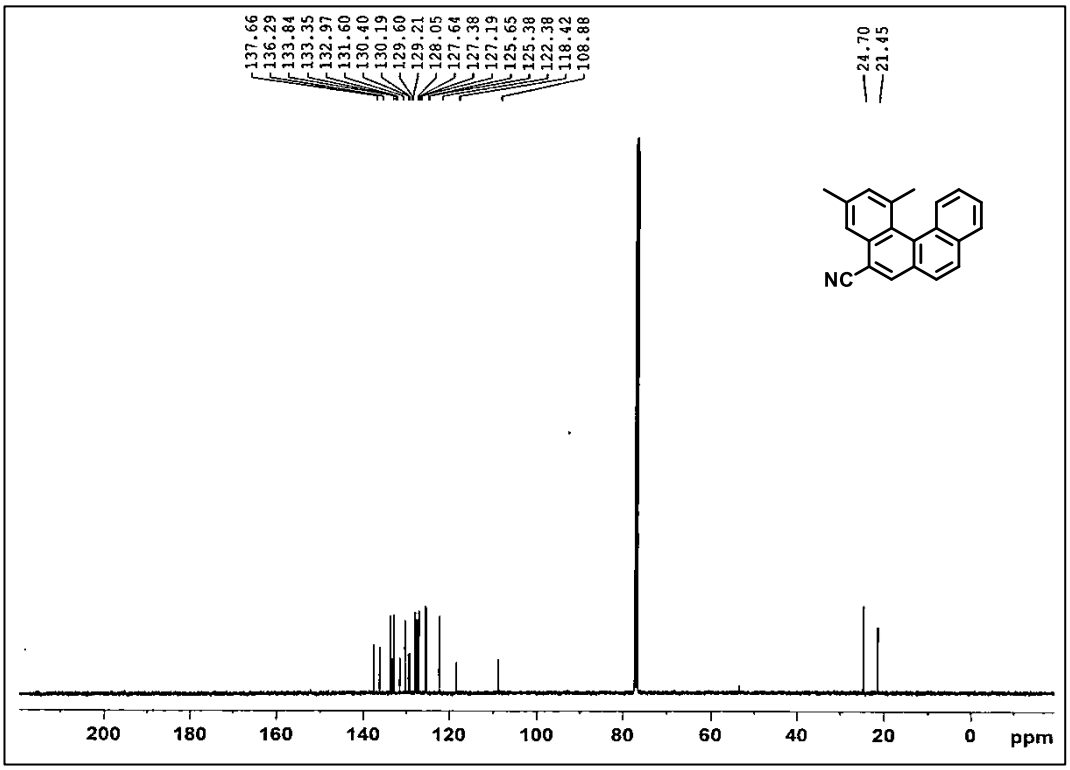

^{13}C NMR Spectra of compound **239** ($CDCl_3$, 100MHz)

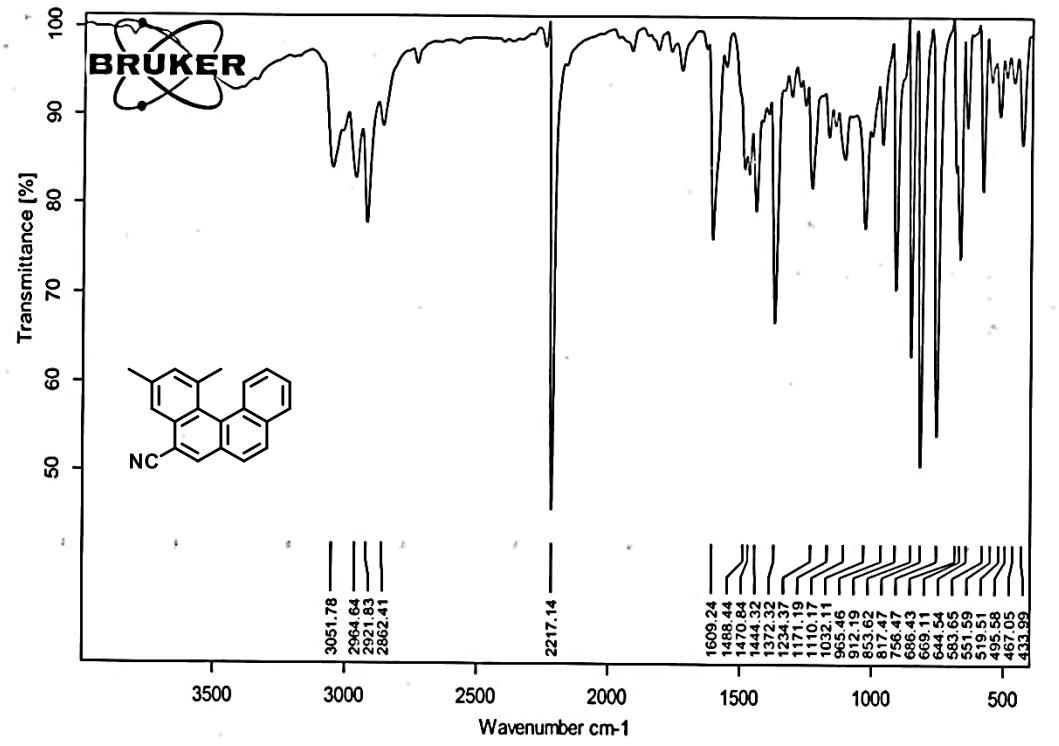

IR Spectra of compound **239**

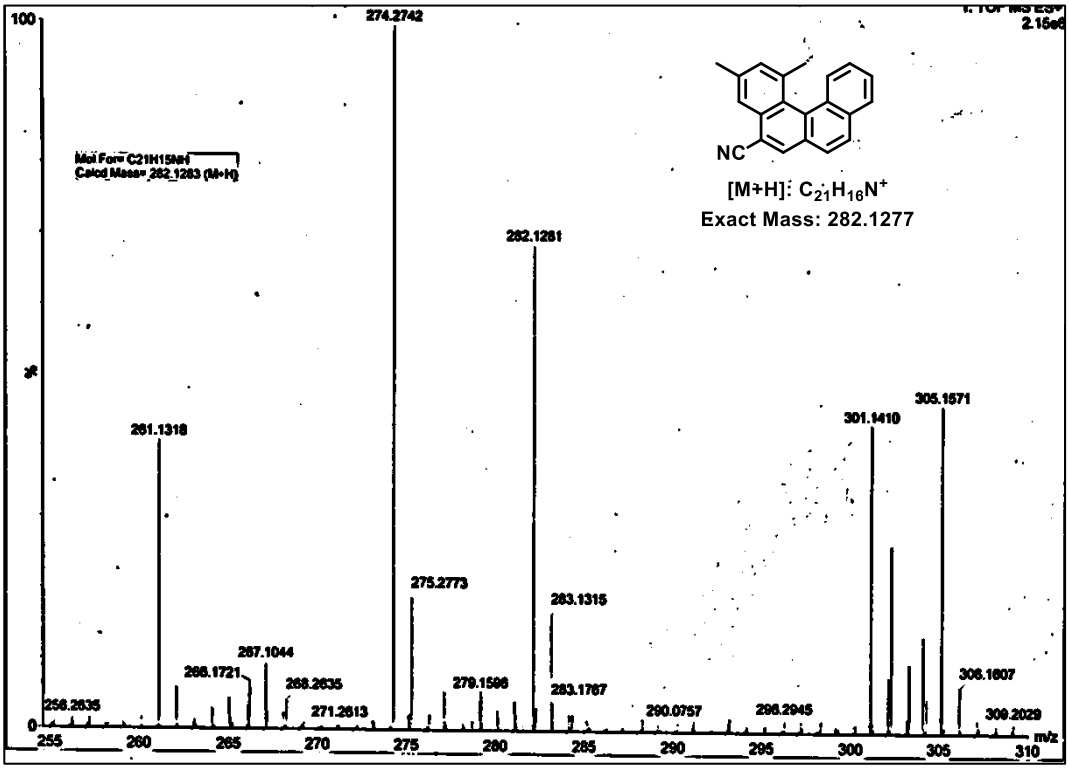

HRMS Spectra of compound **239**

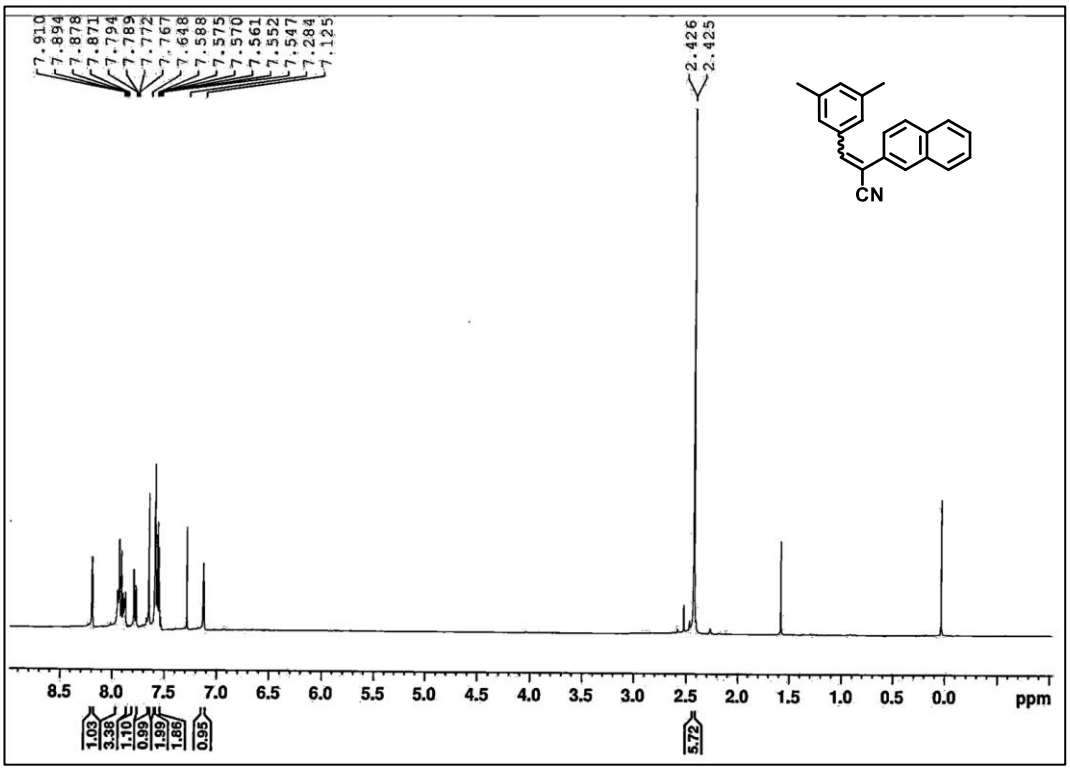

^{1}H NMR Spectra of compound **241** ($CDCl_3$, 400MHz)

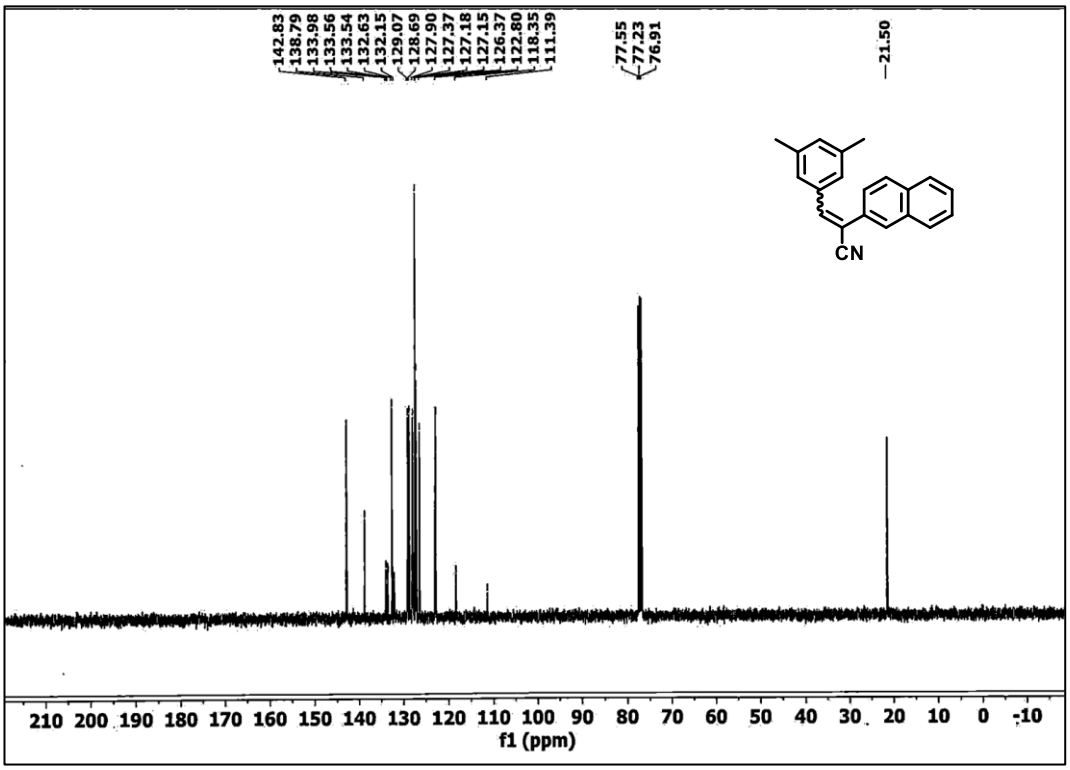

^{13}C NMR Spectra of compound **241** ($CDCl_3$, 100MHz)

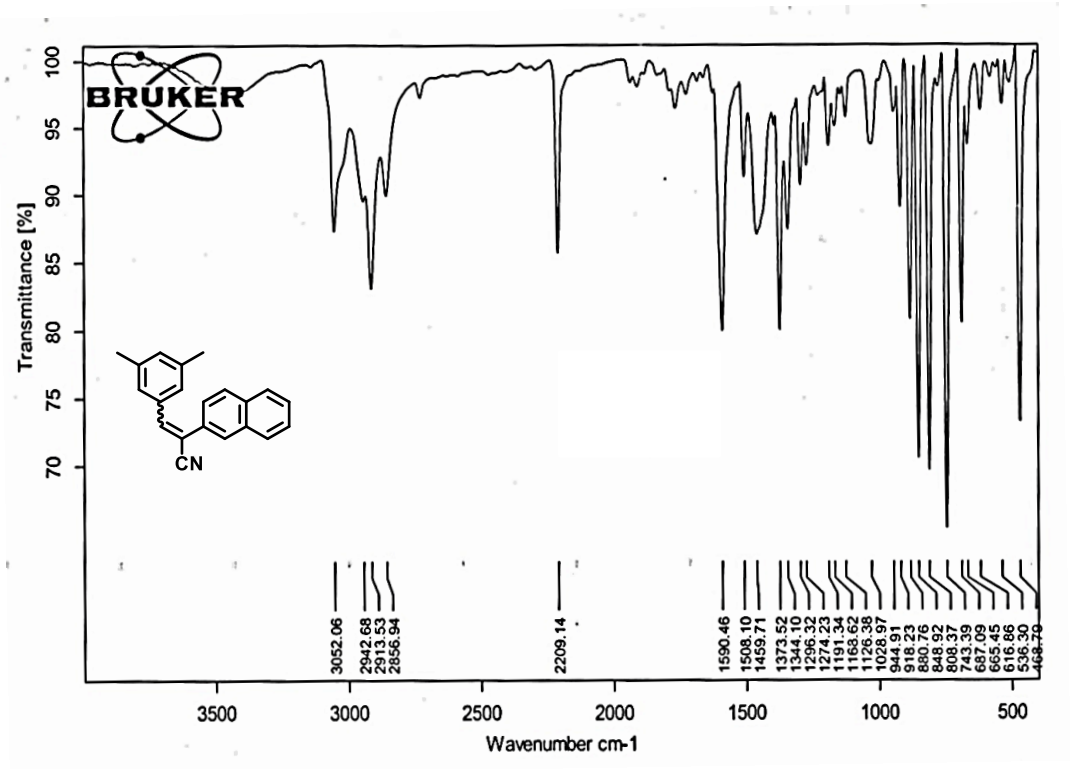

IR Spectra of compound **241**

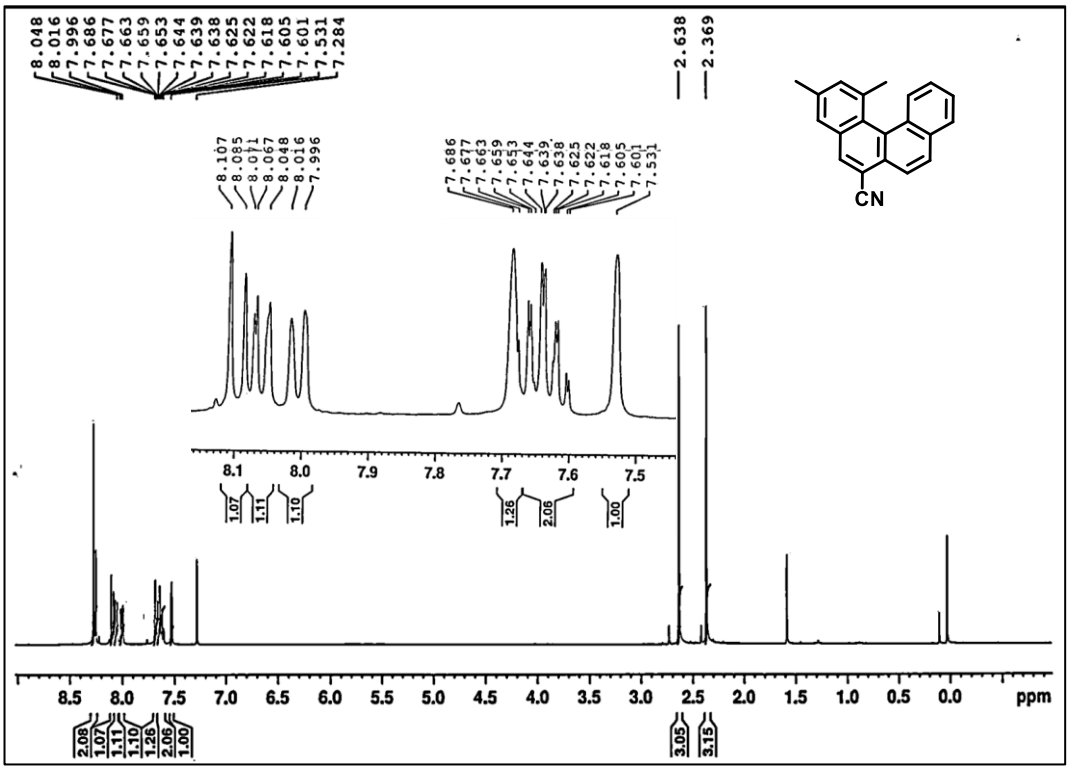

^{1}H NMR Spectra of compound **242** ($CDCl_3$, 400MHz)

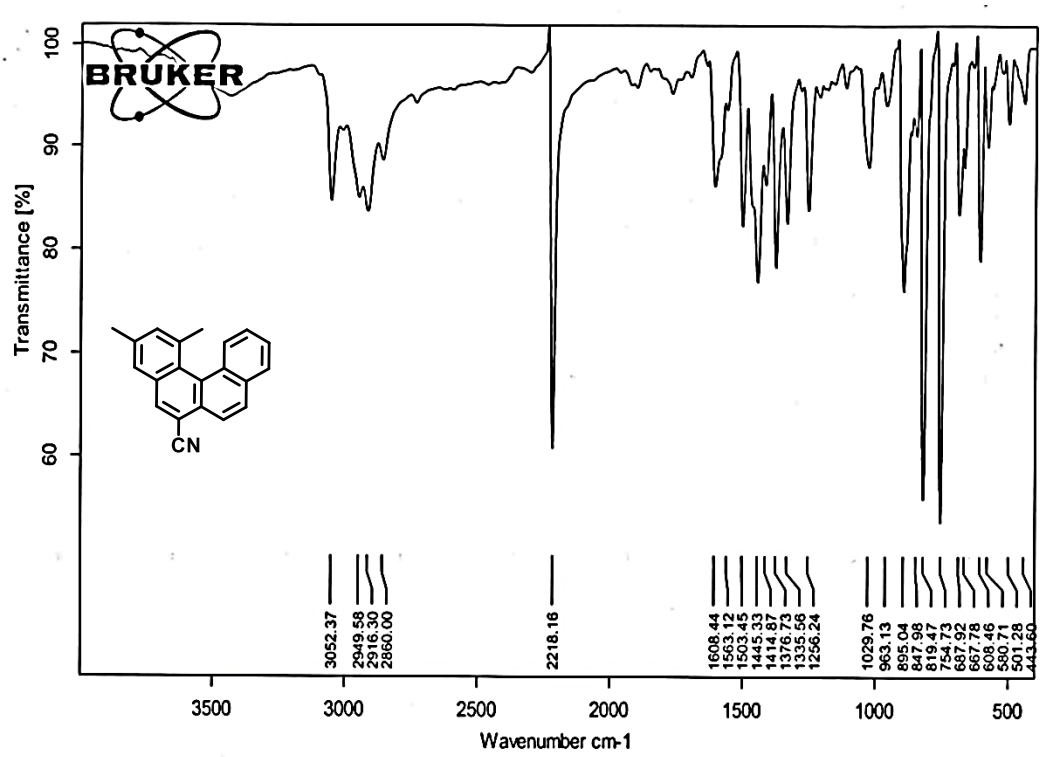

IR Spectra of compound **242**

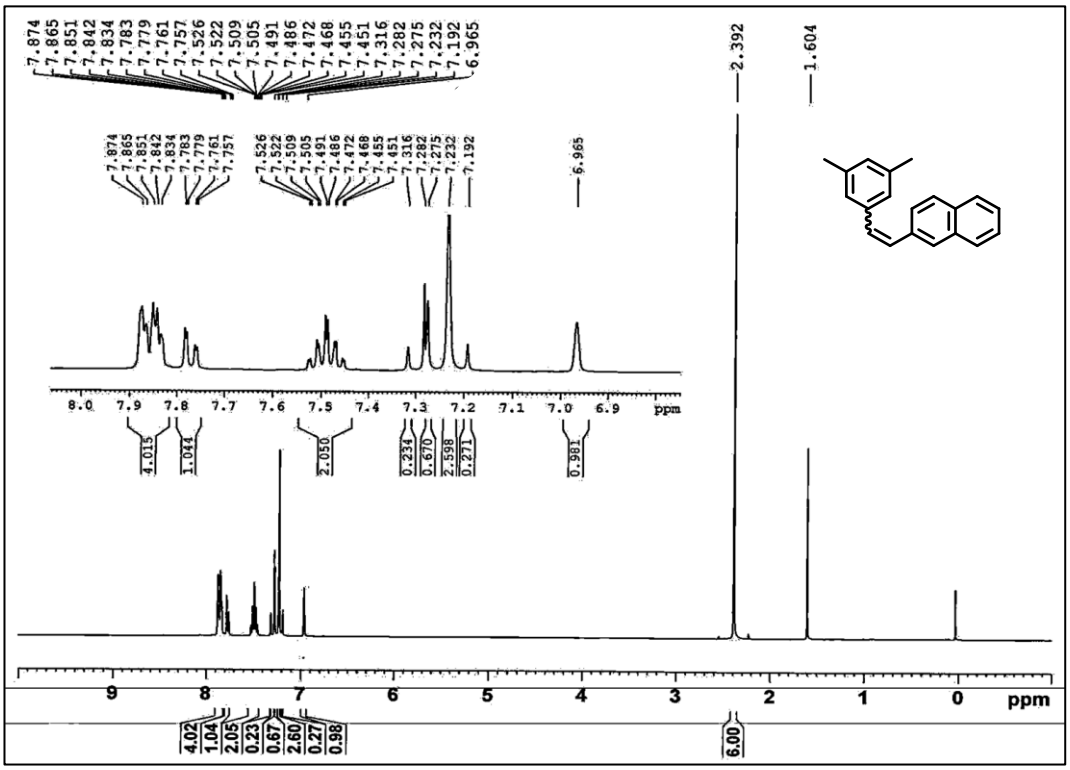

^{1}H NMR Spectra of compound **234** ($CDCl_3$, 400MHz)

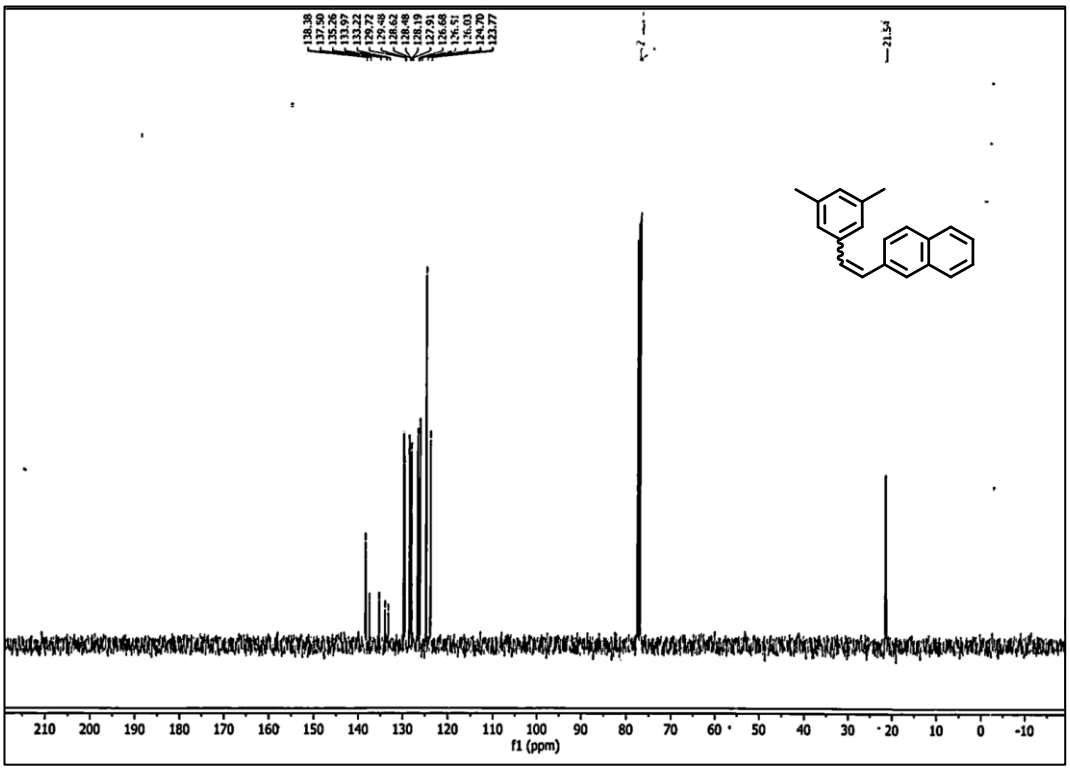

^{13}C NMR Spectra of compound **234** ($CDCl_3$, 100MHz)

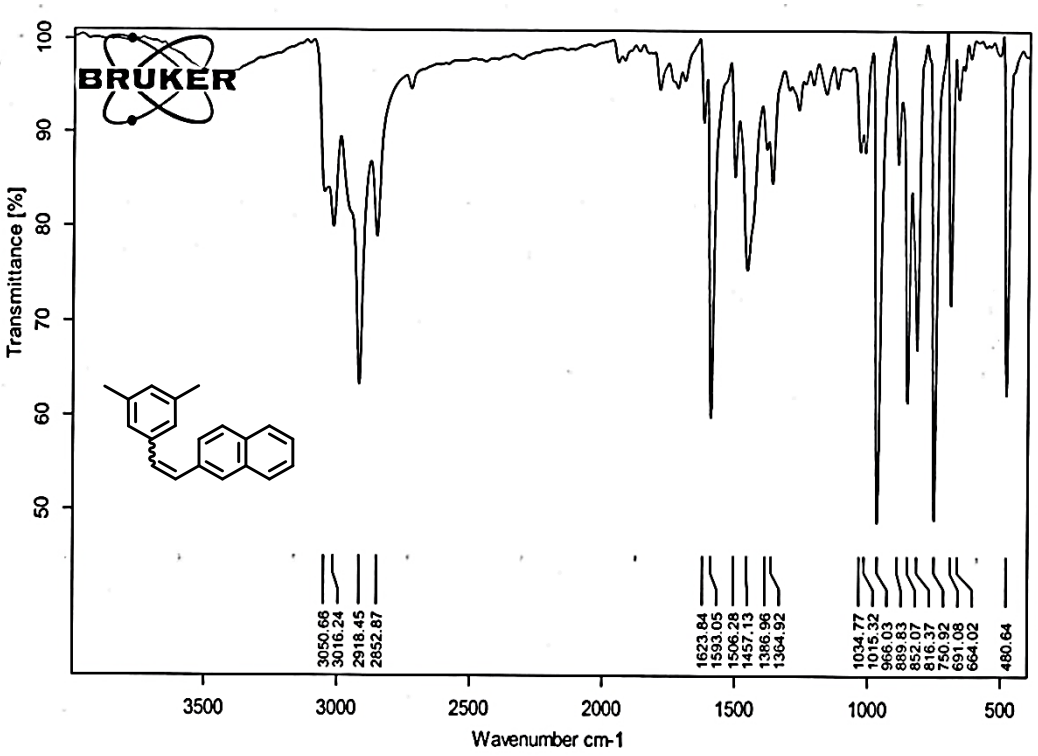

IR Spectra of compound **234**

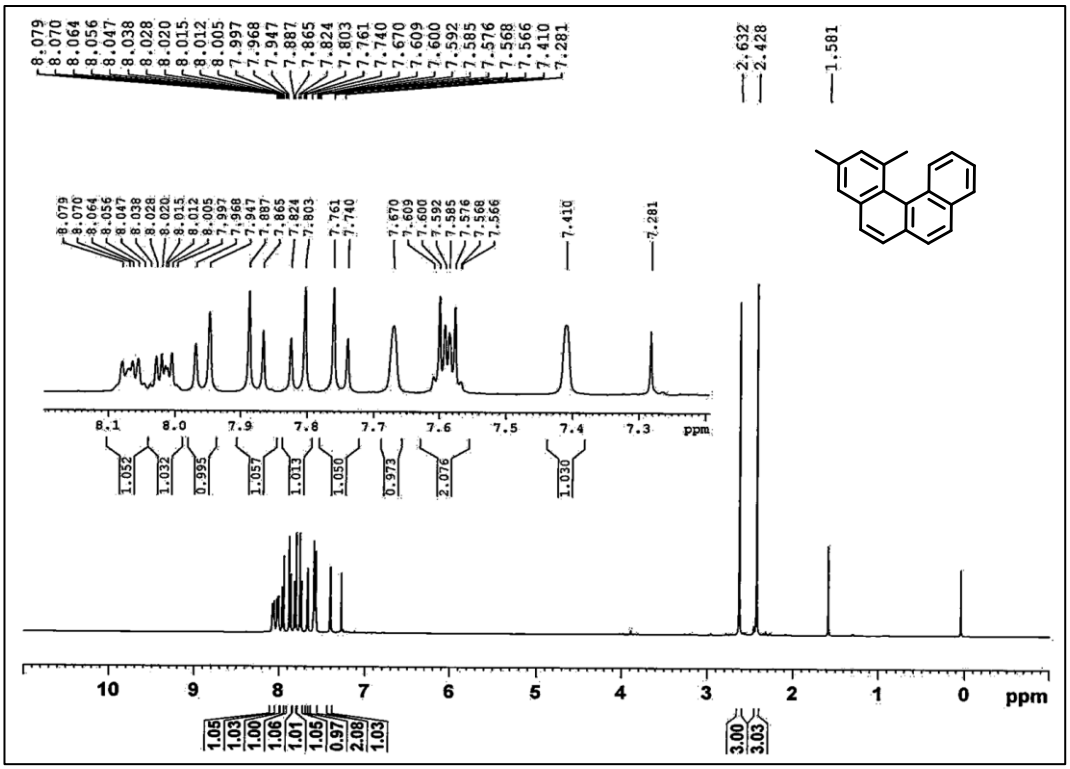

^{1}H NMR Spectra of compound **235** ($CDCl_3$, 400MHz)

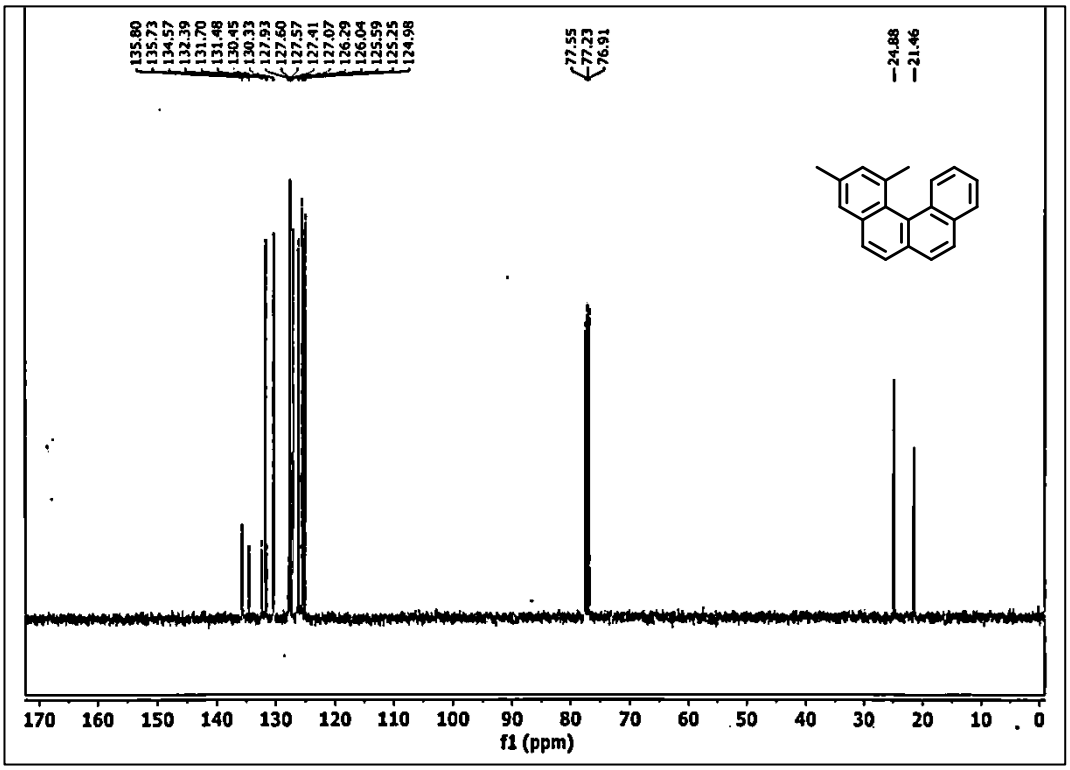

^{13}C NMR Spectra of compound **235** ($CDCl_3$, 100MHz)

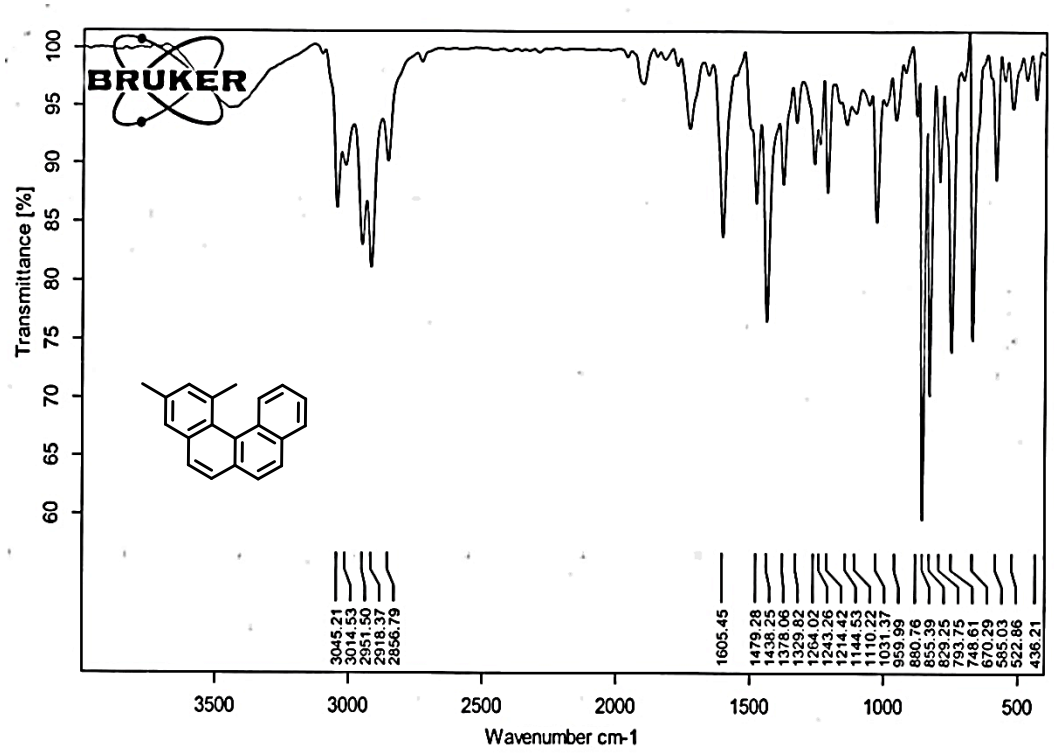

IR Spectra of compound **235**

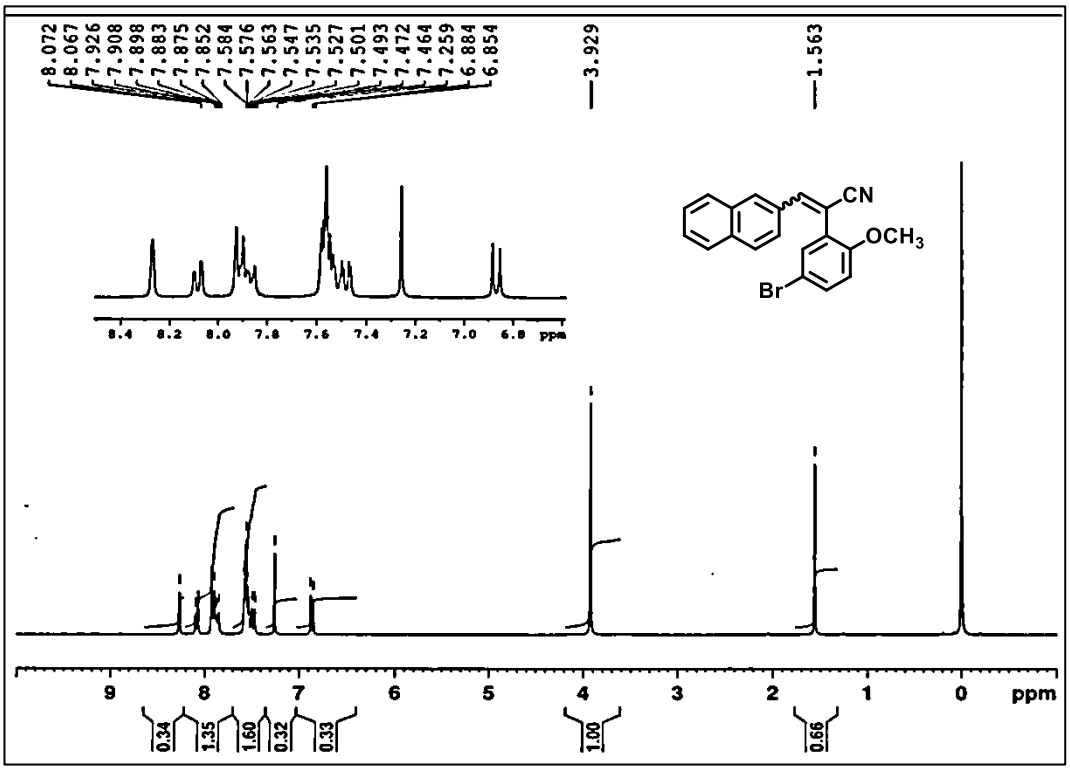

^{1}H NMR Spectra of compound **251** ($CDCl_3$, 400MHz)

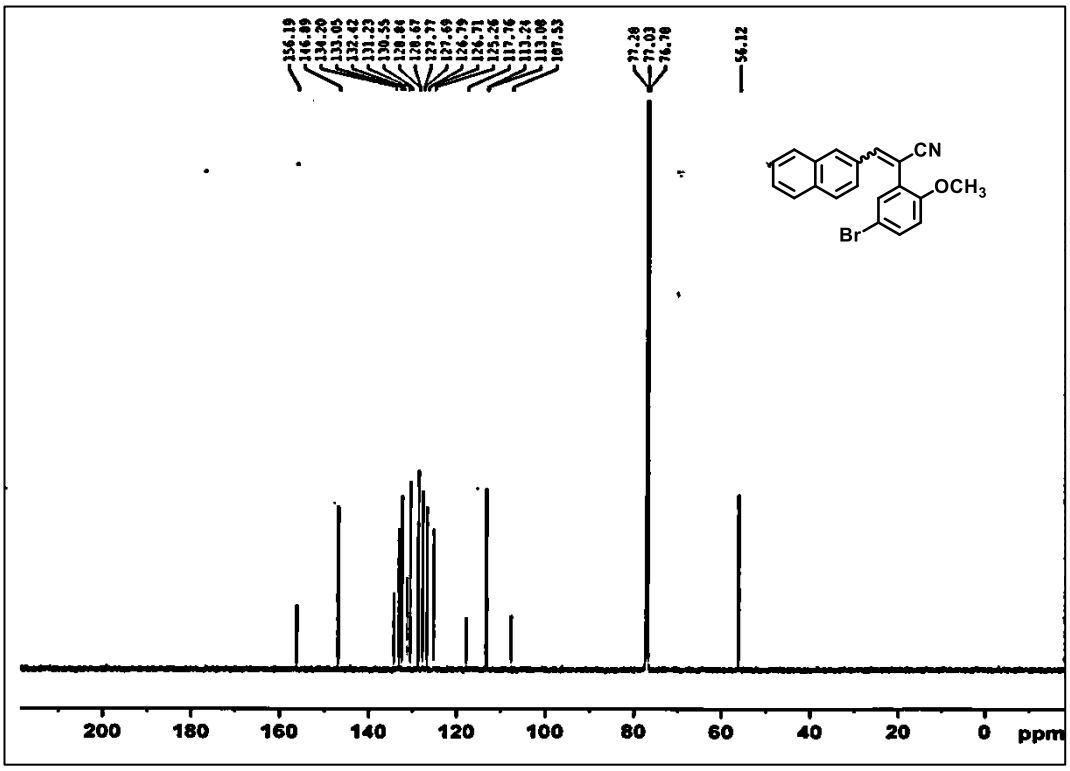

^{13}C NMR Spectra of compound **251** ($CDCl_3$, 100MHz)

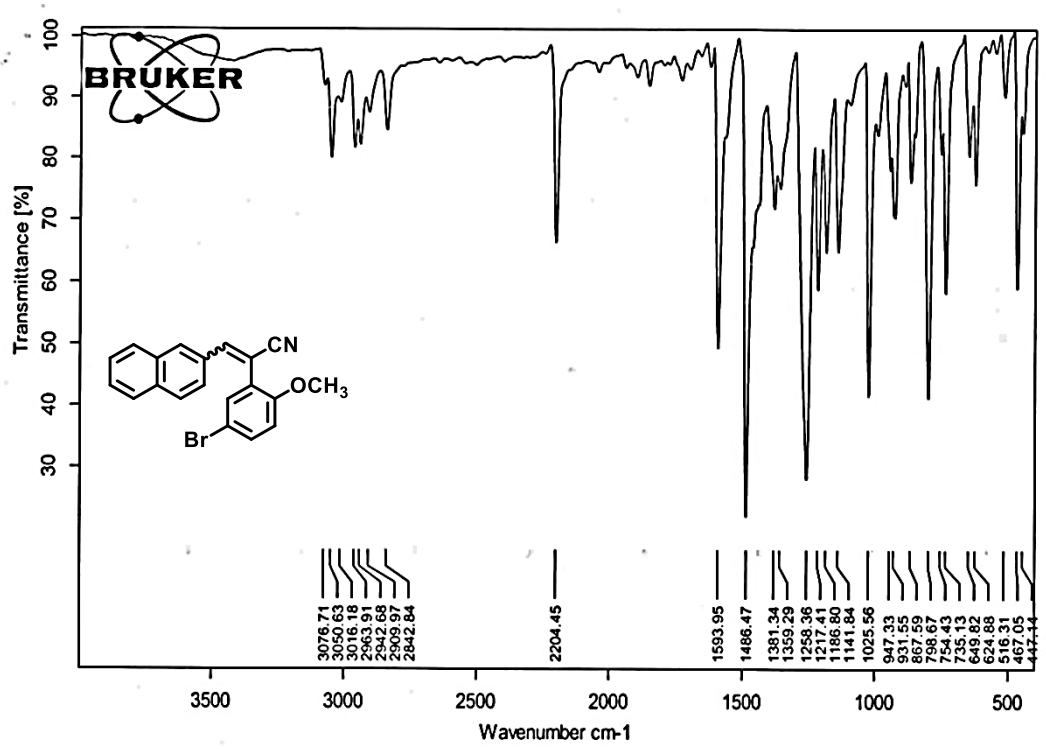

IR Spectra of compound **251**

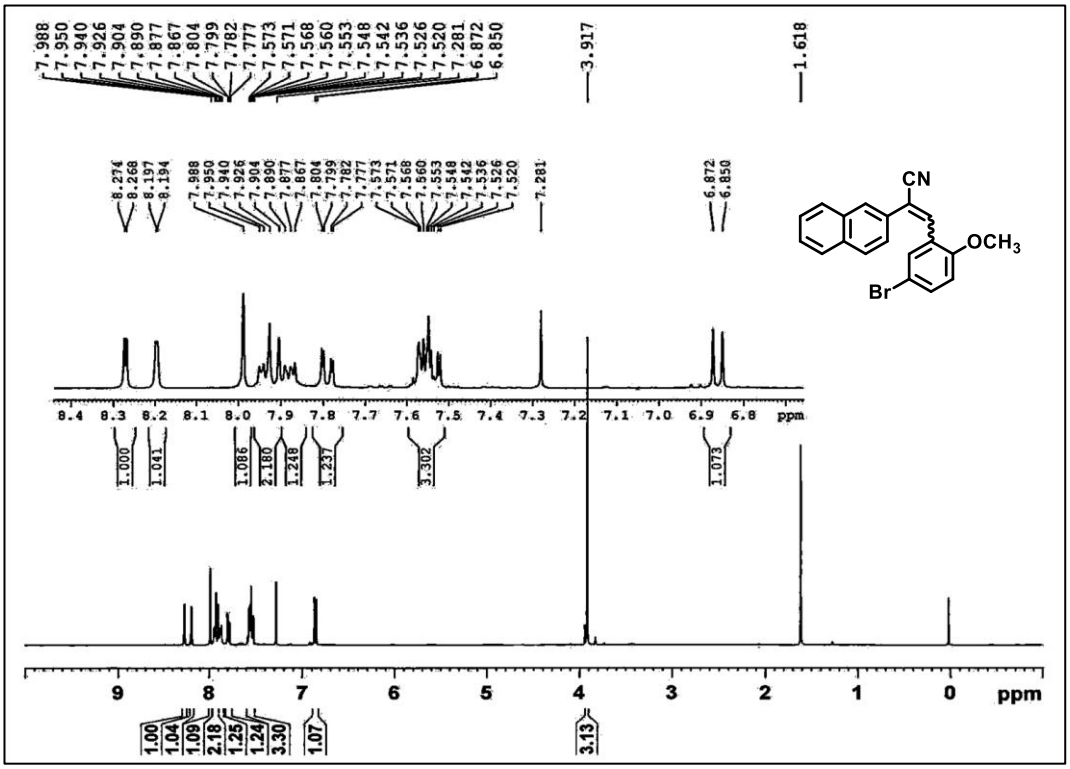

^{1}H NMR Spectra of compound **246** ($CDCl_3$, 400MHz)

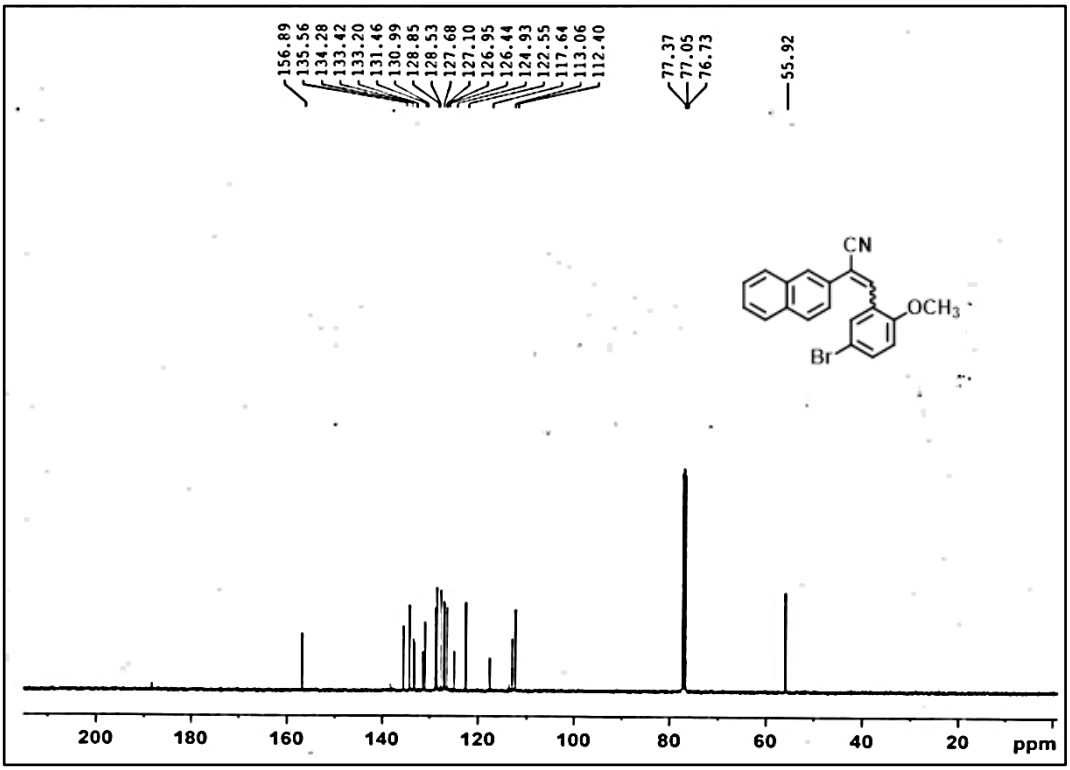

^{13}C NMR Spectra of compound **246** ($CDCl_3$, 100MHz)

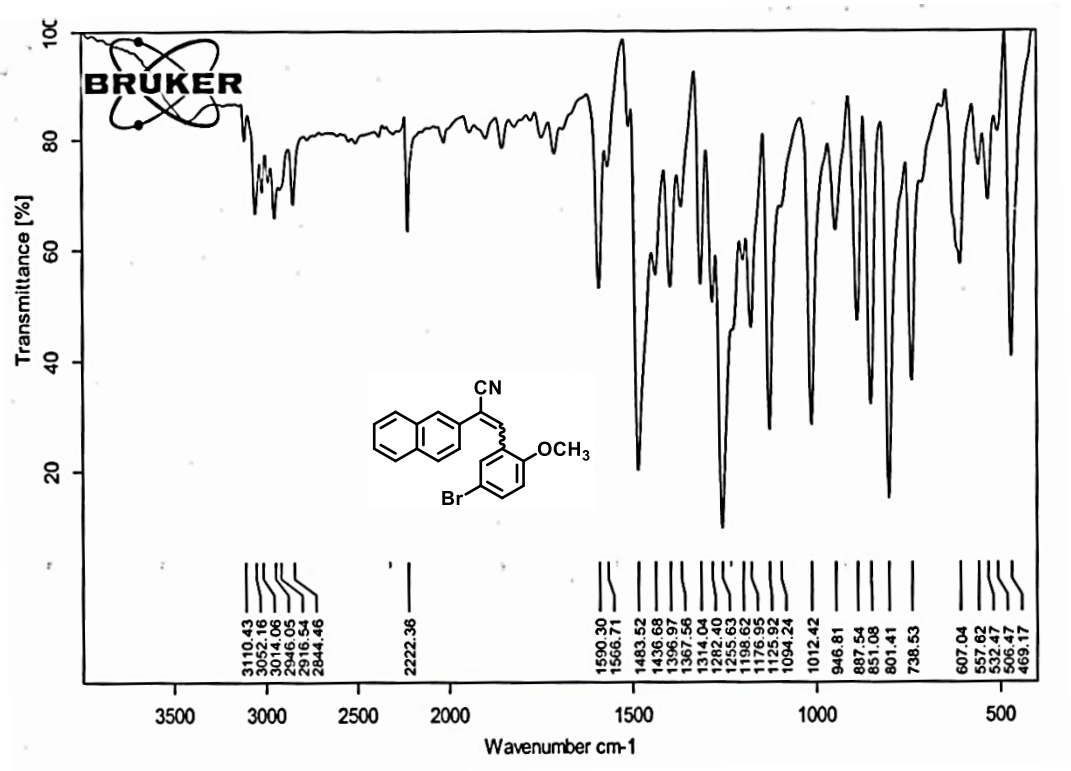

IR Spectra of compound **246**

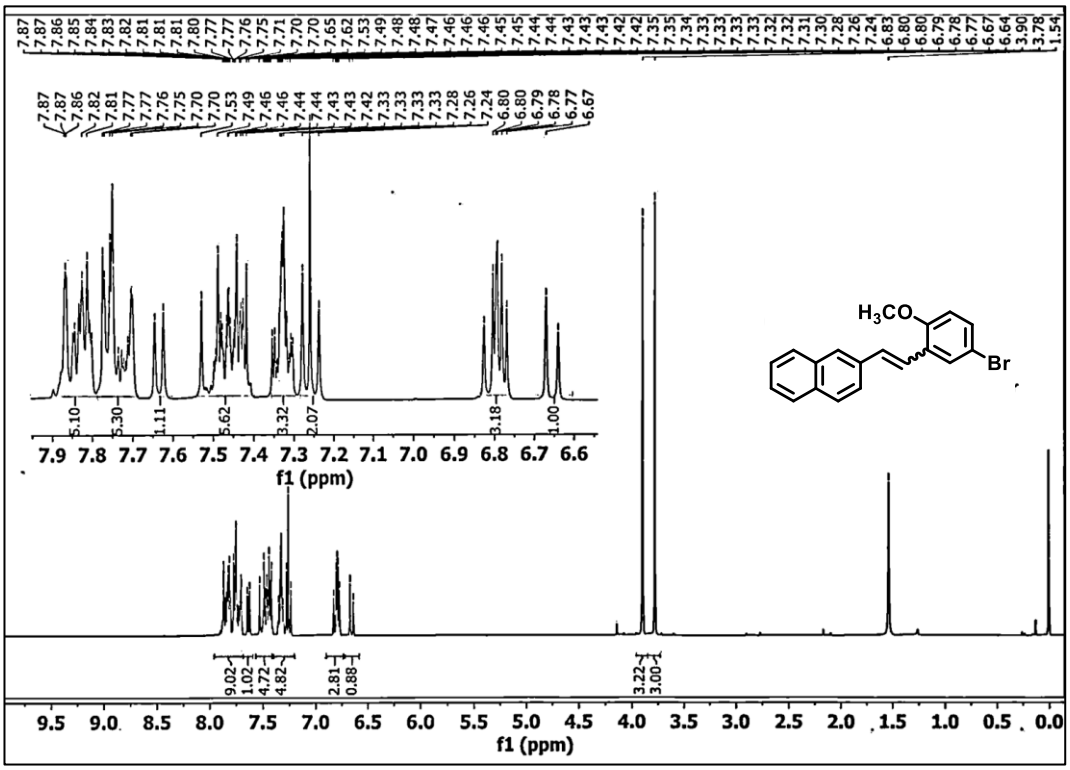

^{1}H NMR Spectra of compound **260** ($CDCl_3$, 400MHz)

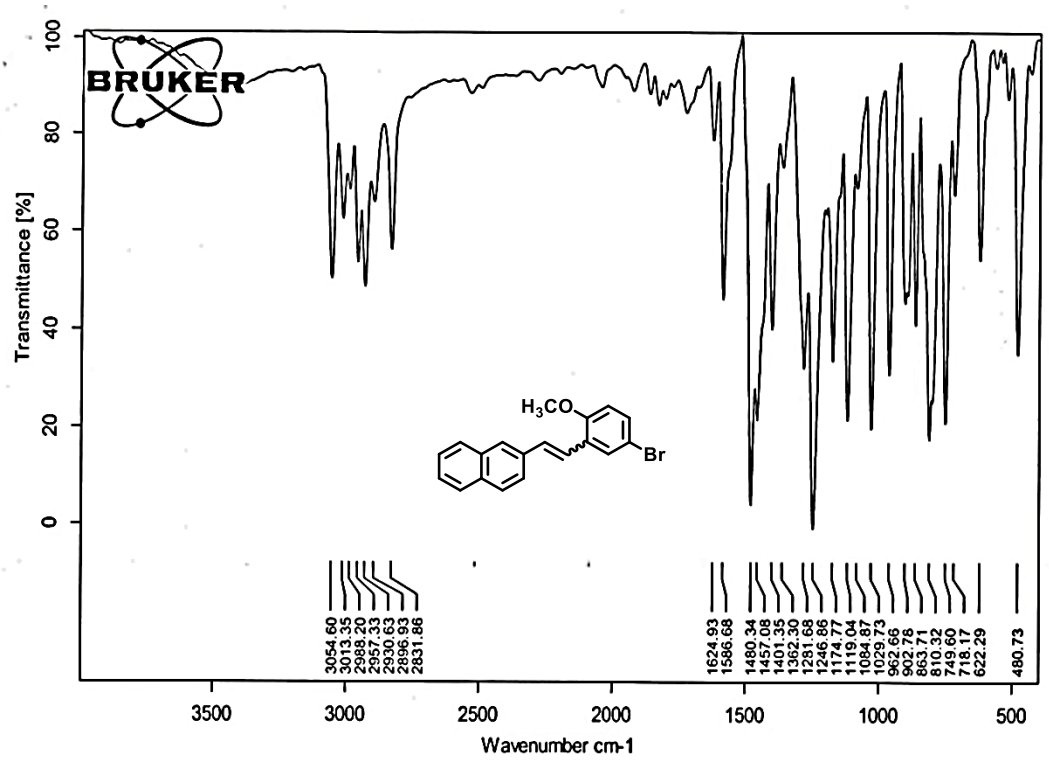

IR Spectra of compound **260**

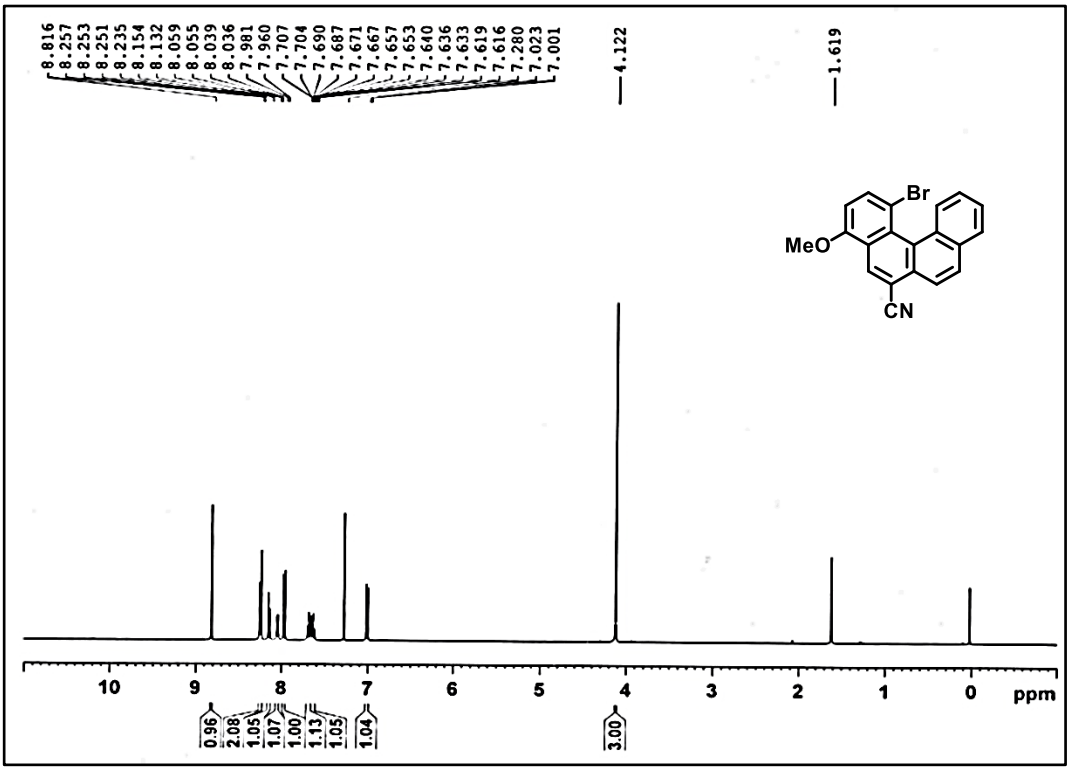

^{1}H NMR Spectra of compound **247** ($CDCl_3$, 400MHz)

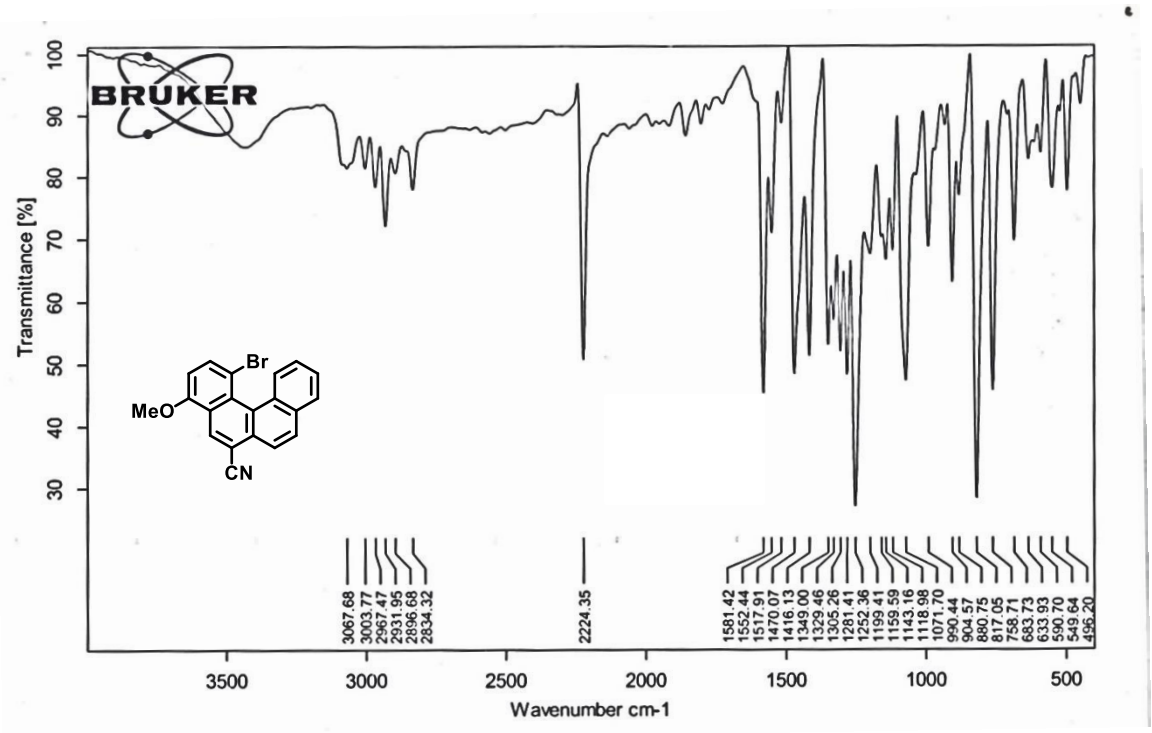

IR Spectra of compound **247**

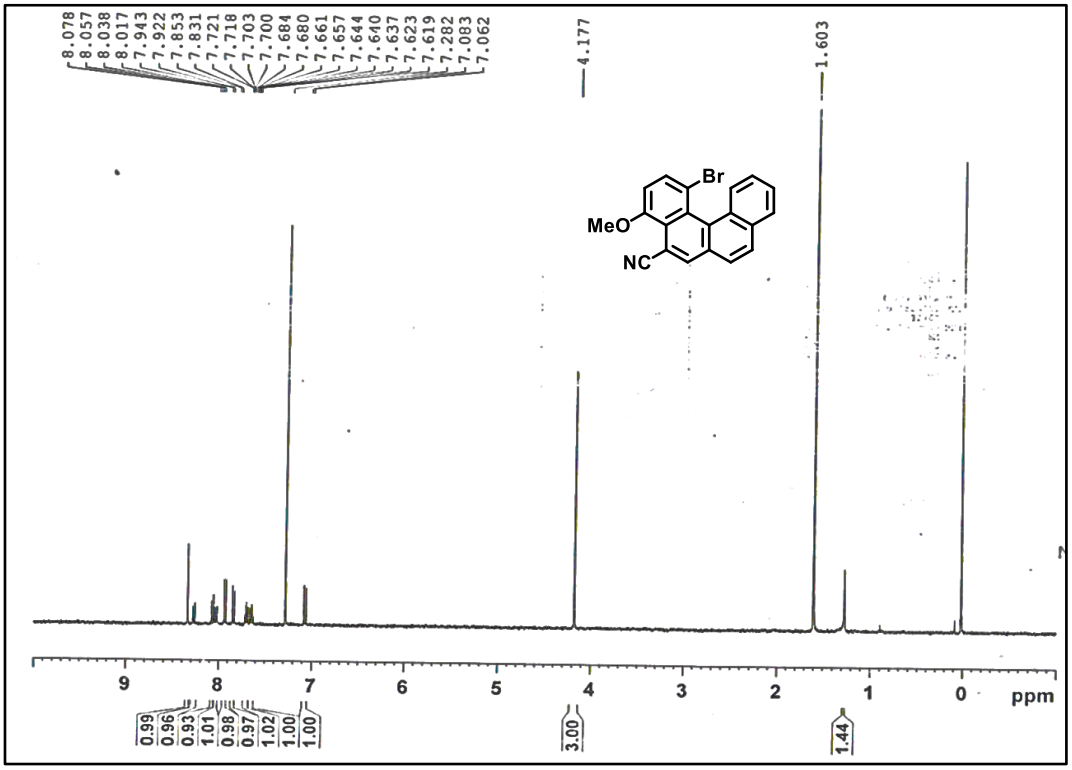

^{1}H NMR Spectra of compound **257** ($CDCl_3$, 400MHz)

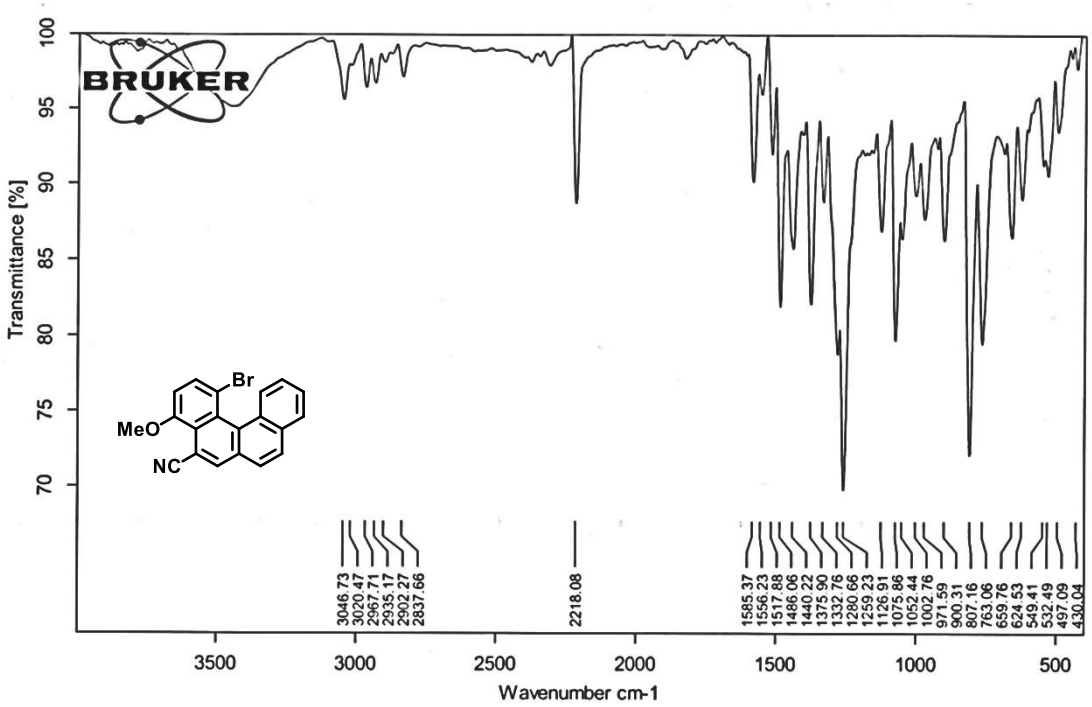

IR Spectra of compound **257**

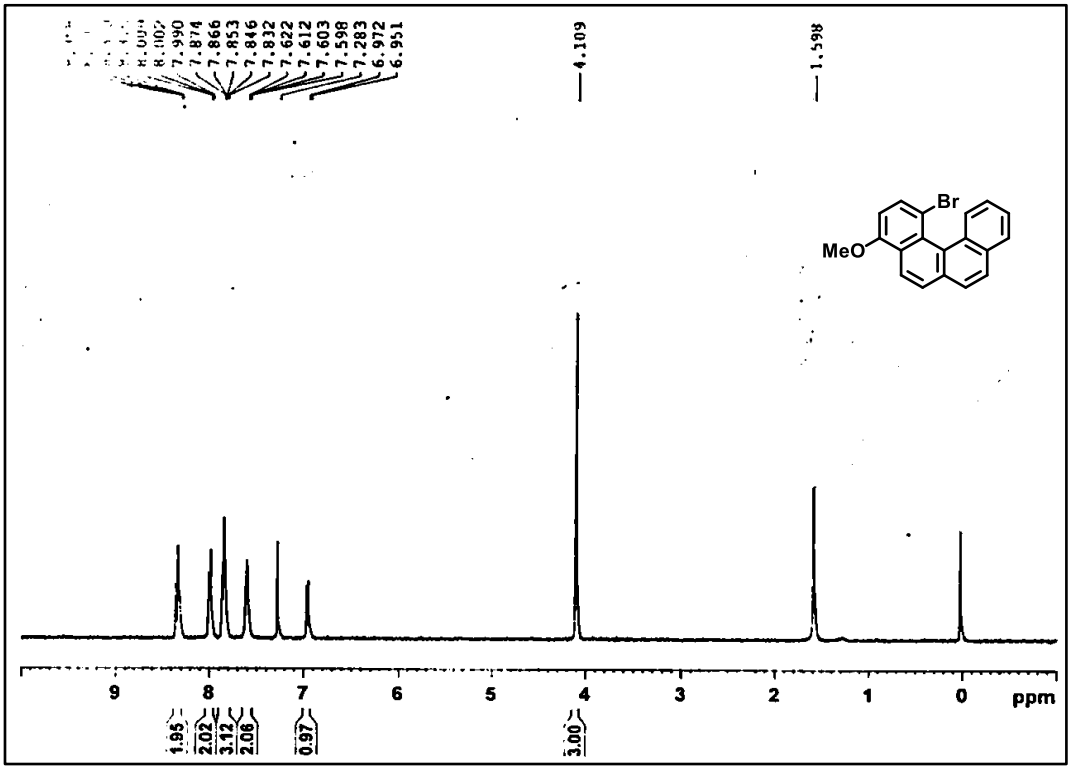

^{1}H NMR Spectra of compound **261** ($CDCl_3$, 400MHz)

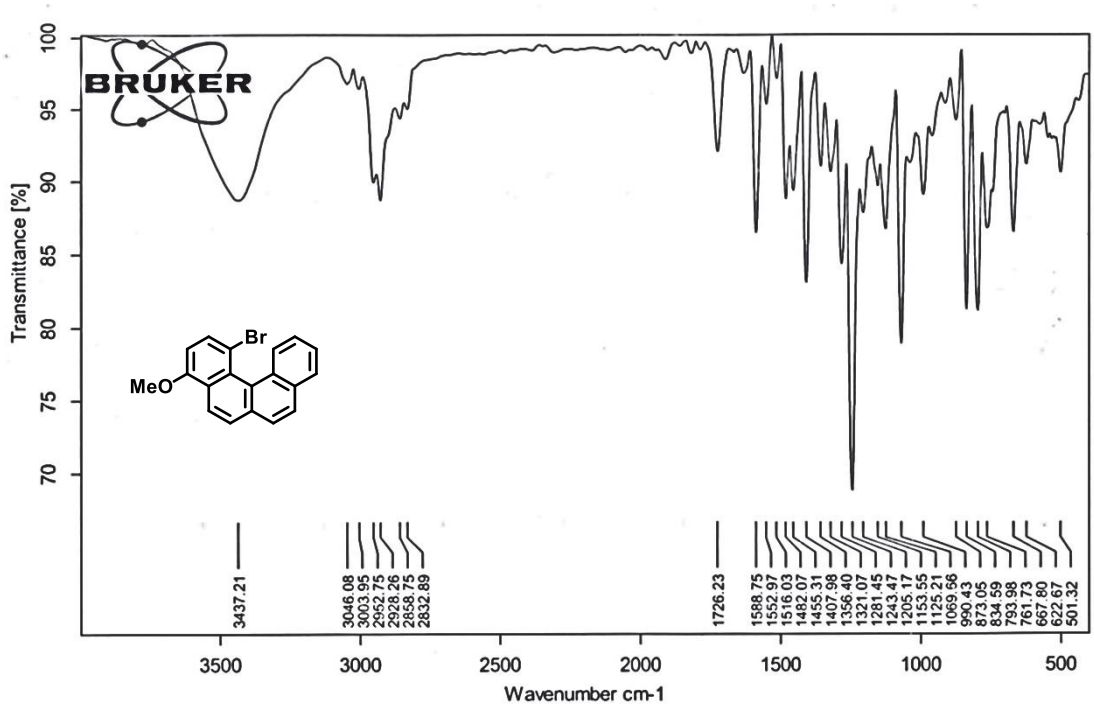

IR Spectra of compound **261**

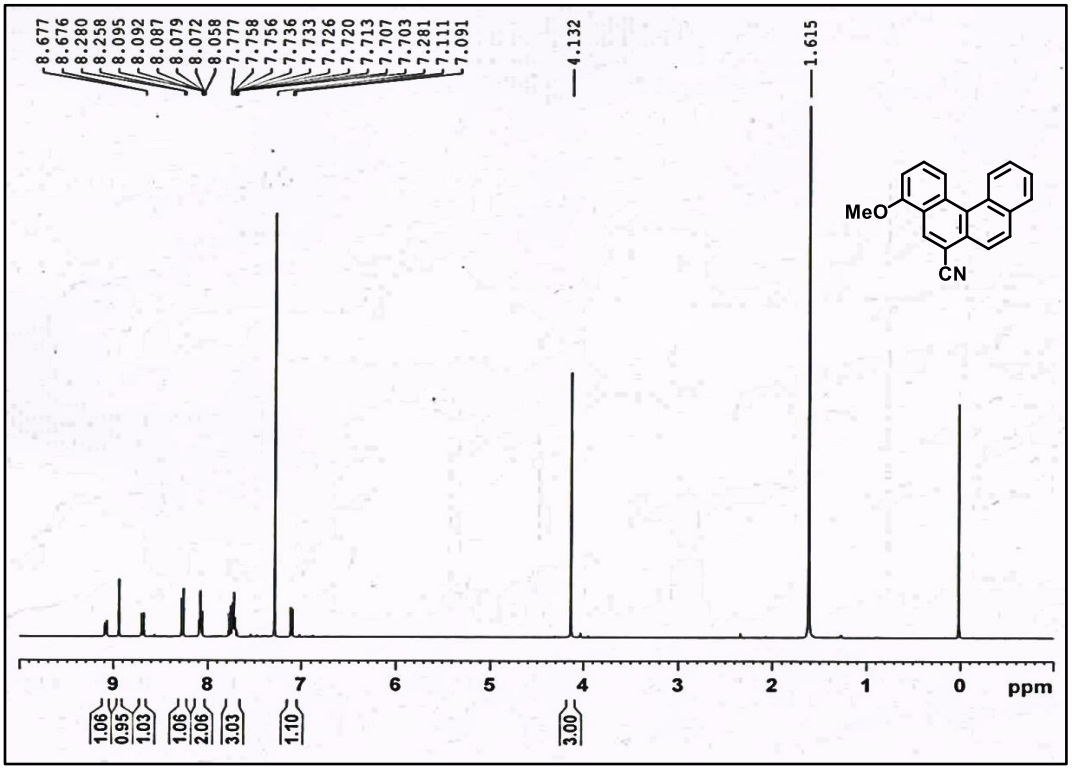

^{1}H NMR Spectra of compound **248** ($CDCl_3$, 400MHz)

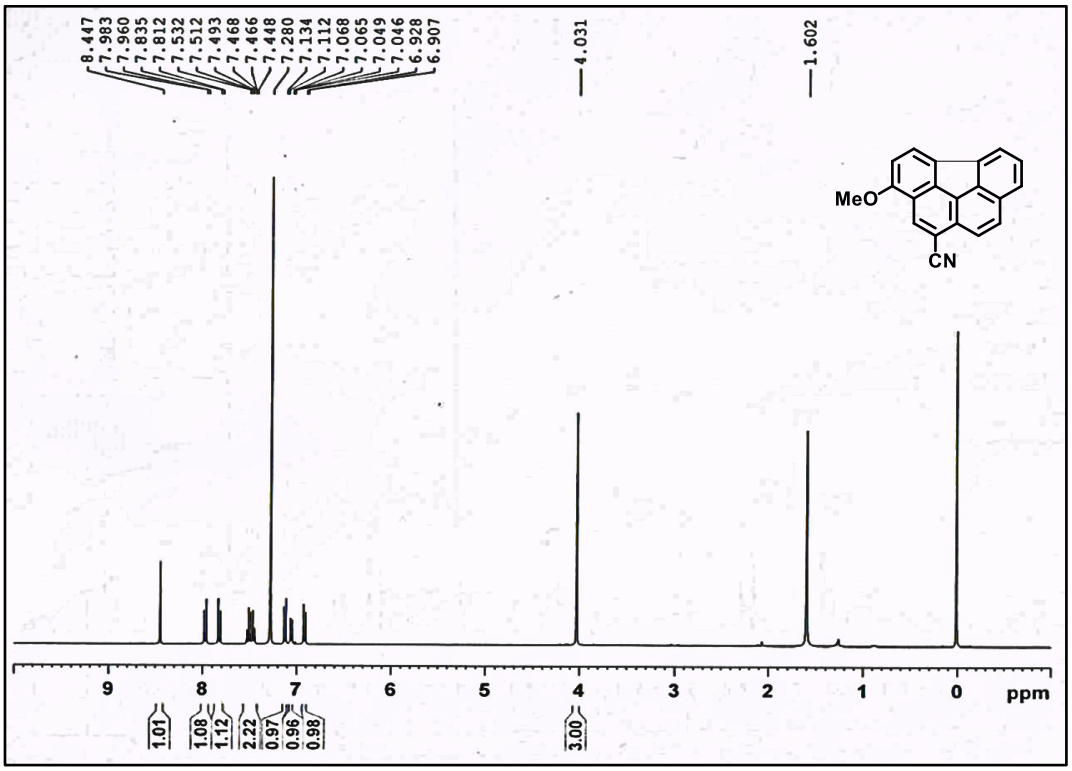

^{1}H NMR Spectra of compound **249** ($CDCl_3$, 400MHz)

2.4.2.8 Crystallographic Data:

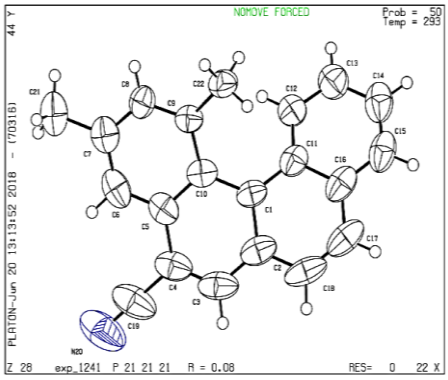

ORTEP diagram of compound (*P*)-239 (CCDC No. 1918596)
(50% probability factor for thermal ellipsoids)

Table 11 Crystal data and structure refinement for compound (*P*)-239

Empirical formula	$C_{21}H_{16}N$
Formula weight	282.35
Temperature/K	293(2)
Crystal system	orthorhombic
Space group	P212121
a/Å	5.8560(12)
b/Å	11.369(3)
c/Å	22.613(6)
α/°	90
β/°	90
γ/°	90
Volume/Å^3	1505.6(6)
Z	4
ρcalcg/cm^3	1.246
μ/mm^{-1}	0.072
F(000)	596.0
Radiation	MoKα λ = 0.71073
2Θ range for data collection/°	6.486 to 57.52
Index ranges	$-7 \leq h \leq 6$, $-15 \leq k \leq 12$, $-30 \leq l \leq 21$
Reflections collected	5039
Independent reflections	3089 [R_{int} = 0.0547, R_{sigma} = 0.0888]
Data/restraints/parameters	3089/0/205
Goodness-of-fit on F2	1.040
Final R indexes [I>=2σ (I)]	R_1 = 0.0814, wR_2 = 0.1972
Final R indexes [all data]	R_1 = 0.1322, wR_2 = 0.2420
Largest diff. peak/hole / e Å^{-3}	0.40/-0.22
Flack parameter	-6.2(10)

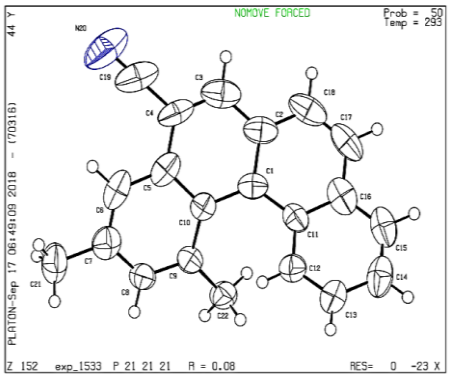

ORTEP diagram of compound (*M*)-239 (CCDC No. 1850915)
(50% probability factor for thermal ellipsoids)

Table 12 Crystal data and structure refinement for (*M*)-239

Empirical formula	$C_{21}H_{15}N$
Formula weight	281.36
Crystal system	orthorhombic
Space group	P212121
a/Å	5.8266(17)
b/Å	11.338(4)
c/Å	22.560(9)
α/°	90
β/°	90
γ/°	90
Volume/Å^3	1490.3(9)
Z	4
ρcalcg/cm^3	1.2539
μ/mm^{-1}	0.073
F(000)	592.2
Radiation	Mo Kα λ = 0.71073
2Θ range for data collection/°	6.5 to 57.42
Index ranges	$-7 \leq h \leq 7$, $-15 \leq k \leq 7$, $-16 \leq l \leq 28$
Reflections collected	3823
Independent reflections	2877 [R_{int} = 0.0826, R_{sigma} = 0.2314]
Data/restraints/parameters	2877/0/201
Goodness-of-fit on F2	0.996
Final R indexes [I>=2σ (I)]	R_1 = 0.0808, wR_2 = 0.1432
Final R indexes [all data]	R_1 = 0.2628, wR_2 = 0.2550
Largest diff. peak/hole / e Å^{-3}	0.63/-0.50
Flack parameter	-13.3(18)

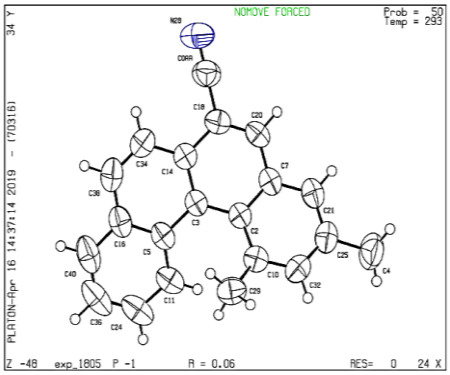

ORTEP diagram of compound 242 (CCDC No. 1918597)
(50% probability factor for thermal ellipsoids)

Table 13 Crystal data and structure refinement for compound 242

Empirical formula	$C_{21}H_{15}N$
Formula weight	281.34
Temperature/K	293(2)
Crystal system	triclinic
Space group	P-1
a/Å	7.3686(6)
b/Å	10.6754(6)
c/Å	11.0035(7)
α/°	62.766(6)
β/°	83.798(6)
γ/°	78.665(6)
Volume/Å^3	754.44(9)
Z	21
ρ_{calc}g/cm^3	1.238
μ/mm^{-1}	0.072
F(000)	304.0
Radiation	MoKα (λ = 0.71073)
2Θ range for data collection/°	6.52 to 58.22
Index ranges	$-9 \leq h \leq 9$, $-14 \leq k \leq 14$, $-14 \leq l \leq 14$
Reflections collected	16759
Independent reflections	3641 [R_{int} = 0.0221, R_{sigma} = 0.0166]
Data/restraints/parameters	3641/0/201
Goodness-of-fit on F^2	1.560
Final R indexes [I>=2σ (I)]	R_1 = 0.0620, wR_2 = 0.2147
Final R indexes [all data]	R_1 = 0.0823, wR_2 = 0.2299
Largest diff. peak/hole / e Å^{-3}	0.66/-0.17

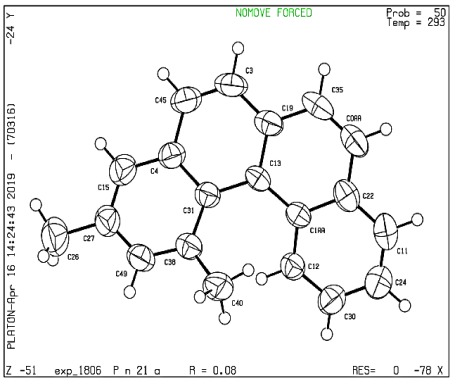

ORTEP diagram of compound 235 (CCDC No. 1918598)
(50% probability factor for thermal ellipsoids)

Table 14 Crystal data and structure refinement for compound 235

Empirical formula	$C_{20}H_{16}$
Formula weight	256.33
Temperature/K	293(2)
Crystal system	orthorhombic
Space group	$Pn2_1a$
a/Å	8.765(2)
b/Å	8.413(3)
c/Å	18.879(5)
α/°	90
β/°	90
γ/°	90
Volume/Å^3	1392.1(7)
Z	4
ρ_{calc}g/cm^3	1.2230
μ/mm^{-1}	0.069
F(000)	544.2
Radiation	Mo Kα (λ = 0.71073)
2Θ range for data collection/°	6.34 to 58.18
Index ranges	$-10 \leq h \leq 11$, $-11 \leq k \leq 10$, $-24 \leq l \leq 23$
Reflections collected	7814
Independent reflections	3208 [R_{int} = 0.0895, R_{sigma} = 0.0747]
Data/restraints/parameters	3208/1/183
Goodness-of-fit on F^2	1.090
Final R indexes [I>=2σ (I)]	R_1 = 0.0782, wR_2 = 0.1842
Final R indexes [all data]	R_1 = 0.1142, wR_2 = 0.2201
Largest diff. peak/hole / e Å^{-3}	0.29/-0.33

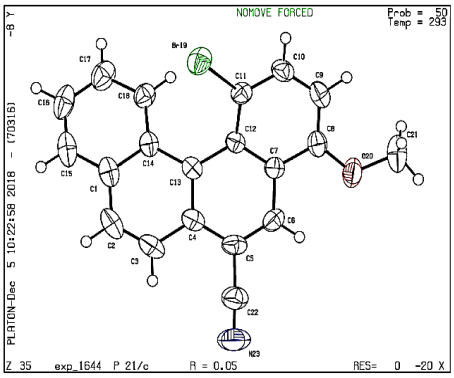

ORTEP diagram of compound 247 (CCDC No. 1883256)
(50% probability factor for thermal ellipsoids)

Table 15 Crystal data and structure refinement for compound 247

Empirical formula	$C_{20}H_{12}BrNO$
Formula weight	362.23
Temperature/K	293(2)
Crystal system	monoclinic
Space group	$P2_1/c$
a/Å	10.5724(11)
b/Å	19.0151(16)
c/Å	7.6556(8)
α/°	90
β/°	95.620(9)
γ/°	90
Volume/Å^3	1531.6(3)
Z	4
ρ_{calc}g/cm^3	1.5707
μ/mm^{-1}	2.687
F(000)	727.2
Radiation	Mo Kα (λ = 0.71073)
2Θ range for data collection/°	6.64 to 57.68
Index ranges	$-13 \leq h \leq 14$, $-23 \leq k \leq 25$, $-9 \leq l \leq 10$
Reflections collected	9393
Independent reflections	3454 [R_{int} = 0.0483, R_{sigma} = 0.0689]
Data/restraints/parameters	3454/0/209
Goodness-of-fit on F^2	1.027
Final R indexes [I>=2σ (I)]	R_1 = 0.0507, wR_2 = 0.0987
Final R indexes [all data]	R_1 = 0.0989, wR_2 = 0.1179
Largest diff. peak/hole / e Å^{-3}	0.79/-0.68

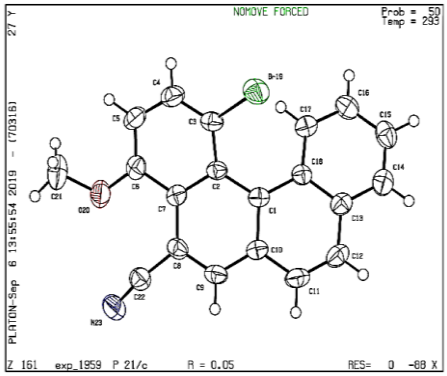

ORTEP diagram of compound 257 (CCDC No. 1955512)
(50% probability factor for thermal ellipsoids)

Table 16 Crystal data and structure refinement for compound 257

Empirical formula	$C_{20}H_{12}BrNO$
Formula weight	362.22
Temperature/K	293(2)
Crystal system	monoclinic
Space group	$P2_1/c$
a/Å	8.7055(8)
b/Å	22.6737(17)
c/Å	8.0327(6)
α/°	90.00
β/°	108.908(8)
γ/°	90.00
Volume/Å^3	1500.0(2)
Z	4
ρ_{calc}g/cm^3	1.604
μ/mm^{-1}	2.744
F(000)	728.0
Radiation	MoKα (λ = 0.71073)
2Θ range for data collection/°	6.12 to 58.06
Index ranges	$-11 \le h \le 11$, $-29 \le k \le 30$, $-9 \le l \le 10$
Reflections collected	16847
Independent reflections	3601 [R_{int} = 0.0752, R_{sigma} = N/A]
Data/restraints/parameters	3601/0/209
Goodness-of-fit on F^2	1.004
Final R indexes [I>=2σ (I)]	R_1 = 0.0503, wR_2 = 0.0861
Final R indexes [all data]	R_1 = 0.1100, wR_2 = 0.1039
Largest diff. peak/hole / e Å^{-3}	0.41/-0.46

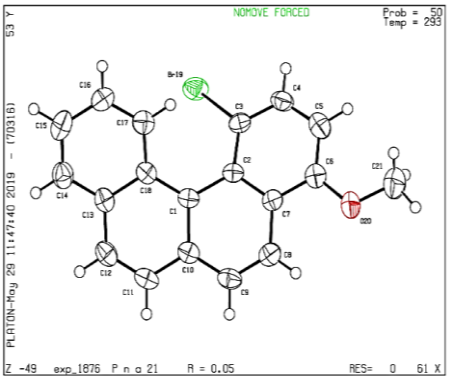

ORTEP diagram of compound 261 (CCDC No. 1920596)
(50% probability factor for thermal ellipsoids)

Table 17 Crystal data and structure refinement for compound 261

Identification code	exp_1876
Empirical formula	$C_{19}H_{13}BrO$
Formula weight	337.20
Temperature/K	293(2)
Crystal system	orthorhombic
Space group	$Pna2_1$
a/Å	8.8096(8)
b/Å	8.3718(5)
c/Å	19.2024(18)
α/°	90.00
β/°	90.00
γ/°	90.00
Volume/Å^3	1416.2(2)
Z	4
ρ_{calc}g/cm^3	1.582
μ/mm^{-1}	2.898
F(000)	680.0
Radiation	MoKα (λ = 0.71073)
2Θ range for data collection/°	7.04 to 58.62
Index ranges	$-11 \leq h \leq 11$, $-11 \leq k \leq 9$, $-26 \leq l \leq 24$
Reflections collected	9057
Independent reflections	3304 [R_{int} = 0.0613, R_{sigma} = 0.0912]
Data/restraints/parameters	3304/1/191
Goodness-of-fit on F^2	1.007
Final R indexes [I>=2σ (I)]	R_1 = 0.0501, wR_2 = 0.0656
Final R indexes [all data]	R_1 = 0.0961, wR_2 = 0.0807
Largest diff. peak/hole / e Å^{-3}	0.61/-0.38

2.5 References:

[1] J. M. Chance, B. Kahr, A. B. Buda, J. S. Siegel, *J. Am. Chem. Soc.* **1989**, *111*, 5940–5944.

[2] K. K. Baldridge, J. S. Siegel, *J. Am. Chem. Soc.* **1993**, *115*, 10782–10785.

[3] G. Hennrich, *Linear Nonlinear Opt. Org. Mater. VI* **2006**, *6331*, 63310G.

[4] H. Hope, J. Bernstein, K. N. Trueblood, *Acta Crystallogr. Sect. B* **1972**, *28*, 1733–1743.

[5] P. Lennartz, G. Raabe, C. Bolm, *Adv. Synth. Catal.* **2012**, *354*, 3237–3249.

[6] L. T. Scott, M. M. Hashemi, M. S. Bratcher, *J. Am. Chem. Soc.* **1992**, *114*, 1920–1921.

[7] A. Borchardt, A. Fuchicello, K. V Kilway, K. K. Baldridge, J. S. Siegel, *J. Am. Chem. Soc.* **1992**, *114*, 1921–1923.

[8] Y. Deng, D. Yu, X. Cao, L. Liu, C. Rong, T. Lu, S. Liu, *Mol. Phys.* **2018**, *116*, 956–968.

[9] A. Borchard, K. Hardcastle, P. Gantzel, J. S. Siegella, *Tetrahedron Lett.* **1993**, *34*, 273–276.

[10] C. Kübel, K. Eckhardt, V. Enkelmann, G. Wegner, K. Müllen, *J. Mater. Chem.* **2000**, *10*, 879–886.

[11] A. Sygula, A. H. Abdourazak, P. W. Rabideau, *J. Am. Chem. Soc.* **1996**, *118*, 339–343.

[12] T. J. Seiders, K. K. Baldridge, J. S. Siegel, *J. Am. Chem. Soc.* **1996**, *118*, 2754–2755.

[13] O. V Shishkin, L. Gorb, P. Hobza, J. Leszczynski, *Int. J. Quantum Chem.* **2000**, *80*, 1116–1124.

[14] T. T. Tidwell, *Tetrahedron* **1978**, *34*, 1855–1868.

[15] J. F. Liebman, A. Greenberg, *Chem. Rev.* **1976**, *76*, 311–365.

[16] V. Balasubramaniyan, *Chem. Rev.* **1966**, 567–641.

[17] X. Qiao, M. A. Padula, D. M. Ho, N. J. Vogelaar, C. E. Schutt, R. A. Pascal, *J. Am. Chem. Soc.* **1996**, *118*, 741–745.

[18] L. Tong, D. M. Ho, N. J. Vogelaar, C. E. Schutt, R. A. Pascal, *Tetrahedron Lett.* **1997**, *38*, 7–10.

[19] L. Tong, D. M. Ho, N. J. Vogelaar, C. E. Schutt, R. A. Pascal, *J. Am. Chem. Soc.* **1997**, *119*, 7291–7302.

[20] X. Qiao, I. Pelczer, R. A. Pascal Jr., *Chirality* **1998**, *10*, 154–158.

[21] Pascal Robert A., L. Barnett, X. Qiao, D. M. Ho, *J. Org. Chem.* **2000**, *65*, 7711–7717.

[22] F. H. Herbstein, *Acta Crystallogr. Sect. B* **1979**, *35*, 1661–1670.

[23] S. Sarkar, T. N. G. Row, *Int. Union Crystallogr.* **2017**, *4*, 37–49.

[24] G. A. Sim, *Acta Crystallogr. Sect. B* **1982**, *38*, 623–625.

[25] A. A. Freer, D. D. MacNicol, P. R. Mallinson, C. D. Robertson, *Tetrahedron Lett.* **1989**, *30*, 5787–5790.

[26] R. H. Barbour, A. A. Freer, D. D. MacNicol, *J. Chem. Soc., Chem. Commun.* **1983**, 362–363.

[27] D. D. MacNicol, P. R. Mallinson, C. D. Robertson, *J. Chem. Soc.,Chem. Commun.* **1985**, 1649–1651.

[28] D. D. MacNicol, W. M. McGregor, P. R. Mallinson, C. D. Robertson, *J. Chem. Soc., Perkin Trans. 1* **1991**, 3380–3382.

[29] H. A. M. Biemans, C. Zhang, P. Smith, H. Kooijman, W. J. J. Smeets, A. L. Spek, E. W. Meijer, *J. Org. Chem.* **1996**, *61*, 9012–9015.

[30] R. W. Franck, E. G. Leser, *J. Org. Chem.* **1970**, *85*, 3932–3939.

[31] J. E. Anderson, R. W. Franck, W. L. Mandella, *J. Am. Chem. Soc.* **1972**, 4608–4614.

[32] J. Handal, J. G. White, R. W. Franck, Y. H. Yuh, N. L. Allinger, *J. Am. Chem. Soc.* **1977**, 3345–3349.

[33] J. E. Anderson, R. W. Franck, *J. Chem. Soc. Perkin Trans. 2* **1984**, 1581–1582.

[34] H. V. Bekkum, T. J. Nieuwstad, J. V. Barneveld, P. Klapwijk, B. M. Wepster, *Recueil* **1969**, *88*, 1028.

[35] D. F. Tavares, J. P. Borger, *Can. J. Chem.* **1966**, *44*, 1323–1324.

[36] C. D. Deboer, W. G. Herkstroeter, A. P. Marchetti, A. G. Schultz, R. H. Schlessinger, *J. Am. Chem. Soc.* **1973**, 3963–3969.

[37] A. Okamoto, R. Mitsui, H. Oike, N. Yonezawa, *Chem. Lett.* **2011**, *40*, 1283–1284.

[38] B. J. E. Anderson, C. J. Cooksey, *J. Chem. Soc., Chem. Commun.* **1975**, 942–943.

[39] J. Clayden, C. Mccarthy, M. Helliwell, *Chem. Commun.* **1999**, 2059–2060.

[40] J. Ciayden, C. S. Frampton, N. Westlund, *Tetrahedron* **1999**, *55*, 14161–14184.

[41] A. Ahmed, R. A. Bragg, J. Clayden, L. W. Lal, C. Mccarthy, *Tetrahedron* **1998**, *54*, 13277–13294.

[42] J. Clayden, C. S. Frampton, *J. Chem. Soc., Perkin Trans. 1* **2000**, 1379–1385.

[43] K. Yamamoto, N. Oyamada, S. Xia, Y. Kobayashi, M. Yamaguchi, H. Maeda, H. Nishihara, T. Uchimaru, E. Kwon, *J. Am. Chem. Soc.* **2013**, *135*, 16526–16532.

[44] H. Aikawa, Y. Takahira, M. Yamaguchi, *Chem. Commun.* **2011**, *47*, 1479–1481.

[45] A. F. Pozharskii, V. A. Ozeryanskii, E. A. Filatova, O. V Dyablo, O. G. Pogosova, G. S. Borodkin, A. Filarowski, D. V Steglenko, *J. Org. Chem.* **2019**, *84*, 726–737.

[46] V. A. Ozeryanskii, A. F. Pozharskii, A. K. Artaryan, N. V Vistorobskii, Z. A. Starikova, *European J. Org. Chem.* **2009**, 1241–1248.

[47] T. Kusukawa, S. Tanaka, K. Inoue, *Tetrahedron* **2014**, *70*, 4049–4056.

[48] H. Naeimi, A. Raeisi, M. Moradian, *Arab. J. Chem.* **2017**, *10*, S2723–S2728.

[49] F. Ashraf, R. Khajuria, K. Zaman, *J. Chem. Pharm. Res.* **2013**, *5*, 33–36.

[50] J. A. Hyatt, P. W. Raynolds, *J. Org. Chem.* **1984**, *49*, 384–385.

[51] A. Okamoto, N. Yonezawa, *Chem. Lett.* **2009**, *38*, 914–915.

[52] A. Okamoto, R. Mitsui, H. Oike, N. Yonezawa, *Chem. Lett.* **2011**, *40*, 1283–1284.

[53] D. Ioffe, A. Kampf, in *Kirk-Othmer Encycl. Chem. Technol.*, American Cancer Society, **2002**.

[54] M. M. Sprung, *Ind. Eng. Chem. Anal. Ed.* **1941**, *13*, 35–38.

[55] V. Srivastava, A. S. Negi, J. K. Kumar, U. Faridi, B. S. Sisodia, M. P. Darokar, S. Luqman, S. P. S. Khanuja, *Bioorg. Med. Chem.* **2006**, *16*, 911–914.

[56] K. P. Latha, H. M. Vagdevi, M. N. Kumaraswamy, *Int. J. Pharm. Chem. Biol. Sci.* **2017**, *7*, 388–392.

[57] B. Saed, H. Sabzyan, *Spectrochim. Acta Part A Mol. Biomol. Spectrosc.* **2019**, *222*, 117133.

[58] B. Wang, X. Qiao, Z. Yang, Y. Wang, S. Liu, D. Ma, Q. Wang, *Org. Electron.* **2018**, *59*, 32–38.

[59] B.-C. Chen, C.-X. Lin, N.-P. Chen, C.-X. Gao, Y.-J. Zhao, C.-D. Qian, *Front. Microbiol.* **2018**, *9*, 1593.

[60] E. V Vetrova, S. V Kurbatov, S. N. Borisenko, A. V Lekar, S. S. Khizrieva, N. I. Borisenko, V. I. Minkin, *Russ. J. Phys. Chem. B* **2017**, *11*, 1255–1259.

[61] I. Kim, Y. H. Song, N. Singh, Y. J. Jeong, J. E. Kwon, H. Kim, Y. M. Cho, S. C. Kang, K.-W. Chi, *Int. J. Nanomedicine* **2015**, *10 Spec Is*, 143–153.

[62] *Chem. Sci.* **2019**, *10*, 5470–5475.

[63] W. D. Good, *J. Chem. Thermodyn.* **1973**, *5*, 715–720.

[64] M. A. Frisch, C. Barker, J. L. Margrave, M. S. Newman, *J. Am. Chem. Soc.* **1963**, *85*, 2356–2357.

[65] M. S. Newman, A. S. Hussey, *J. Am. Chem. Soc.* **1947**, *69*, 3023.

[66] R. Munday, I. O. Sutherland, *J. Chem. Soc.* **1968**, 80.

[67] H. Scheriibl, U. Fritzsche, A. Mannschreck, *Chem. Ber.* **1984**, *117*, 336–343.

[68] F. Imashiro, A. Saika, Z. Taira, *J. Org. Chem.* **1987**, *52*, 5727–5729.

[69] R. N. Armstrong, H. L. Ammon, J. N. Darnow, *J. Am. Chem. Soc.* **1987**, *109*, 2077.

[70] A. Mannschreck, E. Gmahl, T. Burgemeister, F. Kastner, V. Sinnwell, *Angew. Chem. lnt. Ed. Engl.* **1988**, *27*, 270–271.

[71] R. E. Gerkin, *Acta Crystallogr.* **2000**, *C56*, 1220–1221.

[72] S. Sternhell, C. W. Tansey, *Aust. J. Chem.* **1990**, *43*, 1577–80.

[73] S. Grimme, I. Pischel, M. Nieger, F. Vogtle, *J. Chem. Soc. Perkin Trans. 2* **1996**, 2771–2774.

[74] R. Cosmo, T. W. Hambley, Sternhell Sever, *Tetrahedron Lett.* **1987**, *28*, 6239–6240.

[75] R. Cosmo, T. W. Hambley, S. Sternhell, *J. Org. Chem.* **1987**, *52*, 3119–3123.

[76] R. Cosmo, T. W. Hambley, S. Sternhell, *Acta Crystallogr. Sect. B* **1990**, *B46*, 557–562.

[77] H. Bock, M. Sievert, Z. Havlas, *Chem. – A Eur. J.* **1998**, *4*, 677–685.

[78] N. S. Kim, D. M. Thamattoor, *Acta Crystallogr.* **2017**, *E73*, 539–542.

[79] C. Kiefl, H. Zinner, M. A. Cuyegkeng, A. Eiglsperger, *Tetrahedron Asymmetry* **2000**, *11*, 3503–3513.

[80] S. Rozen, S. Dayan, *Angew. Chem. lnt. Ed.* **1999**, 3471–3473.

[81] K. Bera, S. Sarkar, S. Jalal, U. Jana, *J. Org. Chem.* **2012**, *77*, 8780–8786.

[82] F. B. Mallory, C. W. Mallory, *Photocyclization of Stilbenes and Related Molecules*, John Wiley And Sons, **1984**.

[83] F. Bell, D. H. Waring, *J. Chem. Soc.* **1949**, 2689–2693.

[84] J. Szeliga, A. Dipple, *Chem. Res. Toxicol.* **1998**, *11*, 1–11.

[85] I. A. for R. on Cancer, K. I. D. of B. at N. C. for N. and Toxicology, in *IARC Sci. Publ.*, **1994**, p. 466.

[86] R. Weitzenböck, H. Lieb, *Monatshefte für Chemie* **1912**, *33*, 549–565.

[87] H. Weitzenbock, R.; Lieb, *Monatsh. Chem.* **1918**, *39*, 315.

[88] F. Mayer, T. Oppenheimer, *Berichte der Dtsch. Chem. Gesellschaft* **1918**, *51*, 510–

516.

[89] J. W. Cook, *J. Chem. Soc.* **1931**, 2524–2528.

[90] T. Crystal, G. M. J. Schmidt, *J. Chem. Soc.* **1954**, 3302–3313.

[91] W. Levin, A. W. Wood, R. L. Chang, Y. Ittah, M. Croisy-Delcey, H. Yagi, D. M. Jerina, A. H. Conney, *Cancer Res.* **1980**, *40*, 3910–3914.

[92] A. W. Wood, R. L. Chang, W. Levin, D. E. Ryan, P. E. Thomas, M. Croisy-Delcey, Y. Ittah, H. Yagi, D. M. Jerina, A. H. Conney, *Cancer Res.* **1980**, *40*, 2876–2883.

[93] N. Perin, I. Martin-Kleiner, R. Nhili, W. Laine, M.-H. David-Cordonnier, O. Vugrek, G. Karminski-Zamola, M. Kralj, M. Hranjec, *Med. Chem. Commun.* **2013**, *4*, 1537–1550.

[94] W. Jerina, D. M.; Sayer, J. M.; Yagi, H.; Delcey, M. C.; Ittah, Y.; Thakker, D. R.; Wood, A. W.; Chang, R. L.; Levin, *Biological Reactive Intermediates II, Part A*, Plenum Press, New York, **1982**.

[95] M. S. Newman, W. B. Wheatley, W. B. Wheatley, *J. Am. Chem. Soc.* **1948**, *70*, 1913–1916.

[96] M. S. Newman, M. Wolf, *J. Am. Chem. Soc.* **1952**, *74*, 3225–3228.

[97] M. K. Lakshman, P. L. Kole, S. Chaturvedi, J. H. Saugier, H. J. C. Yeh, J. P. Glusker, H. L. Carrell, A. K. Katz, C. E. Afshar, W. Dashwood, et al., *J. Org. Chem.* **2000**, *122*, 12629–12636.

[98] S. Kumar, *J. Org. Chem.* **1997**, *62*, 8535–8539.

[99] S. Bae, H. Mah, S. Chaturvedi, T. M. Jeknic, W. M. Baird, A. K. Katz, H. L. Carrell, J. P. Glusker, T. Okazaki, K. K. Laali, et al., *J. Org. Chem.* **2007**, *72*, 7625–7633.

[100] M. S. Newman, D. Lednicer, *J. Am. Chem. Soc.* **1956**, *78*, 4765–4770.

[101] D. D. (Newmann, M. S.; Phillips, *J. Am. Chem. Soc.* **1959**, *81*, 3667.

[102] M. S. Newman, R. M. Wise, *J. Am. Chem. Soc.* **1956**, *78*, 450–454.

[103] H. Okubo, M. Yamaguchi, C. Kabuto, *J. Org. Chem.* **1998**, *63*, 9500–9509.

[104] M. Yamaguchi, H. Okubo, D. Nakano, *J. Org. Chem.* **2001**, *66*, 557–563.

[105] F. Feng, T. Miyashita, H. Okubo, M. Yamaguchi, *J. Am. Chem. Soc.* **1998**, *120*, 10166–10170.

[106] F. Feng, **1999**, *55*, 14855–14864.

[107] M. Yamaguchi, S. Honzawa, S. Chiba, H. Okubo, *Heterocyclces* **2002**, *57*, 1091–1099.

[108] K. Nakamura, H. Okubo, M. Yamaguchi, *Org. Lett.* **2001**, *3*, 1097–1099.

[109] H. Sugiura, Y. Takahira, M. Yamaguchi, *J. Org. Chem.* **2005**, *70*, 5698–5708.

[110] S. Honzawa, H. Okubo, K. Nakamura, S. Anzai, M. Yamaguchi, C. Kabuto, *Tetrahedron Asymmetry* **2002**, *13*, 1043–1052.

[111] S. D. Dreher, T. J. Katz, K. Lam, A. L. Rheingold, *J. Org. Chem.* **2000**, *65*, 815–822.

[112] T. Shimizu, M. Kobayashi, *Chem. Lett.* **1986**, *15*, 161–164.

[113] H. Okubo, D. Nakano, M. Yamaguchi, C. Kabuto, *Chem. Lett.* **2000**, *29*, 1316–1317.

[114] H. Sugiura, D. Sakai, H. Otani, K. Teranishi, Y. Takahira, R. Amemiya, M. Yamaguchi, *Chem. Lett.* **2006**, *36*, 72–73.

[115] M. S. Newman, R. G. Mentzer, G. Slomp, *J. Am. Chem. Soc.* **1963**, *85*, 4018–4020.

[116] M. S. Newman, W. B. Lutz, *J. Am. Chem. Soc.* **1956**, *78*, 2469–2473.

[117] C. M. Kemp and S. F. Mason, *Tetrahedron* **1966**, *22*, 629–635.

[118] D. E. Adelson, M. T. Bogert, *J. Am. Chem. Soc.* **1937**, *59*, 1776–1782.

[119] C. L. Hewett, *J. Chem. Soc.* **1938**, 1286–1291.

[120] J. Szmuszkovicz, E. J. Modest, *J. Am. Chem. Soc.* **1950**, *72*, 566–570.

[121] M. S. Newman, H. V. Anderson, K. H. Takemura, *J. Am. Chem. Soc.* **1953**, *75*, 347–349.

[122] D. L. Nagel, R. Kupper, K. Antonson, L. Wallcave, *J. Org. Chem.* **1977**, *42*, 3626–3628.

[123] T. Hu, J. Y.; Paudel, A.; Seto, N.; Feng, X.; Era, M.; Matsumoto, T.; Tanaka, J.; Elsegood, M. R.; Redshaw, R.; Yamato, *Org. Biomol. Chem.* **2013**, *11*, 2186.

[124] J. Y. Hu, X. Feng, A. Paudel, H. Tomiyasu, U. Rayhan, P. Thuéry, M. R. J. Elsegood, C. Redshaw, T. Yamato, *Eur. J. Org. Chem.* **2013**, 5829–5837.

[125] D. B. Amabilino, R. M. Kellogg, *Isr. J. Chem.* **2011**, *S1*, 1034–1040.

[126] A. R. A. Palmans, *Mol. Syst. Des. Eng.* **2017**, *2*, 34–46.